

## **General Disclaimer**

### **One or more of the Following Statements may affect this Document**

- This document has been reproduced from the best copy furnished by the organizational source. It is being released in the interest of making available as much information as possible.
- This document may contain data, which exceeds the sheet parameters. It was furnished in this condition by the organizational source and is the best copy available.
- This document may contain tone-on-tone or color graphs, charts and/or pictures, which have been reproduced in black and white.
- This document is paginated as submitted by the original source.
- Portions of this document are not fully legible due to the historical nature of some of the material. However, it is the best reproduction available from the original submission.

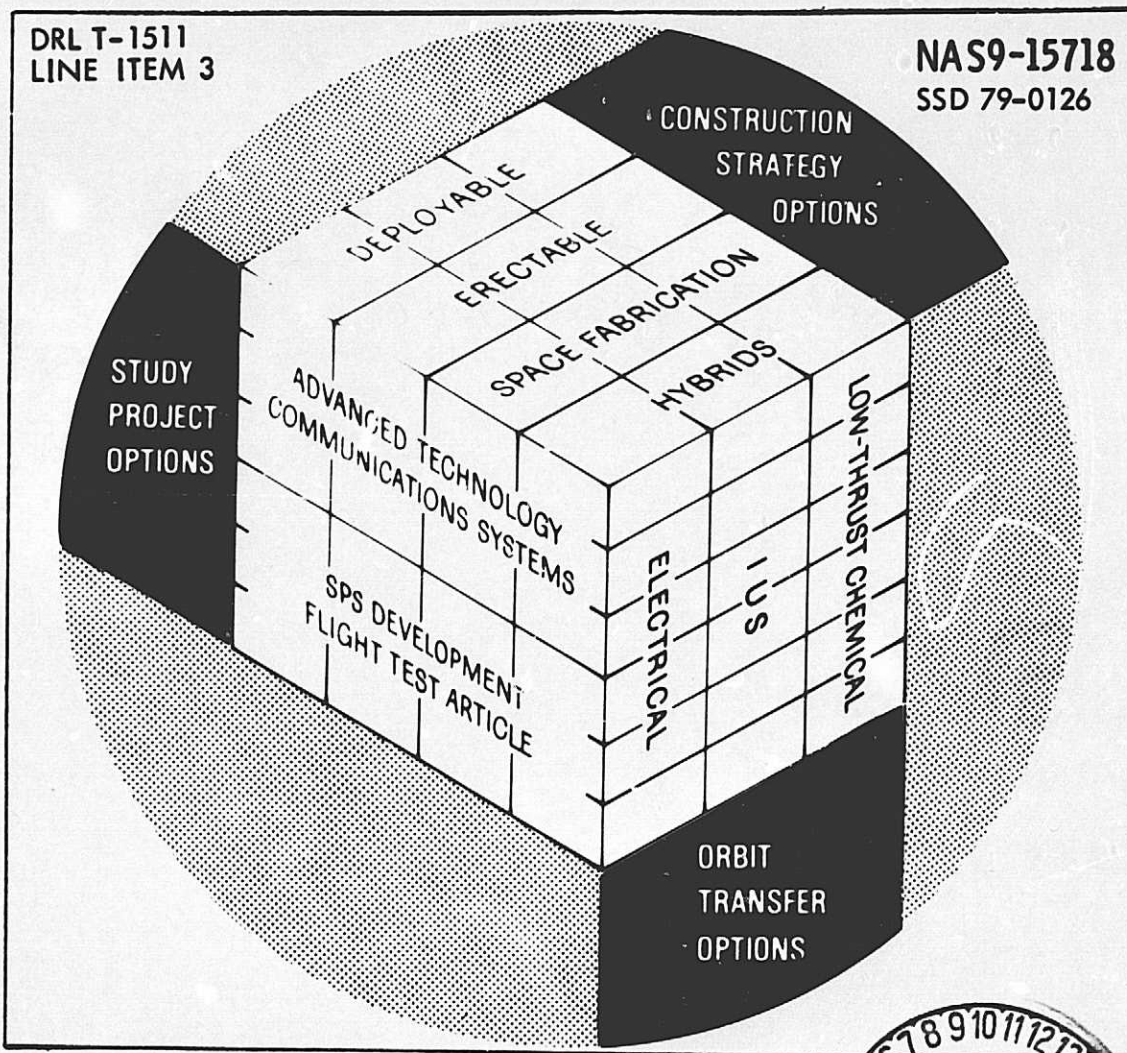
CR-160298

# SPACE CONSTRUCTION SYSTEM ANALYSIS

## SPECIAL-EMPHASIS STUDIES

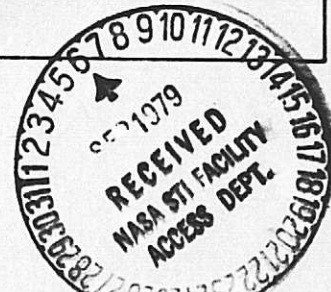
### FINAL REPORT

### JUNE 1979



Rockwell International

Satellite Systems Division  
Space Systems Group  
12214 Lakewood Boulevard  
Downey, CA 90241



(NASA-CR-160298) SPACE CONSTRUCTION SYSTEM ANALYSIS. PART 1: EXECUTIVE SUMMARY. SPECIAL EMPHASIS STUDIES Final Report (Rockwell International Corp., Downey, Calif.) 186 p HC A09/MF A01

N79-30269

CSCI 22A G3/12

Unclas  
31939

SSD 79-0126

SPACE CONSTRUCTION SYSTEM ANALYSIS STUDY

SPECIAL EMPHASIS STUDIES

Final Report

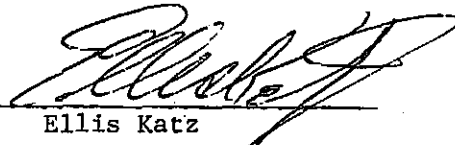
Contract No. NAS9-15718

DRL T-1511

Line Item 3

June 1979

Approved by

  
Ellis Katz



Rockwell International  
Space Division

## FOREWORD

This report summarizes the results of three special emphasis studies related to Space Construction Systems Analysis. The document is a product of Contract NAS9-15718, Space Construction System Analysis Study, which was conducted for the National Aeronautics and Space Administration, Johnson Space Center, by Satellite Systems Division, Space Systems Group, Rockwell International Corporation.

The study was performed under the direction of Ellis Katz, Study Manager. The following persons made significant contributions to the analyses reported herein.

R. D. Donovan  
W. Fredericks  
H. S. Greenberg  
R. Hart  
A. S. Jones  
R. L. Kaiser  
A. N. Lillenas  
H. L. Myers  
A. J. Stefan  
R. R. Thompson  
R. S. Totah

Major documents resulting from Part 1 of the contract effort are listed below:

Space Construction System Analysis,  
Project Systems and Mission Descriptions,  
Task 1 Final Report, SSD 79-0077  
April 26, 1979

Space Construction System Analysis, Task 2 Final Report -  
System Analysis of Space Construction, SSD 79-0123,  
June 1979

Space Construction System Analysis, Task 3 Final Report -  
Construction System Shuttle Integration, SSD 79-0124,  
June 1979

Space Construction Data Base  
SSD 79-0125, June 1979

Space Construction System Analysis, Special Emphasis Studies Final Report, SSD 79-0126, June 1979
--

## CONTENTS

<u>SECTION</u>	<u>PAGE</u>
1.0 INTRODUCTION AND SUMMARY	1-1
2.0 DEPLOYABLE SOLAR ARRAY	2-1
2.1 ARTICULATED FOLDABLE TRUSS STRUCTURE/SOLAR ARRAY CONCEPT	2-1
2.1.1 Improved Packaging	2-1
2.1.2 Wings	2-8
2.1.3 Heat Rejection	2-8
2.1.4 Electrical Power	2-10
2.1.5 Center Mounting	2-10
2.1.6 Deployment From Orbiter Bay	2-11
2.1.7 Orbiter Bay Packaging	2-12
2.1.8 Structural Analysis	2-14
2.1.9 Interior Solar Panel Analysis	2-25
2.2 SOLAR ELECTRIC PROPULSION SYSTEM (SEP) TYPE SOLAR ARRAY CONCEPT	2-26
2.2.1 Concept Variation	2-26
2.2.2 Heat Rejection	2-26
2.2.3 Deployment Mast	2-26
2.2.4 Total Power System	2-26
2.2.5 Structural Analysis	2-32
2.3 SUMMARY	2-36
2.4 REFERENCES	2-36
3.0 LINEAR VERSUS AREA SHAPED ERECTABLE PLATFORM STUDY	3-1
3.1 INTRODUCTION AND SUMMARY	3-1
3.2 PLATFORM DESIGN	3-2
3.2.1 Study Approach/Configuration	3-2
3.2.2 Structural Analyses	3-7
3.2.3 General Conclusions From Structural Analysis	3-11
3.2.4 References	

PRECEDING PAGE BLANK NOT FILMED



## CONTENTS (Con't.)

<u>SECTION</u>	<u>PAGE</u>
3.3 CONSTRUCTION OPERATIONS	3-15
3.3.1 Configuration Considerations	3-15
3.3.2 Assembly Operations - General Considerations	3-15
3.3.3 Area Platform Assembly Process	3-22
3.3.4 Area Platform Timeline Factors	3-33
3.3.5 Linear Platform Assembly Process	3-34
3.3.6 Linear Platform Timeline Factors	3-38
3.3.7 Timeline Comparisons	3-39
3.3.8 Significant Findings	3-44
3.3.9 References	3-45
4.0 COMMUNICATIONS PLATFORM STUDY	4-1
4.1 INTRODUCTION AND SUMMARY	4-1
4.2 THE NEED FOR A TELECOMMUNICATIONS PLATFORM	4-2
4.2.1 Current DOMSAT Constellation Capability	4-4
4.2.2 Traffic Projections	4-9
4.2.3 Capability	4-11
4.2.4 Technical and Regulatory Factors	4-11
4.3 PRELIMINARY DESIGN	4-14
4.4 THE APPLICATIONS TEST PLATFORM	4-17
4.4.1 Applications Test Platform Communication Subsystem	4-21
4.4.2 Description of Electronic Mail System Concept	4-22
4.4.3 Applications Test Satellite Design Parameters	4-31
4.4.4 Basic Transponders for Continuation of ATS-6 Experiments	4-35
APPENDIXES	
A. CONSTRUCTION PROJECT DRAWINGS	
B. LINK CALCULATIONS FOR 12/14 GHz EARTH STATIONS AT USER LOCATIONS	
C. TRAFFIC CAPACITY OF COMMUNICATIONS PLATFORM AS LIMITED BY ANTENNA SIDE LOBES	



## ILLUSTRATIONS

<u>FIGURE</u>		<u>PAGE</u>
2-1	Deployable Solar Array Concepts	2-2
2-2	Folding Panel Concept	2-3
2-3	Structural Folding Concept	2-4
2-4	Variations on Panel Concept	2-5
2-5	Conductors and Routing	2-7
2-6	Heat Rejection Concept	2-9
2-7	Center Mounting Arrangement	2-11
2-8	Orbiter Payload Bay Stowage Arrangement	2-11
2-9	Deployment Mechanism Concept	2-12
2-10	Orbiter Payload Bay C.G. Limitations	2-13
2-11	Solar Array Variations Versus Payload Bay Limitations	2-13
2-12	Deployable Solar Array - Area and Truss Structure Weight Versus Load Factor	2-15
2-13	Solar Array Truss Configuration	2-16
2-14	Solar Array Truss Configuration (for Sizing)	2-20
2-15	Typical Strut Loading	2-24
2-16	SEPS-Type Concept	2-27
2-17	Options for SEPS Design	2-28
2-18	Conductors and Routing	2-29
2-19	Deployment Mast Arrangement Concept	2-30
2-20	Total Power System Delivery Capability	2-31
2-21	Summary - Deployable Solar Arrays	2-37
3.2-1	Stowed Antenna Reflector/Feed Package - Alternate Configuration	3-4
3.2-2	Baseline "Area" Shaped Advanced Communications Technology Platform	3-5
3.2-3	Alternate "Area" Shaped Advanced Communications Technology Platform	3-6
3.2-4	Thrust Structure - Baseline Configuration	3-7
3.2-5	NASTRAN Half Model of Structure - Orbit Transfer Loads	3-12
3.2-6	NASTRAN Model Operational Configuration Modal Analysis	3-12
3.2.7	Communication Platform Growth Potential	3-13
3.3-1	Linear Shaped Erectable Platform	3-16
3.3-2	Area Shaped Erectable Platform	3-17
3.3-3	Assembly Concept for Tetrahedral Area Platform, Using Short Trapeze and Two Standard Length Shuttle RMS Arms	3-19
3.3-4	Assembly Concept for Tetrahedral Area Platform, Using Long Trapeze and Starboard Construction Boom	3-20
3.3-5	Assembly Concept for Linear Platform	3-21
3.3-6	Assembly Sequence for Area Platform	3-23
3.3-7	Module Installation Concept	3-31

# ILLUSTRATIONS (Con't.)

<u>FIGURE</u>		<u>PAGE</u>
3.3-8	RMS Effective Length	3-32
3.3-9	Assembly Sequence of Pentahedral Linear Platform	3-35
3.3-10	LSS Assembly Timeline	3-39
4-1	Scenario of Space Communications for Continental U.S.A.	4-1
4-2	Satellite Constellation	4-5
4-3	C&Ku Band Orbital Arcs	4-6
4-4	Platform Utilization	4-15
4-5	Satellite Communications Requirements and Capabilities	4-18
4-6	Applications Test Platform Program Schedule	4-19
4-7	A Frame in a TDMA System	4-23
4-8	Typical Attenuation Caused by Rain for Clarksburg, Maryland	4-26
4-9	Number of Total Occurrences of 1-Inch Per Hour or Greater Rainfall Rate for a 30-Year Period	4-28
4-10	Regions Where Indicated DB of Attenuation at 12 GHz is Exceeded for 0.01 Percent of the Time	4-29
4-11	Basic Two-Channel Transponder Block Diagram for Electronic Mail Experiment	4-33
4-12	CTS Communications Transponder and Beacon	4-36
4-13	Communications Subsystem (Simplified Block Diagram)	4-38





## TABLES

	<u>PAGE</u>
2-1 Area/Power Versus Solar Panel Concept	2-10
2-2 Member Axial Compression Loads (N) for Axial Compression, Torque, Bending Moment Load Factors	2-21
2-3 Typical Design Data	2-22
2-4 Solar Array Candidate Design Characteristics	2-23
2-5 Deployment Mast Configurations	2-33
3.2-1 Comparative "Linear" Versus "Area" Shaped Platform Characteristics	3-8
3.2-2 Comparative Platform Structural Deformation Contributions to Antenna Pointing Error	3-9
3.3-1 Physical Comparison	3-15
3.3-2 Assembly Groundrules	3-18
3.3-3 Timeline Assembly Activity Time Allowances	3-33
3.3-4 RMS Operational Guidelines	3-36
3.3-5 Kit Assembly Time Summary (RMS Operations)	3-37
3.3-6 Kit Assembly Time Summary	3-37
3.3-7 Time Allocations for Assembly Comparisons	3-40
3.3-8 Timeline Details	3-41
3.3-9 Timeline Comparison Summary	3-43
4-1 Current U.S. DOMSAT Transponders	4-7
4-2 Postulated Growth	4-8
4-3 Traffic Projections/Assumptions	4-10
4-4 Traffic Projections	4-10
4-5 Satellite Communications Capability Assumptions	4-12
4-6 Satellite Communications Capability	4-12
4-7 Factors Which Alter the Forecast	4-13
4-8 Applications Test Platform Validation Areas	4-20
4-9 Potential Up- and Downlink Frequency Bands for Electronic Mail Transmissions in GHz	4-25
4-10 Summary of Possible Applications Test Platform Satellite Antennas	4-32
4-11 Characteristics of Transponders in Figure 4-11	4-34
4-12 Baseline CTS 12/14 GHz Transponder Characteristics	4-37
4-13 Baseline ATS-6 Type 2.6/6 GHz TV Transponder Characteristics	4-40
4-14 ATS-6 Communications Subsystem Characteristics	4-41

## 1.0 INTRODUCTION AND SUMMARY

During the course of the Space Construction System Analysis Study, several studies of a generic nature were identified as worthy of analysis. This document presents the results of three such generic concept analyses.

The first study concerns the issue of the maximum size of deployable solar power array which might be packaged into a single orbit payload bay. It explores various concepts for configuring and mechanizing a solar array which could be attached at a single juncture (e.g., a berthing port) on a large space satellite.

The second study is concerned with the optimal overall shape of a large erectable structure for large satellite projects. Specific concern is given to those which may have platforms either of column-like, "linear" shapes or, in contrast, more nearly equal length and width dimensions (herein called "area" shapes for convenience of discussion). This study was performed to evaluate what penalties might have been incurred by favoring a linear shaped project configuration in order to facilitate construction operations. Specific concerns were potential weight increase, reduced stiffness, and consequent impacts on pointing accuracy and stability/control systems.

The third study addresses issues of electronic communication optimization related to number of antennas and their diameters, number of beams, traffic growth projections and frequencies. This study is more concerned with the question of what should be constructed in space than how it should be constructed. However, it has a strong potential impact on design of the systems, their arrangement on the structure, their power demands and the pointing accuracies needed for the antennas and the basic spacecraft. This study is a portion of the effort to define trends in satellite communications technology development and supports the analytical effort planned for Part 2 of the Space Construction System Analysis Study.

The results of these special emphasis studies were significant, generally favorable and supportive of the earlier selected approaches. For example, it was found feasible to package a deployable solar array into a single orbiter payload bay, which could generate over 250 kilowatts of electrical power. Also, it was found that the linear-shaped erectable structure is better for ease of construction and installation of systems, and compares favorably on several other counts. Finally, the study of electronic communication technology indicated that proliferation of individual satellites will crowd the spectrum by the early 1990's, so that there will be a strong tendency toward a small number of communications platforms over the continental U.S.A. with many antennas and multiple, spot beams.

## 2.0 DEPLOYABLE SOLAR ARRAY

A study of deployable solar array concepts was initiated to determine the maximum feasible size that could be delivered to low earth orbit (LEO) within the payload bay of a single Shuttle orbiter. The solar array is assumed to be part of a large space vehicle assembled in LEO (approximately 220 nmi) and then boosted to geosynchronous orbit by electric propulsion. Switch gear and other electrical equipment necessary to condition the output of the solar array is to be mounted in a separate module and is not part of the solar array itself.

Two concepts were developed to satisfy these conditions: (1) an articulated foldable truss structure/solar panel concept, and (2) a single mast supported solar panel similar to the Solar Electric Propulsion System (SEPS) program concept. Figure 2-1 illustrates these two concepts. A description of these concepts follows, including characteristics and supporting structural analysis.

### 2.1 ARTICULATED FOLDABLE TRUSS STRUCTURE/SOLAR ARRAY CONCEPT

The basic design is shown on Drawing 42662-4 (Appendix A). It is a constant 1-m-deep truss, 252 m long by 16 m wide. The length is divided into 63 bays of equal length (4 m) which can be stowed to occupy a cross-section of the orbiter bay, 2.35 m by 3.3 m (Figure 2-2). The folding arrangement is illustrated in Figure 2-3. The structural members are fabricated from epoxy-graphite rectangular tubing with aluminum end-fitting clevises. The sizing of these members for strength and for minimum natural frequency requirements is discussed in the Structural Analysis section.

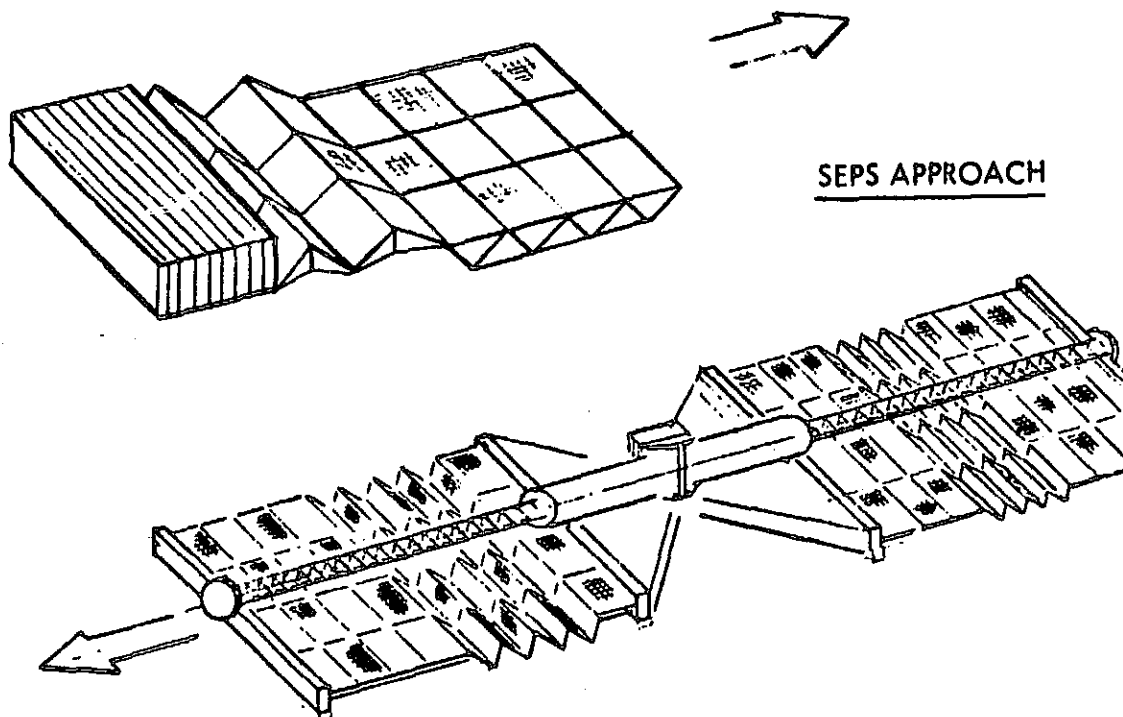
Two concepts for increasing the solar panel area of the basic design were developed: (1) an improved packaging concept, and (2) the addition of "wings" to the basic structure. Figure 2-4 illustrates these concepts.

#### 2.1.1 Improved Packaging

By using most of the available 4.57-m-diameter of the orbiter bay, an increased length and depth of the truss is achieved as shown on Dwg. 42662-28 (Appendix A). The 252 m length of the basic design increases to 391 m, and the depth of the center bay increases from 1 m to 1.77 m. It should be noted that this truss is double-tapered, i.e., the center bay is deeper than the two ends.

The solar array consists of 63 mechanical sections which vary in length from 4.296 m to 7.080 m. The width of all mechanical sections is the same. Depending on its length, each mechanical section contains either 8, 12, or 16 electrical panels. The electrical panels are adopted from the PEP Solar Array System as depicted in Lockheed Report LMSC-D665410 (NAS9-15595), and use the 5-year EOL value of 336.6 W of output power per panel.

## FOLDING PANEL APPROACH



### REQUIREMENTS

- >250 KW POWER
- SUB-ARRAY SWITCHING
- PACKAGABLE IN ORBITER BAY
- DEPLOY LEO
- SEP ORBIT TRANSFER

### DESIGN APPROACH

- SILICON SOLAR CELL BLANKET
- 240 V POWER TO INTERFACE
- FLAT ELECTRICAL CONDUCTORS
- PASSIVE HEAT REJECTION

Figure 2-1 Deployable Solar Array Concepts

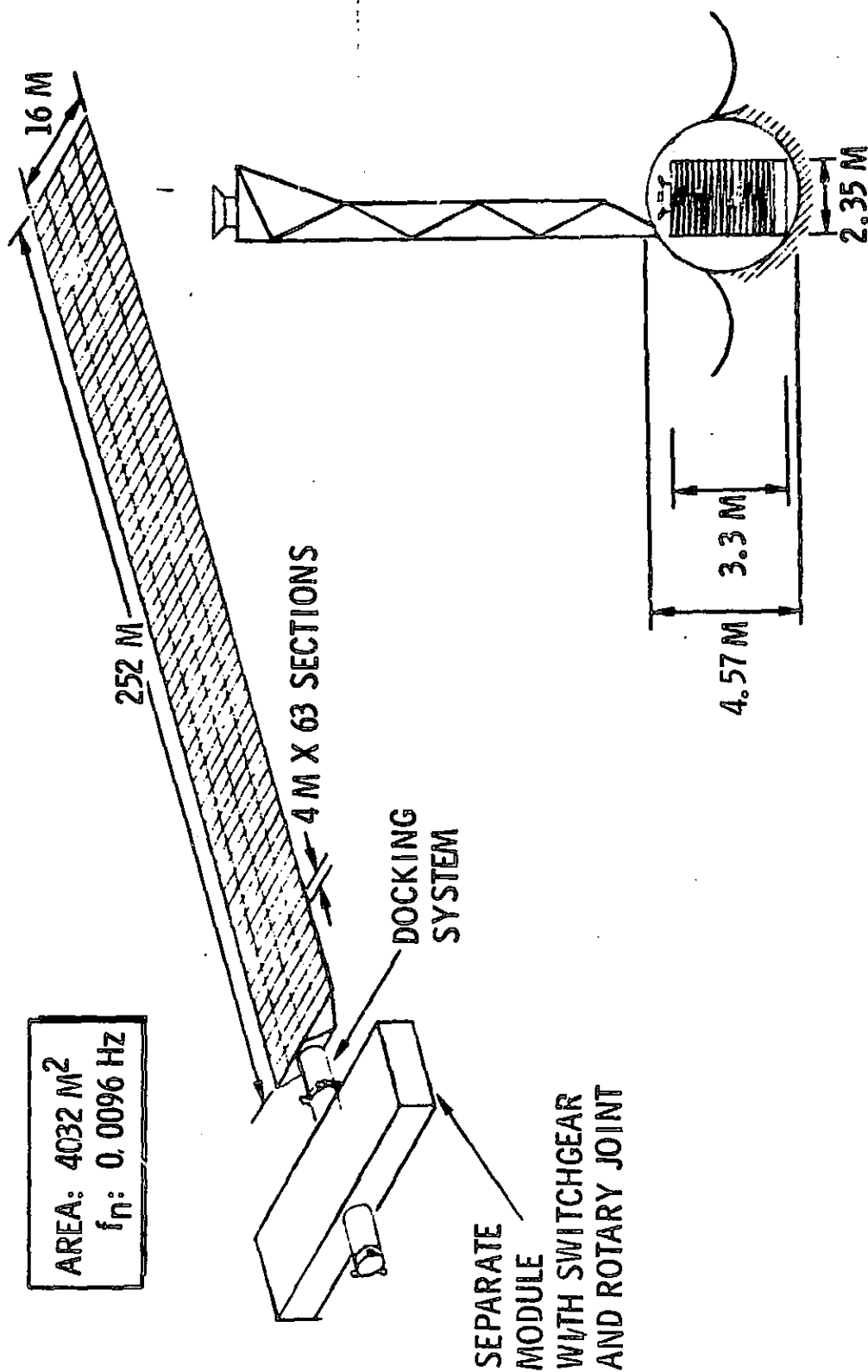


Figure 2-2 Folding Panel Concept

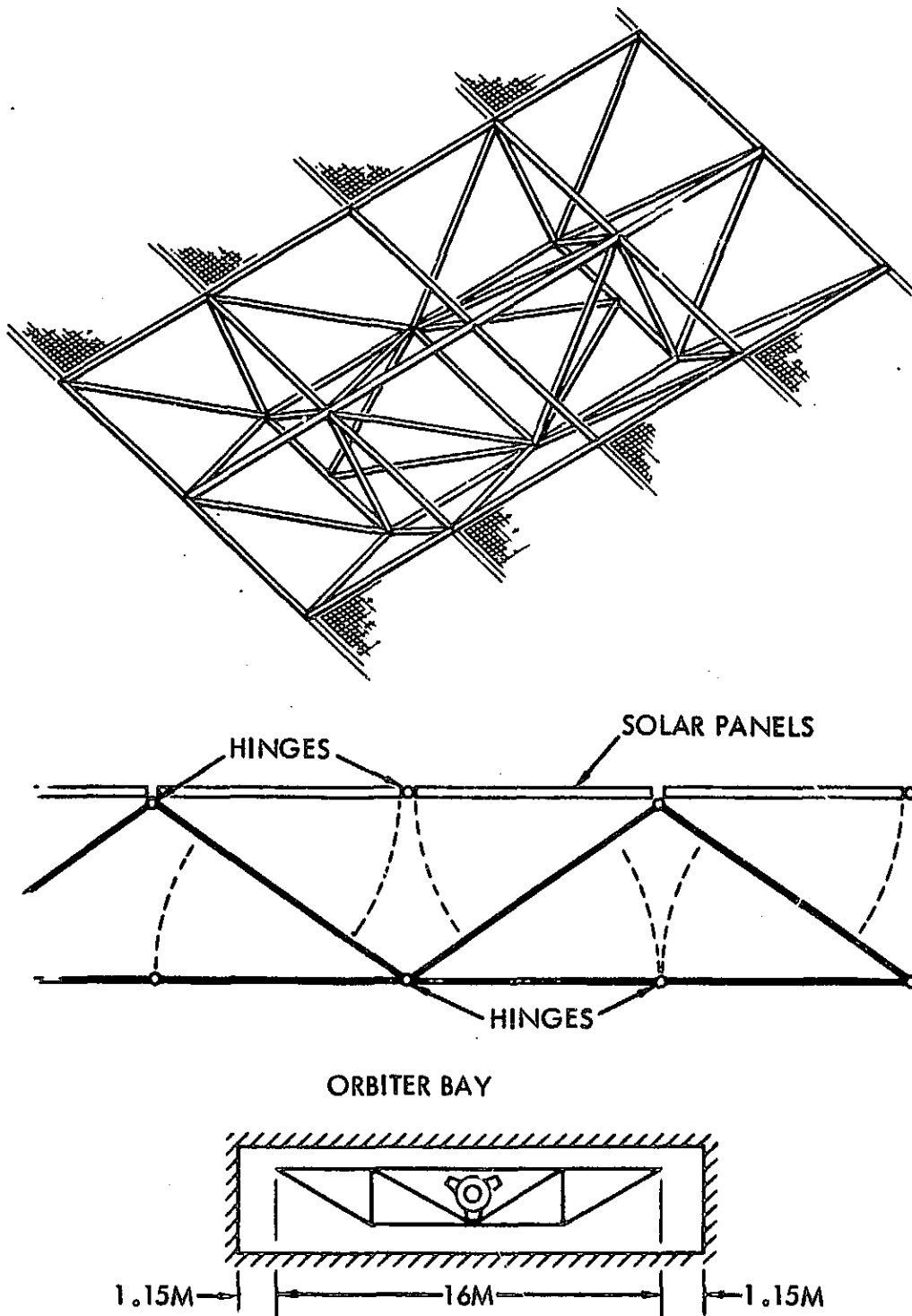
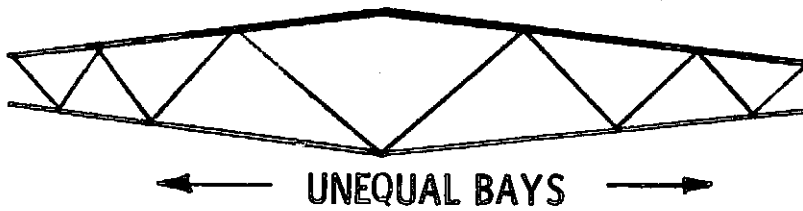
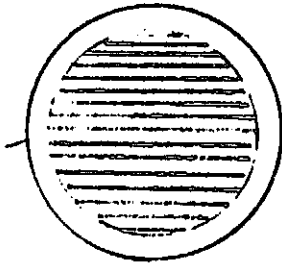


Figure 2-3 Structural Folding Concept

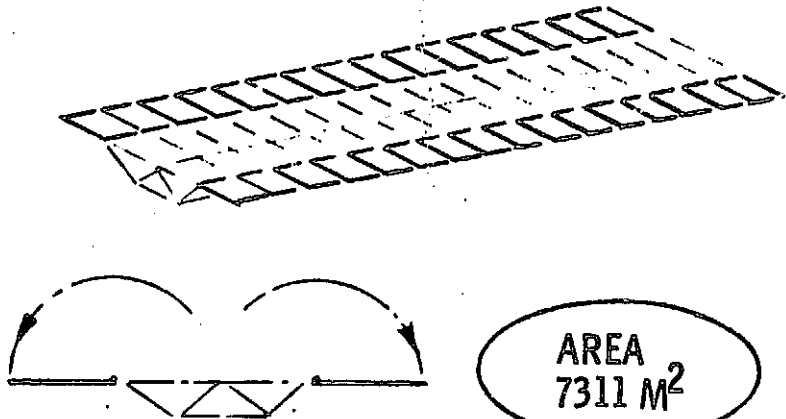
BASIC WITH IMPROVED PACKAGING



AREA  
6256 M<sup>2</sup>

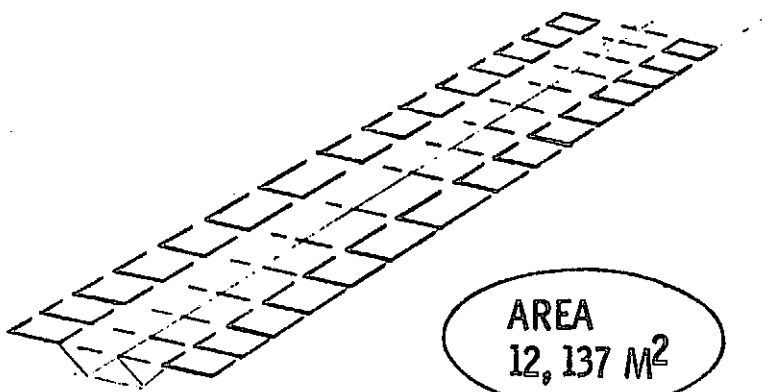


BASIC WITH "WINGS" ADDED



AREA  
7311 M<sup>2</sup>

WITH IMPROVED PACKAGING AND "WINGS"



AREA  
12,137 M<sup>2</sup>

Figure 2-4 Variations on Panel Concept

A 240-V base output voltage at a transmission efficiency of  $\eta = 0.96$  was used for this exercise. By series-parallel connections of the panels, a variety of voltages may be obtained. A flat cable conductor consisting of 3-mil-thick aluminum (6101-T6) encapsulated with one-mil Kapton using a 1-mil thickness of high-temperature polyester adhesive was used for the array harness. A variation of the conductor width provides a nearly constant voltage drop in each conductor.

Conductors are mounted on the back of the array and are routed longitudinally to the base of the array. Multiple paths may be used so as to minimize the thickness of the layer buildup and be compatible with the fold mechanism. More than two conductors may be brought from each panel if multiple voltages are required. Figure 2-5 illustrates the conductor routing scheme. Conductor mass was calculated at 65°C. Conductor temperatures were determined by thermal analysis based on location and current flow. The equation used for calculating the conductor size is:

$$A = \frac{\gamma I \ell}{\Delta V} ;$$

the equation used for calculating the conductor mass is:

$$W = \rho A \ell ;$$

where

A = Cross-sectional area

I = Amperes flowing in circuit

$\gamma$  = Resistivity of wire ( $2.828 \times 10^{-6} \Omega/\text{cm}$  for Al at 20°C)

$\ell$  = Length of conductor

V = Voltage drop in conductor

W = Conductor mass

$\rho$  = Density of aluminum ( $2.7 \text{ gm/cm}^3$ )

The conductor resistivity as a function of temperature is

$$\gamma = \gamma_0 [1 + 0.0039 \Omega/\text{cm} (T - T_0)] .$$

It may be seen that the mass of the conductor varies as  $\ell^2$ .

Conductors will be terminated in connectors at the base of the array. These connectors will tie across the docking ports into the switch gear module. The switch gear will series-parallel panel leads together to obtain various voltages and power levels as required. Circuit protective devices will be located in the switch box to protect the array from shorts and ground which may result in catastrophic effects. Power regulators will be provided to condition the power. These switch boxes will feed into a power distribution box where the user may readily tie into the power as desired.



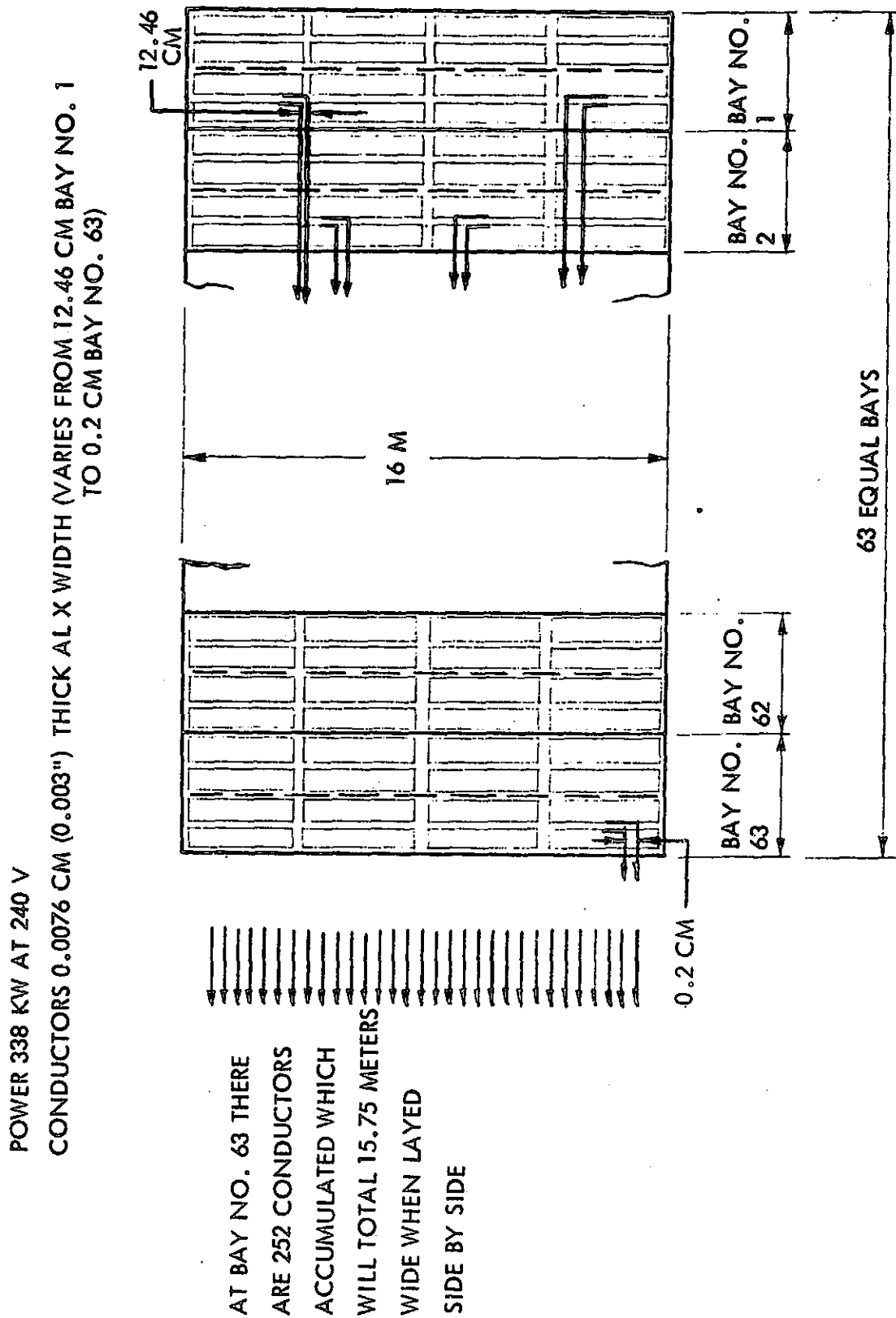


Figure 2-5 Conductors and Routing  
for Basic Array

### 2.1.2 Wings

The "wings" shown on Drawing 42662-28\* can double the effective area of a solar array without adding to the stowed volume envelope. The wings can be folded within the 16-m width of the main solar array truss. Each wing is attached to the longerons or main horizontal members by a hinge which can be a series of clevises, or a continuous piano hinge. Edge members are used to stiffen the wing and each consists of a spring-loaded member which is held flat against the wing until deployment is initiated. The wings can be deployed in one of two fashions:

- Deploy the entire main framework first and then release the wings by pulling a lanyard. The wings are deployed by springs.
- The main framework is deployed section by section from the orbiter bay. The wings can be unfolded one by one as each section of the frame is deployed and erected. Each wing requires a catch or short lanyard to retain it in the folded position. It is possible that unfolding of the wing and locking it in the open position can be accomplished either by EVA or by the RMS.

### 2.1.3 Heat Rejection

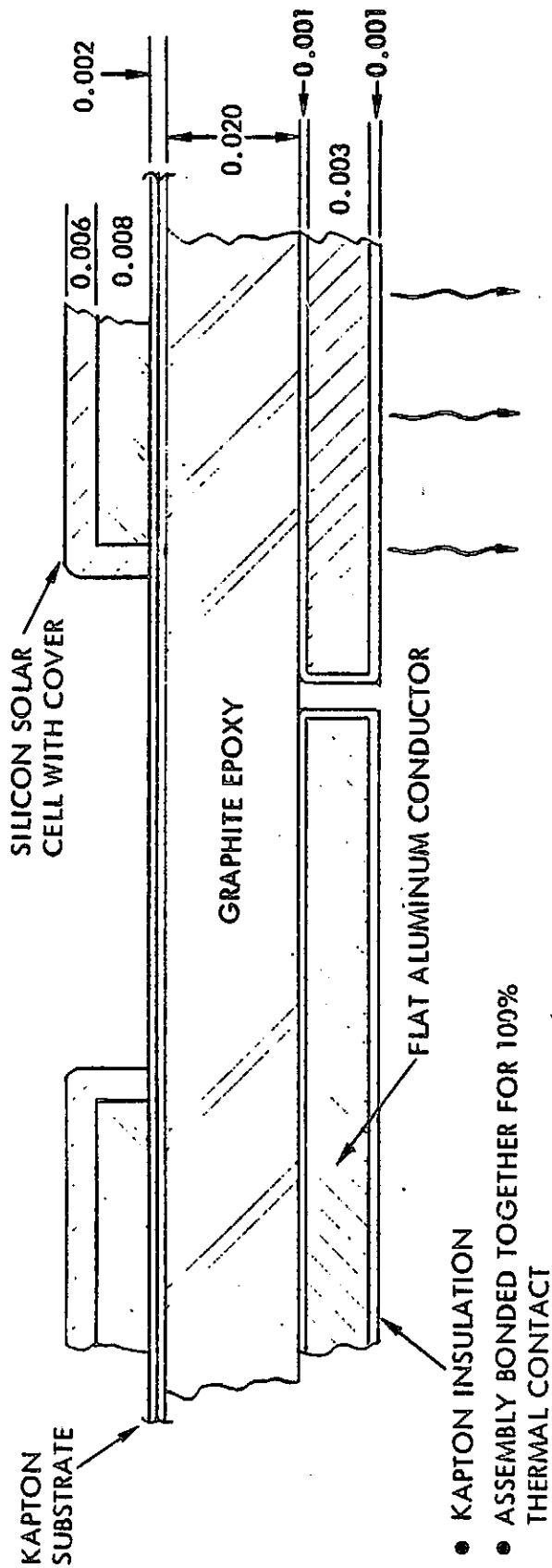
Due to the long length—391 meters—of this solar array and the conductor routing concept, the heat rejection from the solar cells is inhibited and the radiation heat rejection concept utilized in the SEPS panel concept is ineffective.

The solar panel of the Lockheed-developed SEPS consists of solar cells mounted on a substrate which, in turn, is bonded to a stiffener grid/panel. The grid/panel is 0.41mm thick and is 95% open grid. The solar cells are thus able to reject heat by radiation through the open grid. The conductors are relatively narrow and are mounted to one side of the panel. However, when the array length is substantially increased, the conductors pose a problem because of their increased cross-section. It is desirable to spread the conductors in a wide thin pattern over the backside of the stiffener to permit the panels to package in a "closely stacked" pattern. When this is done, the solar cells can no longer radiate through the open grid because the assembly of substrate-grid-conductor forms a good thermal insulator. However, by replacing the open grid/panel with a solid 0.51mm panel the solar cells can reject heat by conduction. Figure 2-6 illustrates this arrangement. The temperature gradients across the solar array assembly, the temperature of the solar cells, and their corresponding efficiencies are indicated. The 252-m equal bay truss without wings corresponds to the one-conductor case, and the large 391-m unequal bay truss with wings corresponds to the six-conductor case. The efficiency of the solar cell decreases from 11.45% for the no-conductor case to 10.25% for the six-conductor case.

The six-conductor is a worst-case condition which exists at one end only of the 391-m unequal bay truss with wings. The conductors beginning at the far end of the solar array are comparatively narrow and are stacked one deep.

---

\*See Appendix A



	$\Delta T$ ACROSS TOTAL THICKNESS °F	$\Delta T$ ACROSS GRAPHITE EPOXY °F	TEMP OF SOLAR CELL °F	EFFICIENCY OF SOLAR CELL
CROSS SECTION WITH NO CONDUCTORS	0.15	0.15	125	11.45%
WITH ONE LAYER OF CONDUCTOR	0.30	0.12	160.6	10.26%
WITH SIX LAYERS OF CONDUCTORS	1.01	0.12	160.8	10.25%

Figure 2-6 Heat Rejection Concept

The conductors accumulate to 15.75 m wide, stacked six deep at the power delivery end of the array (Figure 2-5); therefore, approximately 50% of the area of the solar array is covered by conductors.

#### 2.1.4 Electrical Power

Various amounts of electrical power can be generated, depending on the amount of available solar panel installation area utilized. Two methods of populating the available area with solar cells were considered:

- Using the Lockheed SEPS panel, which is 0.754 m by 4 m
- Filling all of the available area with solar cells

The areas and power obtained by combining the structural concepts, wing variations, and population methods are shown in Table 2-1.

Table 2-1 Area/Power Vs. Solar Panel Concept

	Populated with SEP Panels		Fully Populated	
	(m <sup>2</sup> )	(kW)	(m <sup>2</sup> )	(kW)
Basic truss, equal bays	4032	338	4032	447
Truss, unequal bays	6256	607	6256	694
Truss, equal bays with 100% wings	7311	676	8064	894
Truss, unequal bays with 100% wings	12137	1214	12512	1388
Truss, unequal bays with 50% wings	9196	910	9384	1041

#### 2.1.5 Center Mounting

A possibility which exists, but has not as yet been explored, is that of positioning the attachment between the solar array and the large space vehicle at the center of the solar array rather than at one end. Some of the advantages which might occur from this design are:

- Reduced electrical conductor length and, consequently, reduced cross-section and weight
- Reduced stack height of conductors because of the above, and because the solar array is divided into halves
- Increased stiffness of the truss
- Lower control torque
- Higher natural frequency of the truss

A typical design for center mounting is shown in Figure 2-7.

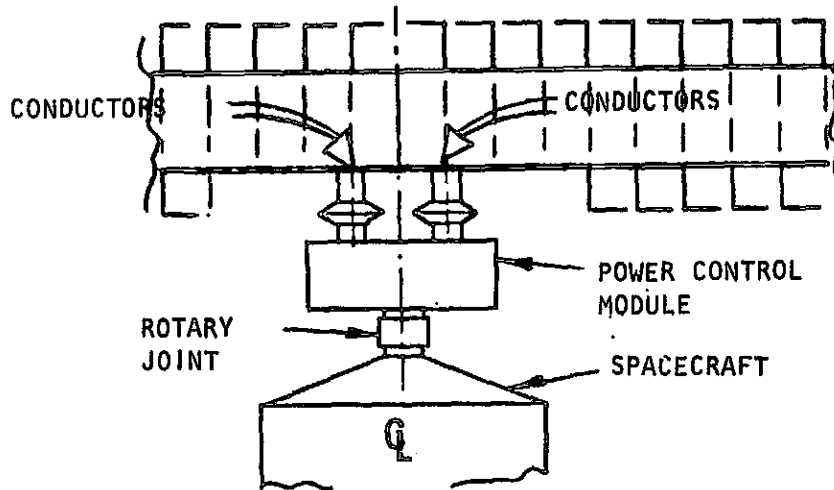


Figure 2-7 Center Mounting Arrangement

#### 2.1.6 Deployment from Orbiter Bay

No study was made of the equipment required to mount the solar array in, or to deploy it from, the orbiter bay. When stowed in the orbiter bay, the basic equal bay truss design leaves a reasonable margin on four sides for a deployment mechanism. The unequal bay truss, however, reaches to within 0.3 m of the orbiter bay diameter and only the two ends of the truss are accessible for a deployment mechanism (Figure 2-8).

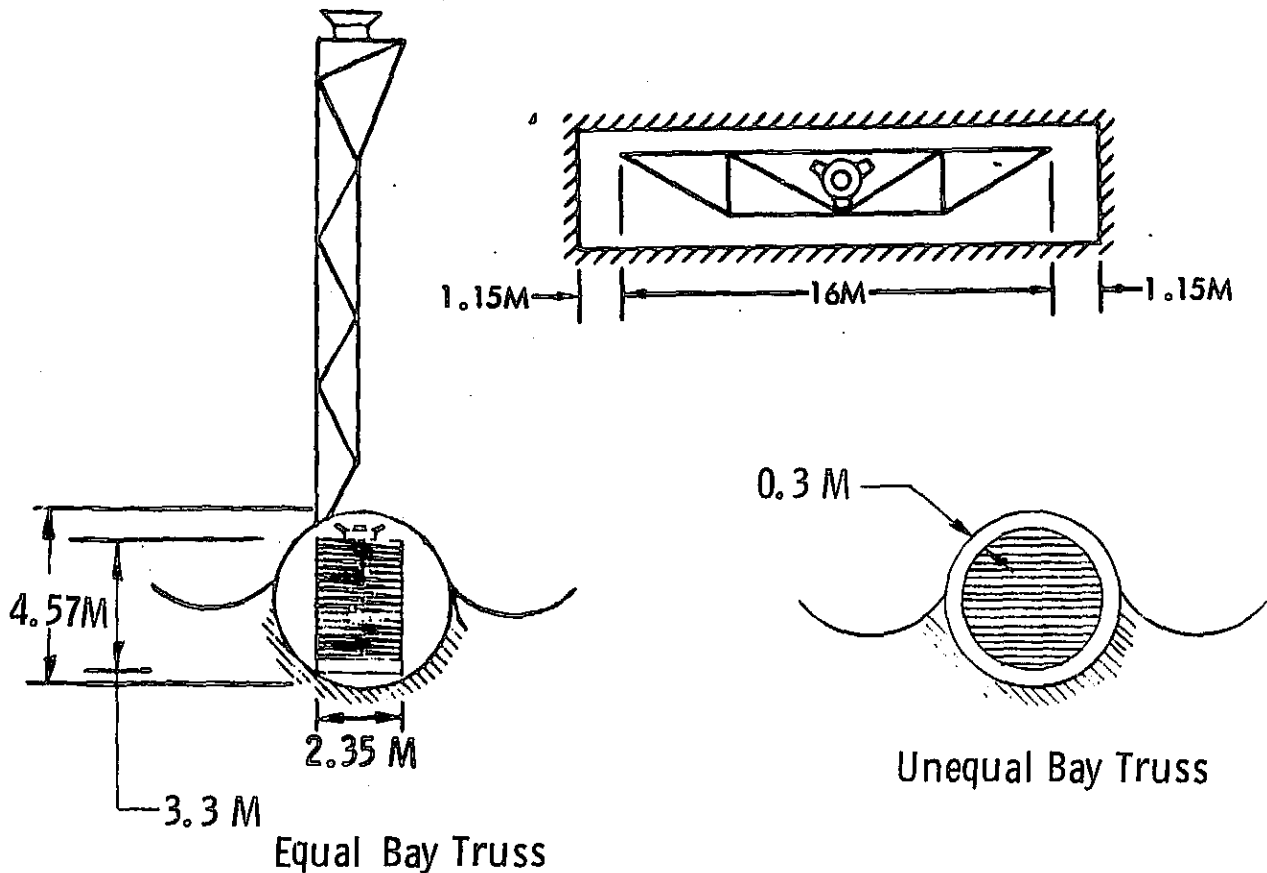


Figure 2-8 Orbiter Payload Bay Stowage Arrangement

A deployment mechanism would be required to perform the following functions:

- Retain the stowed truss in the "stacked" configuration after the orbiter doors are opened.
- Release the first layer of the stack.
- Erect the first bay and lock into shape (this might be done by the RMS and/or EVA).
- Move the stack up one notch and release the second layer, etc.

Figure 2-9 illustrates an automatic deployment concept. Concepts utilizing the orbiter RMS may also be applicable.

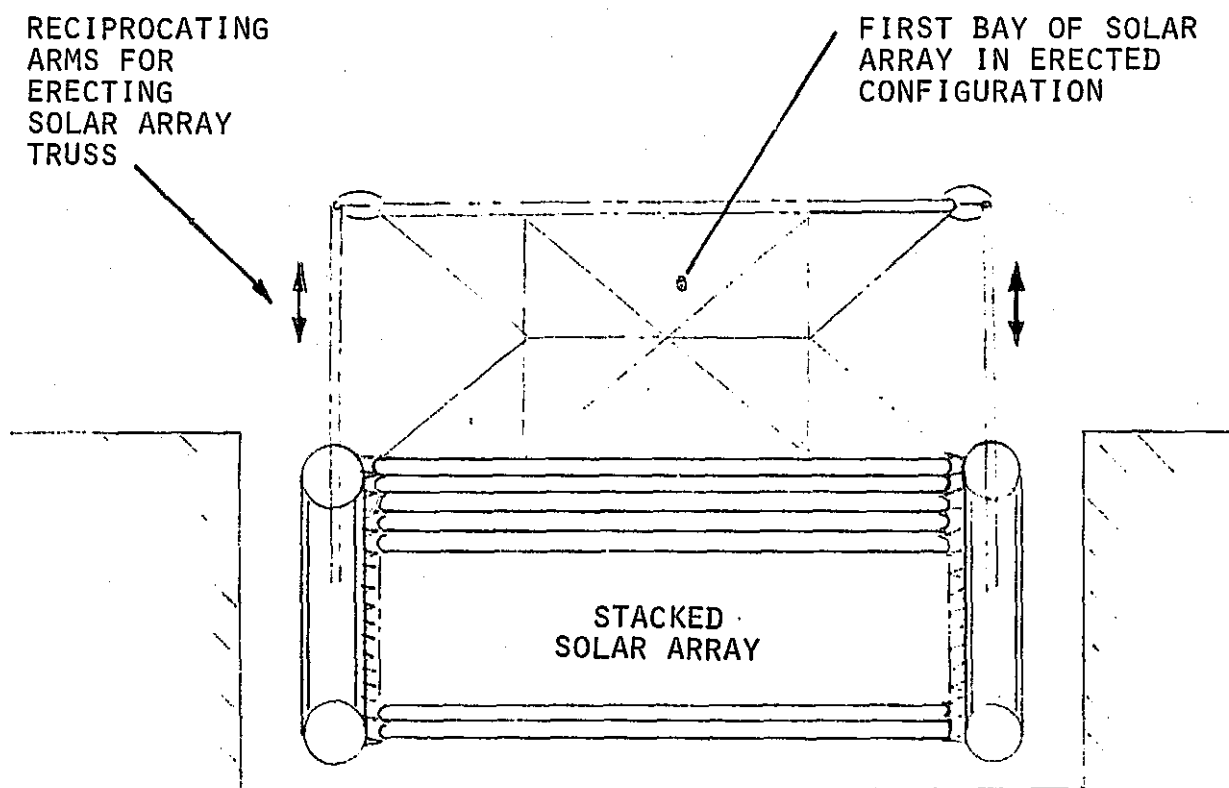


Figure 2-9 Deployment Mechanism Concept

#### 2.1.7 Orbiter Bay Packaging

In addition to the payload bay volume limits, the payload center of gravity (c.g.) also has limitations. Because the truss-type solar array concept is essentially a symmetrical arrangement, its c.g. will, therefore, be located in the center of the orbiter payload bay. This condition limits the payload weight

to 12,474 kg (27,500 lb). However, by providing 6345 kg (14,000 lb) of ballast at the aft bulkhead of the payload bay, a payload of 23,100 kg (51,000 lb) with its c.g. at the bay geometrical center will meet the limits of the orbiter c.g. envelope. Figure 2-10 illustrates this condition. Figure 2-11 illustrates the various solar array arrangements and their relationship to the maximum payload limit with no ballast and the maximum payload limit with ballast. It is necessary, however, to either jettison the ballast or to reposition it in the orbiter payload bay in order to remain within the orbiter landing c.g. limit.

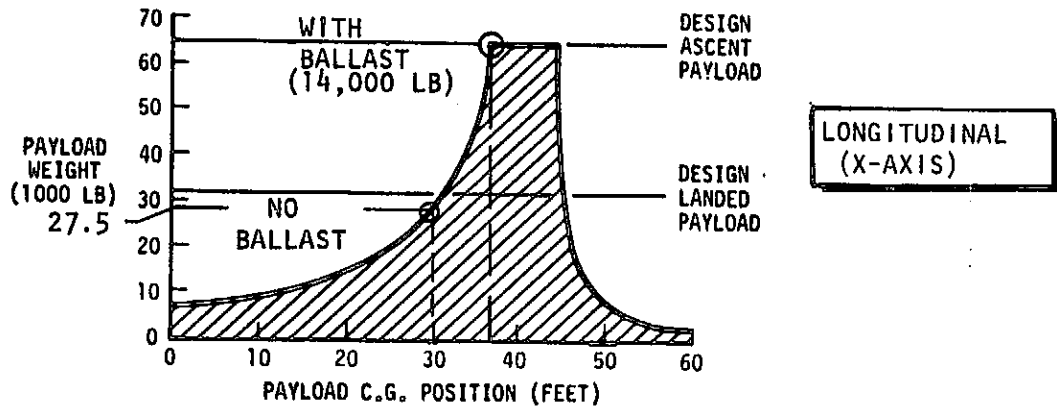


Figure 2-10 Orbiter Payload Bay C.G. Limitations

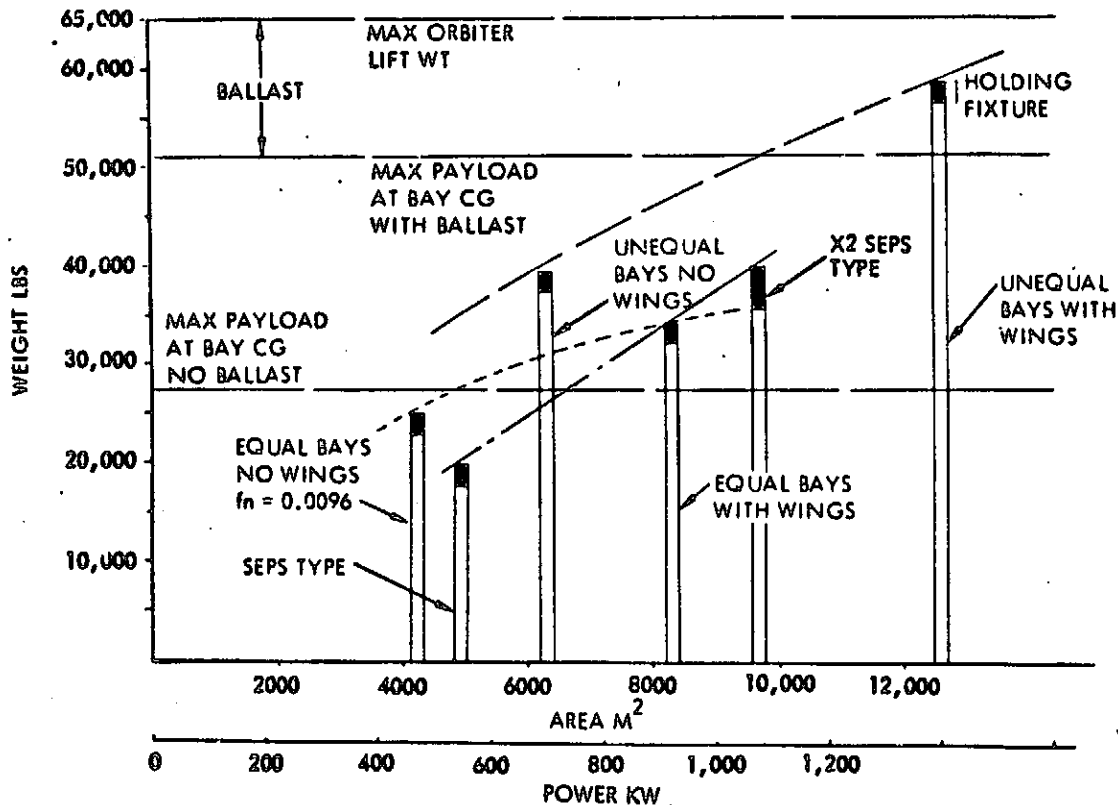


Figure 2-11 Solar Array Variations Vs. Payload Bay Limitations

## 2.1.8 Structural Analyses

### Introduction

The objective of the structural analyses was to support the preliminary design evaluation of the solar panel array described on Drawing 42662-28 (Appendix A) in regard to:

- Assessment of the basic concept feasibility.
- Determination of the solar array area that can be delivered into low earth orbit by the Shuttle as a function of the operational loading environment.

As a result of the conceptual reviews and the analyses (described herein), the basic structural concept of the supporting space truss, in regard to member arrangement, sizes, packageability, and structural suitability for the predicted load environments is regarded as quite feasible. It is, however, possible that the blanket panels may require a low level of pretension to mutually satisfy thermal isolation and blanket in-plane load stability requirements. The structural concept of the wings appears feasible but will require further study for assurance of feasibility of deployment, locking, and structural suitability.

Since the solar array area deliverable to orbit is directly related to the levels of loading to be imposed upon the array, the reduction of area as a function of the increased torsional or bending load factors is illustrated in Figure 2-12. The reduction of area is from the baseline design of 390x25.6m. The associated space truss structure weight variation is also shown in the figure.

### Configuration Description

Drawing 42662-28 (Appendix A) illustrates that the solar blanket array is supported by a space truss. Two typical bays of the truss are shown in further detail on Figure 2-13. The space truss is packaged by folding the typical planar trusses, such as that defined by nodes 1-4-6-9-12-10-7-3, about the hinge axes shown and by folding the longitudinal members and torsion-resistant bracing about the fold axes shown. The folded members are provided with self-locking hinges to provide moment continuity compatible with the required Euler column behavior. This space truss is, and has been, configured to be a statically determinate structure for the following significant reasons:

- There will be no thermal induced axial loads in the individual column members regardless of temperature differences between separate members (thermal stresses due to non-linear gradients across member depths can occur but are not significant).
- Complete deployment and rigidization of the truss will not be precluded by member length changes due to temperature or initial fabrication deviations. (Permissible deviations from array flatness will result, however).



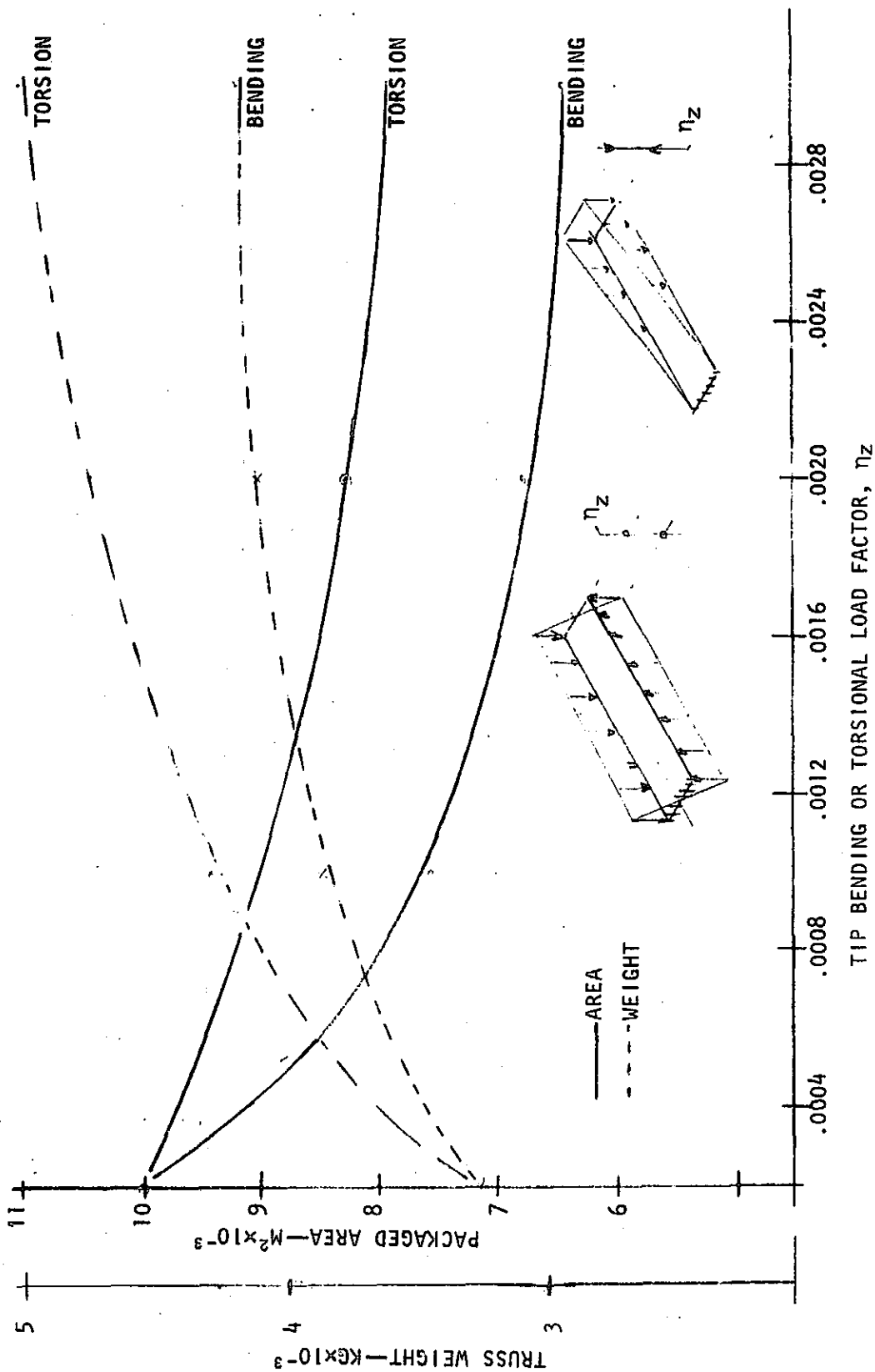


Figure 2-12 Deployable Solar Array—Area and Truss Structure Weight Vs. Load Factor

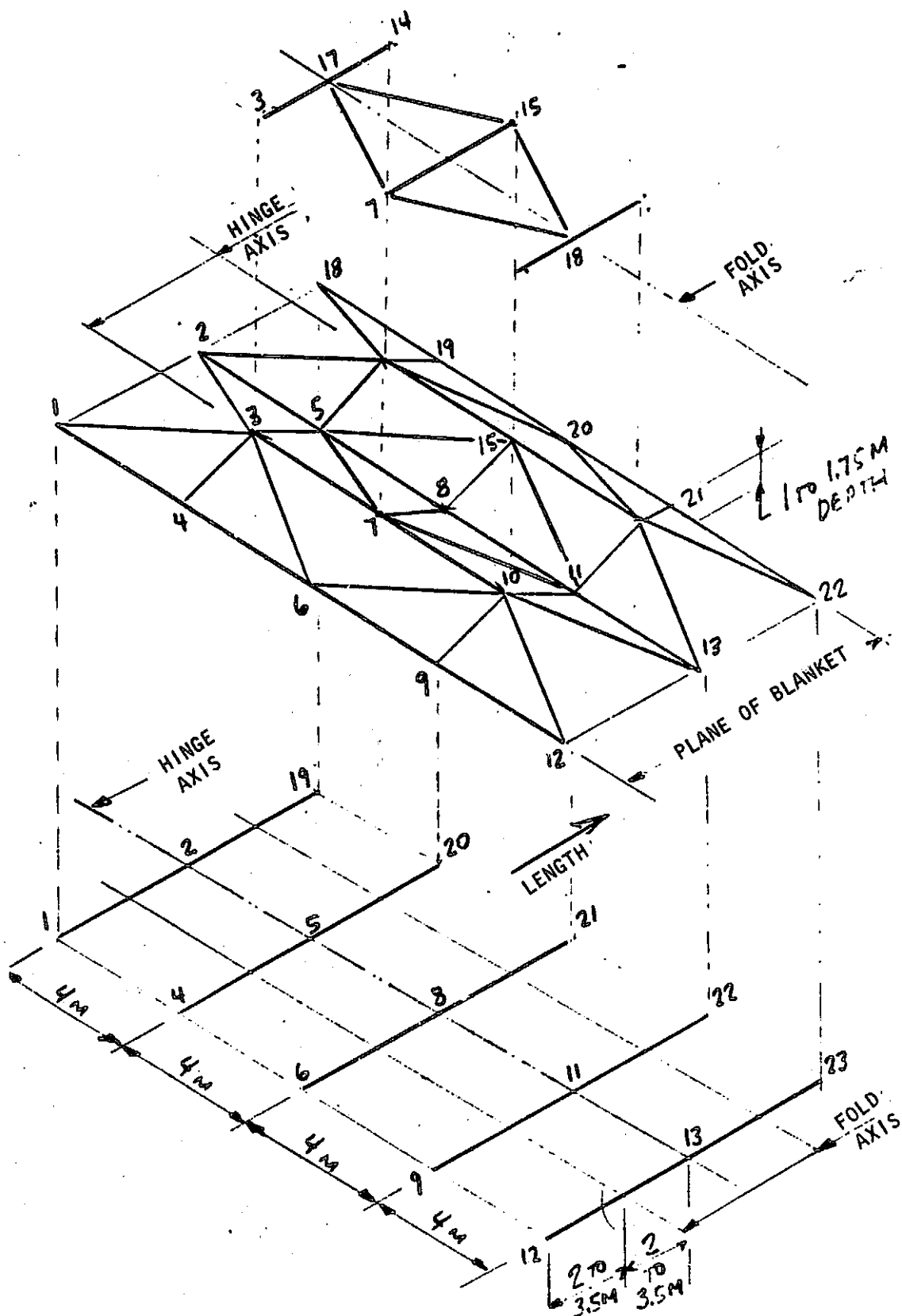


Figure 2-13 Solar Array Truss Configuration

It is pertinent to note that in view of the foregoing, the confidence in the predicted primary loads environment is independent of thermal distribution predictions.

The interior solar blanket panels are supported by the five longitudinal members shown in Figure 2-13. The attachments between the solar blanket and the five longerons will provide free relative thermal contraction/expansion of the blanket, but maintain adequate support for the blanket. A low-level ( 8.76 N/m ) tension spring system may be utilized.

The basic wing structure blanket is supported by ribs cantilevered from the basic truss framework and ties into planar truss members at typical nodes such as 1-4-6-9-12 as shown on Figure 2-13.

It is worth noting that deployment of this structure will be such that rigidization of each bay is achieved in a suitable fixture before it is extended outward. The fixture will provide sufficient support so that the extended structure is adequately supported.

#### Structural Requirements

The following structural requirements were considered in the structural review and/or analyses pertaining to this solar array. The structure shall survive, with no detrimental deformation, the following conditions:

- Ground handling, shipping, and installation into the Shuttle cargo bay.
- The Shuttle launch vibration and steady-state acceleration loads imposed upon the packaged configuration.
- The loads incurred from initiation of deployment through final securement of the last bay. These loads include atmospheric drag, solar pressure, and gravity-gradient torques.
- The stresses resulting from non-linear temperature gradients across the individual members, and the secondary stresses due to thermal gradient induced deflections.
- The loads induced by linear and rotational accelerations applied to the entire solar panel array.

For this feasibility study, the solar panel array has been assumed to be cantilevered from a large space structure system. The c.g. of the entire system was assumed to be at the solar array support. The load factors were varied according to the parametric analyses described herein and include  $\eta_z$  directed as shown in Figure 2-12, and  $\eta_x$  the longitudinal compression factor.

The structure shall survive the following additional requirements:

- Control System Requirement. It is highly desirable that the minimum modal frequency (from the study of the SPS test article configuration) should be no less than 0.0040 Hz. The exact value of 0.0040 Hz is not regarded as a non-yielding requirement; however, the minimum modal frequency will be maintained in proximity to that value.
- Dimensional Stability. The solar array is to maintain orientation within  $9^\circ$  of the sun despite the thermal gradients across the solar blankets and inertia loads applied normal to the plane of the array.

### Analysis Methodology

The analysis methodology applied to determine the data shown in Figure 2-12 and to establish the feasibility of this solar panel array is contained herein. These analyses were based on the following assumptions:

- Adequate care will be exercised in the fabrication, ground handling and shipping of the solar panel array for either the discrete parts and/or the total packaged assembly.
- A compact packaging arrangement during Shuttle launch to preclude damage due to mechanical vibration and steady-state acceleration loads.
- Deployment at a controlled rate, by a suitable fixture, that will limit deployment loads due to rate of extension. Further, the fixture design itself should not impose loads in excess of the basic structure capability. The deployment loads, of course, must be sustained concurrent with the particular gravity gradient or atmospheric drag loads.
- Careful design of the hinges so that local moments due to friction are limited to less than one pound inch, yet joint tightness (no slop) is maintained.

The specific analyses performed on the space truss, and interior panel blankets are described below.

Space Truss Analysis. As stated previously, the individual members of this space truss will not experience axial loads due to temperature differences throughout this statically determinate structure. This phenomenon is documented in Reference 1, and has been verified for this particular structure by thermal analyses using NASTRAN. The NASTRAN model is as shown in Figure 2-13. Temperature differentials were separately imposed upon members 1-2, 3-17, and 17-14, 15-17, 5-8, 9-11, and 4-6. Prior to the NASTRAN run, static determinacy was verified by a bar member and joint count.

The loads imposed by unit inertial loads for Cases 1, 2, and 3 for the member groups shown in Figure 2-14 are tabulated in Table 2-2. It is pertinent to note the member arrangement of Figure 2-14 is the earlier member arrangement, and differs slightly from that of Figure 2-13. The difference is negligible to the trend data generated.

A total uniformly distributed weight of  $2.27 \text{ kg/m}^2$  was used throughout the analysis. This is conservative since the conductor and structure weight are highest at the support base. Consistent with the aforementioned weight, the wing cantilever has been limited to 4.8 m (subsequent to Dwg. 42662-28 preparation) to be compatible with the cargo weight limitation of approximately 23,045 kg (50,700 lb). The baseline array is, therefore,  $390 \times 25.6$  meters. (The structural desirability of limiting the wing cantilever is also quite pertinent.)

The unit loading data were applied to several discrete load cases to determine the data shown in Figure 2-12. The data were proportionately adjusted to account for unit load changes due to array length changes. Table 2-3 is a typical example of the tabulated data for a  $7600\text{-m}^2$  array ( $25.6 \times 297 \text{ m}$ ) which is good for the following concurrent load factors:

- Axial compression  $\eta_x = 0.001$
- Rotational acceleration  $\eta_z = 0.0002$
- Bending acceleration  $\eta_z = 0.0010$

The results of the other data points, performed in a similar manner, are shown in Table 2-4. In all cases, the effects of gravity gradient, and drag-induced bending moments and shears were absorbed within the conservatism of the distributed load. The individual column sizes were determined for this parametric analysis as described below.

The limit capability of the columns was determined from the equation

$$P = \frac{\pi^2 EI}{\ell^2} \times \frac{1}{(1.5)^2}$$

where the two factors of 1.5 are the safety factor, and a factor to limit secondary bending. The limitation of secondary bending values is to preclude deleterious beam column magnification of moment and deflection due to eccentric application of axial load, thermal deflection, fabrication deviation, and in the case of the members supporting the solar panel blanket, the  $\eta_z$  induced vertical deflection. An example from Table 2-3 is illustrated as follows for the group (6) member shown in Figure 2-15, having an initial fabrication deviation from straightness  $s = 0.001 \times 4 = 4 \text{ mm}$  (0.16 in.). For this beam column, the parameter

$$u = \frac{\ell}{2} \sqrt{\frac{P}{EI}},$$

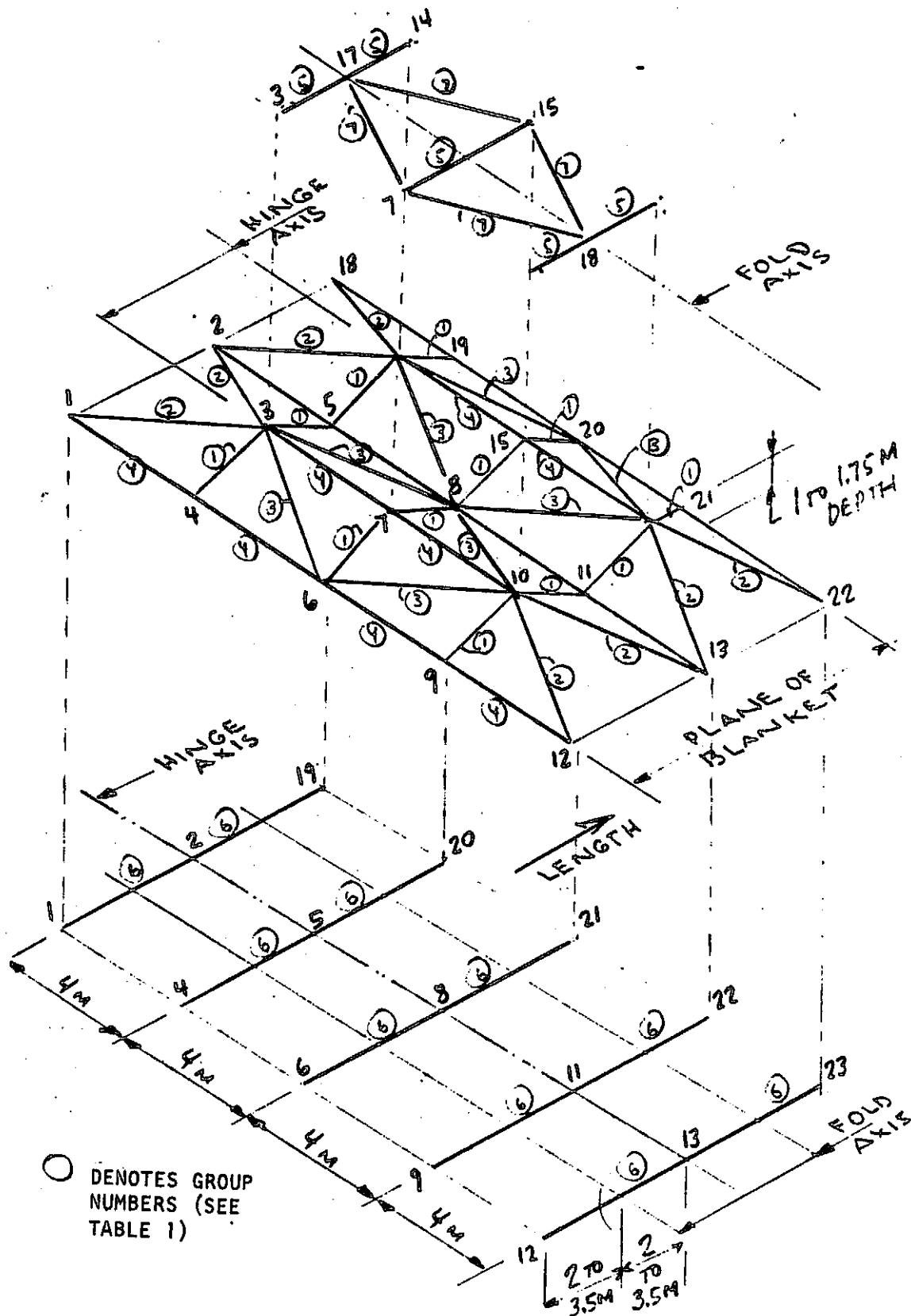


Figure 2-14, Solar Array Truss Configuration (for Sizing)

Table 2-2 Member Axial Compression Loads (N) for Axial Compression, Torque,  
Bending Moment Load Factors  
(390 m x 25.6 m Design)

Group Members*	Location/ Configuration	Bending Load Factor = 0.001 g	Axial Load Factor = 0.0001 g	Torsion Load Factor = 0.0001 g
1	At support	0.	0	5.3
2	Depth is 1 meter	16.9	0	43.0
3	Bay length is 4 m	8.5	0	151.3
4		14.7	0	37.8
5		961.0	0	99.2
6		579.0	4.5	19.1
7		0.	0	217.2
1	At mid-span	0.	0	5.8
2	Depth is 1.75 m	16.9	0	15.6
3	Bay length is 7 m	8.5	0	54.7
4		11.1	0	10.7
5	Bay length is 7 m	171.3	0	47.6
6		102.4	2.3	9.4
7		0.	0	84.5
*Group members as shown in Figure 2-3.				

Table 2-3 Typical Design Data  
(25.6×297 m Array-Bending Load Factor = 0.0010)

Group	Location	Limit* Compress Load (N)	Member Length (m)	Rectangular Tube Sizes (cm)
1	Tip	Negl.	2.2	1.59×1.59×.064
	Mid	Negl.	4.1	2.38×2.38×.064
	Support	Negl.	2.2	1.59×1.59×.064
2	Tip	Negl.	4.5	2.38×2.38×.064
	Mid	134	5.7	2.38×3.10×.081
	Support	155	4.5	2.38×2.38×.064
3	Tip	Negl.	4.5	2.38×2.38×.064
	Mid	101	5.7	2.38×3.20×.064
	Support	172	4.5	2.38×3.20×.064
4	Tip	Negl.	4.0	1.59×1.59×.064
	Mid	89	4.0	2.38×2.38×.064
	Support	134	4.0	2.38×2.38×.064
5	Tip	Negl.	4.0	1.90×1.90×.24
	Mid	992	7.0	2.7×10.8×.24
	Support	5638.	4.0	2.7×11.6×.53
6	Tip	Negl.	4.0	1.9×1.9×.064
	Mid	601	7.0	2.7×5.4×.30
	Support	3370	4.0	2.7×10.8×.27
7	Tip	0	4.5	2.38×2.38×.064
	Mid	62	5.3	2.38×2.38×.064
	Support	114	4.5	2.38×2.38×.064
*Minimum strength is 100 N (22.5 lb) limit load. Torsion load factor = .0002, axial load factor = 0.001				



Table 2-4 Solar Array Candidate Design Characteristics

Case	Array Area Size (m×m)	Array Area Size (m <sup>2</sup> )	Truss Structure Weight (kg)	Vertical Bending Load Factor (g)	Torsion Load Factor (g)	Maximum Member Depth (mm)	Minimum Frequency (Hz)
1	390×25.6	9984	3260	0.0001	0.0002	19	0.0045
2	347×25.6	8883	4268	0.0001	0.0010	22	0.0057
3	328×25.6	8397	4768	0.0001	0.0020	24	0.0064
4	250×25.6	6400	5310	0.0001	0.010	33	>0.0064
5	328×25.6	8397	3677	0.0005	0.0002	24	>0.0045
6	297×25.6	7600	3860	0.0010	0.0002	27	>0.0045
7	390×16	6240	3440	0.00014	0.0005	19	0.0057
8	250×25.6	6400	4120	0.0030	0.0002	33	>0.020

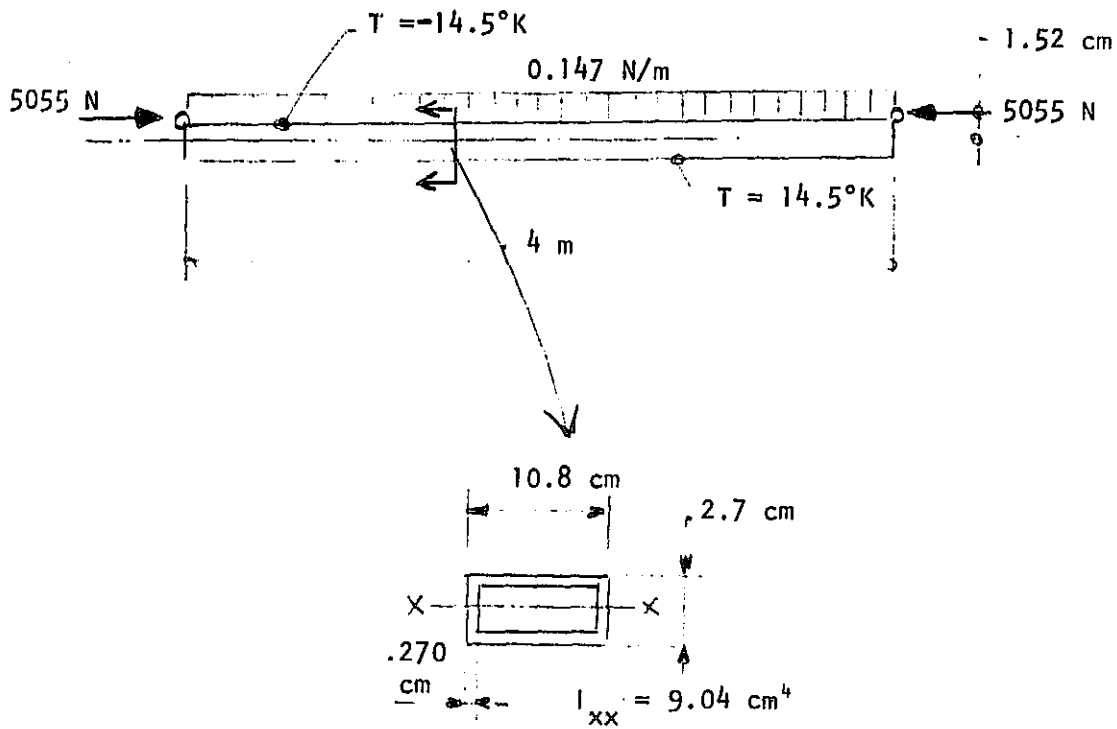


Figure 2-15 Typical Strut Loading

and for the ultimate load of 5055 N (1136 lb) = 1.273. Considering first the effect of just the eccentricity  $e = 1.52$  cm (0.60 in.), the maximum ultimate moment at the center of the span =  $5055 \times 1.52 / \cos u = 262$  Nm (2323 lb-in.), and the total axial and bending induced ultimate compressive stress =  $46.4 \times 10^6$  N/m<sup>2</sup> (6718 psi). The local buckling capability from  $3.0 E(t/b)^2$  is much greater. The bending moment and deflection due to the uniform load (without the axial loading) is negligible. The moment due to the axial load and thermal induced deflection is determined from  $92.8 / \cos u - 92.8 = 224$  Nm (1979 lb-in.). The effect of initial straightness is negligible by comparison. It is apparent the combined thermal and axial load induced stresses are acceptable.

### 2.1.8 Interior Solar Panel Analysis

The following survey analyses were performed to verify the feasibility of the basic solar blanket design.

The peak transverse inertial loading for the 4-m span is 0.0663 N/m<sup>2</sup>. For a panel partially fixed (the panels span across the longerons), the maximum ultimate moment is 0.0034 Nm (0.030 lb-in.) and the maximum stress (0.5 mm thick graphite-epoxy laminate) is  $3.1 \times 10^6$  N/m<sup>2</sup> (450 psi), which is acceptable. The maximum limit deflection would be 4.8 cm (1.9 in.) which is 1.2% of the span and is not representative of deleterious panel rotation. However, unquestionably, a small pretension would reduce the peak deflection. An alternate means of stiffening the panel (if necessary) would be to place 1.5-mm-deep stiffeners parallel and between the conductors.

Figure 2-6 illustrates a typical section through the solar panel blanket. Thermal analyses indicate the peak gradient across the section to be 65°K (1.12°F). The peak angle due to the "bi-metallic" behavior (for an unconstrained 4-m-long span) is 1.4 degrees and not deleterious.

The peak in-plane inertial loading has been limited to 0.001 g (with solar electric power, values of 0.0001 are appropriate). For this loading, the 1.5-mm-deep stiffeners are very beneficial. The allowable limit load per meter =

$$\frac{4\pi^2 E}{12(1-u^2)} (t/b)^2 \times t \times \frac{1}{1.5} \times \frac{1}{5}$$

where 1.5 is the safety factor and 5 is an uncertainty factor to allow for eccentricities—thermal deflection, non-straightness, etc. Substituting  $I$  for  $t^3/12$ , the permissible load on the total 4-m-wide panel is 3.1 N (0.70 lb). The applied load is 0.62 N (0.14 lb). Here, too, the use of pretension appears desirable.

The feasibility of the wing structure is independent of the primary solar array concept previously discussed. The foregoing stands on its own. The rudimentary deflection and stress analyses have identified no obvious problems, but further effort would be required for an adequate level of confidence in the feasibility.

## 2.2 SOLAR ELECTRIC PROPULSION SYSTEM (SEPS) TYPE SOLAR ARRAY CONCEPT

This design concept is an expanded version of the Lockheed-developed SEPS solar array. The basic SEPS 4-m $\times$ 0.75-m solar panel is utilized. The configuration developed, that would be packageable within the orbiter bay, is illustrated in Figure 2-16. It consists of two masts, each extending 150 m from a central canister, with each mast deploying four solar blankets each 4 m wide by 150 m long. The total solar array area is 4800 m<sup>2</sup>.

### 2.2.1 Concept Variation

Two of these solar arrays can be packaged within the orbiter payload bay, providing the delivery to low earth orbit of 9600 m<sup>2</sup> of solar array. A variation of this concept, as illustrated in Figure 2-17, utilizes solar panels that exceed the 0.75-m SEPS panel dimension in order to develop a single solar array unit that will fill the orbiter bay. The deliverable area of this concept is antitipated to be less than 9600 m<sup>2</sup> because of the electrical conductor area and weight associated with this single large array.

The electrical conductor and routing issue is similar to that previously discussed for the articulated foldable truss concept. Figure 2-18 illustrates the conductor routing for a single 150-m solar array blanket. This arrangement would be repeated for each of the four blankets that constitute one side of the total solar array.

### 2.2.2 Heat Rejection

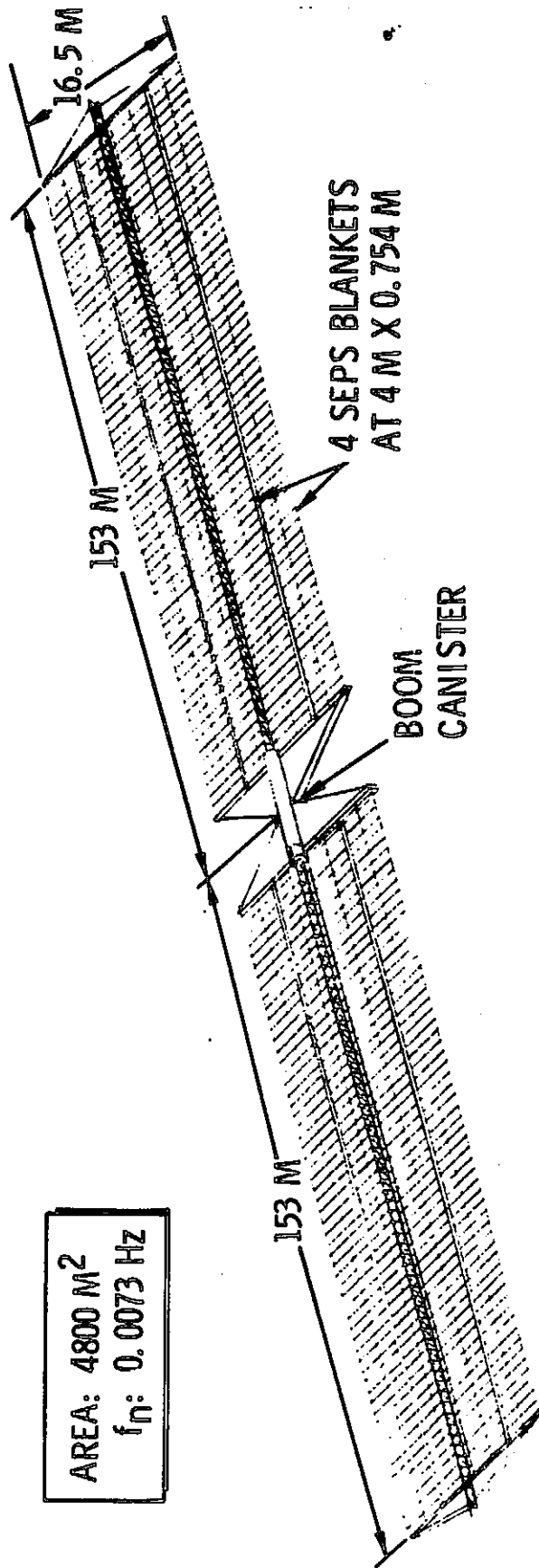
The heat rejection concept described for the articulated foldable solar array concept will also be applicable to the SEPS array concept, i.e., conduct the heat through the solar cell substrate, and through the electrical conductors bonded to the underside of the substrate.

### 2.2.3 Deployment Mast

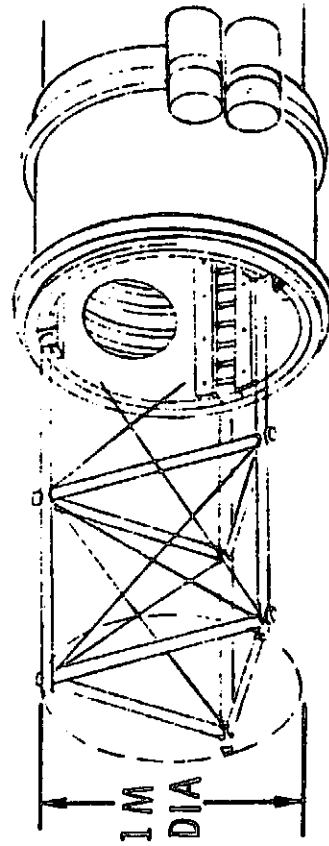
The length of the mast stowage canister for the 150-m deployment is 7.1 m. Consequently, these canisters must be rotated in relationship to their operating location in order to be packageable within the 4.57-m-diameter orbiter bay. Figure 2-19 illustrates a concept that achieves this relationship for orbiter payload bay packaging. The canisters are offset from each other and from the centerline of the solar array. The solar array blanket tension will be adjusted to create equal loads on the support beams, thus minimizing bending reactions on the mast. The Structural Analysis section will discuss this condition in further detail.

### 2.2.4 Total Power System

The thrust of this study was to determine the maximum solar array area that could be transported to LEO in a single launch, considering that the power controls, conditioning and storage subsystems would be delivered on other flights. However, it becomes apparent that the delivery of a total power system, including the solar arrays, controls and power storage, in a single launch would be

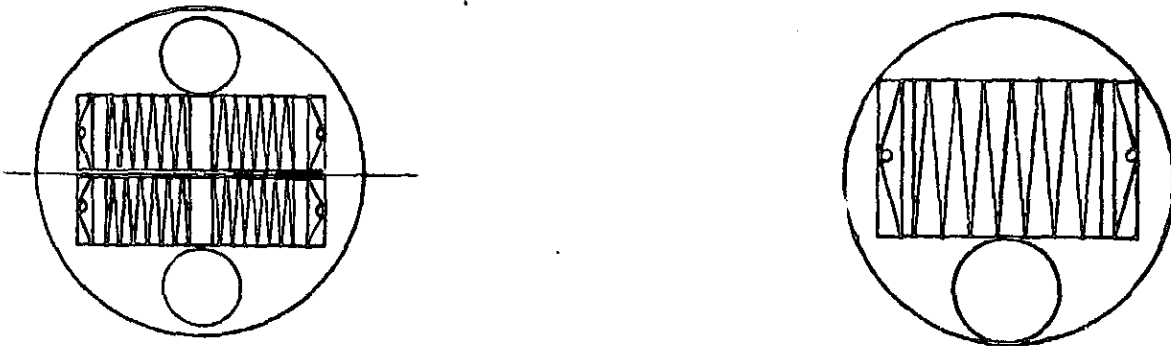


### BOOM DETAIL



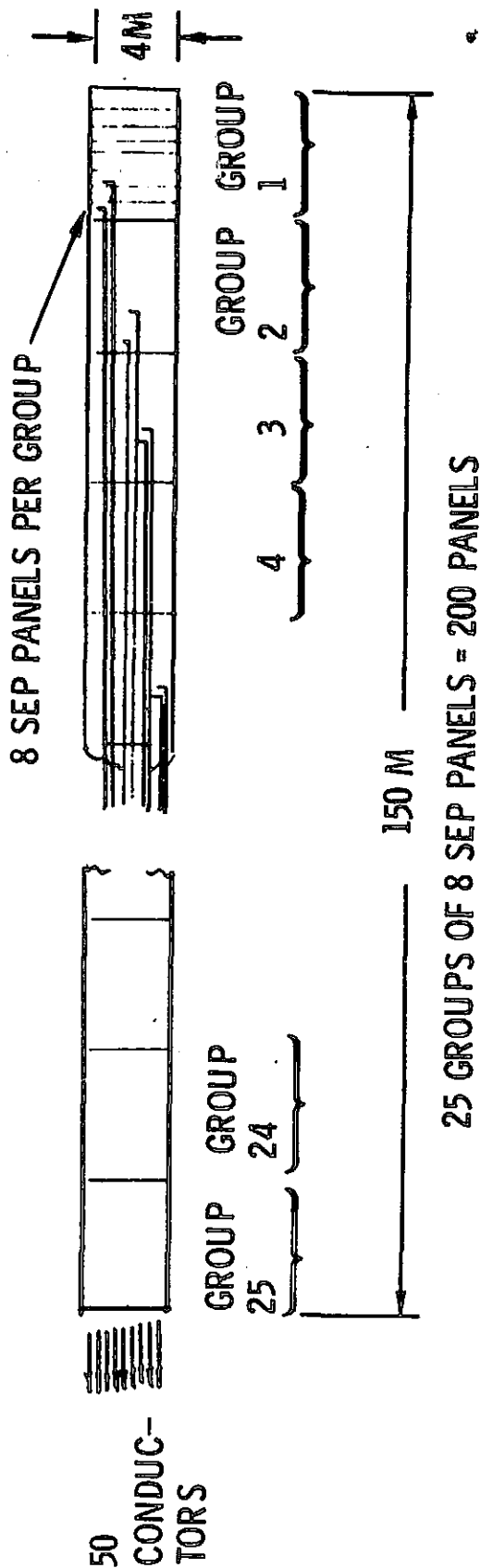
### PACKAGED IN ORBITER BAY

Figure 2-16 SEPS-Type Concept



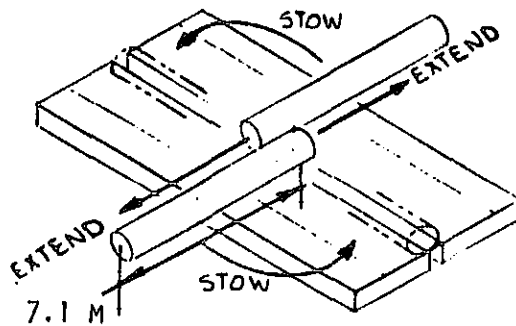
- PACKAGE TWO SEPS ASSYS IN ORBITER  
AREA =  $4800 \text{ M}^2 \times 2 = 9600 \text{ M}^2$
- DESIGN SEPS ARRAYS WITH PANEL  $> 0.754 \text{ M}$   
AREA  $< 9600 \text{ M}^2$  BECAUSE OF CONDUCTOR  
INCREASE IN WEIGHT AND CROSS SECTION

Figure 2-17 Options for SEPS Design

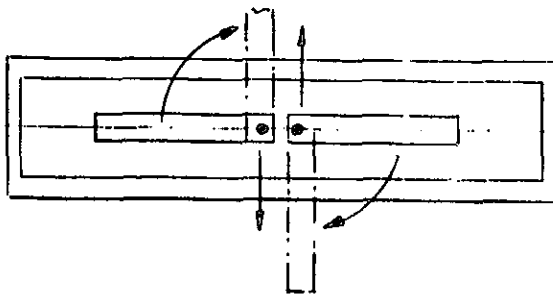


- 1 PAIR OF FLAT ELECTRICAL CONDUCTORS FROM EACH GROUP OF 8 PANELS
- TOTAL NUMBER OF CONDUCTORS = 50
- ALL CONDUCTORS 0.003" THICK ALUMINUM WITH 0.001" KAPTON INSULATION
- WIDTH OF EACH CONDUCTOR FROM GROUP 1 = 7.44 CM
- WIDTH OF ACCUMULATED CONDUCTORS (1 LAYER HIGH) AT GROUP 25 = 1.86 M
- CONDUCTORS BONDED TO BACK SIDE OF BLANKET

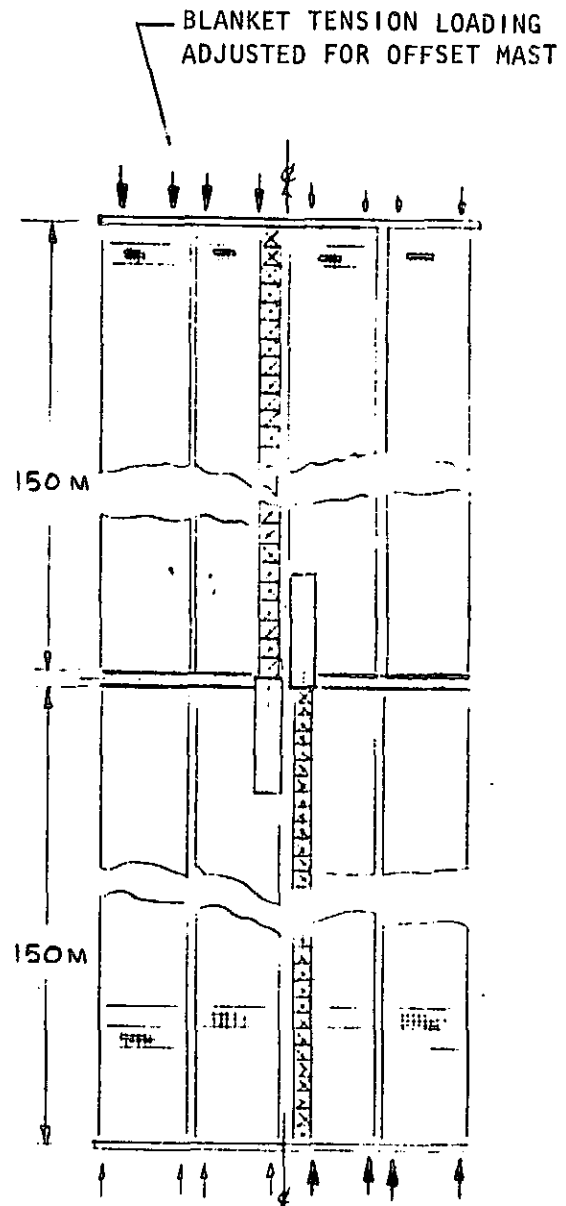
Figure 2-18 Conductors and Routing



MAST ROTATION CONCEPT



PAYLOAD BAY STOWAGE  
ARRANGEMENT



MAST/SOLAR ARRAY  
EXTENDED

Figure 2-19 Deployment Mast Arrangement  
Concept



desirable. Figure 2-20 defines the volume and weight limits of the orbiter payload bay for total power systems. The total power system for a 536-kW capability, which represents the basic SEPS concept illustrated in Figure 2-16, is indicated on Figure 2-20 and shows that this system is within the volume and weight capability of the orbiter, and could be delivered to LEO in a single launch.

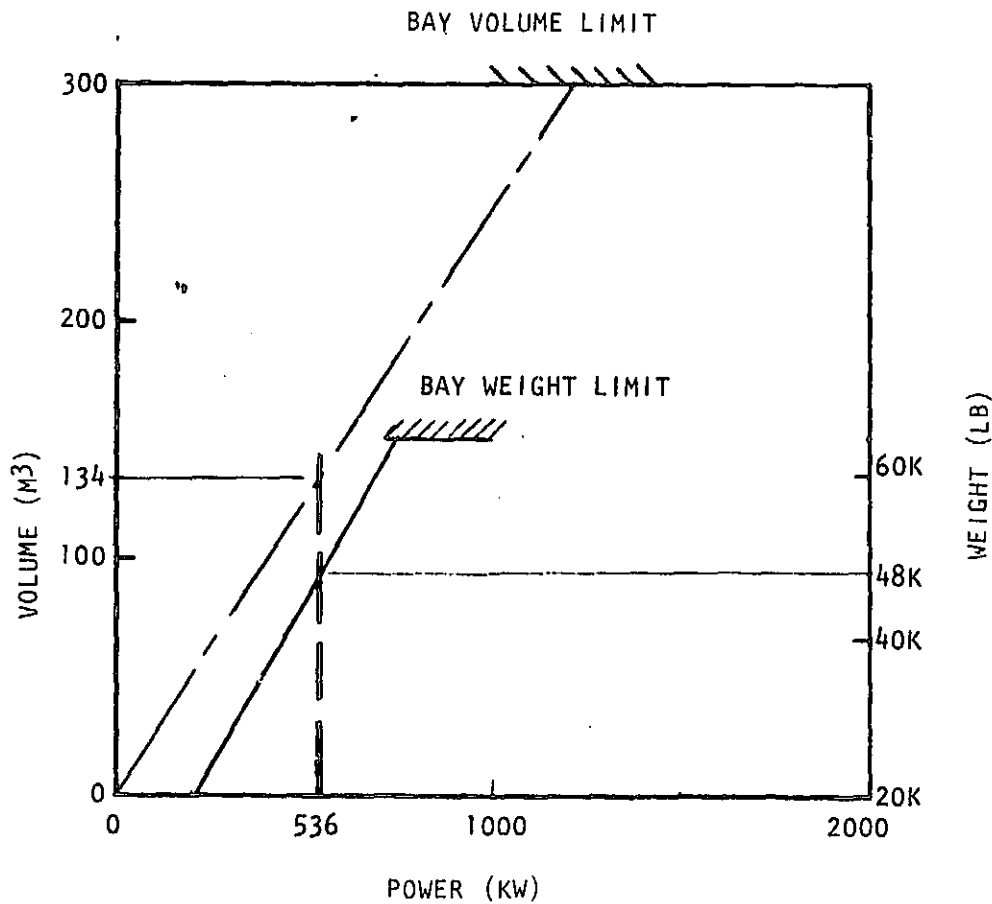


Figure 2-20 Total Power System Delivery Capability

## 2.2.5 Structural Analysis

### Introduction

This section describes the analysis performed to assess the structural feasibility of a large solar array (up to 4800 m<sup>2</sup>), constructed of SEPS panels (Figure 2-16) that are deployed, positioned, and pretensioned by an Astromast-type compression member. The structural requirements outlined in the deployable truss concept structural analysis section are all directly applicable, except for the minimum modal requirement of 0.0074 Hz. For this solar array, a minimum modal frequency of 20 times that of the frequency of earth orbital gravity-gradient disturbance torques are used. Similarly, the comments pertaining to adequate care during fabrication, adequate packaging into the Shuttle cargo bay, and controlled deployment are also directly applicable.

### Analysis

A review of the total system requirements indicated that the minimum modal frequency requirement was the most significant structural requirement. The combination of the axial compression loading (to pretension the SEPS arrays), including the moment due to the pretension offset and inertia loadings of the same character as that discussed previously, is provided by the high stiffness requirement.

Referring to Figure 2-16, the structural concept is that of a membrane (SEPS array) stretched between the extreme ends of the deployable compression boom. The combined structural system, comprised of a tension membrane and compression boom, must have a minimum modal frequency of 0.0074 Hz.

Since the primary purpose of this study was a comparison with the deployable space truss array (which was cantilevered from its end rather than supported at the middle), this concept was also analyzed as cantilevered from a spacecraft. The configuration shown on Figure 2-16 was analyzed as a 16-m array of varying lengths cantilevered from a spacecraft with the blanket spanning the total length. The significant reduction of required boom flexural rigidity, with support of the array at its center, is evident by comparison of the data for the designs of 300-m and 150-m long arrays that are shown in Table 2-5.

The data of Table 2-5 were determined as follows: To provide an overall minimum modal frequency of 0.0074 Hz for the combined system of stretched membrane and boom, Dunkerley's formula was used to define the separate minimum natural frequencies for each system. Hence

$$1/f^2 = 1/(f_{sb})^2 + (1/f_{boom})^2$$

where  $f$  is the overall natural frequency. A multitude of solutions satisfy this formula, with determination of the optimum being beyond the purposes of this study. For this study, a ratio of 2 to 1 was used, i.e.,  $f_{boom}/f_{sb} = 2.0$ . The required separate frequencies obtained were 0.0085 and 0.017 Hz for the blanket and boom, respectively.

Table 2-5 Deployment Mast Configurations

Array Length (m)	Pretension (N/m)	EI req'd for Freq. ( $N\ m^2$ ) $\times 10^{-6}$	EI req'd for Column ( $N\ m^2$ ) $\times 10^{-6}$	GJ req'd for Freq. ( $N\ m^2$ ) $\times 10^{-6}$	Canister Diameter (m)	Longitud- inal Rods Diameter (cm)	Canister Length (m)	X-Cable Diameter (mm)
50	1.6	0.43	0.030	0.0027	1.0	0.44*	1.8	0.36
100	6.6	6.9	0.48	0.011	1.0	1.20	3.2	0.72
150	14.8	35	$2.4 \times 10^7$	0.024	1.0	2.70	7.1	1.10
200	26.4	110	7.7	0.044	1.5	3.20	8.2	0.95
300	59.3	560	39	0.098	3.0	3.60	9.5	0.72
*Local rod element in column is critical condition								

The natural frequency of a stretched membrane is determined by the formula

$$f_{sb} = \frac{1}{2\ell} \sqrt{\frac{\tau}{\rho}} \quad \text{where}$$

$\tau$  = tension in newtons per meter  
 $\rho$  = mass in kilograms per meter  
 $\ell$  = length in meters

Therefore, for a required frequency of 0.0085 Hz, this equation is rewritten to be:

$$\tau = .00029 \rho \ell^2$$

The natural frequency of a cantilever beam subjected to a concentrated mass at its end is determined from

$$f_{boom} = \frac{1}{2\pi} \sqrt{\frac{3EI}{m\ell^3}}$$

where EI is the flexural stiffness in newton meters squared  
m is the mass in kilograms  
 $\ell$  is the length in meters

For a required frequency of 0.017 Hz, the required EI is defined by

$$EI = 0.0038 m\ell^3$$

Since m is half the solar blanket mass it is defined by

$$m = 16 \times \ell/2 \times \rho = 8\rho\ell$$

Hence, the required  $EI = 0.0304 \rho \ell^4$ . In the above analysis  $\rho = 2.27 \text{ kg/m}$ , reducing the above equations to

$$\tau = 0.00066 \ell^2 \text{ and}$$

$$EI = 0.069 \ell^4$$

To assure the validity of the above equation for EI, it is essential that the secondary effects due to the column compression be insignificant. The column capability is defined by the following. The limit pretension-induced column loading is  $16 \tau$ ;

$$\text{hence } 16\tau = \pi^2 EI_{col} / (2\ell)^2 \times 1/1.5 \times 1/3.0;$$

where 1.5 is the applied safety factor and the factor of 3.0 is to assure that secondary effects are negligible. The factor of 2 is the equivalent length for a cantilever supported column (expected to be conservative for this pretension induced loading). Rewriting

$$EI_{col} = 0.0048 \ell^4$$

the torsional natural frequency required was determined from

$$f = \frac{1}{2\pi} \sqrt{\frac{K_T}{I}}$$

where  $K_T$  is the torsional spring constant in N m per radian

$I$  is the inertia in  $\text{kg m}^2$

Using  $K_T = GJ/L$  and  $I = \rho/12 (16)^3 \ell/2$  for the 16-m-wide array, and a required frequency of 0.0085 (for the torsion case, the blanket array frequency is at least twice that of the value in the bending mode), the following equation is obtained:

$$GJ = 0.480 \rho \ell^2$$

where  $\rho$  is the mass in  $\text{kg/m}^2$ ,  $GJ$  is the torsional stiffness in  $\text{N m}^2$ .

The values determined from the foregoing equations are shown in Table 2-5. The mast configuration and diameter are shown in Figure 2-16. The significant results of Table 2-5 are as follows.

- The Astromast-type column dimensions become excessive to the space available in the cargo bay for array lengths significantly above 200 m.
- The maximum model frequency requirement in the bending mode is much more significant than the column requirement associated with the pretension.

It is pertinent to mention the characteristics of these designs were reviewed with the Astro Research Corporation and are regarded as technically feasible.

The designs of Table 2-5 can withstand various combinations of inertia loads of sufficient magnitude that no problems are foreseen in this regard. This is due to the high  $EI$  and  $GJ$  values required to satisfy the minimum model frequency requirement.

## 2.4 SUMMARY

This study indicates that a deployable-type solar array capable of delivering 400 kW to 500 kW of power can be delivered to LEO in a single Shuttle launch. A major technology development is indicated in the area of heat rejection for both of the concepts investigated. The use of ballast to meet payload c.g. limits for some cases was also indicated. Figure 2-21 lists the principal characteristics of the two design concepts.

The delivery of a 500-kW-total power system to LEO in one Shuttle launch, including the power controls and power storage, necessary to obtain a constant power level, appears to be a feasible concept. This arrangement utilizes the SEPS-type deployable solar array.

## 2.5 REFERENCES

1. B. A. Boley and J. H. Weiner, *Theory of Thermal Stresses*, John Wiley and Sons, New York, 1960.

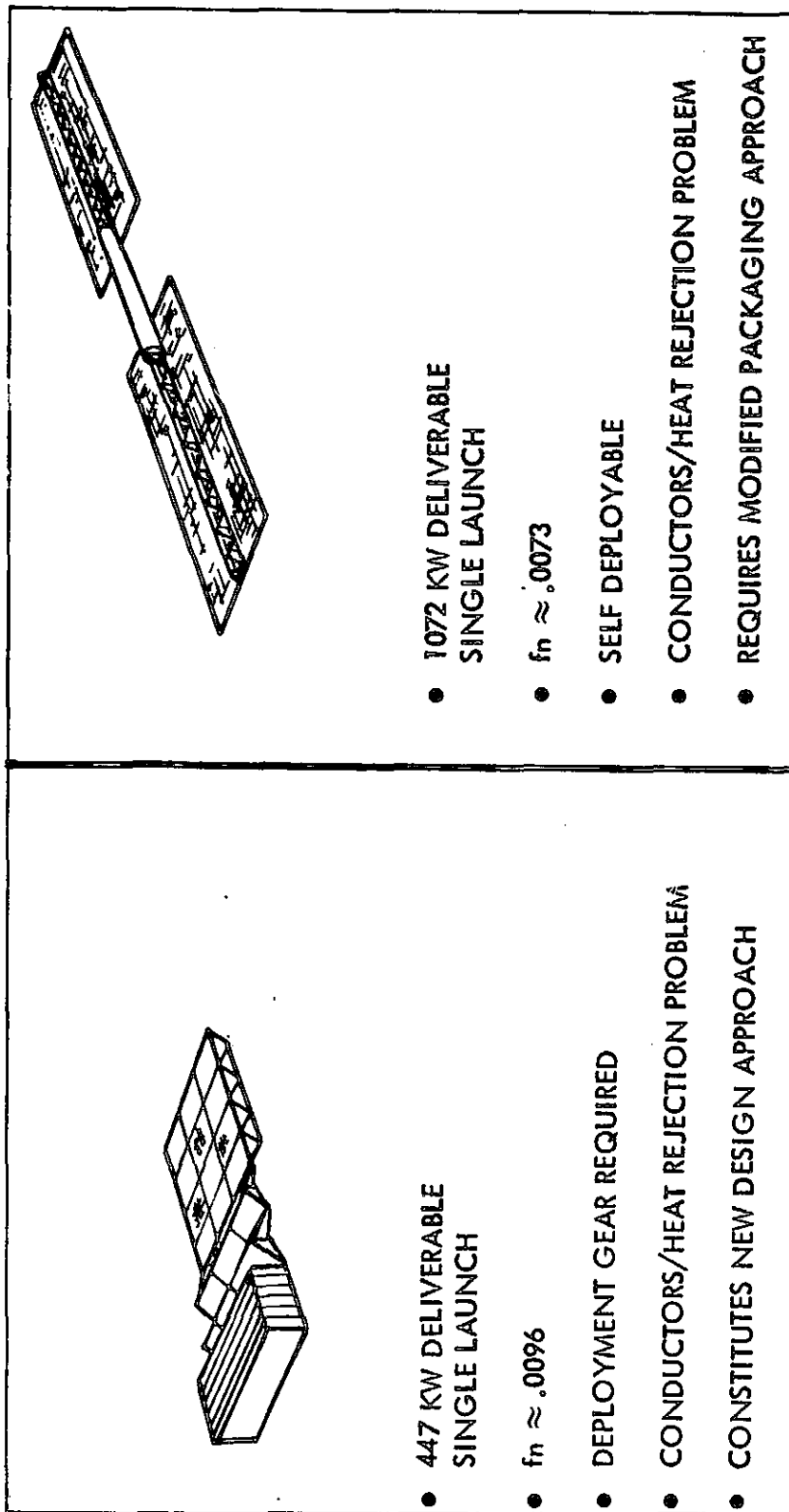


Figure 2-21 Summary—Deployable Solar Arrays

### 3.0 LINEAR SHAPED VERSUS AREA SHAPED ERECTABLE PLATFORM CONFIGURATIONS

#### 3.1 INTRODUCTION AND SUMMARY

The Task I study (Reference 1, Section 3.0) documents the significant requirements and configuration/subsystem characteristics, of an erectable, "linear" shaped advanced technology communications platform. The "linear" shaped platform, rather than an "area" shaped platform, was selected and studied because "simplicity of space construction" was considered to be the most significant platform design objective (rather than, for example, minimum system weight or maximum performance). Appropriately, recurring questions pertinent to the foregoing are:

1. It is significantly simpler to construct an erectable "linear" shaped platform as compared to an equivalent "area" shaped platform?
2. Would an "area" shaped platform result in a significant weight savings, increased antenna pointing accuracy, less stringent structural system, or reduced propulsion and control system requirements?
3. Over what ranges of communication platform size are conclusions to 1 and 2 appropriate?

This mini-study was directed to resolve these questions. The study approach, baseline configuration, analyses, and detailed results that support the following conclusions, are described herein.

Results of the analyses of structure design and construction operations are summarized in the following statements:

#### Structural Considerations

1. The "linear" shaped erectable platform is superior to the "area" shaped erectable platform for lengths up to at least 480 meters, because it requires:
  - a) fewer members
  - b) fewer joints
  - c) less weight
2. The "area" shaped platform may nominally provide a small advantage in reduced structural deformation affecting antenna pointing errors (2.1 minutes versus 4.2 minutes if the thrust is in plane).
3. Modal frequency of the erectable linear shaped platform for orbit transfer (0.05 Hz) is expected to be acceptable to the guidance and control system design.



4. The modal frequency of the operational configuration of the erectable linear shaped platform (0.23 Hz) is determined by the local solar panel structure behavior, and is also considered acceptable and would not change significantly if supported by an area shaped platform.
5. A factor favoring the erectable area shaped platform is that all struts are of equal length (except for the thrust structure in one case). The linear configuration requires a set of longer (17.0 meter) diagonal struts, as well as the standard length (12.0 meter).

#### Conclusions From Construction Operations Considerations

1. The area shaped platform requires additional construction equipment - a second RMS and a trapeze.
2. Simplicity of operations favors the linear shaped erectable platform, which does not require simultaneous operation of two RMS's or "walking" the orbiter from one position to another.
3. Installation of modules using the RMS is enhanced by the linear shaped configurations which can be oriented to avoid the orbiter tail and wing obstructions.
4. Power and signal line installations are similar in two configuration approaches, but the linear shaped configuration requires more inter-connects (42 versus 26 for the area shaped platform). The impact of this additional number may be offset by less complex and more automatic assembly equipment and procedures facilitated by the linear configuration.

Combining all the above considerations, the majority favor a linear configuration when the relative sizes of structure and antennas and other modules are similar to the construction projects studied.

### 3.2 PLATFORM DESIGN

This section describes the design and structural analyses performed in support of this comparative study of "linear" and "area" shaped advanced technology communication platforms.

#### 3.2.1 Study Approach/Configuration

An equitable comparison between the "area" and "linear" shaped erectable platforms is possible if the platforms are indeed comparable, i.e., they are configured to the same requirements. These requirements are summarized as follows:

1. Provision for mounting of four - 6.0m, 7.5m, 13.8m, and 20.5m diameter offset feed antennas as shown on Drawing 42662-25 (Reference 1).
2. Provision for growth, which was assumed to be four additional offset feed antennas up to 13.8 meters in diameter. These antennas are installed in synchronous orbit.
3. East-west orientation of all the antennas.
4. A minimum electrical clearance of 5° between the antenna reflectors and adjacent feed columns, to minimize diffraction of the beam-width envelope.
5. Arrangement of the higher frequency antennas closest to the solar panels to minimize power distribution system weight.
6. The same solar panel array in regard to size, weight, and structural configuration.
7. The same RCS weights and system including use of one pound thrusters for attitude control.
8. The same antenna weights, structural configuration, and stiffness characteristics as that delineated in Table 3.3.2-2 (Reference 1) for the baseline "area" shaped platform (orbit transfer thrust essentially in the plane of platform). The alternate configuration (thrust perpendicular to plane of platform) has a slightly different antenna configuration that is shown on Figure 3.2-1.
9. The same subsystem weights resulting in the same total weight tabulated in Table 3.4 1 (Reference 1). The actual differences in assumed and actual weight of the area shaped platform subsystems have second order affects on the comparative data.
10. The same orbit transfer propulsion system, comprised of the five stages described in Section 3.3.6 (Reference 1), that provides a maximum T/W = .20.

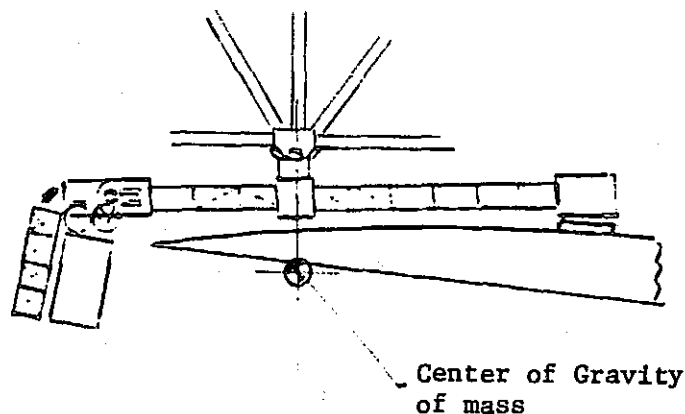


Figure 3.2-1 Stowed Antenna Reflector/Feed Package - Alternate Configuration

11. Construction from the orbiter with the reach capability of a standard RMS restricting the length of the individual tapered struts to no more than 12 meters.

The erectable "linear" shaped and "area" shaped configurations that satisfy the foregoing requirements are pictorially described on Drawing 42662-25 (Reference 1) and Figures 3.2-2 and 3.2-3 respectively. The "linear" platform is further described in Section 3.3.1 (Reference 1). A further description of the "area" shaped platform is as follows:

The platform structure is a tetrahedral truss constructed of 12 meter long tapered graphite epoxy composite material struts. The 6.0m, 7.5m, 13.8m, and 20.5m antennas are attached to the lower plane elements through moment connections with docking ports of the same concept as that used in the linear platform and shown in Figure 3.3.1-1 (Reference 1). The intersurface and top elements utilize pin-connected joints.

As was the case in the "linear" platform, the significant differences in structural function and load level placed upon the bottom plane, top plane, and intersurface members resulted in three different member sizes for the basic platform.

The solar panel array, RCS pods, and control moment gyro package are mounted to the basic platform structure by hexapod structures, all comprised of 12 meter long struts configured as shown in Figure 3.3.1-2 (Reference 1) for the linear platform RCS pods. However, the thrust structure for the baseline configuration (Figure 3.2-4) utilizes different length elements (as in the "linear" shaped platform) to center the thrust line (at the end bay adjacent to the thrust structure) midway between the top and bottom plane. In the baseline configuration the thrust line through the mass center of gravity is inclined at an angle of 3.8 degrees with the platform planar surface. In the alternate configuration, since the thrust line is perpendicular to the plane of the platform, significant bending moments (during orbit transfer) on the

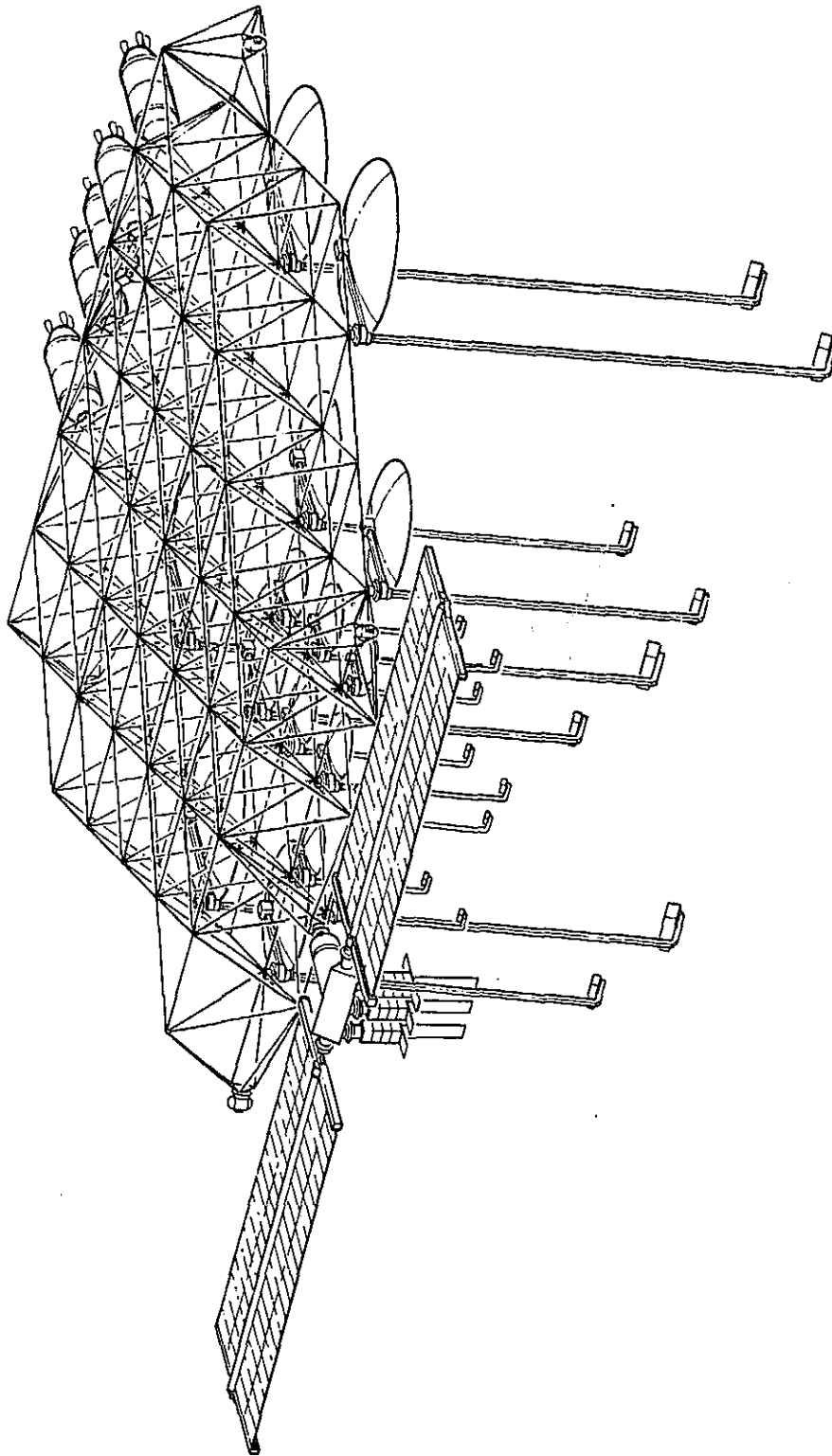


Figure 3.2-2    Baseline "Area" Shaped Advanced Communications Technology Platform

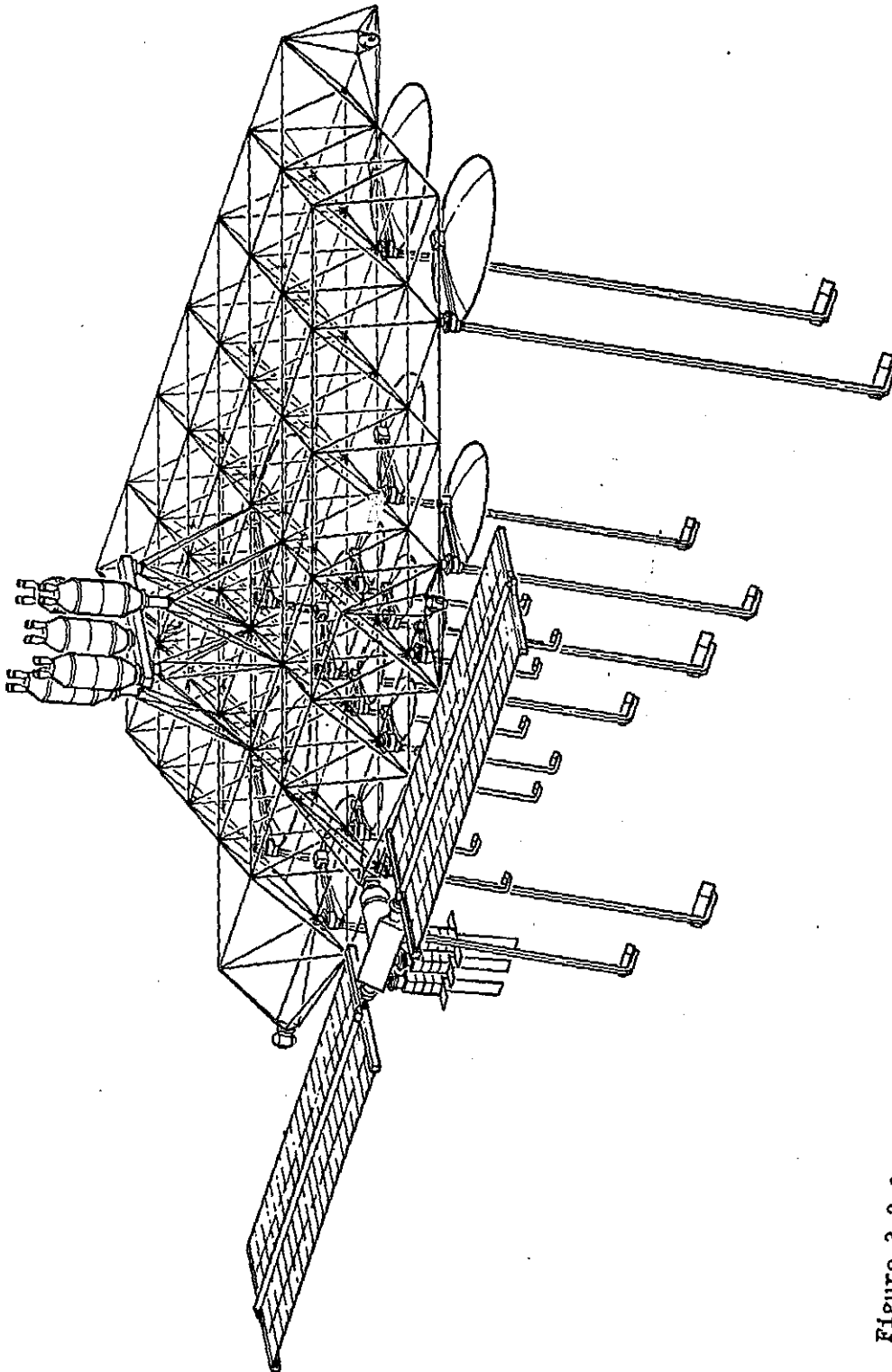


Figure 3.2-3 Alternate "Area" Shaped Advanced Communications Technology Platform

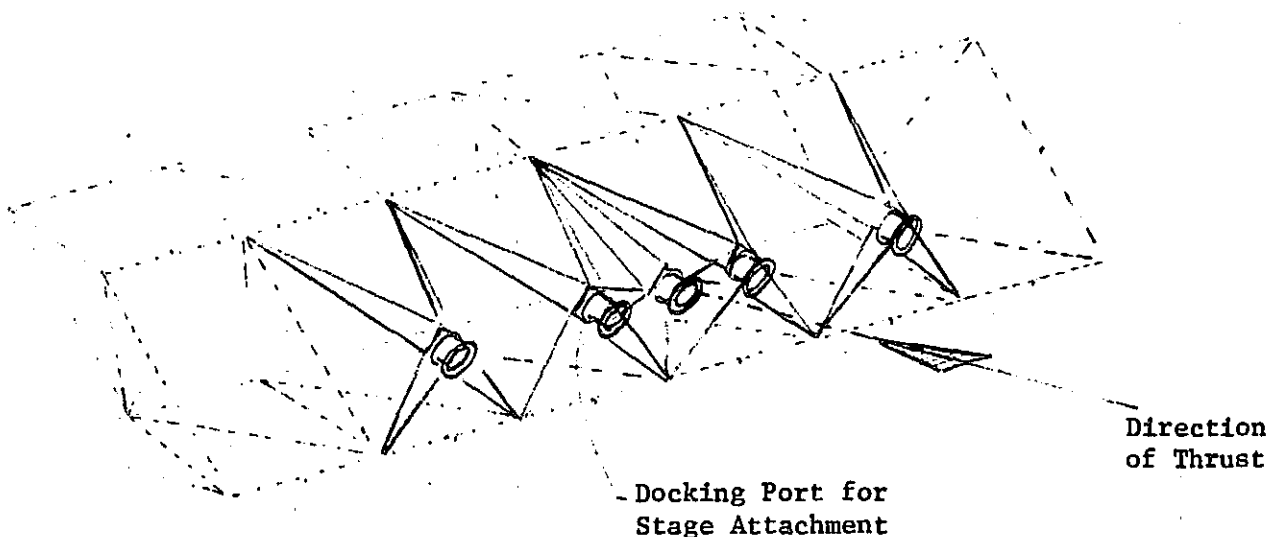


Figure 3.2-4 Thrust Structure - Baseline Configuration

docking port to lower element member joints, are avoided by placing the static location of the center of gravity of the antenna/feed stowed package so that a line joining it and the centroid of the joint is parallel to the thrust (Figure 3.2-1). This is the basic difference in the alternate configuration, which uses the thrust structure shown in Figure 3.2-3.

As in the "linear" shaped platform, the feed columns and solar panels are stowed during the orbit transfer maneuver.

It is pertinent to note that three other configurations drawn without adherence to requirement 5 did not result in platform areas less than 90% of that shown on Figures 3.2-2 or 3.2-3. Relaxation of this requirement for the "linear" shaped configuration would not reduce the configuration length. In view of the foregoing and other miscellaneous design considerations, it is quite possible the "area" shaped platform shown could be reduced to 85% of the area shown which, however, is not significant to the conclusions drawn.

The detailed structural analyses for this "area" shaped platform that were directed to satisfy the structural requirements delineated in Section 3.3.1 (Reference 1) are described herein. However, for review convenience, the results are tabulated in Table 3.2-1 together with that of the comparable "linear" platform data.

### 3.2.2 Structural Analyses

As in the "linear" shaped platform structural analysis, an ultimate safety factor of 1.5 was used.

Table 3.2-1 Comparative "Linear" Versus "Area" Shaped  
Platform Characteristics

Characteristic	Linear Platform	Area Platform (Thrust In-Plane)	Area Platform (Thrust Normal to Platform)
Structure Mass*	3352 Kg	4730 Kg	4345 Kg
Operational Min. Frequency	.022 Hz	.023 Hz	.023 Hz
Orbit Transfer Min. Frequency	.140 Hz	.213 Hz	.078 Hz
Errors (Minutes)			
Antenna	2.8	2.8	2.8
Overall Platform	.6	.2	.2
Local Supports	3.6	1.9	5.0
TOTAL	7.0	4.9	8.0
Member Distribution**			
	No. Max. Dia. Min. Dia. Wall Gage	No. Max. Dia. Min. Dia. Wall Gage	No. Max. Dia. Min. Dia. Wall Gage
Bottom Cords	61 30.5 24.0 .12	124 30.5 25.4 .081	124 21.6 10.8 .064
Top Cords	19 44.0 22.0 .09	95 34.3 17.1 .064	95 33.0 16.5 .064
Pyramidal	88 20.3 10.15 .064	116 21.6 10.8 .064	116 38.0 19.0 .064
Diagonals	20 20.3 10.15 .064	- - - -	- - - -
RCS Pods	24 20.3 10.15 .064	24 27.4 13.7 .064	24 26.6 13.3 .064
Solar Pods	6 30.5 15.2 .064	6 27.4 13.7 .064	6 26.6 13.3 .064
Thrust Structure	65 Miscellaneous	40 Miscellaneous	26 Miscellaneous
TOTAL Members	283	405	391
No. of Joints*	53	70	70

\*Comparative, not total (equals not included). \*\*Dimensions are in cm.

Table 3.2-2 Comparative Platform\* Structural Deformation  
Contributions to Antenna Pointing Error (Minutes)

Item	Linear Platform		Area Platform (Thrust-In-Plane)		Area Platform (Thrust $\perp$ to Plane)	
	Overall Platform	Local Elements	Overall Platform	Local Elements	Overall Platform	Local Elements
Thermal	.5	3.3	.20	1.6	.20	2.7
Attitude Control	<.10	.30	Neg	.3	Neg	2.3
Total	4.2		2.1		5.2	

\*The antenna contributions are the same.



### Orbit Transfer Thrust - Truss Element Sizing

The structural element sizes shown in Table 3.2-1 were determined using the same column stability and beam-column analysis techniques that were applied to the "linear" shaped platform. The internal loads were determined from a NASTRAN model of half of the structure, as shown in Figure 3.2-5, that was constrained by symmetrical boundary conditions. Since this truss is deeper and less than one-third the length of the "linear" platform, overall stability requirements are not critical.

### Orbit transfer Configuration Modal Analysis

The minimum modal frequencies of the baseline and alternate "area" platforms are respectively .213 and .078 Hz and are associated with the vertical displacement of the stowed 13.8m antenna reflector/feed package located at the edge of the platform. These values are directly determined by the flexural inertia of the lower truss elements, and do not represent the overall platform flexural deflection. To the contrary, the "linear" shaped platform minimum modal frequency is .140 Hz and is associated with the overall platform response rather than the local antenna package response.

### Operational Configuration Modal Analysis

The NASTRAN model shown in Figure 3.2-6 was used to determine the values of .023 Hz shown in Table 3.2-1. The negligible change in values across the three designs, despite the difference in the bottom element moments of inertia, is due to the criticality of the solar panel array which is governing the value quoted. To verify this, reduction of the lower plane elements from an effective moment of inertia of 1.7 to .10, in the alternate configuration, resulted in reduction of the minimum frequency to .010 Hz, with lateral deflection of the deployed 13.8 meter antenna feed package being the critical mode.

### Dimensional Stability Analysis

The results of the analyses performed to determine the "area" platform dimensional stability quality are summarized in Table 3.2-2. The comparable data for the "linear" platform is also shown. The data generated was based upon:

1. A maximum thermal gradient of 50°F between the average top and bottom plane elements.
2. A thermal gradient of 220°F across the bottom plane local elements supporting the antennas.
3. The same RCS induced inertial forces on the antenna feed package masses for both "area" shaped and "linear" shaped platforms.

Table 3.2-2 illustrates that the minimum and maximum errors which occur with respect to the baseline and alternate "area" shaped platforms. However, the table illustrates the maximum error, including the antenna deformations (to be 8.1 minutes). The requirement of six minutes (Reference 1) was determined from an arbitrary 33 1/3% allocation of a total error of 18 minutes. Hence, all the designs are regarded as adequate since the peak values have been determined by algebraic addition of the peak incremental values that are not necessarily concurrent or in the same sense.

It is pertinent to note that major contributions to all the platform errors are due to the local flexural behavior of the members directly supporting the antennas, and not the overall platform structural behavior. Also, the basic local element sizes for strength appear to be adequate for stiffness although a transient dynamic analyses (beyond the scope of this study) is required for final confirmation.

### 3.2.3 General Conclusions

In general, these analyses have unquestionably confirmed the correctness of the Phase I selection of the "linear" shaped platform configuration. The "area" platform exhibits no significant advantages, unless the reduced error of 2.1 minutes is significant (in which case an open section lateral element would be used on the "linear" shaped platform to reduce the thermal gradient error). The disadvantages of the area platform consisting of more members, more joints, and increased weight is more significant. At best, a platform with 85% of the area would still weigh more, and have more members than the "linear" shaped platform and would also have the disadvantages of construction that are discussed in Sections 3.3 and 3.4. Further, this conclusion is expected to be applicable at least up to "linear" platform lengths of 480 meters. This is based upon the data of Table 3.2-1 and Figure 3.2-7 (extracted from Reference 2). Referring to Table 3.2-2, the total platform error of 4.2 minutes is expected to increase to only 5.4 minutes since the local values are the same. The antenna values are also the same. The model frequency (Figure 3.2-7) of .05 Hz (during orbit transfer) is expected to be acceptable to the guidance and control system design. Also, the operational configuration frequency of .023 Hz was determined by the local solar panel structure behavior, and will not change significantly.

### 3.2.4 References

1. Space Construction System Analysis Project Systems and Mission Description, Task 1 Final Report - Satellite Systems, Rockwell International  
SSD 79-0077, April 26, 1977
2. Space Construction System Analysis, Project Systems Review - Satellite Systems, Rockwell International,  
PD 79-08, March 21, 1979

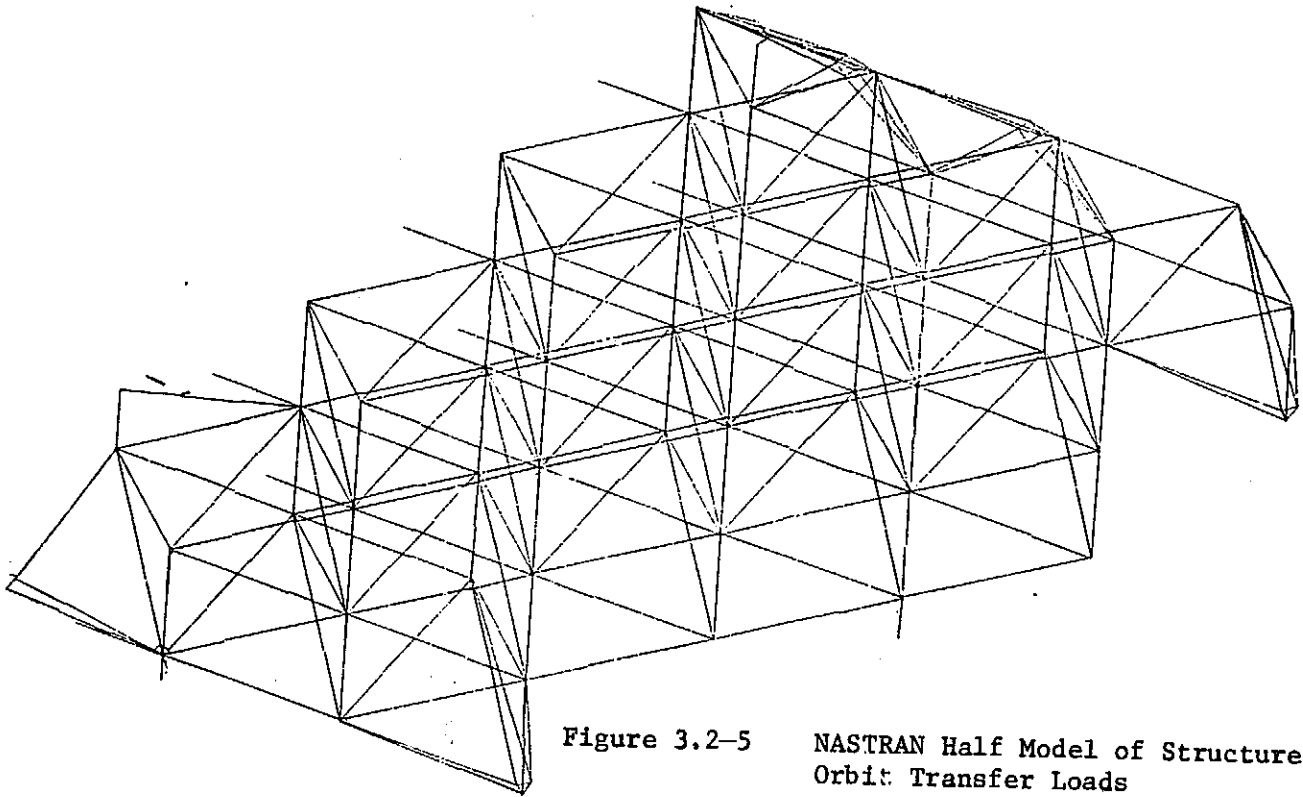


Figure 3.2-5 NASTRAN Half Model of Structure -  
Orbit Transfer Loads

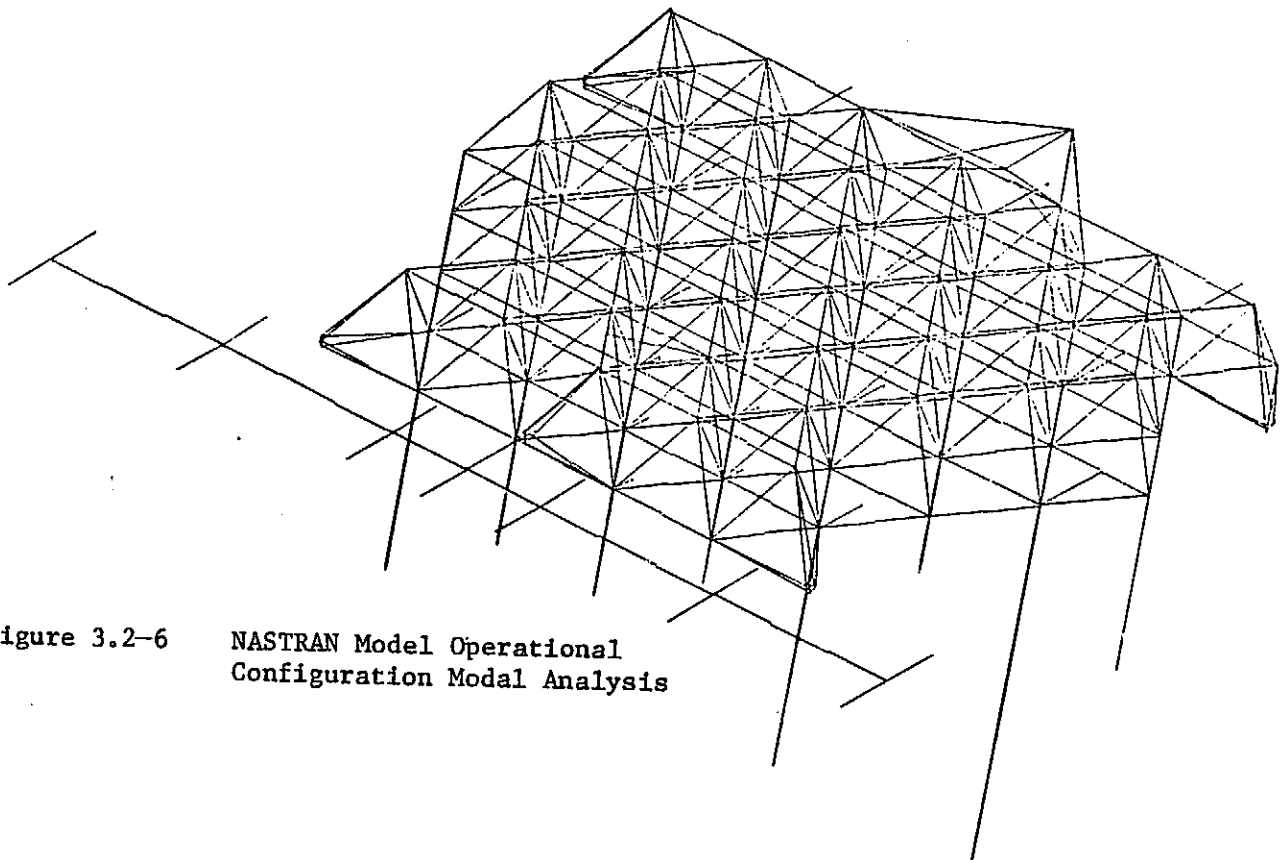


Figure 3.2-6 NASTRAN Model Operational  
Configuration Modal Analysis

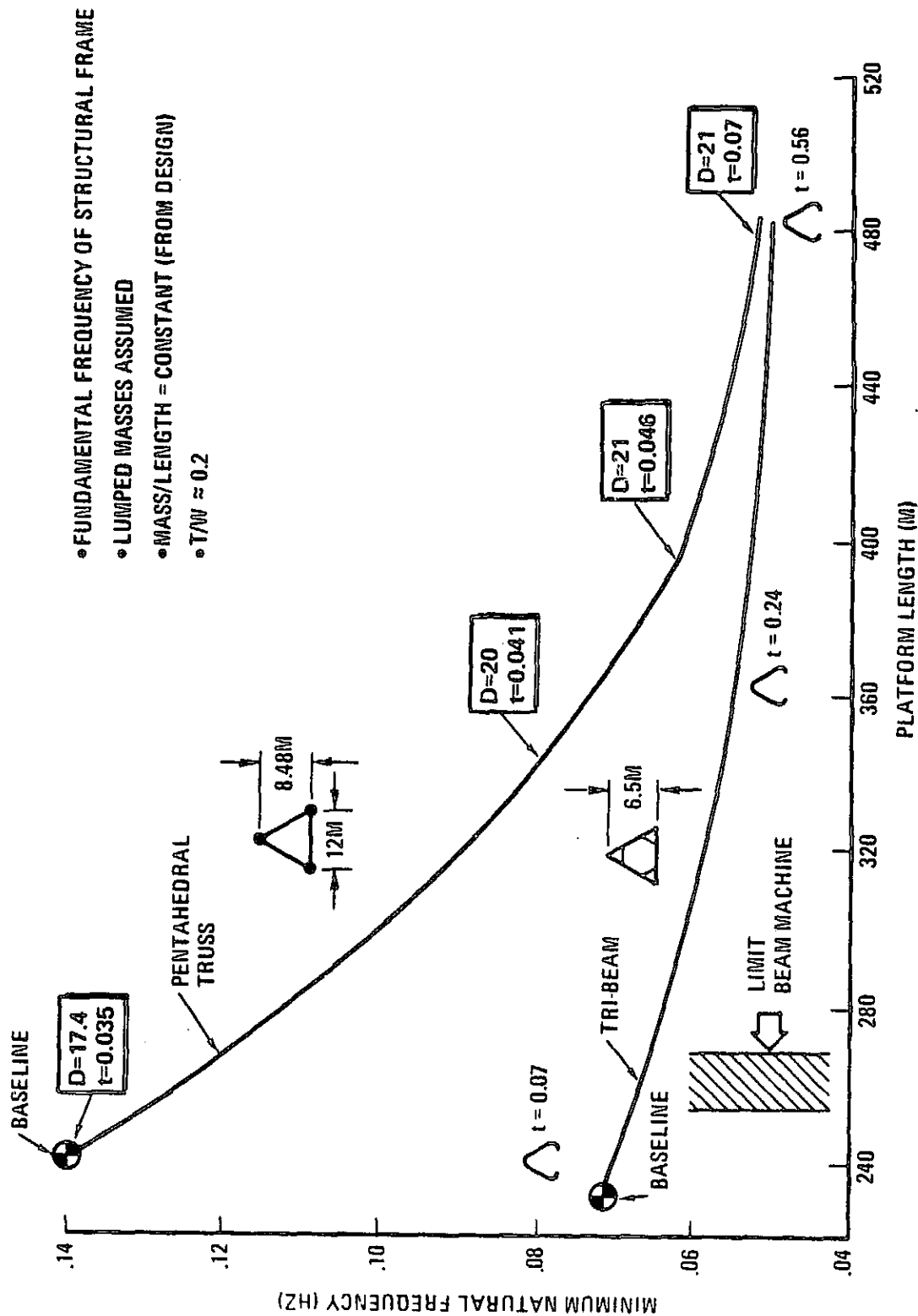


Figure 3.2-7 Communication Platform Growth Potential

### 3.3 CONSTRUCTION OPERATIONS

#### 3.3.1 Configuration Considerations

Two structural configurations are being considered as models for analysis in this construction operations study, a linear platform consisting of a string of 20 pentahedral cells, Figure 3.3-1, and an area platform consisting of tetrahedral cells as shown in Figure 3.3-2. A comparison of the key basic structure elements was conducted, revealing the physical characteristics shown in Table 3.3-1.

Table 3.3-1 Physical Comparison

	Area Platform	Linear Platform
No of Struts (12.0m)	339	160
No of Struts (17.0m)	0	20
Total Struts	339	180
No. of Unions (9 pt)	88	65
Unused Joints	114	225
Area, M <sup>2</sup>	4645	2880
Area (M <sup>2</sup> ) Strut	13.7	1600

Table 3.3-1 highlights some significant differences in the basic structure. There are similarities, however, in both configurations that are worth noting. For example, secondary structures that may be required for the installation of mission equipment and subsystems would be similar for both configurations. Also, similar, for purposes of this study, are the basic design concepts of structural elements, consisting of columns and unions/joints.

Note that the structural models used for these operations analyses are consistent and comparable in the context of a generic concept study, but do not precisely represent the structures or module attach concepts described in other main stream study final reports of the Space Construction System Analysis Study (References 1, 2 and 3).

#### 3.3.2 Assembly Operations

The assembly operations of a large space structure constitute an important factor in establishing its feasibility. In comparing the assembly operations which are required for both the linear and area platforms, a set of ground rules was established as shown in Table 3.3-2.

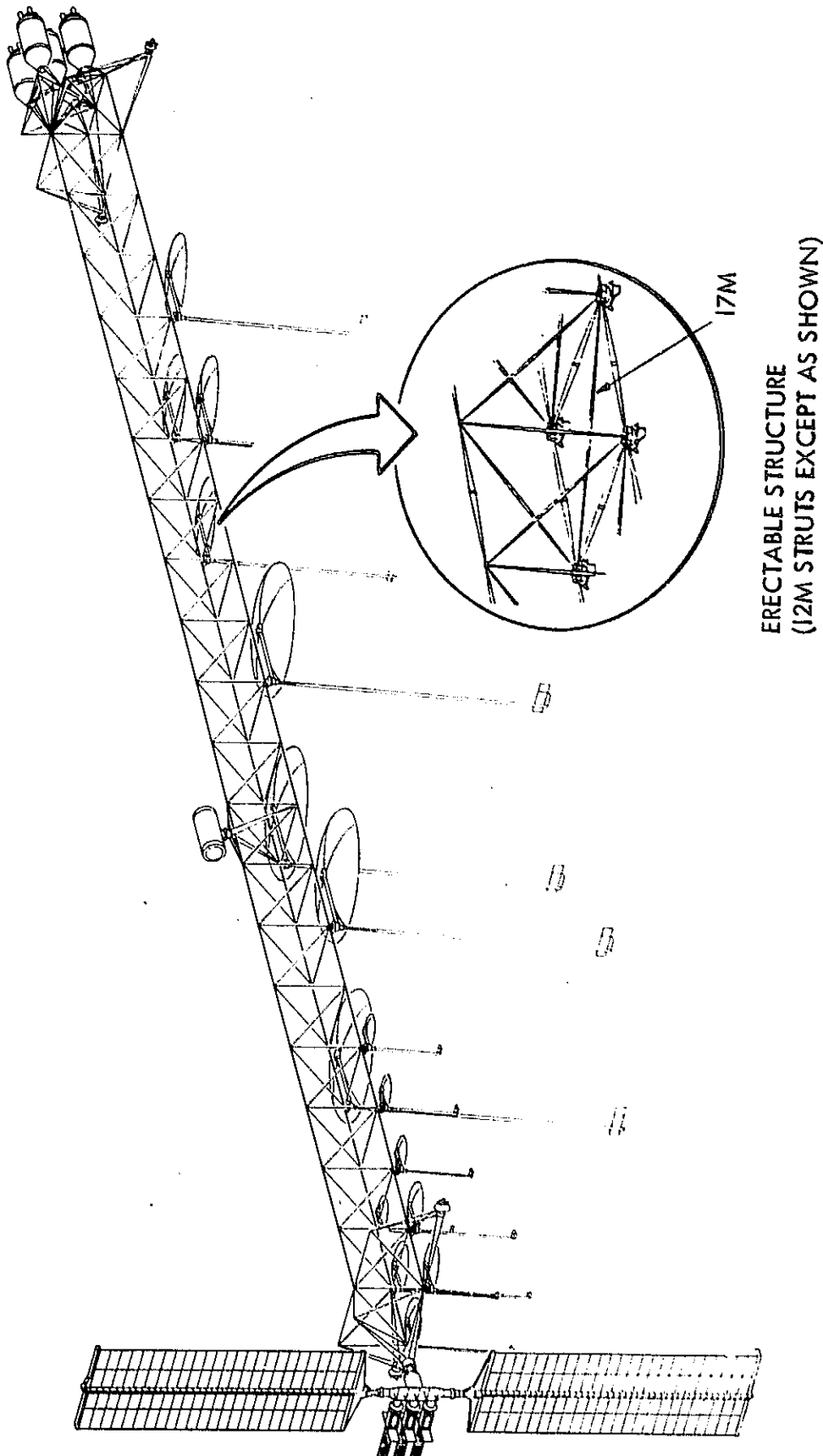


Figure 3.3-1 Linear Shaped Erectable Platform

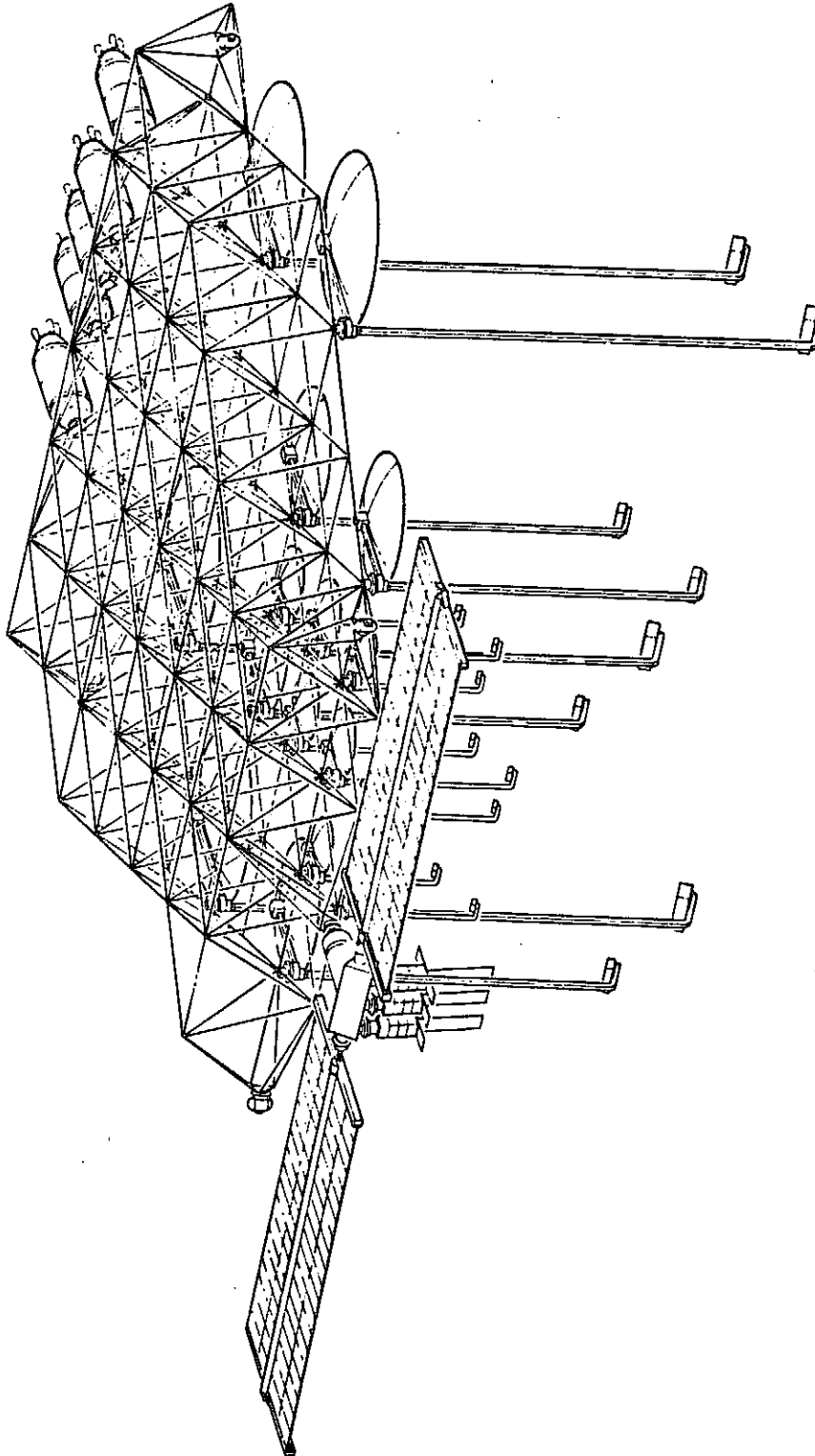


Figure 3.3-2 Area Platform

Table 3.3-2 Assembly Ground Rules

1. Orbiter to serve as construction base.
2. Construction does not require more than one orbiter at a time.
3. Orbiter systems and performances per Volume XIV.
4. Remote manipulator performance per RMS specification.
5. Assembly compatible with nestable columns.
6. No routine EVA for assembly activities.
7. No preferential attitude for assembly

The assembly procedure for the area platform for the current study is that of cell kit assembly approach utilized in previous studies.\* In these previous studies, the same procedures were investigated for different scale effects (paced by strut lengths), which affected the required sizes of holding fixtures and remote manipulators. Figures 3.3-3 and 3.3-4 illustrate the essential elements of the structures and construction equipment for two different size considerations. In either case, the assembly procedure calls for assembling of cell kits (specific combinations of struts and unions) using a remote manipulator and aid of an orbiter-mounted assembly fixture. These cell kits are then progressively joined (using a remote manipulator) to build up the area platform structure, which is stabilized with respect to the orbiter by a "trapeze" fixture. In Figure 3.3-3 the equipment used is two standard type Shuttle RMS's and a minimum trapeze fixture. This is the concept analyzed for purposes of the following reported study timelines. In Figure 3.3-4 the structure and equipment is analogous, but the struts are longer, the starboard manipulator (called a construction boom) is approximately twice the length of the standard Shuttle RMS, and the trapeze fixture is also much longer.

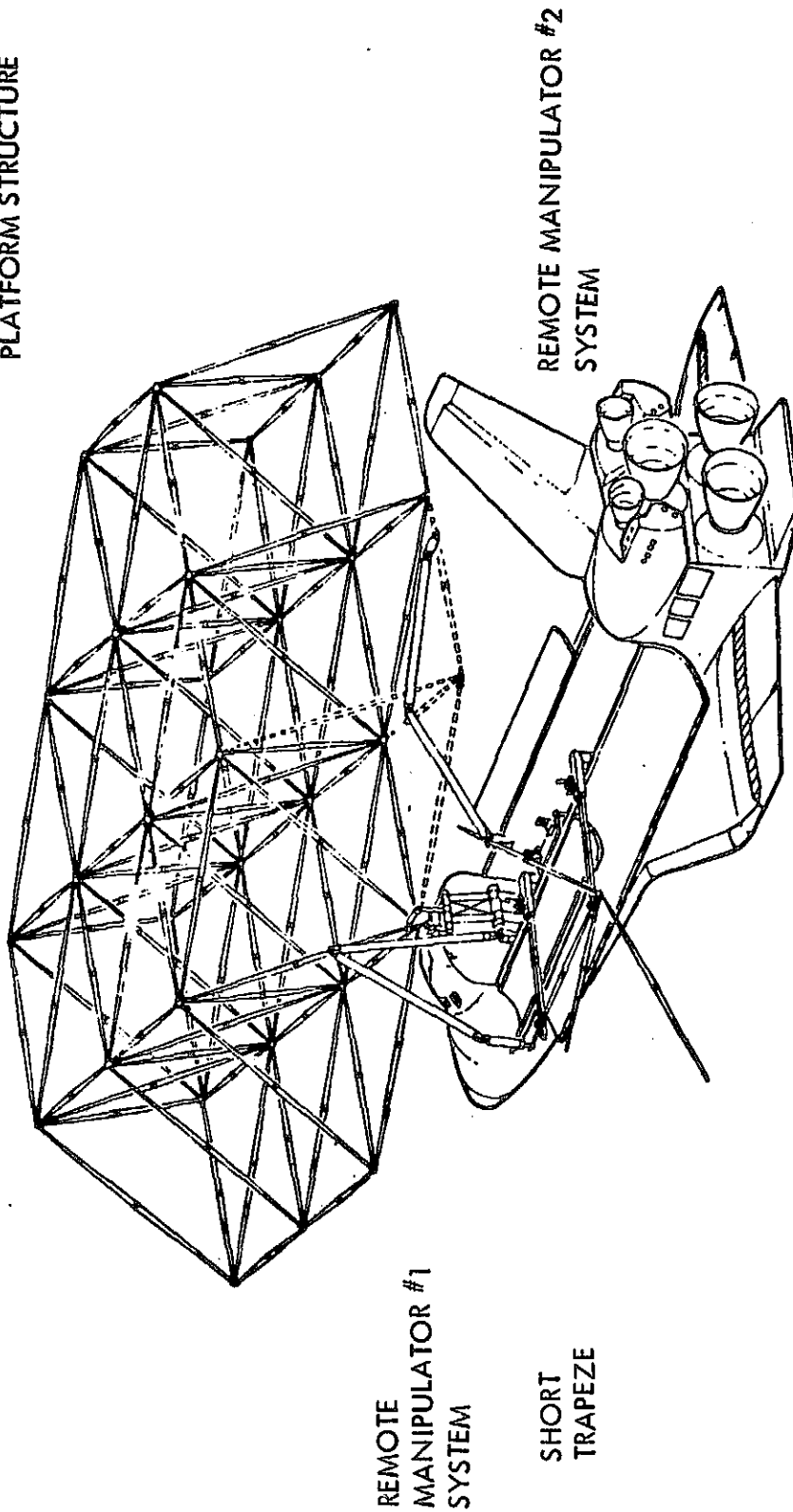
In following descriptions of large area platform assembly procedures, the large-scale equipment and structure shown in Figure 3.3-4 are used in the illustrations, because these graphics were readily available from previous studies. However, the associated timelines have been scaled to be compatible with shorter struts, the shorter trapeze and the use of the two standard RMS's illustrated in Figure 3.3-3.

For the linear platform, the assembly procedure is a continuous process of attaching individual elements to the platform until completion. The process is illustrated in Figure 3.3-5. Although the illustration assumes a structural growth path in line with the Orbiter's Y-axis, a Z-axis orientation is conceivable where operator visibility could be enhanced during mission equipment and subsystem installation.

\*References 4 and 5



ERECTABLE TETRAHEDRAL  
PLATFORM STRUCTURE



CELL KIT

CONSTRUCTION FIXTURE

Figure 3.3-3 Assembly Concept for Tetrahedral Area Platform,  
Using Short Trapeze and Two Standard Length  
Shuttle RMS Arms

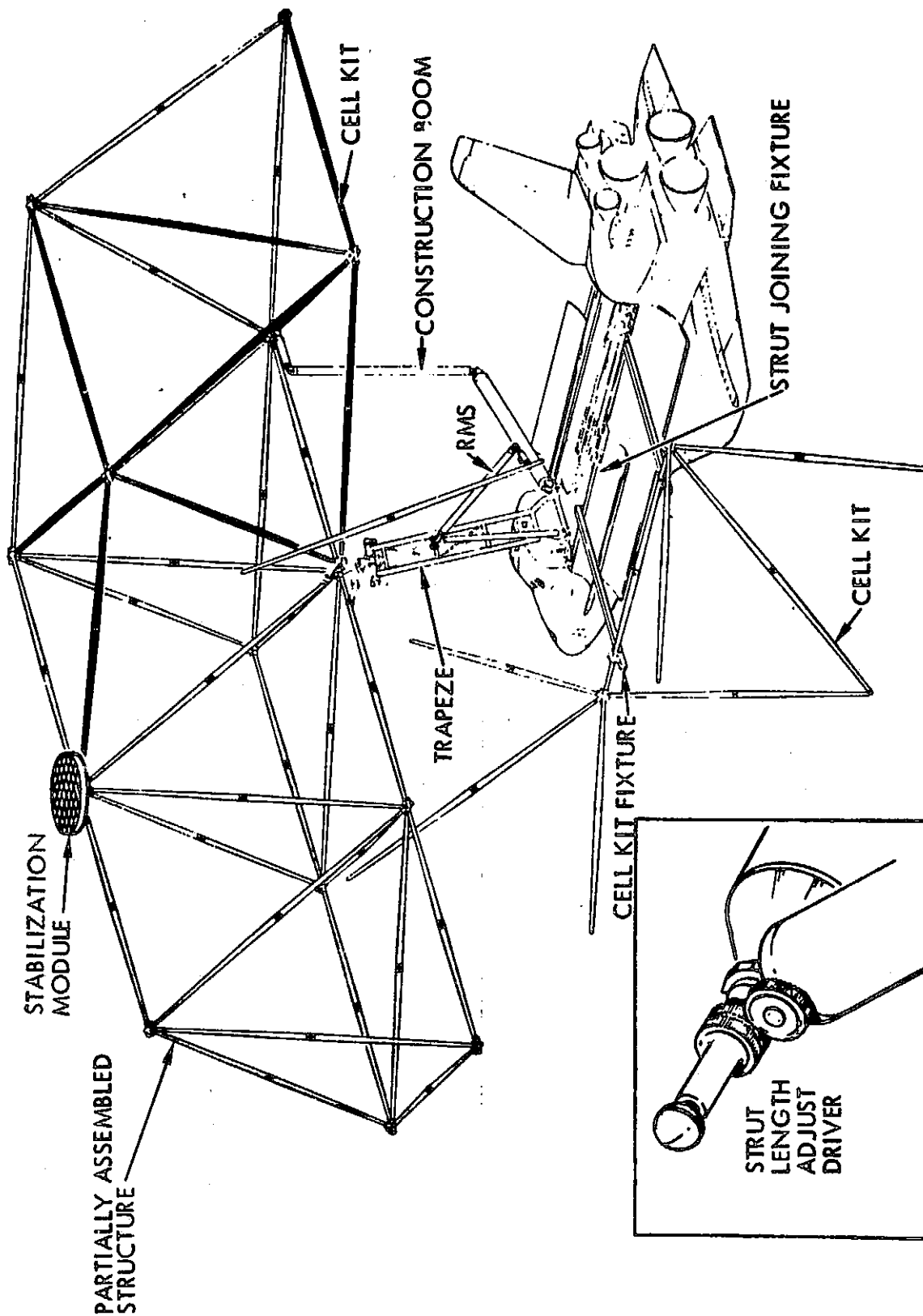


Figure 3.3-4 Assembly Concept for Tetrahedral Area Platform Using Long Trapeze and Starboard Construction Boom

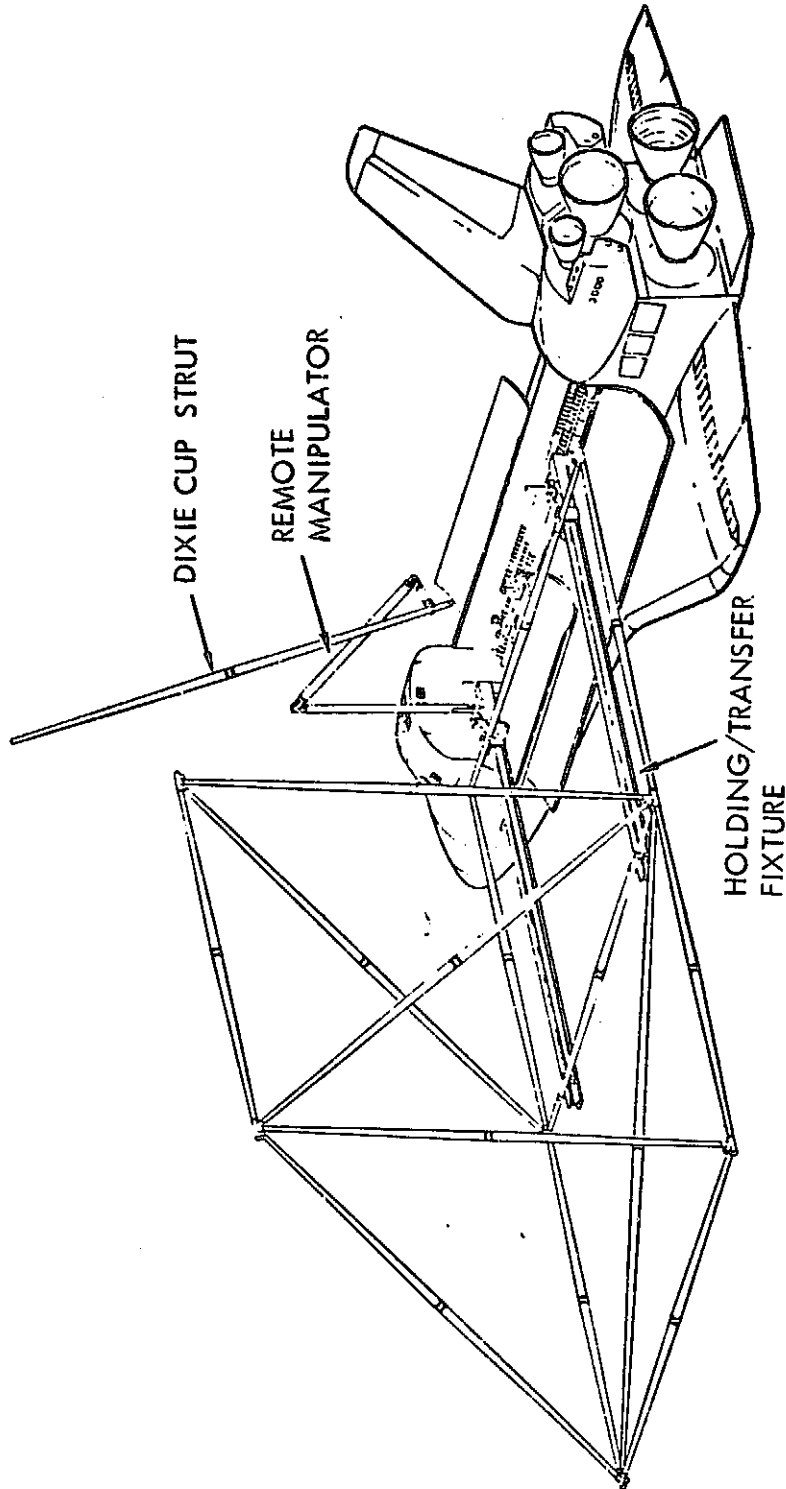


Figure 3.3-5 Assembly Concept for Linear Platform

### 3.3.3 Area Platform Assembly Process

#### Construction Equipment

Using the nestable columns and ball-socket joints as the basic structural elements, the construction equipment required for the assembly operations of an area platform are identified as follows (See Figure 3.3-3).

1. The standard Remote Manipulator System (RMS) which is to be utilized mainly to extract the nestable column segments from their stacked position, join each two segments together and perform the cell kit assembly. This RMS is designated as RMS #1.
2. A second 15.24m (50 ft) RMS is planned for inclusion in the Orbiter. The function of the second RMS will be to transfer the cell kit from its assembly fixture to the partially assembled main structure and effect the joining of the columns to the unions. This RMS is designated as RMS #2.
3. One docking/holding trapeze which will provide a positive controlled spacing between the orbiter and the main structure.
4. One construction fixture which is a combination of column assembly tool to mate each of two column segments together, and a cell kit assembly tool.
5. Various supports and mechanisms within the orbiter cargo bay to restrain the column segment stacks and the union-joints during launch and to permit their extraction upon demand.
6. Closed circuit television (CCTV) and lighting provisions.

#### Assembly Operations

Figure 3.3-6 depicts the various assembly stages of a standard cell kit. Hence, it assumes that initial and subsequent cell kits have been assembled and attached together. Subsequent to the completion of any cell kit attachment, the trapeze will be undocked from the main structure, the orbiter advanced one cell and the trapeze redocked to the partially assembled main structure. Sketch (a) of the figure depicts that point in time while:

1. RMS #2 (upper arm shown only in the vertical position) is in the process of attaching another cell kit. Simultaneously, RMS #1 latches onto the end of a new stack of column segments as they are packed inside the orbiter cargo bay.
2. In sketch (b), RMS #1 lifts one end of the column segments stack out of the cargo bay, while the opposite end of the stack is restrained and supported by a rotating ratchet-type mechanism.

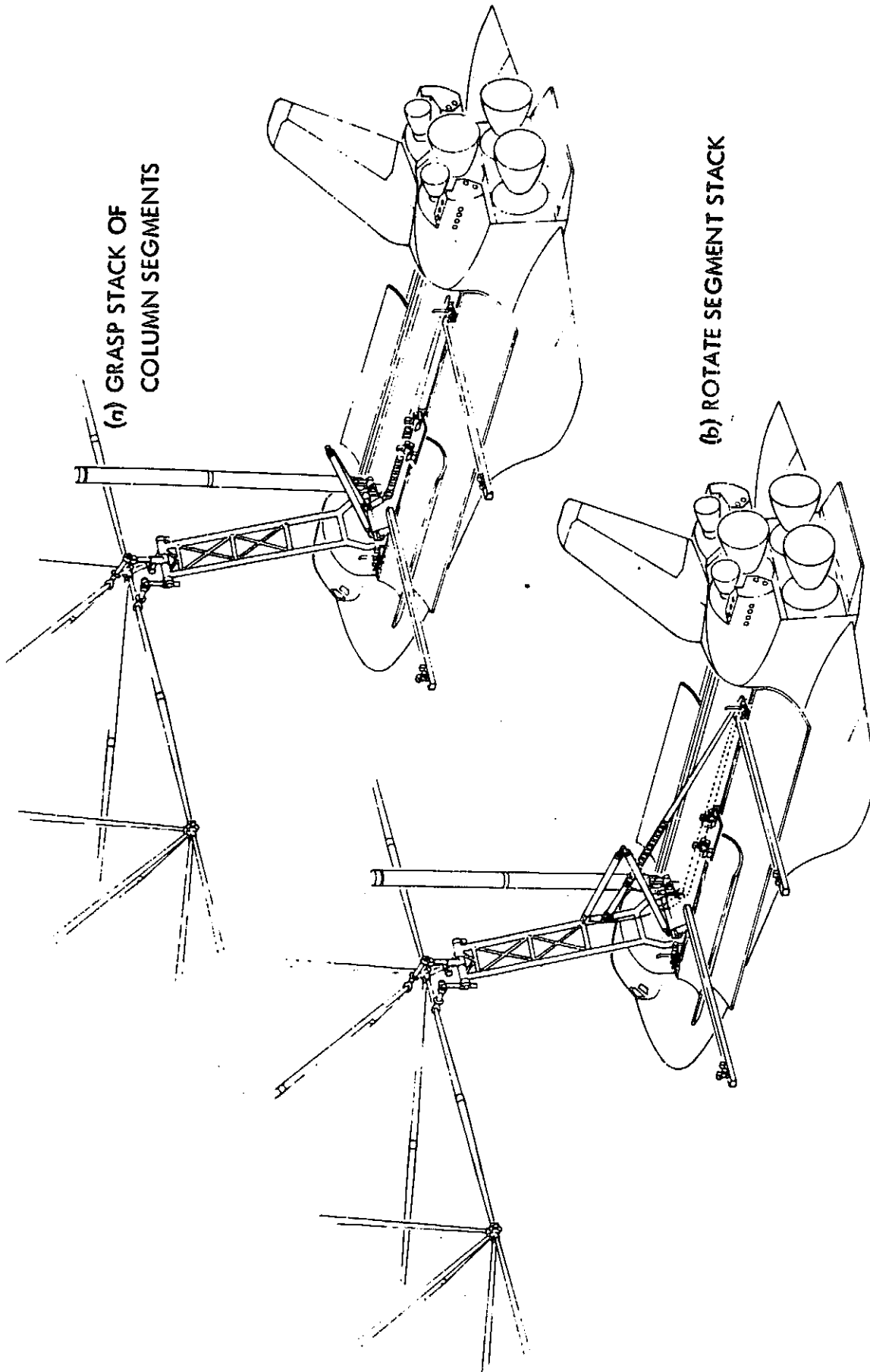


Figure 3.3-6A Assembly Sequence for Tetrahedral Area Platform

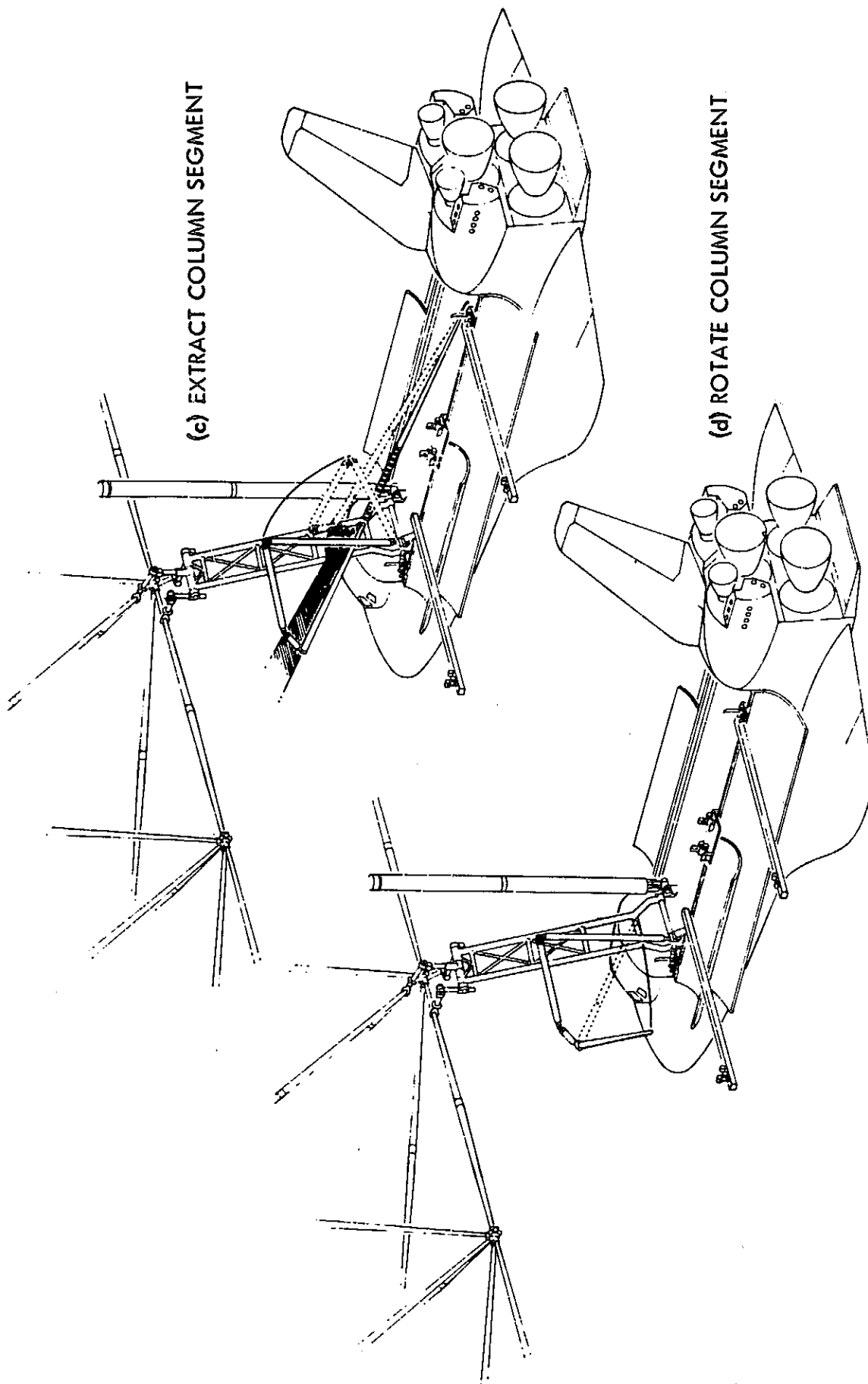


Figure 3.3-6B Assembly of Tetrahedral Area Platform (Con't.)

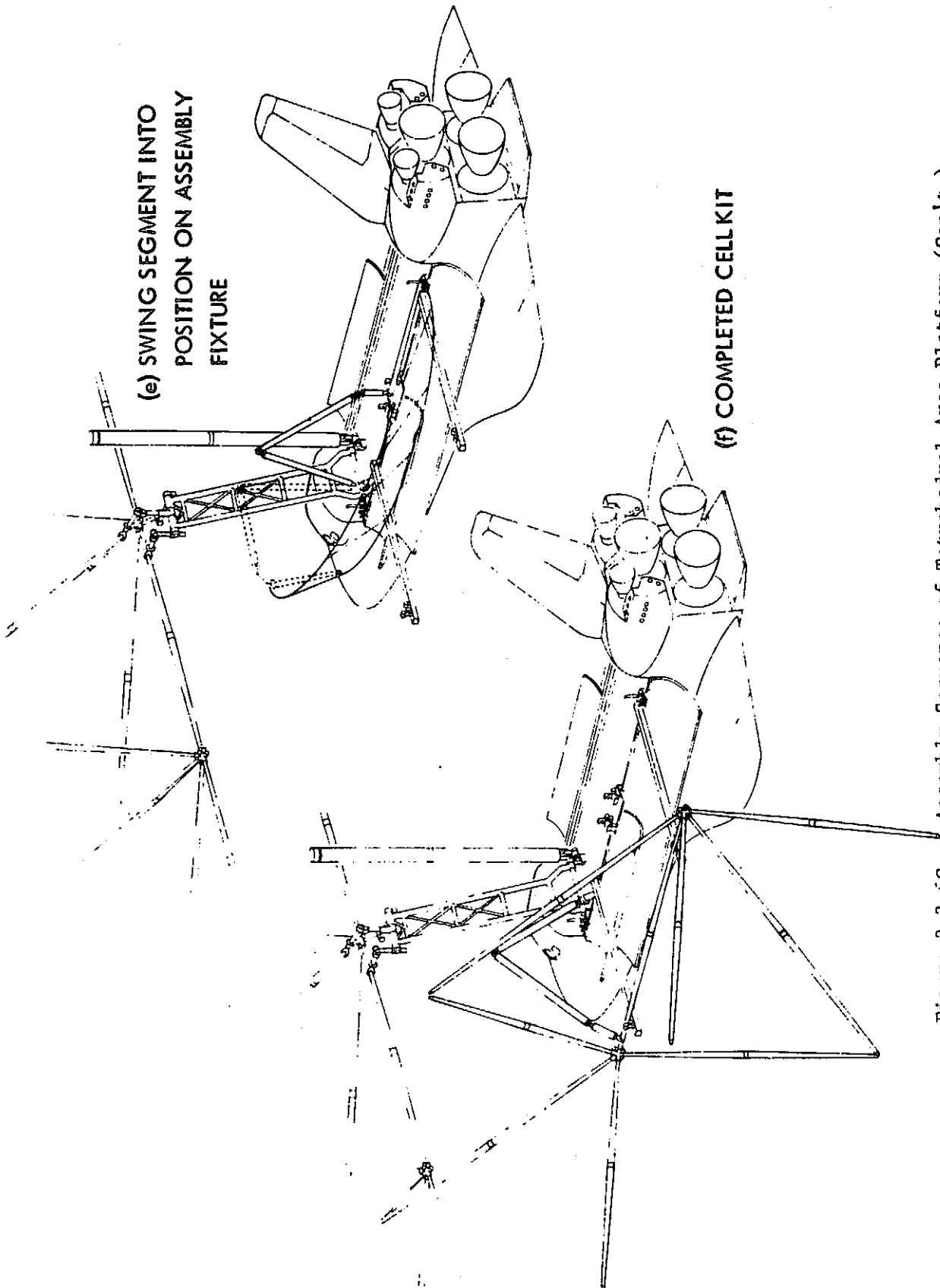


Figure 3.3-6C Assembly Sequence of Tetrahedral Area Platform (Con't.)

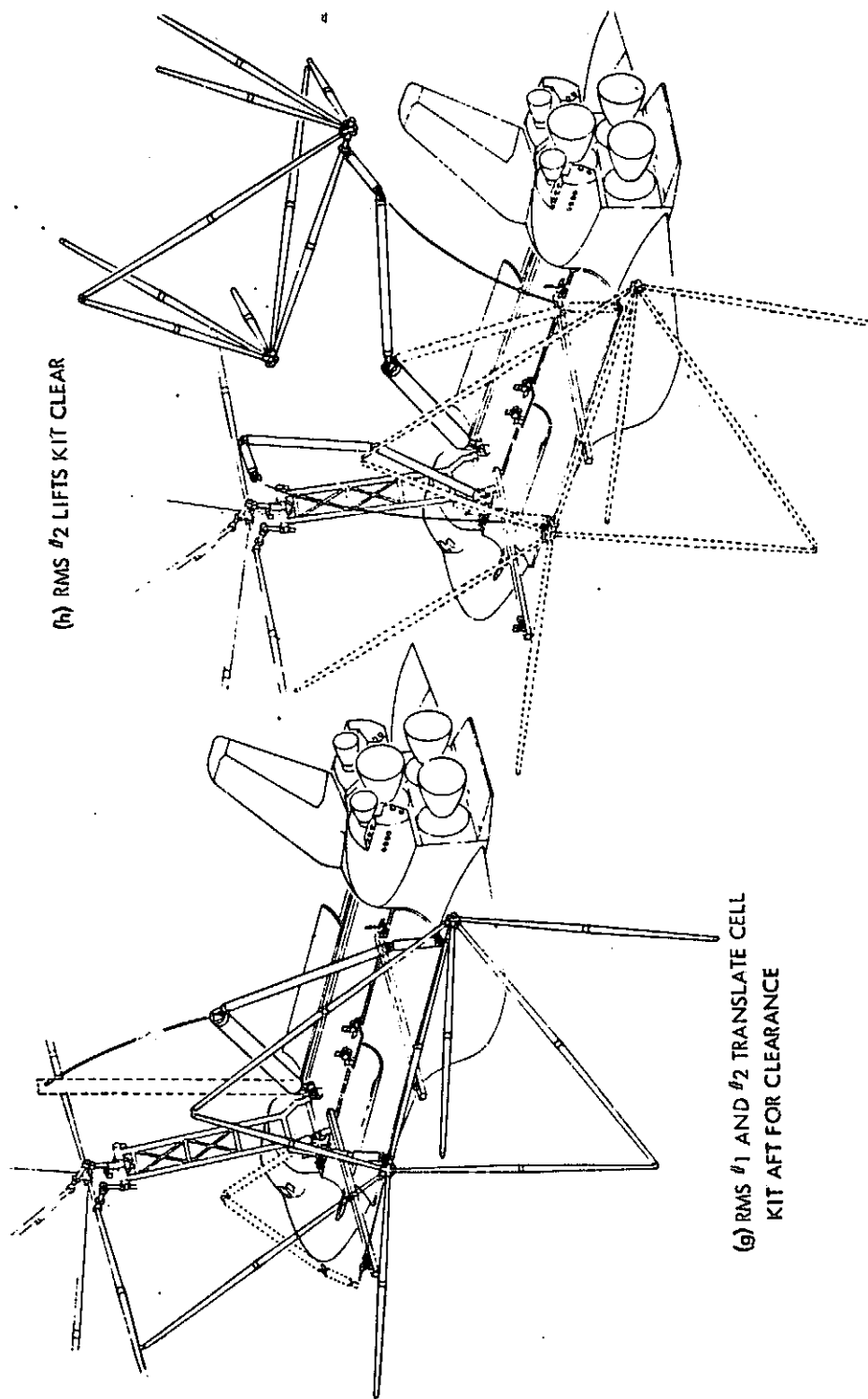


Figure 3.3-6D Assembly Sequence of Tetrahedral Area Platform (Con't)



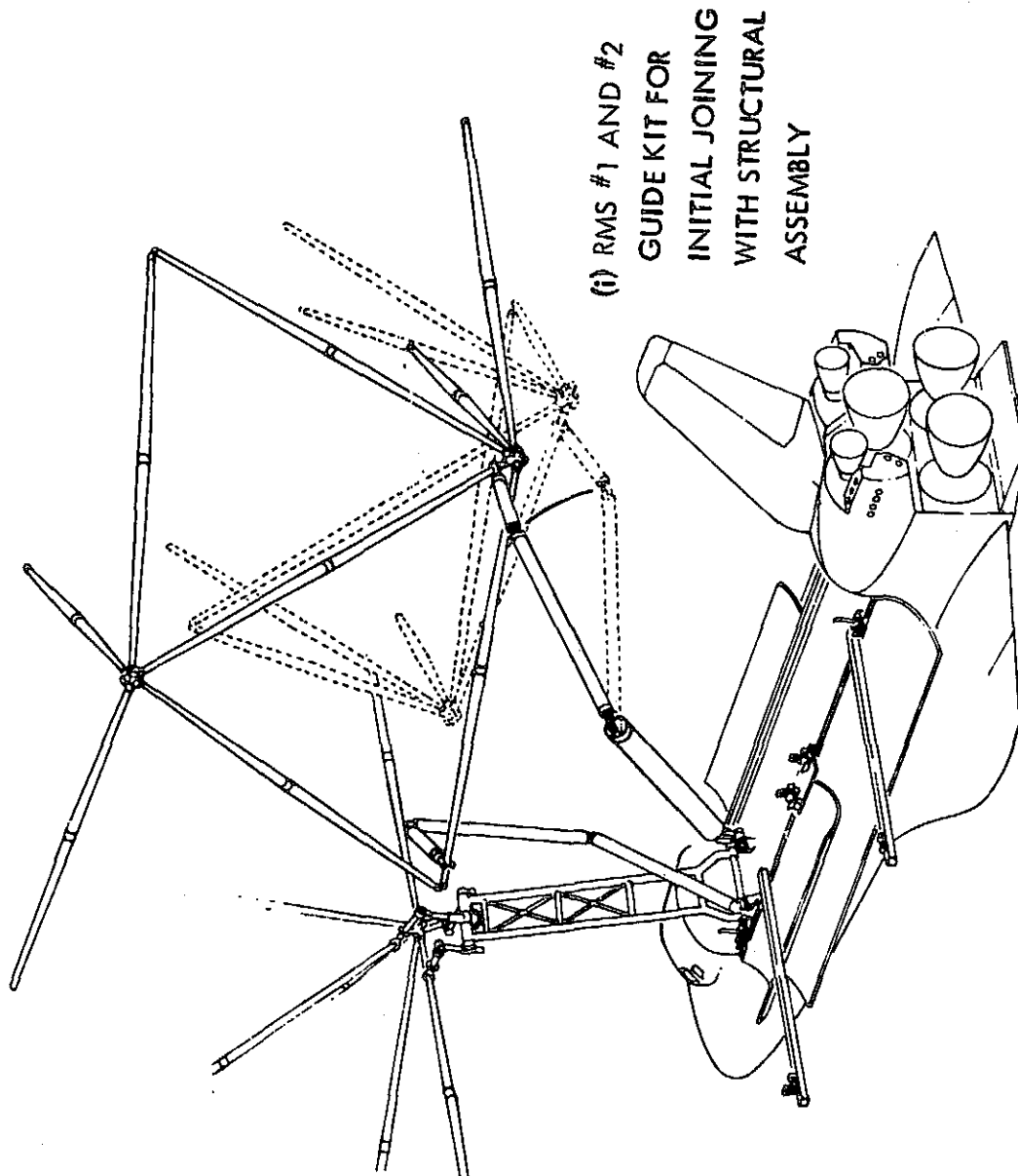


Figure 3.3-6E Assembly Sequence of Tetrahedral Area Platform (Con't.)

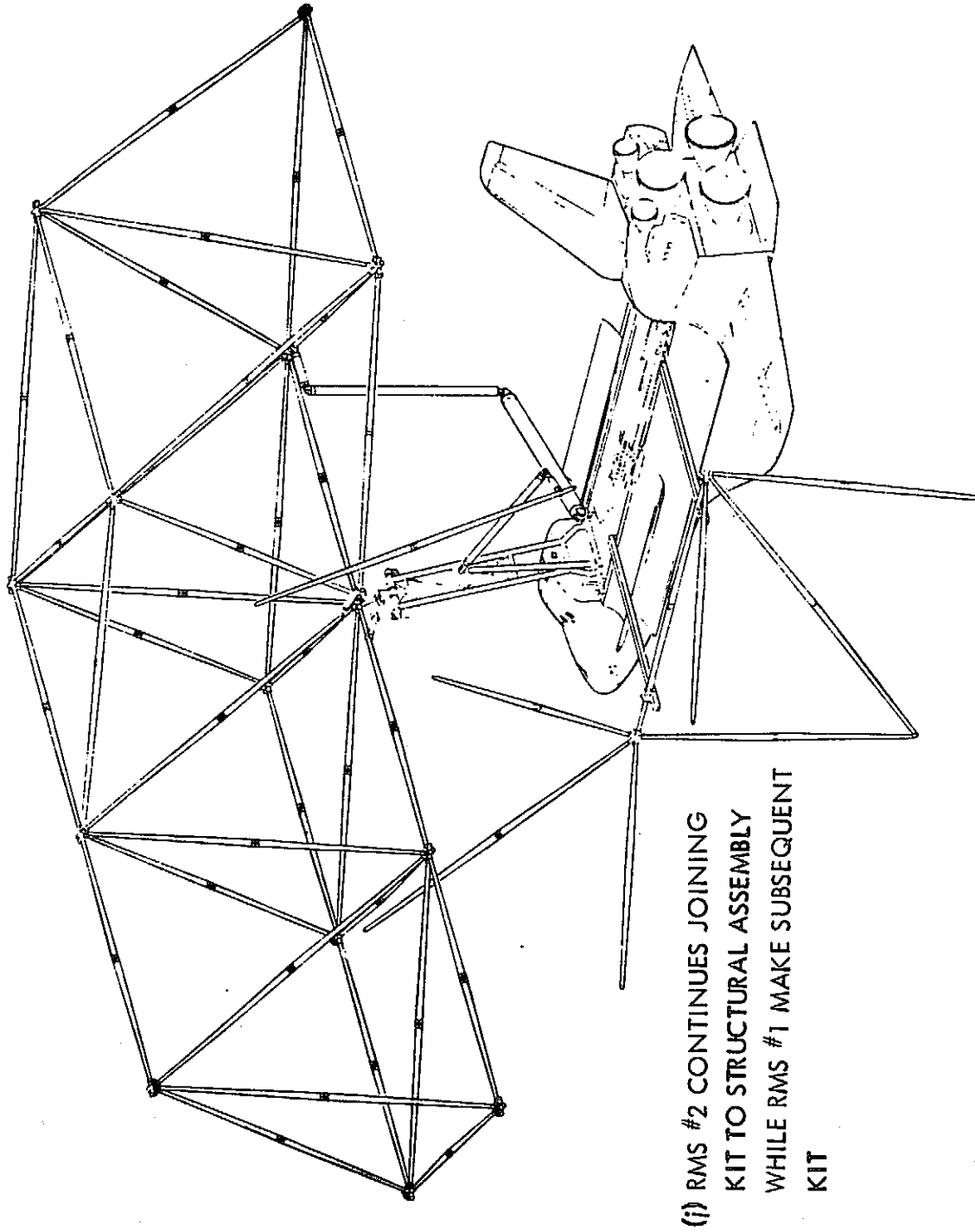


Figure 3.3-6F Assembly Sequence of Tetrahedral Area Platform (Con't.)

3. RMS #1, then, extracts one column segment out of the stack, as shown in sketch (c), while lifting and rotating to avoid the trapeze.
4. In sketch (d), the end arm of RMS #1 rotates the column segment clear of the trapeze, the orbiter forward bulkhead, and the upper arm RMS #1.
5. The RMS subsequently swings the column segment 180° and places it on one end of the column assembly fixture as shown in sketch (e).
6. Steps 1 through 5 are repeated for another column segment and the two strut segments are mated together in the strut assembly fixture.
7. Steps 1 through 5 are repeated twice where two unions instead of two column segments are secured from the cargo bay and coupled to the assembled full column, one at each end, while it is still in the column assembly fixture.
8. RMS #1 lifts the subassembly of one full column and two unions and places it across the cell kit assembly fixture.
9. Steps 1 through 5 are repeated twice to assemble a second full column.
10. RMS #1 lifts the second column from the column assembly fixture, transfers it to the cell kit assembly fixture and effects a coupling of one end of the second column to one of the unions. The second column, at this point in time, is in a plane 45° from the vertical. By design, this was dictated by the placement of the initial column in the cell kit assembly fixture in order to provide adequate clearance between the cell kit as it is being assembled and the partially assembled main structure.
11. Steps 1 through 5 and 9 and 10 are repeated sufficiently to assemble and attach two more full columns in the 45° position.
12. At this point in time, the initial column of the cell kit which is laying across the cell kit assembly fixture is rotated 60° away from the orbiter.
13. Step 11 is repeated for two more columns.
14. Step 12 is repeated.
15. Step 11 is repeated for three more columns to complete the cell kit assembly.

16. RMS #1 lifts the completed cell kit out of its assembly fixture, as shown in sketch (f). Note that the cantilevered end of one column is directly underneath the partially assembled main structures.
17. RMS #1 translates the completed cell kit laterally (towards the aft end of the orbiter) in order to withdraw all parts of the cell kit from underneath the main structure as shown in sketch (g). (g). Meanwhile, RMS #2 grips the end of the common column of the cell kit.
18. RMS #1 releases its grip on the cell kit and RMS #2 lifts the cell kit up and towards the main structure as shown in sketch (h).
19. RMS #2 rotates the cell kit 140°, as shown in sketch (i), ending in a position very much similar to its final attachment position. RMS #1, at this time, effects the first joint while the cell kit is being held by RMS #2. Subsequently, RMS #1 will start another cycle in its operational sequence.
20. The end arm of RMS #2 releases its grip on a common column and effects the coupling of the remaining columns to their respective unions as seen in sketch (i). Meanwhile, RMS #1 is ready to extract one column segment from its stack similar to its operation in sketch (b).

The above described procedure was used as the basis for the timeline analysis reported in the next section. It should be noted, again, that a great number of variations of the above described procedure could be visualized. It is believed, however, that the described assembly sequence will provide a conservative approach for initial analyses.

A concept for the assembly of mission equipment and subsystem is depicted in Figure 3.3-7. The concept utilizes RMS #1 as a transport agent for transferring mission equipment and subsystem from the stowed position in the orbiter cargo bay to the installation site, and effects the installation. The concept also utilizes RMS #2 as a berthing/docking agent and its TV cameras as the installation guide. The concept is applicable with equal suitability to both the area and the linear platform configurations. However, certain features inherent in the area platform need to be pointed out. If a central site on the platform is required for the installation of a particular mission module, a nearby docking site for the orbiter is dictated. This situation presents two possible conditions as shown in Figure 3.3-8 where the effective length of the RMS is reduced by that portion that lies within the physical envelope of the orbiter.

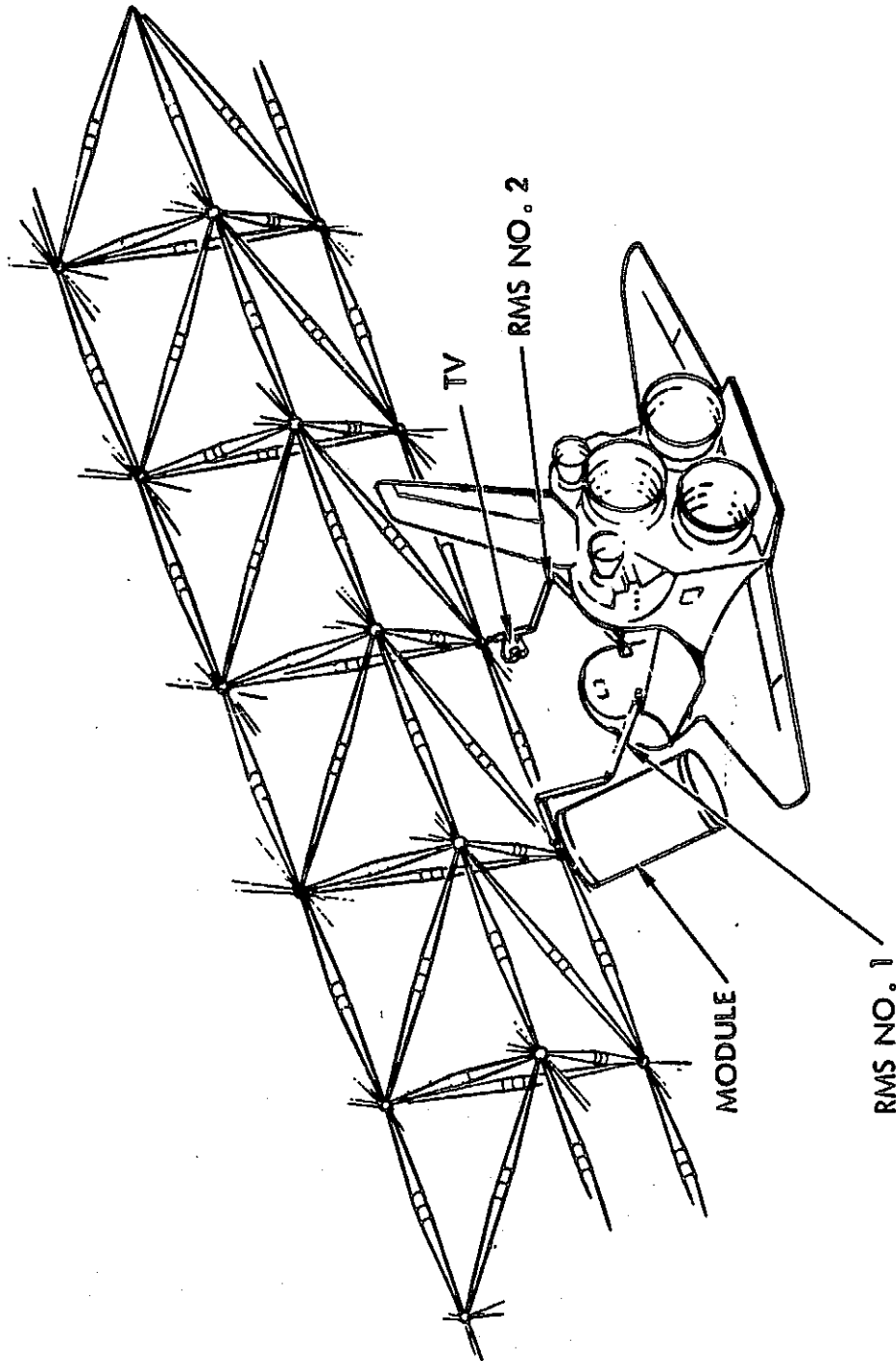


Figure 3.3-7 Module Installation Concept

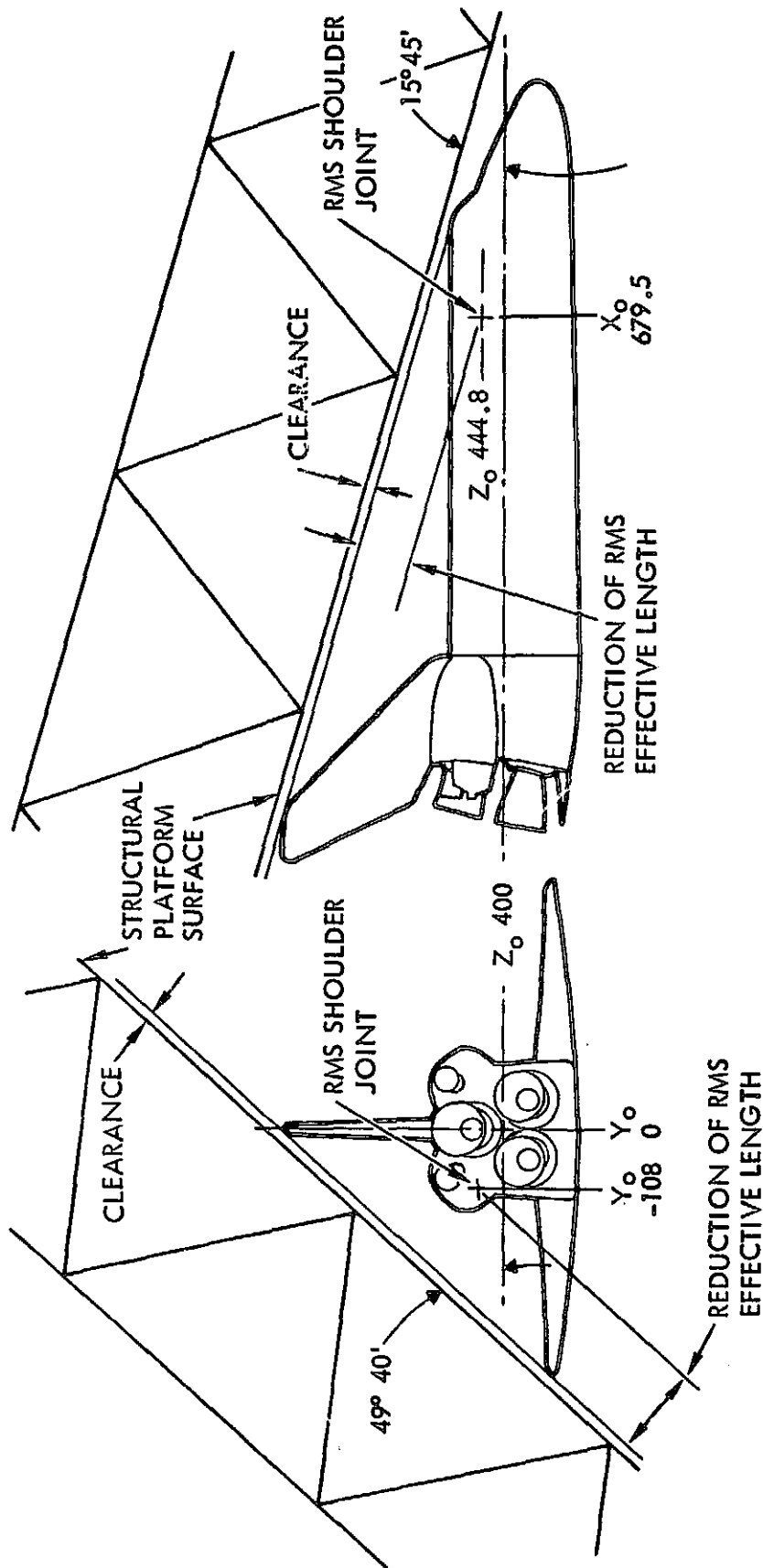


Figure 3.3-8 RMS Effective Length

### 3.3.4 Area Platform Timeline Factors

This report section presents the results of a preliminary timeline analysis for the tetrahedral area platform assembly. The timeline is based on the assembly sequence detailed in the previous section. The timeline, of necessity, requires a number of assumptions and first time estimates for the mission procedures for the initial concept definitions of this nature. The assumptions and estimates on which the timeline steps are identified and the time summation procedures indicated. The general estimation procedure was to identify basic steps in the operational sequence and then apply a consistent set of application rules to the particular operational step.

The major set of sequential events for the assembly were tied to the RMS activities of grasping, translating, releasing, and joining the various construction elements into the finished products. Estimates were made for reasonable tip speed velocities and different allowances were made for the allowable translation speed depending on whether the RMS was empty (or lightly loaded) or whether a completed kit assembly was being transported or rotated as part of the assembly procedure.

The orbiter RMS is an essential part of the selected assembly procedure. The RMS operational specifications, as presently indicated in the available references, do not adequately identify the operational times and other details desired. The information available in several references was selected and summarized in Table 3.3-2. This background information was utilized in establishing a first set of velocity allowances for the assembly procedure. The preliminary time allocations are listed in Table 3.3-3.

Table 3.3-3 Timeline Assembly Activity Time Allowances

<u>Translation</u>	Tip Speed <u>m/min (ft/min)*</u>
RMS - Empty	30.48 (100)
RMS - Kit Assembly	7.62 (25)
<u>Rotation</u>	Kit Rotation Velocity** <u>(deg/min)</u>
RMS - Kit Assembly	30
<u>Final Closure and Grapple Time</u>	<u>Time (min)</u>
RMS	0.60
-----	
*Uniform acceleration/deceleration in 3.05m (10 ft) assumed	
**Uniform acceleration/deceleration in 15 deg. assumed	

The times required for all the detailed steps for one basic kit (nine columns and two unions) assembly and one basic kit installation were estimated. The time steps were then analyzed for consistency and values adjusted as seemed appropriate. The total number of operations, average translation or rotational dimensions, and average times for each type operation was then established. Table 3.3-4 provides the resulting summary of activities for the basic kit assembly. Table 3.3-5 gives a similar summary for the kit installation operations.

Some variations of these two major operational areas are required when mission equipment and subsystems are to be included in the assembly and installation routine. For the total mission, allowances must be made for the initial orbiter and construction aids startup and shutdown activities as well as for crew breaks for meals and other activities. Orbiter translations from one assembly location to the next also must be included in the construction time allocations.

### 3.3.5 Linear Platform Assembly Process

#### Construction Equipment

Based on similar assumptions as in the case of the area platform, the assembly operations of a linear platform required the following equipment (See Figure 3.3-5).

1. The standard RMS for the column segment assembly and full column assembly functions.
2. One construction fixture which is a combination of a column assembly tool to mate two segments together and a holding tool to hold the partially assembled structure while in the process of attaching additional columns. The holding tool will also include provisions for translating the structure one cell at a time for subsequent column installations.
3. Various supports and mechanisms within the orbiter cargo bay to restrain the column segment stacks and the union-joints during launch and to permit their extraction upon demand.
4. Closed circuit television and lighting provisions.

#### Assembly Operations

Figure 3.3-9 depicts the various assembly stages of the linear platform. The assembly procedure is similar to that of the area platform in its initial steps. In fact, Steps 1 through 10 of the assembly operations in Section 3.3.3 are applicable to the linear platform. The only exception is that a holding tool is used instead of cell kit assembly tool. Subsequent to the first 10 steps, the process of assembling columns and attaching them to the partially assembled structure is repeated until one cell (bay) has been completed. At that point, the holding tool translates the entire structure one cell (bay) away from the orbiter and the process continues in constructing another bay.



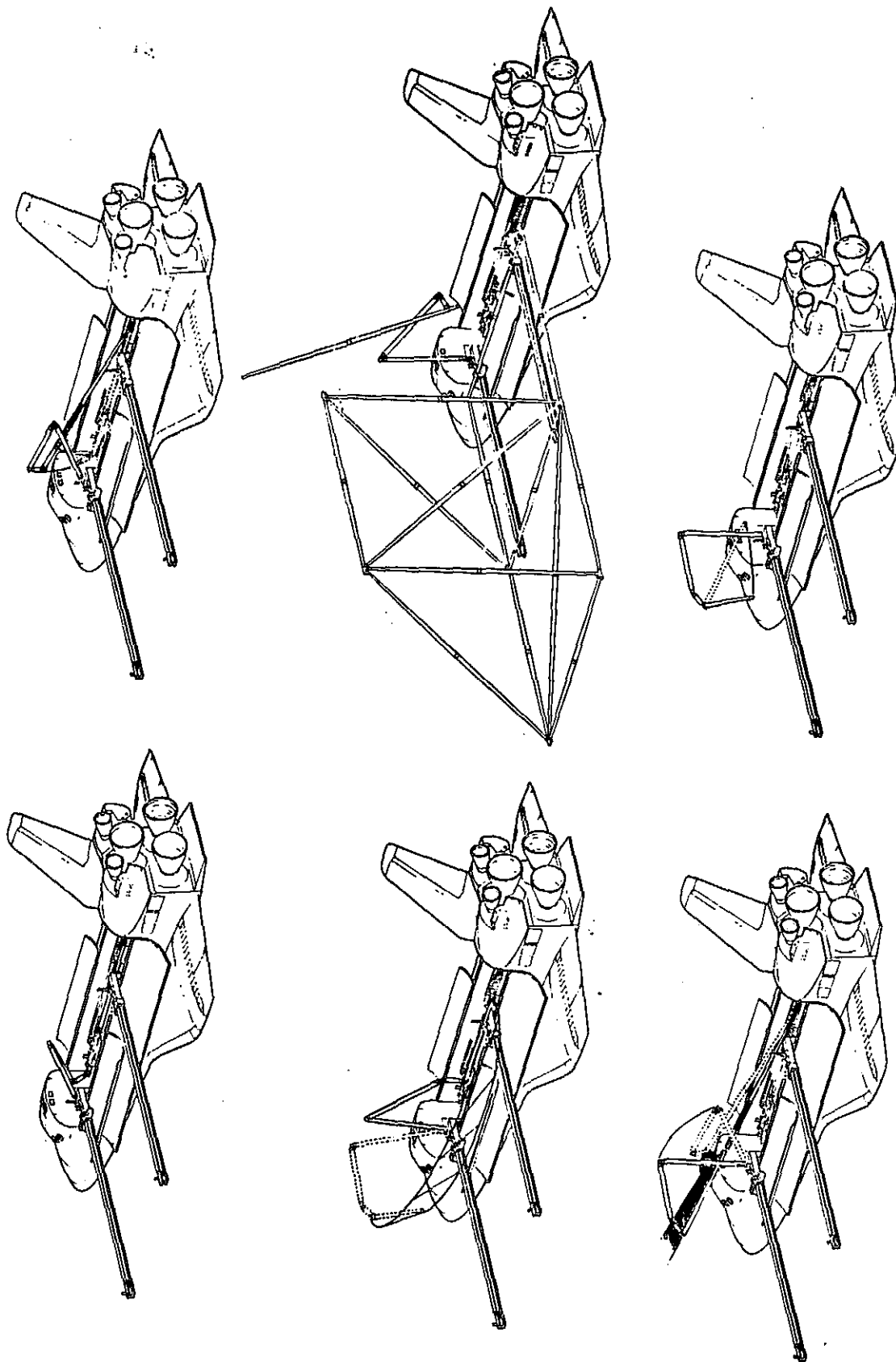


Figure 3.3-9 Assembly Sequence of Pentahedral Linear Platform



Table 3.3-5 Kit Assembly Time Summary  
(RMS #1 Operations)

Type of Operation	Number Operations	Average Time (min)	Time Per Kit (min)
1. RMS #1 translation, empty or light load	68	0.507	34.48
2. RMS #1 translation with kit assembly	1	1.60	1.60
3. RMS #1 column rotations	8	.94	7.50
4. RMS #1 final closure and grasp operations	28	.60	16.80
5. RMS column joining operations (in kit assembly fixtures)	27	.70	18.90
6. Slack time allocation	--	--	<u>.72</u>
Total Kit Assembly Time			80.00

Table 3.3-6 Kit Installation Time Summary  
(RMS #2 Operations)

Type of Operation	Number Operations	Average Time (min)	Time Per Kit (min)
1. RMS #2 translations, empty	9	.507	4.60
2. RMS #2 translations with kit assembly	2	2.40	4.80
3. RMS #2 kit rotations	2	3.50	7.00
4. RMS #2 final closure and grasp or joining operations	10	0.80	8.00
5. Slack time allocation	--	--	<u>.60</u>
Total Kit Installation Time			25.00

For installing mission equipment and subsystems, an equivalent procedure to that of the area platform can be utilized for the linear platform, which was illustrated in Figure 3.3-7. In that event, situations as shown in Figure 3.3-8 do not present themselves because the orbiter easily takes a posture, while docked to the platform, where its rudder and wings are not in proximity to the platform. Furthermore, if the assembly concept opted for a structural growth path in the orbiter's Z-axis, the effectiveness of the lighting provisions and visibility are enhanced.

### 3.3.6 Linear Platform Timelines Factors

As mentioned previously, the assumed assembly procedures for the linear platform have many operations similar to those used for the area platform standard cell kit assembly. The assembly of the nested struts can be identical in each case and the assembly of the linear platform cell in the holding tool uses many steps similar to the area platform cell kit assembly.

The linear platform "standard" cell is composed of eight 12-meter struts and one 17-meter diagonal strut (see Figure 3.3-1), plus three unions. The equivalent basic building unit for the area platform requires nine struts plus two unions. Because of the use of the non-standard 17-meter strut and the requirement for 14 joining connections (versus 10 for the cell kit assembly), the cell assembly time allocation for the linear platform cell was estimated at 90 minutes versus the 80 minutes for the area kit assembly (Table 3.3-5).

Table 3.3-6 shows an estimate of approximately 25 minutes as the requirement for the transfer and attachment of an area platform cell kit. The kit is moved from the assembly fixture to the proximity of the previously assembled platform and attached by use of both RMS #1 and RMS #2. It is estimated that RMS #1 can return to strut assembly after 10 minutes of dual RMS operations. For the linear platform, the equivalent operation consists only of transferring the completed linear platform "outboard" from the cell assembly location to allow the next cell to be constructed. An allowance of 15 minutes was made for this translation operation for the linear platform. A further comparison of the two platform assemblies will be shown in the next section.

### 3.3.7 Timeline Comparisons

It is desired to provide a summary of the times required to complete the structural assembly of the two platform models being compared in the study. Figure 3.3-10 shows an assembly timeline summary presented in Reference #4 (Page 13-38). The procedure and ground rules used in the previous study were followed in the present comparisons and the basic items are included in the Table 3.3-7 summary.

Item 5 of Table 3.3-7 refers to the allowance of time required for the orbiter to "walk" along the partially completed area structure in order to be in the proper location for the next cell kit attachment. The linear platform assembly process does not require this activity.

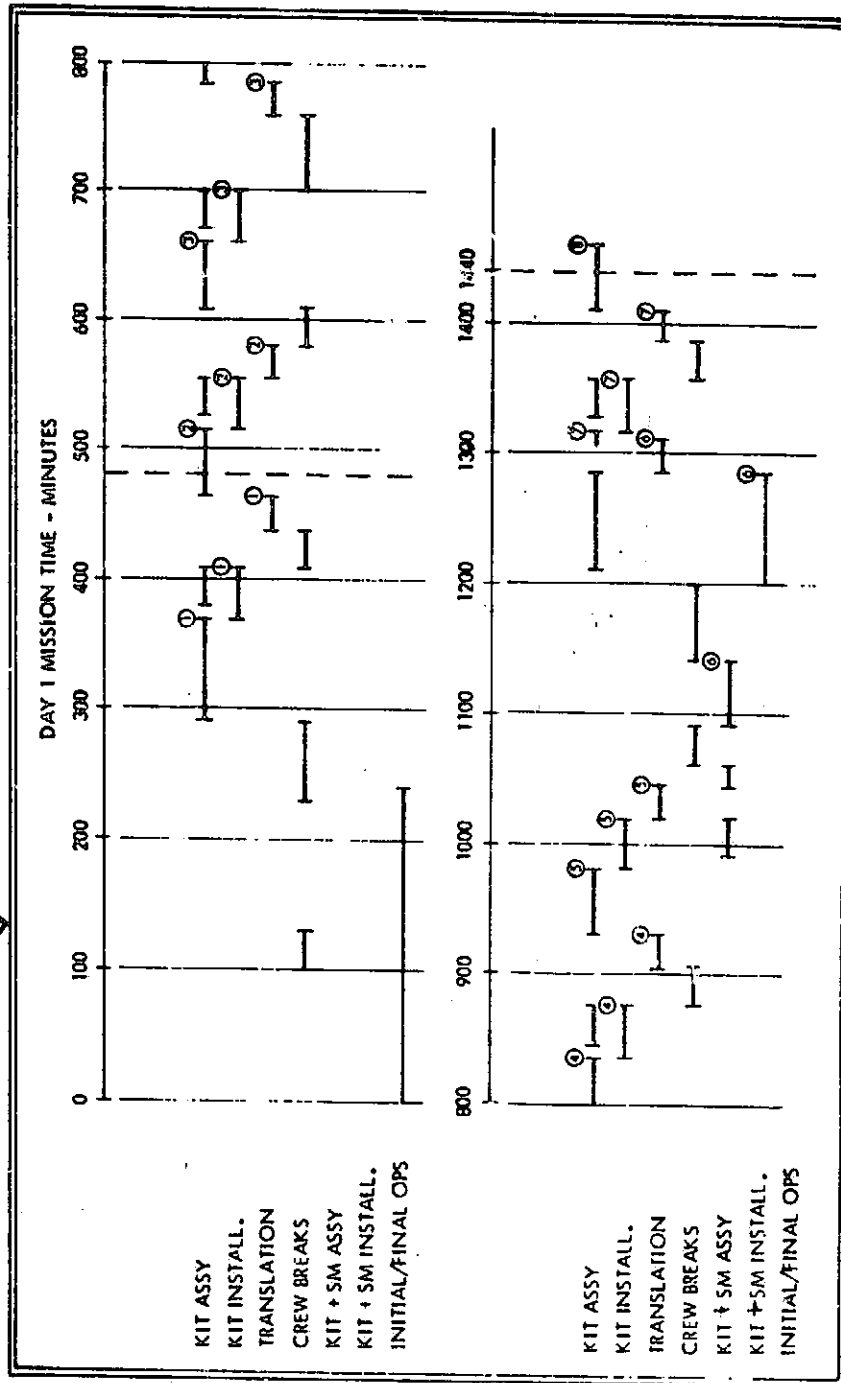
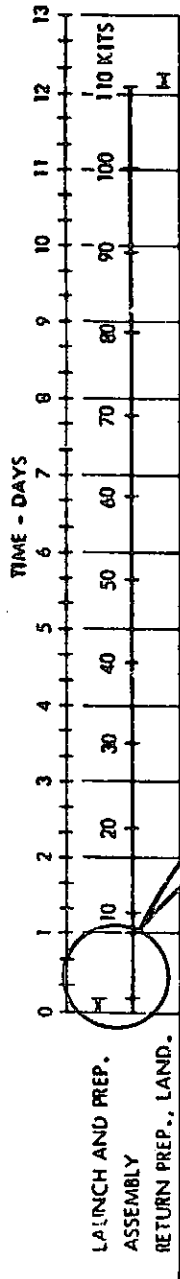


Figure 3.3-10 LSS Assembly Timeline

Table 3.3-7. Time Allocations for Assembly Comparisons

	Area			Linear		
1. Cell components						
Struts		9			9	
Unions		2			3	
2. Approximate kits/ cells required for complete platform		38			20	
3. Kit and cell assembly time alloca.		80 min.			90 min.	
4. Kit installation (15 min. of Item 3 during this activ- ity)		25 min.			—	
5. Translate orbiter relative to next kit installation location		25 min.			—	
6. Translate (12 m) linear structure in assembly fixture to next cell installa- tion location		—			15 min.	
7. Crew "break" dura- tions: (a) noon		60 min.			60 min.	
(b) morning/after- noon		30 min.			30 min.	
8. Approximate daily crew break start times (min.), three shifts:						
Morning	100	580	1060	100	580	1060
Noon	220	700	1190	220	700	1190
Afternoon	400	880	1360	400	880	1360
9. First day prepara- tion		240 min.			240 min.	
10. Last day shutdown		240 min.			240 min	

Table 3.3-8. Timeline Details

(Time in Minutes)					
Area			Linear		
Activity	$\Delta$	$\Sigma$	Activity	$\Delta$	$\Sigma$
<u>DAY 1</u>			<u>DAY 1</u>		
Preparation	240	240	Same	240	240
Noon break	220-280	280	Same		280
Kit 1 assembly	(280-360) 80	360	Cell 1 assembly	90	370
Transl. & install	(360-385) 25	385	Translate	15	385
Orbiter trans-					
late (A)	(385-400) 15	400	Start Cell 2 (A)	15	400
Afternoon break	30	430	Break	30	
Orbiter trans-					
late (B)	(430-440) 10	440	Complete Cell 2 (B)	75	505
Kit 2 assy (A)	(370-385) 15	-	Translate	15	520
Kit 2 assy (B)	(440-505) 65	505	Cell 3 assy (A)	60	580
Transl. & install	(505-530) 25	530			
Orbiter transl.	(530-555) 25	555			
Kit 3 assy (A)	(515-530) 15	-			
Kit 3 assy (B)	(555-580) 25	580			
Morning break	30	610	Break	30	610
Kit 3 assy (C)	(610-650) 40	650	Cell 3 assy (B)	30	640
Transl. & install	(650-675) 25	675	Translate	15	655
Orbiter transl.	25	700	Cell 4 assy (A)	45	700
Noon break	60	760	Noon break	60	760
Kit 4 assy (A)	(660-675) 15	-	Cell 4 assy (B)	45	805
Kit 4 assy (B)	(760-825) 65	825	Translate	15	820
Transl. & install	(825-850) 25	850	Cell 5 assy (A)	60	880
Orbiter transl.	(850-875) 25	875			
Kit 5 assy (A)	(835-850) 15	-			
Kit 5 assy (B)	(875-880) 5	880			
Afternoon break	30	910	Break	30	910
Kit 5 assy (C)	(910-970) 60	970	Cell 5 assy (B)	30	940
Transl. & install	(970-995) 25	995	Translate	15	955
Orbiter transl.	(995-1020) 25	1020	Cell 6 assy	90	1045
Kit 6 assy (A)	(980-995) 15	-	Translate	15	1060
Kit 6 assy (B)	(1020-1060) 40	1060			
Morning break	(1060-1090) 30	1090	Break	30	1090
Kit 6 assy (C)	(1090-1115) 25	1115	Cell 7 assy	90	1180
Transl. & install	(1115-1140) 25	1140	Translate (A)	10	1190
Orbiter transl.	(1140-1165) 25	1165			

Sheet 1 of 2

Table 3.3-8. Timeline Details (Cont.)

(Time in Minutes)					
Area			Linear		
Activity	Δ	Σ	Activity	Δ	Σ
Kit 7 assy (A)	(1125-1140) 15				
Kit 7 assy (B)	(1165-1190) 25	1190			
Noon break	(1190-1250) 60	1250	Noon break	60	1250
Kit 7 assy (C)	(1250-1290) 40	1290	Translate (B)	5	1255
Transl. & install	(1290-1315) 25	1315	Cell 8 assy	90	1345
Orbiter transl.	(1315-1340) 25	1340	Translate	15	1360
Kit 8 assy (A)	(1300-1315) 15	-			
Kit 8 assy (B)	(1340-1360) 20	1360			
Afternoon break	(1360-1390) 30	1390	Break	30	1390
Kit 8 assy (C)	(1390-1435) 45	1435	Cell 9 assy (A)	50	1440
Translate and install (A)	(1435-1440) 5	1440			
<u>DAY 2</u>			<u>DAY 2</u>		
Transl. & install	(0-20) 20	20	Cell 9 assy (B)	40	40
Orbiter transl.	(20-45) 5	45	Translate	15	55
Kit 9 assy (A)	(5-20) 15	-	Cell 10 assy (A)	45	100
Kit 9 assy (B)	(45-100) 55	100			
Morning break	(100-130) 30	130	Break	30	130
Kit 9 assy (C)	(130-140) 10	140	Cell 10 assy (B)	45	175
Transl. & install	(140-165) 25	165	Translate	15	190
Orbiter translate	(165-190) 25	190	Cell 11 assy (A)	30	220
Kit 10 assy (A)	(150-165) 15	-			
Kit 10 assy (B)	(190-220) 30	220			
Noon break	(220-280) 60	280	Noon break	60	280
<u>END 24 HOURS ASSEMBLY OPERATIONS</u>					
Approximate rate			Approximate rate		
$= \frac{9.56}{24} = 0.398 \text{ kits/hr}$			$= \frac{10.33}{24} = 0.430 \text{ cells/hr}$		
or 2.51 hr/kit			or 2.32 hr/kit		



Table 3.3-8 summarizes a 24 hour period of assembly activities for both of the platform concepts. The results of this analysis indicate that the rate of construction on a "per kit" or "per cell" basis are not greatly different (2.5 versus 2.3 hours per completion). However, the platform designs which required approximately the equivalent of 38 tetrahedral standard kits for the area platform as compared with 20 pentahedral cells for the linear platform resulted in widely different times for the platform assembly. Table 3.3-9 provides the summary of the timelines for the two platforms. The area platform structure, under the assumed ground rules was estimated to require 4.32 days for completion. The linear platform was similarly estimated to require only 2.28 days. Thus, on the basis of assembly time comparisons, the linear structure provides a marked advantage.

Table 3.3-9 Timeline Comparison Summary

	Area Platform	Linear Platform
1. Preparation for Assembly (4 hr)	0.17 days	0.17 days
2. Area Platform Structure Assembly (38 kit equivalent, 0.398 kits/hr rate: $\frac{38}{.398 \times 24} = 3.98 \text{ days}$	3.98	--
3. Linear Platform Structure Assembly (20 cells at 0.445 cells/hr: $\frac{20}{.43 \times 24} = 1.94 \text{ days}$	--	1.94
4. Assembly Shutdown (4 hr)	<u>0.17</u>	<u>0.17</u>
Totals	4.32 days	2.28 days

### 3.3.8 Significant Findings

#### Similarities

The following project characteristics were found to be essentially similar, and thus not pertinent to a comparison of relative merits of the differing shapes.

- o Structural Components Types
- o Module Installation at Periphery of Platform
- o Construction Equipment Types
  - RMS's
  - Construction Fixture
  - Supports & Mechanisms
  - CCTV & Lighting Provisions
- o Cable and Connector Design

#### Differences

The number of structural components that are required for the linear platform are considerably less than those required to construct the area platform. However, the linear platform requires two different strut sizes (12.0m and 17.0m) whereas only one standard size (12.0m) is needed for the area platform. The longer strut will also dictate a larger construction fixture for the linear platform. Nevertheless, the larger fixture is not expected to be beyond the reach capabilities of the RMS.

Construction equipment requirements provide another advantage for the linear platform. All the equipment required to construct the linear platform will be required for constructing the area platform. Additionally two major pieces, namely, a second RMS and the trapeze are needed for the area platform. Otherwise, similar complexity factors are foreseen for the common equipment of the two platforms.

The assembly operations envisioned for the area platform are considered more complex than the linear platform. This complexity is caused, mainly, by the simultaneous operation of two manipulators and the necessity for "walking" the orbiter from one position to another. The linear platform assembly process avoids these complexities in its continuous construction scene. The installation of mission equipment and subsystems during the construction process can be similar for both platforms in terms of operational sequence. However, the area platform process reduces the effective length of the RMS, as shown in Figure 3.3-8, and its visibility provisions are dependent on CCTV cameras, which, by virtue of their positions, cannot view the actual interfacing surface. The comparatively smaller width of the linear platform makes it possible to avoid the conditions shown in Figure 3.3-8 and, in addition to the CCTV camera, direct visual contact of the interfacing surface by the RMS operator is a distinct possibility. This is especially true if the construction path of the linear platform is parallel to the Z-axis of the orbiter.

The design of power and signal distribution systems are similar for both platforms, in that similar cable and connector designs can be utilized. However, the area platform potentially has an advantage because it requires 26 interconnects, whereas, the linear platform requires 42 interconnects. Nevertheless, it is conceivably less complex to install the interconnects on the linear platform than on the area platform, because the linear configuration lends itself to mass production-type assembly techniques.

### 3.3.9 References

1. Rockwell International  
Space Construction System Analysis, Task 2  
Final Report - System Analysis of Space Construction,  
SSD79-0, Satellite Systems Division, Space Systems  
Group, June 1979
2. Rockwell International  
Space Construction System Analysis,  
Space Construction Data Base, SSD79-0  
Satellite Systems Division, Space Systems Group,  
June 1979
3. Rockwell International  
Space Construction Systems Shuttle Integration,  
SSD 79-0, Satellite Systems Division, Space  
Systems Group, June 1979
4. Rockwell International  
Advanced Technology Laboratory Program for Large  
Space Structures, Parts 1 & 2 Final Report,  
SD 76-SA-0210 (NASA CR-145206), May 1977
5. Katz, E., J. A. Boddy and A. N. Lillenas  
Advanced Technology Laboratory Program for Large  
Space Structures, Part 3 Final Report, Flight  
Experiment Description SD 77-AP-0071-1 (NASA CR-145256)  
Rockwell International, Space Division, June 1977

## 4.0 COMMUNICATION PLATFORM STUDY

### 4.1 INTRODUCTION AND SUMMARY

Collins Transmission Systems Division of Rockwell International is pleased to submit this report to the National Aeronautics and Space Administration, Johnson Space Center, as part of Contract Number NAS9-15718, Space Construction System Analysis Study, under subcontract to the Rockwell Space Systems Group. The Collins Transmission Systems Division has a background of experience and expertise in satellite communications systems. Collins developed Apollo Communications Systems in the mid-sixties, systems which have stood for many years as a standard of performance for space communications systems. More recently, the Transmission Systems Division has provided ground stations for American Telephone and Telegraph Company for their backbone network for the Public Broadcasting System Interconnect System, in which one hundred and sixty-two earth stations were provided, largest contract of this kind let. The Collins Transmission Systems Division is currently under contract to the Public Broadcasting System to supply the National Public Radio Interconnect System (204 earth stations). Both of the latter systems employ the Westar satellite. In addition to these two large programs, the Collins Transmission Systems Division is providing a plethora of small ground stations to many individual users primarily in the television receive only market. This report was developed by the personnel of the Collins Transmission Systems Division and Electronics Operations staff.

The television distribution by satellite market has exhibited extraordinary growth over the past two years. As a result of this growth, new technology is being developed to more properly utilize the allocated bandwidth for satellite transmission systems. Even with the emphasis on new technology and spectrum conservation the demand for satellite communications appears to be growing at a rate faster than ever conceived by those regulatory bodies which have allocated frequency spectrum. As a result, considerable attention has been focused on allocation of additional spectrum to insure that capacity be provided by the satellite operating companies. However, it does appear that saturation will occur at an early date. This report discusses when saturation will occur, based on varying assumptions concerning technical and regulatory decisions, along with market demand.

The study was conducted in two basic segments: Segment one culminated in a presentation to Johnson Space Center on 21 March 1979. This presentation covered the initial segment which investigated the need for additional capabilities for providing additional communications capacity through frequency reuse. Included were topics such as the status and capability of the current satellite constellation, including the satellites in orbit and their transponder configurations, the projected demand for services based upon studies by Rockwell and other organizations, the capability of future satellites, and finally a projection concerning the saturation of the orbital arc and frequency spectrum, resulting in the need for a method of frequency reuse. A multiple beam communications platform was postulated as a method to implement frequency reuse.

The second segment of the study emphasized the evolution of a space platform. Due to the fact that the space platform itself requires a major investment on the part of its owner, the proper definition of this vehicle is mandatory. The second segment of the study further defined the plans for the communications satellites of the eighties to determine the trends and directions of the satellite operating companies. A straw-man system was developed for the ultimate platform to develop the technology areas which are in need of validation. Finally, a projection was made for future work in this area.

The traffic demand projections were based upon voice, data, video, and electronic mail only. Traffic projections for plane/truck location, police, ambulance and emergency services were not made at this time. Also not covered in this report are:

1. Maintenance requirements for the ATP.
2. Special construction techniques for electrical circuits, feedhorns, etc.
3. Upgrading or expansion techniques for growth or for frequency band changes.

In summary, the extraordinary growth of satellite communications, the limited bandwidth, and the crowded occupancy of the orbital arc will result in saturation of 4/6 GHz band in 1989-92 and the 12/14 GHz band in 1993-96 as presented in Figure 4-1. This saturation is due to the poor frequency re-use factor inherent in the single-beam per satellite system in present use. By utilizing multiple-beam satellites, the frequency re-use factor can be greatly increased and the saturation alleviated so that much more traffic can be handled.

Before the multiple-beam system can be designed with confidence, a pilot test with 50 beams should be attempted on the Application Test Platform as noted on the summary chart. By using heavily tapered aperture illumination and low-surface roughness, offset-fed reflectors, the sidelobe levels, isolation, and frequency re-use factors can be determined so that operational antennas can be deployed in the 1990 to 1994 time frame.

The pilot system as first deployed on the ATP will be designed for replacement and/or upgrading. In this manner the operational antennas can later be incorporated on the platform. This capability for docking, refueling, and replacement on the ATP stands in contrast to the ATS-6 program which is limited in this respect. Indeed, once the 50 beam system is proved feasible, NASA can lease the system to a common carrier for commercial use to augment the present single-beam satellite communication system until more capability is needed. At the same time this work is being carried out, much use of the ATP will be utilized in the areas of propagation measurements, RFI, low-cost TV, electronic mail pilot programs, data relay, and emergency aircraft beacon locating. Design of the Applications Test Platform should begin in 1982 or before so that launch could be by 1987.

#### 4.2 THE NEED FOR A TELECOMMUNICATIONS PLATFORM

Due to the extraordinary growth of satellite communications, the limited bandwidth and occupancy of the orbital arc will result in saturation of the domestic satellite communications network at some point in time. To enable the communication needs to be met, there are several avenues for relief,

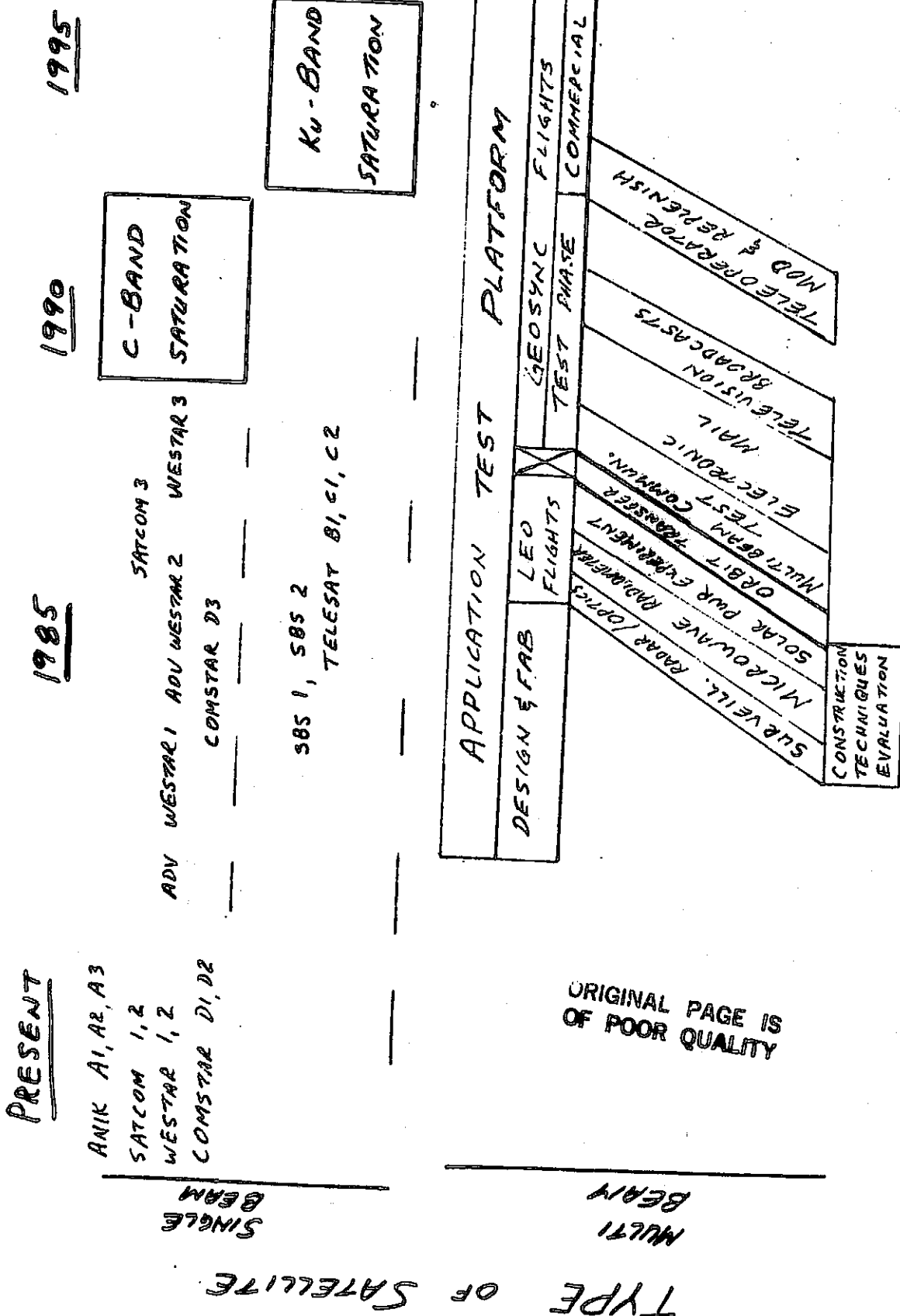


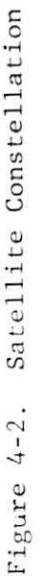
Figure 4-1 Scenario of Space Communications for Continental U.S.A.

including (1) allocation of additional spectrum, (2) better utilization of existing spectrum, and (3) adding additional satellites in the limited orbital space. This study addresses the second point, describing a new technique for frequency reuse based on a space platform employing multiple switched beam antennas.

#### 4.2.1 Current DOMSAT Constellation Capability

Figure 4-2 shows the satellite constellation in synchronous orbit. The two bands describe the satellite configuration in synchronous orbit for C and Ku band\* communications satellites. C band and Ku band are the currently authorized bands which are authorized by the FCC for Commercial Satellite Communications. Note that there are a number of satellites which carry both C and Ku band transponders. Figure 4-3 gives a further description of the satellite configuration. There are currently three United States domestic satellite operating companies, Western Union, Radio Corporation of America, and Comsat, leasing to American Telephone and Telegraph Company. The satellites which these companies operate are known as the Westar satellites, and the Comstar satellites, respectively. In addition, Figures 4-2 and 4-3 show the satellites belonging to other operators such as Telesat, who have the license to provide satellite communications to Canada. Note that satellites approximately placed from seventy degrees to 150 degrees west longitude are capable of illuminating the continental United States. Satellite spacing is restricted to approximately four degrees, due to the fact that each of these satellites (or most of the satellites) have beams which cover the full continental United States, so that interference from an adjacent satellite is possible unless the ground receiving antenna has a narrow beam, much less than four degrees, and with very good side lobes. Each one of the satellites is capable of transmission and reception over a full 500 MHz frequency band. A survey of the utilization of current United States domestic satellite transponders is continually updated by the cable television journal magazine. The results of this survey, somewhat modified by private information from the carriers is indicated in Table 4-1. This shows that of the total number of transponders, 144, the capacity is largely unused. It is expected that this situation may change considerably this summer when a set of restrictions limiting the use of the Comstar satellites is lifted by the Federal Communications Commission. One may note that the Comstar satellite system is used primarily for voice and data, i.e., narrow band communication, whereas the Satcom satellites are used primarily for video transmission. The Westar satellites are used primarily for video but due to the nature of the operator, have considerable voice and data carriage. Note that this table is constructed on the basis of continuous operation. Table 4-2 gives a projection of the near trend growth of the satellites in orbit. These projections are merely estimates and have been taken from personal conversations with individuals who may or may not have correctly forecast the launch dates past 1979. The launch dates are variable due to any number of factors. A failure of a satellite in orbit would cause a total change in the launch plans. Any perturbation due to reallocation of slots due to the WARC would change the capacity complexion. Due to the tie-in between the advanced Westar and the TDRSS transponders

\*C-band allocations are 5925-6425 MHz (uplink) and 3700-4200 MHz (downlink).  
Ku-band allocations are 11,700 to 12,200 MHz (downlink) and 14000 to 14500 MHz (uplink).





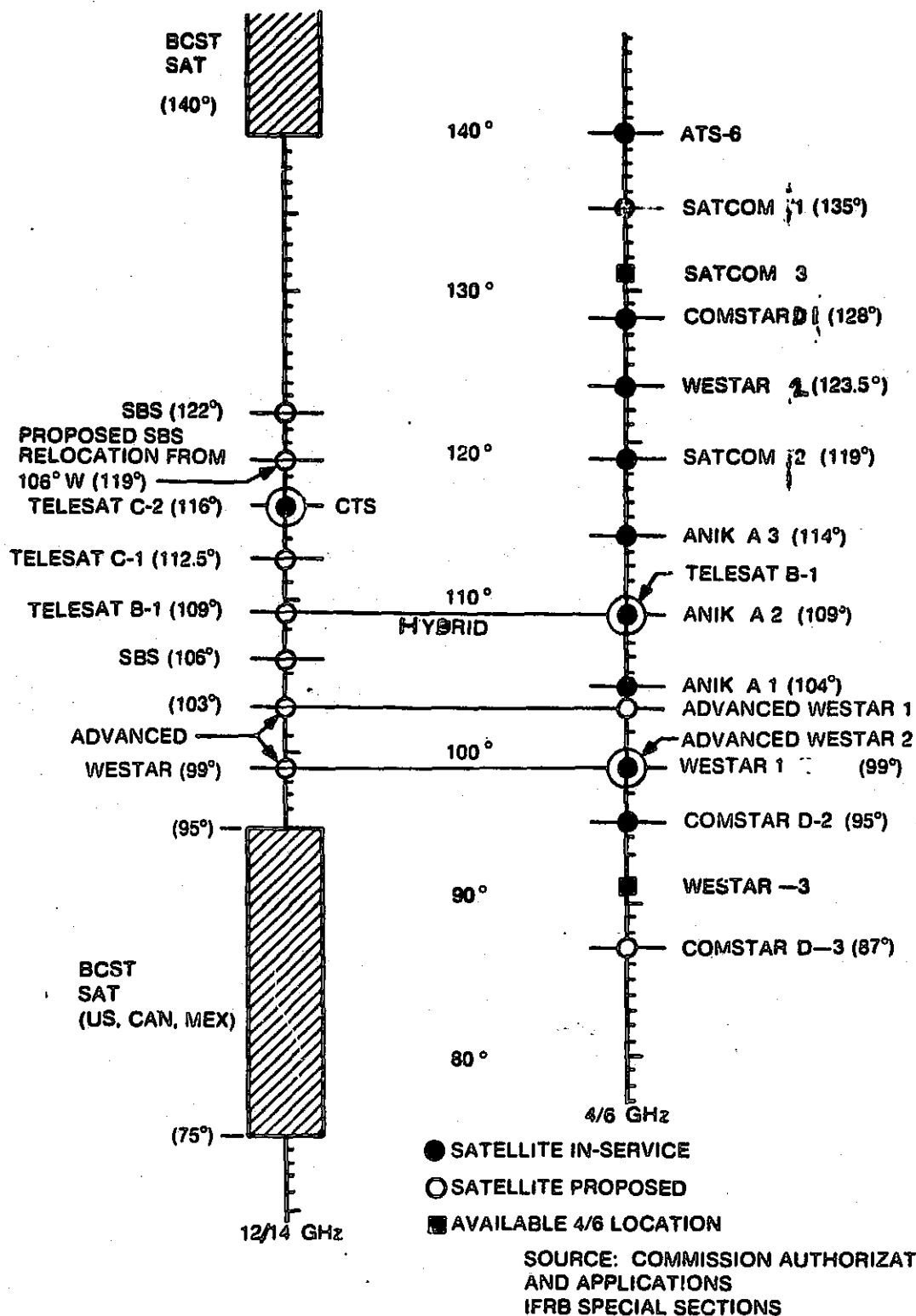


Figure 4-3 C & Ku Band Orbital Arcs



Table 4-1 Current U.S. DOMSAT Transponders

	<u>VOICE/DATA</u>	<u>VIDEO</u>	<u>UNUSED</u>
COMSTAR (AT&T)	8	0	64
SATCOM (RCA)	2	24	22
WESTAR (WESTERN UNION)	<u>8</u>	<u>12</u>	<u>4</u>
TOTAL	18	36	90
			144

Table 4-2 Postulated Growth

OPERATUR	SATELLITE	LAUNCH DATE	CONFIGURATION					LIFE (YRS)	
			C-BAND		KU-BAND				
			#TRANS	BW	#	TRANS	BW		BEAM W
RCA *	F3	1978	24	36					5-7
	F4	Ground Spare	24	36					5-7
	F5	1982	24+4sp	36					7-10
	F6	1982	24+4sp	36					7-10
	F7	Slot Allocation	24+4sp	36					7-10
	F8	Slot Allocation	24+4sp	36					7-10
	W3	1979	12	36					5-7
	AW-1	1982	12	36	2	225	Fixed (T.Z.)	7-10	
Comsat (AT&T Lease)	AW-2	1982	12	36	2	225	Fixed (T.Z.)	7-10	
	C5	1983	24	36	1	500	Scan	7-10	
	C6	1983	24	36	1	500	Scan	7-10	
	C7	1984	24	36	1	500	Scan	7-10	
	C8	Ground Spare	24	36	1	500	Scan	7-10	
	C9	Slot Allocation	24	36	1	500	Scan	7-10	
	C10	Slot Allocation	24	36	1	500	Scan	7-10	

\* Certain satellites have Hawaii and Alaska beams.

C-2

the advanced Westar launches appear to also have some variability. The new Comstar satellites may employ a Ku band scanning beam with a 500 MHz transponder which will certainly require considerable technology development. As a result, the technology risks in this development will require very careful validation prior to launch. These factors all have a bearing on the time table used for these satellites.

#### 4.2.2 Traffic Projections

Table 4-3 described the traffic projection assumptions underlying the projections to follow. One of the major factors in the analysis to follow is the assumption that an additional 250 MHz bandwidth will be granted by the World Administrative Radio Council (WARC). This 250 MHz bandwidth increases the available spectrum for C-band satellite communications by 50 percent. At the same time it is assumed that no additional bandwidth increase of this nature will be achieved for terrestrial radio. It is assumed however, that terrestrial radio will achieve increased utilization of the existing bandwidth through such techniques as digital time assigned speech interpolation. The fiber optics technology is a growth area which is very new and as a result projections in its use are relatively unstable, however, it is assumed that the use of this technology will be restricted to intra-city as opposed to long distance services which would compete with the satellite communications transmissions until the year 1990.

The data growth rate has been assumed to be the same as that of the total market which is roughly twenty percent per annum based on an average of several sources. It is also assumed that the satellite growth rate is equal to that of the total data growth rate. One should also be cautioned that a major part of the so-called data growth is contained in the segment known as electronic mail. The voice growth rate is approximately 10 percent per annum and it is assumed that the satellite voice growth rate is equal to that of the total market for voice long distance services which satellites are very well positioned to supply. The video growth rate was based on specific projections by other authors.

With these assumptions the specific projection based on average loading of transponders is given in Table 4-4. In an August 1978 memorandum to the Federal Communications Commission, American Telephone and Telecommunication's R. W. Warfield stated that "--loads presently vary from 6.4% to 63.2% in 1978--". Familiarity with the American Telephone and Telegraph Company system indicates that the estimated average utilization is roughly 16% (8 transponders), which generally agrees with published logs. Based on this data, the peak to average utilization of the transponder loading for voice, and perhaps data, is roughly four to one. If peak loading were used for the basis of estimate, transponder utilization for voice and data services as well as video would increase to 451 by the year 1990. If, on the other hand, peak loading were used only for voice, the demand is 373 in 1990, and in 2000 demand is 699.

Table 4-3 Traffic Projections/Assumptions

- ENHANCED BANDWIDTH UTILIZATION BUT NO ADDITIONAL BANDWIDTH FOR TERRESTRIAL RADIO.
- FIBER OPTICS ONLY REPLACES GROWTH IN TERRESTRIAL RADIO FOR INTRACITY SERVICES UNTIL 1990.
- DATA GROWTH RATE (TOTAL MARKET)
  - 20% PER ANNUM
  - SATELLITE DATA GROWTH RATE EQUAL TO TOTAL DATA GROWTH RATE.
- VOICE GROWTH RATE (TOTAL MARKET)
  - 10% PER ANNUM
  - SATELLITE VOICE GROWTH RATE EQUAL TO TOTAL VOICE GROWTH RATE.
- VIDEO GROWTH BASED ON SPECIFIC PROJECTIONS.

Table 4-4 Traffic Projections

(EQUIVALENT 36 MHZ TRANSPONDERS)

	<u>VOICE</u>	<u>DATA</u>	<u>VIDEO</u>	<u>TOTAL</u>
1980	14	4	60 ‡	78
1990	36	26	203	265
2000	93	103	224	420

‡ INCLUDES NETWORK PROGRAMMING (24 TRANSPONDERS)

#### 4.2.3 Capability

Table 4-5 lists the assumptions underlying the projection made for satellite communications capability. The current 36 MHz transponders carry considerably less than the 60 MBPS listed in the assumptions in Table 4-5. Rockwell International has supplied equipment to American Telephone and Telegraph Company which will allow over 60 MBPS to be carried within the 36 MHz transponder bandwidth. Preliminary test results have shown that 60 MBPS can be achieved operationally and perhaps higher rates may be accommodated. It is assumed additional C-band allocation will be granted by WARC. As may be noted in Figure 4-3, the area between 75 and 90 degrees west longitude is allocated by WARC to Ku-band broadcast. It is assumed that this particular segment of the orbital arc will continue to be allocated to the broadcast service. However, it is assumed that this direct service, if authorized by the FCC, will not diminish the demand for video services as presently constituted. It is assumed that Ku-band will not be limited to a single polarization, and will exhibit adequate rain performance. Both of these assumptions are somewhat tenuous, because a full scale test has not been made of the Ku-band operations. The CTS has demonstrated that Ku-band is feasible: what has not occurred is an adequate amount of testing to enable one to predict the operational reliability of the system. Table 4-6 describes the satellite communications capability with the foregoing assumptions in mind. The two columns indicating allocated and potential indicate the following: at C-band, an additional Satcom will be launched this year. This accounts for the 24 Satcom transponders in the allocated column. The Westar expansion is due two factors, one factor is that an additional Westar satellite will be shortly launched, and secondly that each of the Westar orbital slots potentially have the capability of doubling their communications capacity through frequency reuse using dual polarization. In addition, the potential column indicates an additional Comstar and an additional Satcom satellite in two easterly orbit locations not currently used. Finally, the bandwidth expansion at C-band assumes a 50% increase in the number of 36 MHz transponders over the total derived from additional satellites, frequencies, polarizations and orbital slots. At Ku-band the projection is somewhat more conservative due to the lack of an operational Ku-band satellite in orbit. In addition the one for four spare allocation is somewhat less than is currently used. As a result, one may conclude that roughly 450 36 MHz transponders is the capacity which can be achieved under the current frequency allocation and orbital arc allocation.

#### 4.2.4 Technical and Regulatory Factors

Table 4-7 indicates some of the factors which may alter the foregoing projections of supply and demand. As alluded to earlier, it may ultimately be possible to attain a 90 megabit per second transmission in a 36 MHz channel. This increases the capacity of existing or proposed satellites with this configuration. A lower spares reserve may be achieved through operational experience. It also may be determined that squeezing in the orbital arc may be possible without undue interference, especially if improvements are made in ground antennas. The 18/30 GHz bands represent additional potential, especially in the western U.S. In the capacity decrease area, the WARC may not add additional bandwidth at C-band, resulting in a marked change in the

Table 4-5 Satellite Communications Capability Assumptions

- 36 MHZ TRANSPONDERS CARRY 60 MBPS
- ADDITIONAL C-BAND ALLOCATION WILL BE GRANTED BY WARC
- 75° TO 95°W LONGITUDE WILL BE ALLOCATED TO Ku-BAND BROADCAST AND WILL NOT DIMINISH DEMAND.
- Ku-BAND NOT LIMITED TO SINGLE POLARIZATION
- Ku-BAND EXHIBITS ADEQUATE RAIN PERFORMANCE

Table 4-6 Satellite Communications Capability

	(EQUIVALENT 36 MHZ TRANSPONDERS)		
	IN ORBIT	ALLOCATED	POTENTIAL
C-BAND			
COMSTAR	72	0	24
SATCOM	48	24	24
WESTAR	24	48	0
BANDWIDTH EXPANSION	<u>0</u>	<u>0</u>	<u>132</u>
C-BAND SUBTOTAL	144	72	180
Ku-BAND			
SBS	0	36	36
WESTAR	0	24	48
COMSTAR	<u>0</u>	<u>0</u>	<u>72</u>
Ku-BAND SUBTOTAL	<u>0</u>	<u>60</u>	<u>156</u>
TOTAL	<u>144</u>	<u>132</u>	<u>336</u>
		612	
LESS 1:4 SPARE ALLOCATION		<span style="border: 1px solid black;">459</span>	

Table 4-7 Factors Which Alter the Forecast

<u>CAPACITY INCREASE</u>	<u>CAPACITY DECREASE</u>
<ul style="list-style-type: none"> <li>• 90 VS 60 MBPS IN 36 MHZ CHANNEL</li> <li>• LOWER SPARES RESERVE</li> <li>• SQUEEZING IN ARC</li> <li>• USE OF 18/30 GHZ BANDS</li> </ul>	<ul style="list-style-type: none"> <li>• WARC DOES NOT ENCHANCE C-BAND</li> <li>• ADDITIONAL SLOTS NOT USED</li> <li>• Ku-BAND PRECIPITATION EFFECTS</li> <li>• DUAL Ku-BAND POLARIZATION EFFECTS</li> </ul>
<u>DEMAND DECREASE</u>	<u>DEMAND INCREASE</u>
<ul style="list-style-type: none"> <li>• RAPID MATURITY OF FIBER OPTICS</li> <li>• SUCCESS OF SINGLE SIDEBAND</li> <li>• DIGITAL TASI ON TERRESTRIAL</li> </ul>	<ul style="list-style-type: none"> <li>• PROJECTIONS BASED ON PEAK LOADS</li> <li>• SHIFT TO SATELLITE FOR TARIFF JUSTIFICATION</li> </ul>



capacity forecast. If additional slots are not used for any reason whatever, either from standpoint of treaty limitations or the unsuitability of slots for use due to low angle or EIRP problems in the Western United States, a decrease of capacity would result. The Ku-band precipitation effects will have to be determined through operational testing, and the Satellite Business Systems satellites will do that; however, it will be in the 1982 time frame. In the demand area, the rapid maturity of fiber optics with a corresponding cost benefit could seriously affect the demand for satellite communications. The success of single sideband and terrestrial radio might allow an expansion of low cost terrestrial capacity over existing routes due to adoption of this new technology. Finally, use of digital time assigned speech interpolation on the terrestrial network could substantially develop the capacity of the terrestrial net thereby decreasing the demand for satellite communications. On the other hand, an increase in demand could result in from projections based on peak loading as opposed to average loading. It has been assumed that the message or data traffic can suffer substantial delays. However, if these delays must be minimized to, say, perhaps with a business day, it may be that the peak load projection should be used for this class of service. Finally, there are many political and regulatory factors which are difficult to project, which might force certain carriers to move communications to their satellite net for reasons related to justification of various tariffs. This again may have an effect to either increase the demand or decrease the demand depending upon whether the tariffs move up or down.

#### 4.3 PRELIMINARY DESIGN

To increase the available spectrum capacity, the space platform can develop narrow beams which allow reuse of the frequency spectrum in each one of the beams. For example the current satellite configurations employ antennas which largely cover the continental United States, as shown in Figure 4-4. A space platform could employ satellite antennas which are large enough to create an extremely narrow beam, from 50 to 200 miles in diameter. With this narrow beam, communications could be confined to the single sector illuminated by that beam as shown in Figure 4-4 on the right. Thus, a single frequency could be used for communications between Dallas and Los Angeles at the same time that the same frequency is being used for communications between Houston and Florida. As the spot size is decreased to take into account centers of traffic, a single spot could cover Manhattan, for example, whereas another spot beam could cover Newark, allowing frequency reuse in both of these high traffic locations. One important distinction, however, is that this narrow beam concept can be used only effectively between single points or perhaps a single point and a few other points. For broadcast services which are currently so popular, especially in the cable television area, the full continental United States should be illuminated for maximum effectiveness, unless a subdivision into four is made to accommodate time zone coverage for peak hour demands, as has been accomplished by Telesat Canada. Due to the regulatory factors, plus the convenience of using existing frequencies, it is assumed that the space platform with the large antennas will operate in the existing C-band allocation. Since this C-band allocation is a shared band of frequencies with the terrestrial services, it may be difficult to get F.C.C. clearance for all positions

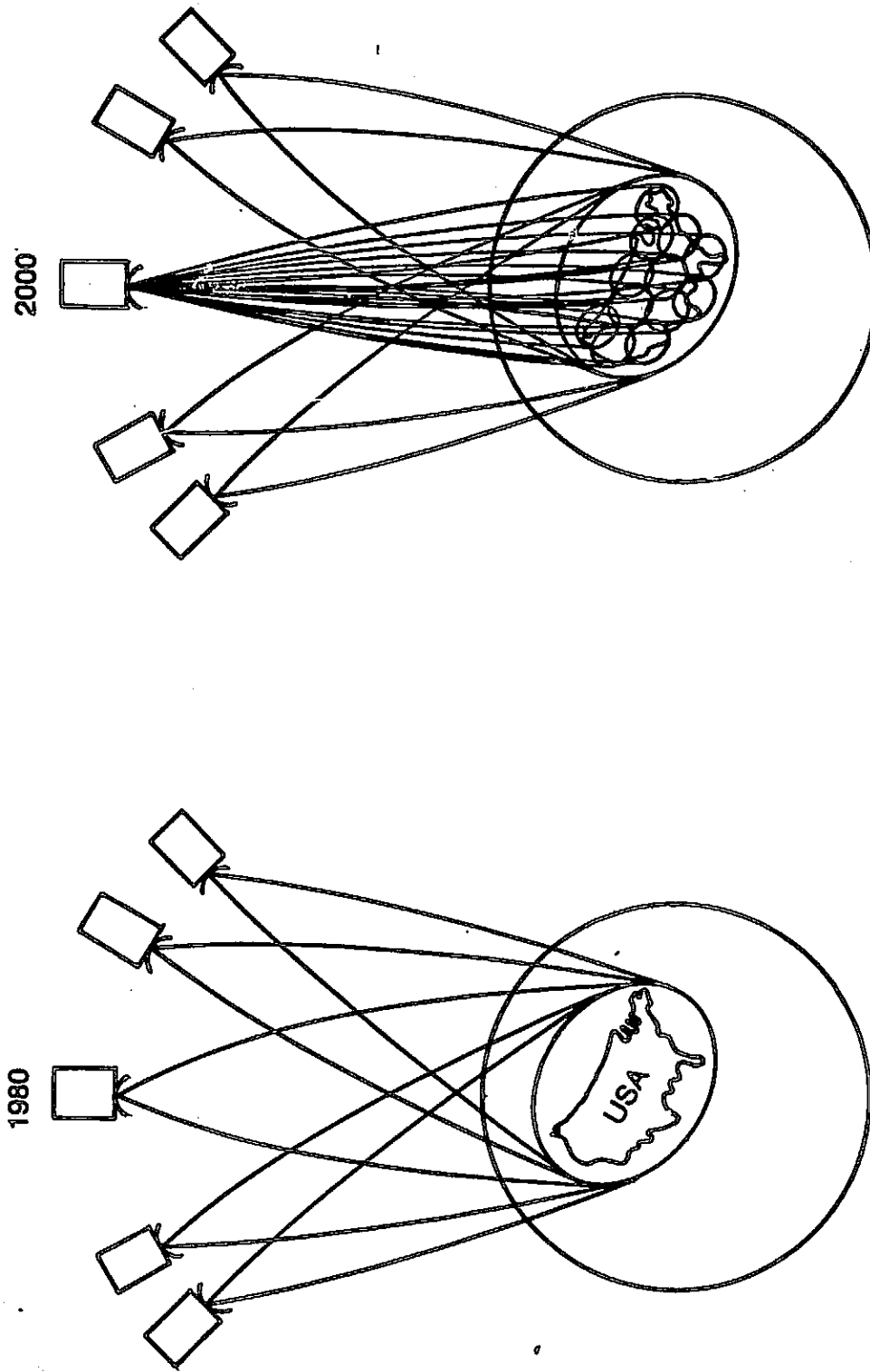


Figure 4-4 Platform Utilization

in the orbital arc which could be utilized by the space platform. As a result, more than one platform may be required to allow any earth station to be able to communicate with a space platform. Alternatively, the space platform may utilize Ku-band, assuming that the feasibility of Ku-band is definitely validated, or conceivably higher frequencies, and avoid the conflict with the terrestrial network. Finally, high quality sidelobes will be required to avoid interference with other satellites which will undoubtedly be in operation in the time frame of interest. It is assumed that satellites similar to those in existence today will continue to provide broadcast services. Orbital slots and frequencies used by these satellites must be protected to avoid interference.

A potential scenario for the utilization of the space platform is not unlike any other communications satellite. The transfer of the ground station communications to this platform would be performed in a similar manner to that of a ground station which moves its antenna from a primary to a backup satellite. The receive power levels would be largely equivalent. The equivalence of these levels is primarily dictated by FCC rules and regulations governing the amount of flux allowed at the earth's surface from a communications satellite. Due to the large platform antenna size the transmitter in the communication satellite would have a very low power, the EIRP, which is the same for the platforms as a conventional satellite, being largely due to the satellite antenna gain. The ground station transmit power level, however, would have to be lowered for the higher gain antenna of the space platform. As a result, the transmit power amplifier would be eliminated in any new designs or refurbished installation. In the existing installations the transmit power amplifier would have to be attenuated or otherwise reduced in power to avoid interference.

In the regulatory area, there will be actions required from the government to initiate utilization of this platform. The point to point traffic would largely phase over to the platform. This has implications over the ownership of this satellite. The point to multipoint, or broadcast traffic would continue to use the conventional satellites with broad beams. Allocations of one or more orbital positions must be made for the platform. This may have far-reaching implications due to the limited extent of the C-band orbital arc and the fact that this arc has already been allocated.

An interesting alternative is use of 20 and 30 GHz allocations. The attraction for these bands is obvious: The antennas are smaller, both on the ground and on the spacecraft. The disadvantage is that precipitation outages at these frequencies may not allow reliable communications. Two other factors enter consideration of these frequencies: (1) entirely new equipment will be required by the ground station owner and (2) technology development will be required at these frequencies. Efforts underway for reasons unrelated to this program are developing technology in the 20 to 30 GHz region. For example, quarter micron gate geometry field effect transistors appear to be capable of providing both power and noise figure required for voice and data services if spot beams are employed in the satellite. With this technology, a lower cost ground station may be produced, providing lower operating costs as well. The advent of a lower cost ground station could offset the potential drawback of

not being able to utilize existing equipment. The combination of multiple beam generation and higher frequencies presents an attractive satellite configuration, as well. Using a 20 GHz downlink, a 50 Mi spot can be generated by a smaller antenna on the spacecraft than a 200 Mi spot. Another attraction of the higher frequency antenna is that due to its small size, an experimental 20/30 GHz payload could be carried on an earlier satellite for feasibility demonstrations both from the standpoint of precipitation tests and multiple beam generation.

The above discussion has indicated that traffic projections show a need for frequency reuse sometime between 1990 and 2000 dependent upon the basis of projections as shown in Figure 4-5. It appears that the space platform with multiple beams frequency reuse is a very attractive solution. The resultant reduction of ground station costs may produce a more cost effective service. Finally, there are many political and technical factors which may accelerate the need for this platform.

#### 4.4 THE APPLICATIONS TEST PLATFORM

The foregoing paragraphs have demonstrated the potential exhaustion of frequency spectrum allocated to Commercial Satellite Communications in the 1990-2000 time frame. A multiple beam antenna system deployed on a telecommunications platform placed in a geosynchronous orbit is a potential solution. There are technology areas requiring validation, however, due to the investment required. The antenna range from 10 to 100 meters depending on the spot size and sidelobe structure and frequency. The number of these antennas are dependent upon beam cross over parameters as well as spot size. The electronics network which provides channelized switching between individual receive and transmit beams also represents a major investment. As described in paragraphs to follow there are additional technology areas to be verified prior to proceeding with full scale development.

It appears that these technology validations may be best approached by in-orbit placement of a subset of the telecommunications platform, known as the applications test platform. This platform, similar in concept to ATS-6, would be a Shuttle-launched satellite with a communications payload capable of demonstrating the technologies contained in the telecommunications platform.

The time phasing of this effort is shown in Figure 4-6. With this schedule, the launch of the full scale platform could be achieved in the early 1990's, coincident with replacement dates of several communication satellites as well as coinciding with a date at which saturation of existing spectrum may occur.

Table 4-8 describes the tests performed by the applications test platform corresponding to the areas in need of technical validation.

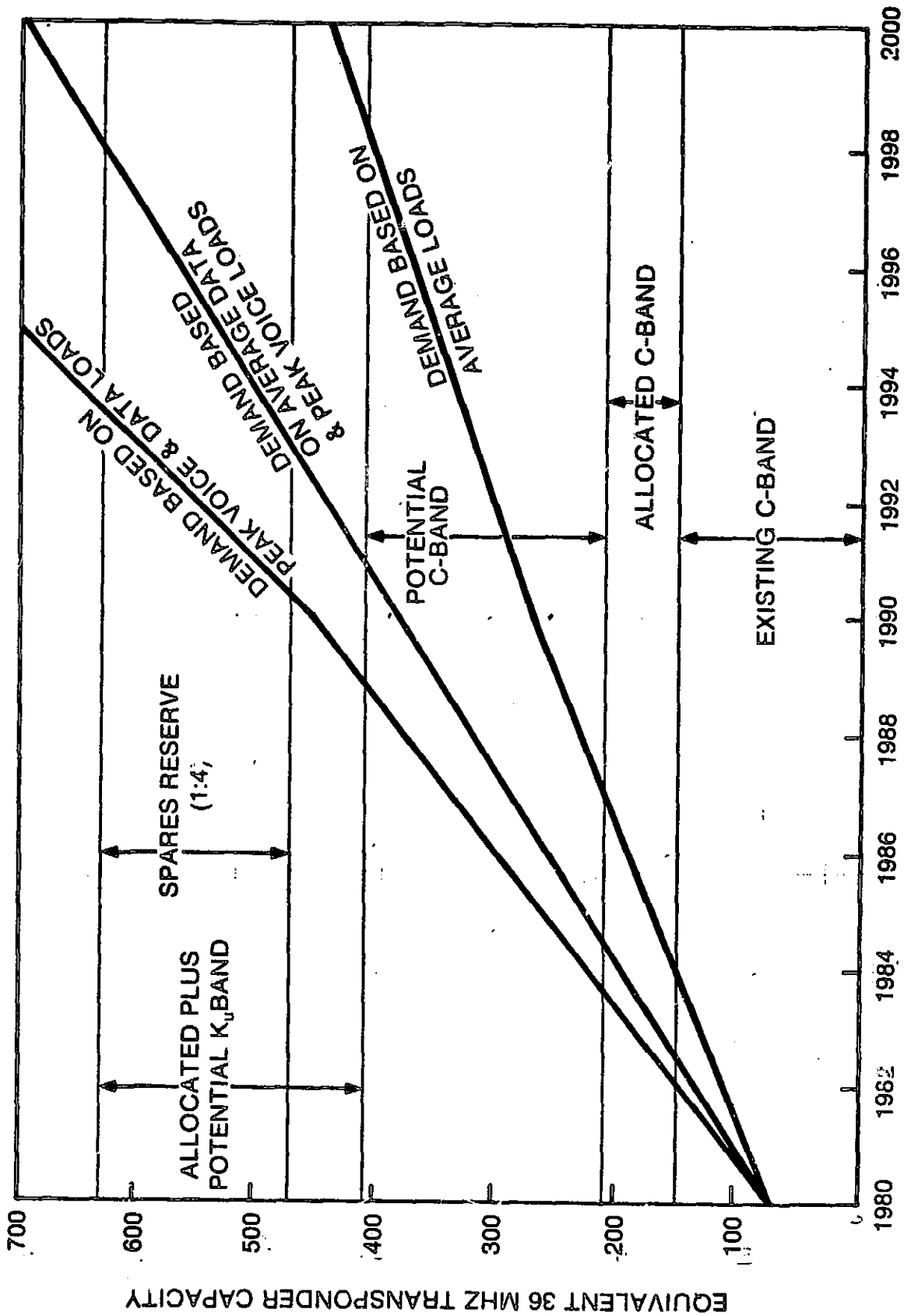


Figure 4-5 Satellite Communications Requirements and Capabilities

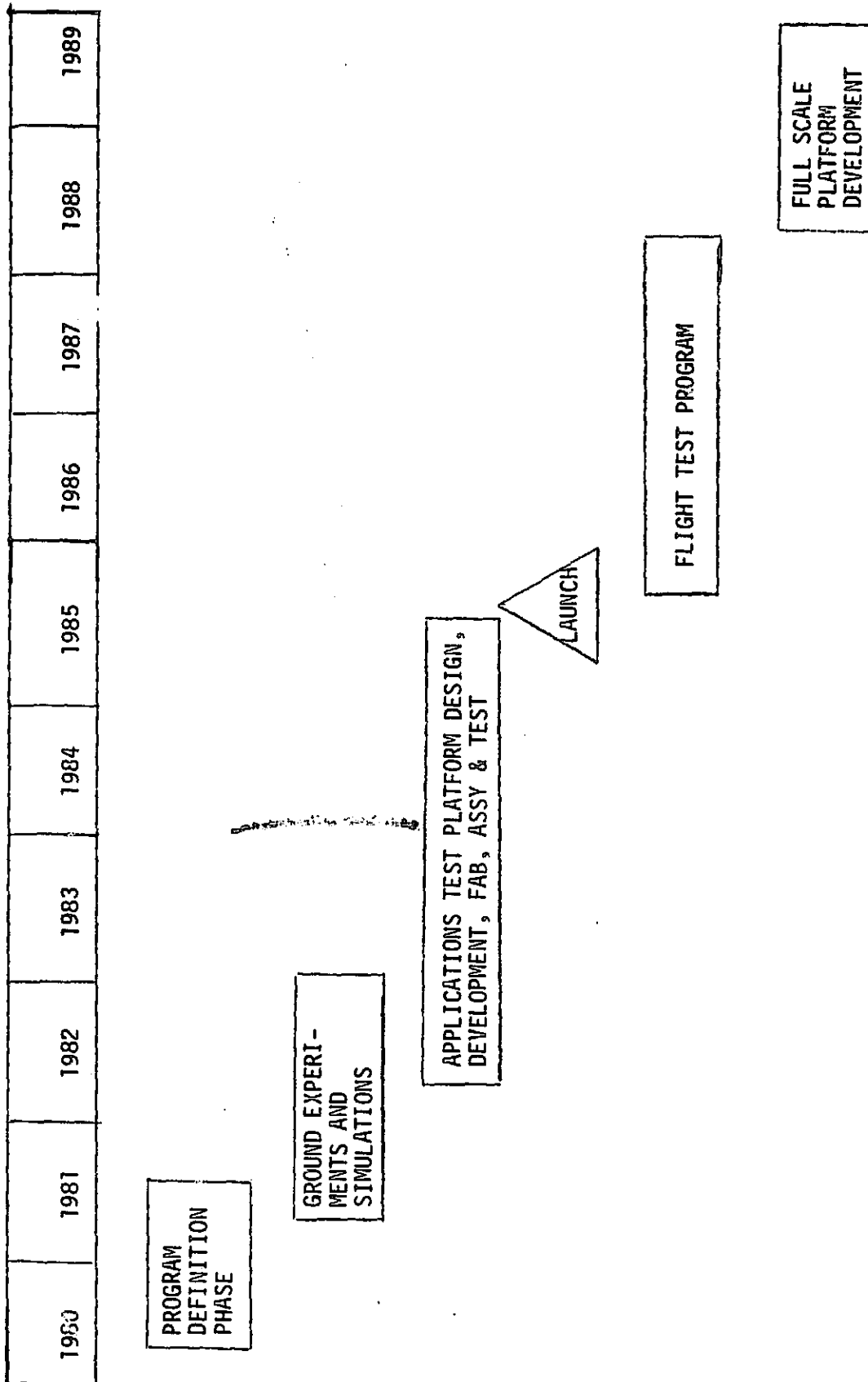


Figure 4-6 Applications Test Platform Program Schedule

Table 4-8 Applications Test Platform Validation Areas

VALIDATION AREA	TEST DESCRIPTION
1. Operation of multiple large antennas simultaneously from a common platform, some at the same frequency.	cross coupling, isolation, alignment and mutual blockage patterns.
2. Multiple beam scanning and forming for large scale frequency reuse.	cross coupling, isolation, alignment
3. C-band point-to-point communications for small low cost earth stations.	continuation of ATS-6 experiments
4. Ku-band point-to-point communications for small low cost earth stations.	continuation of CTS experiments
5. Ku-band propagation measurements.	continuation of CTS experiments
6. RFI measurements at VHF, UHF, L-band and C-band.	continuation of ATS-6 scanned radiometer measurements of radiation received from CONUS
7. S-band ETV to low cost earth stations.	continuation of ATS-6 experiments
8. Ku-band TV Broadcast	confirmation of CTS experiments
9. Emergency Aircraft Beacon location/reporting	VHF scanning antenna with receivers turned to aircraft emergency beacons
10. 20/30 GHz propagation	New 20/30 GHz beacon propagation stations.
11. Large scale electronic mail for medium sized and large terminals	12/14 GHz 5-meter earth stations with TDMA modems in synchronization with satellite scanning beams and switching.
12. Electronic mail for small western terminals	3-foot 20/30 GHz earth stations with TDMA modems in synchronization with satellite switching
13. Computer control, routing and sorting of large scale electronic mail.	12/14 GHz 5-meter earth stations with TDMA modems in synchronization with satellite scanning beams and switching.



#### 4.4.1 Applications Test Platform Communication Subsystem

The communication related experiments which can be provided by the Applications Test Platform (ATO) should include a continuation of the CTS and ATS-6 experiments in spot beam television broadcast and related experiments to small S-band and 12 GHz earth stations. Both the CTS and ATS-6 satellites were very successful in demonstrating the feasibility of operating with very small and low-cost earth stations. At the same time they demonstrated that there was an urgent need for the type of educational, medical, and emergency service which could be provided in the rural and remote portions of the world such as Alaska, most of Canada, Western United States, Appalachians, etc. These satellites are currently approaching their end-of-life and in the past few years have become important service satellites. To date, no commercial satellite system or other governmental system has been implemented to provide the service which the CTS and ATS-6 satellites currently provide. Those who have been benefitting from these as well as those who have been providing these services are very concerned that when the CTS and ATS-6 reach end-of-life that these vital services will be interrupted.

The ATS-6 and CTS satellites have provided a very valuable tool for space-to-earth propagation measurements and some of the charts in this report concerning rain attenuation have been derived from such experiments. However, link budgets and availability analysis requires measurements over many years and many locations in order to obtain adequately large sample sizes for design decisions. Thus, it is very important that the current CTS and ATS-6 propagation experiments continue. This report as well as many other studies indicate that as the satellite spectrum and orbit congestion increases, it may ultimately be necessary to exploit the K-band frequencies.\* To date, the propagation experiments at K-band have been limited because only a few satellites have been launched with K-band beacon packages. Many of those which have been launched to date, had a very short lifetime. Thus, it becomes important that the propagation experiments be expanded to the higher frequency bands.

Because of the increasing congestion of the microwave bands, the radio interference mapping of the United States using scanning spot beams and sensitive receivers pioneered by ATS-6 should be continued.

The new experiments should include transmission experiments to small earth stations at K-band and should include point-to-point communication experiments such as electronic mail. For example, analysis shows that it would be well within the capability of the ATP to transmit high data rates to earth stations in the low rainfall regions of the Western United States at 30 GHz with earth station antennas as small as three feet.

\*K-band allocations are 17,700 to 20,200 MHz for space to earth and 27,500 to 31,000 for earth to space.



We have seen a need for demonstrating the use of these frequency bands to relieve congestion, to provide new services, and to provide old services in a more cost-effective manner. Historically, we have seen that until NASA demonstrates the use of a new space frequency band, the commercial world is very reluctant to move into a new frequency band. Historically, we have also seen in the case of 4/6 GHz and now 12/14 GHz, that within a few years after NASA demonstrates the use of a new frequency band the commercial world will begin to make use of the new band. The electronic mail transmission experiment is a very worthy candidate for the Advanced Technology Platform Satellite since it appears that not only could the mail service benefit from the use of K-band, it also appears that the commercial organizations need a major viable demonstration of satellite electronic mail in order to encourage them to apply themselves fully to provide such services.

#### 4.4.2 Description of Electronic Mail System Concept

This experiment employs spot beam switching at the satellite to provide a Space Switched Time Division Multiple Access (SS TDMA) for point-to-point digital traffic between small user earth stations.

The country would be divided into sectors with each sector generating approximately equal amounts of total traffic. A transponder would be assigned to each sector for purposes of collecting the traffic from each earth station as the satellite beam for that transponder is sequentially switched to the earth stations within that sector. The resulting data stream to the input of the transponder is a TDMA signal with each burst corresponding to one of the earth stations within the sector. Refer to Figure 4-7. Note that the burst length can be different for each earth station in order to match the traffic volume of each earth station. Similarly, the satellite has downlink switching spot beams to provide, in sequence, the digital traffic designated for each earth station within a sector.

The heart of the system is the digital switch which takes the data stream output from each uplink transponder, splits it into individual messages and reassembles the messages into TDMA frames for the downlink transmissions so that each burst contains only traffic for a single earth station.

The digital switch along with the necessary multiplexing and demultiplexing equipments can become quite complicated. Further, in an experimental/operational network of this type it would be highly desirable to provide for a great deal of human supervision and interaction with the switch/processor. It is proposed that a minimum risk and logical evolution of such a system would be for the first experimental system to operate with the "mail sorting/routing" switch/processor on the ground rather than in the satellite. Specifically, it is proposed that the switch/processor be located in a low rainfall area near the central part of western CONUS and be connected to the satellite transponders by 20/30 GHz data links. The footprint for satellite beams should be very small, and the earth station for the "switch/processor" should have a moderately high G/T to insure that the traffic between the ground station and the satellite cannot be easily monitored or interfered with under unauthorized/accidental situations.

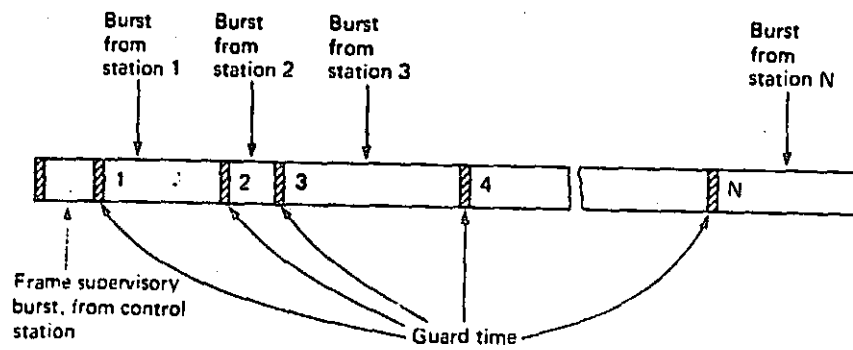


Figure 4-7 A Frame in a TDMA System

In addition to providing point-to-point electronic mail experiments between small western user earth stations, electronic mail transmission experiments between large users in moderate to high rainfall regions should also be demonstrated with some earth stations configured for space diversity reception and/or transmission.

An important feature of this system is the use of scanning or switched small spot beams so the same frequency band can be used simultaneously by many users in the network. That is, the spot beams provide high isolation between transmissions in adjacent sectors even though they are all transmitting at the same frequency. The large platform concept for the satellite which can accommodate several large diameter antennas is assumed for the system/experiment in the following description.

#### Experimental/Operational Frequencies

The choice of the uplink and downlink frequencies for the user earth stations is a trade between the lower frequency bands (such as 4 and 6 GHz) where earth station user equipment costs and precipitation losses are lower and higher frequency bands (such as 12/14 GHz and 20/30 GHz) where the interference and congestion is expected to be lower. Table 4-9 shows several frequency combinations for consideration for the proposed electronic mail experiments using the ATP.

Although a complete performance/cost trade study has not been done, it appears that Case 3 is the most attractive from the standpoint of permitting medium sized antennas at the user earth station with acceptable interference levels. The advantage of 30 GHz over 12 GHz for a downlink is that for the same satellite antenna size, a given spot beam size is approximately 2.5 times smaller. The disadvantages of 30 GHz over 12 GHz are the tighter antenna surface tolerances, higher cost receivers and significantly higher rain and cloud attenuations. Refer to Figure 4-8. For the Applications Test Platform Satellite it is proposed that both 12 GHz and 30 GHz downlinks be used with 30 GHz being restricted to only low rainfall regions or to periods of low rainfall.

Note that it is recommended for the 20/30 GHz bands that 20 GHz be used for uplink and 30 GHz be used for downlink. This is primarily a cost trade since the ground based transmitters which are lower in cost at 20 GHz than at 30 GHz for the same power levels. Further, when it is considered that much higher powers would be required at 30 GHz than at 20 GHz for rain margin and that the ground transmitter costs would be multiplied by the number of earth stations it becomes more economical to use 20 GHz for the uplink transmissions than 30 GHz. These same arguments would seem to also rule out 30 GHz for downlink transmissions. However, the satellite power amplifiers are a one time cost to be spread over the number of stations in the network. Further, the large space platform proposed can easily accommodate a large downlink antenna in order to keep the actual power amplifier output requirements at 30 GHz to a very modest level.

Table 4-9 Potential Up and Downlink Frequency Bands  
for Electronic Mail Transmission in GHz

CASE	USER TO SATELLITE	SATELLITE TO GROUND SWITCH	GROUND SWITCH TO SATELLITE	SATELLITE TO USER
1	6	30	20	4
2	6	12	14	4
3	14	30	20	12
4	20	30	20	30
5	14	30	20	30
6	20	30	20	30

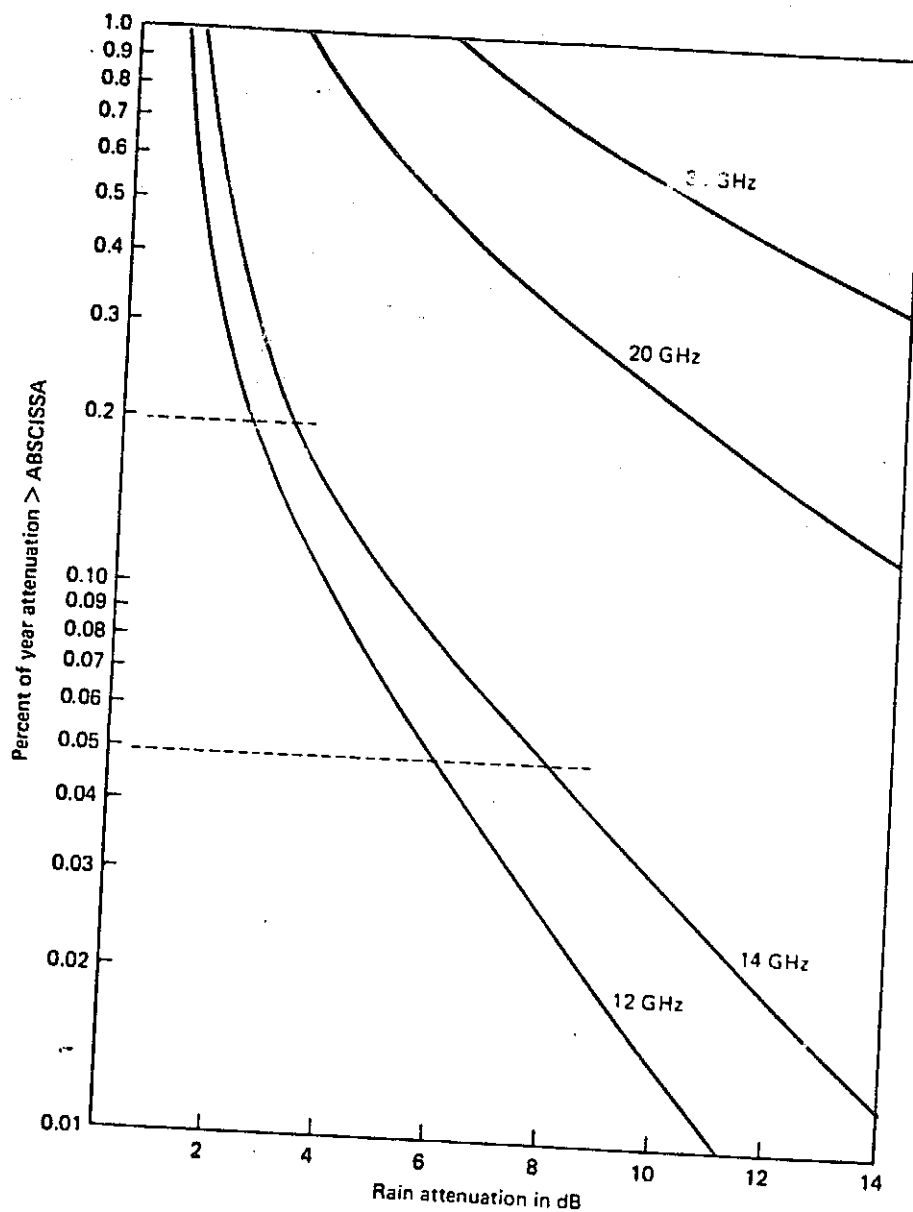


Figure 4-8 Typical Attenuation Caused by  
Rain for Clarksburg, Maryland



Of course, 14 GHz power amplifiers are significantly lower in cost than 20 GHz amplifiers and the rain/cloud attenuation at 14 GHz is much less. On the other hand, 6 GHz and 4 GHz are so heavily used by LOS terrestrial microwave systems and other satellite systems in the vicinity of metropolitan areas where the mail centers are located, the interference at 6 and 4 GHz could be unacceptable. In summary, it is recommended that the electronic mail experiments with the Applications Test Platform Satellite use the frequency bands shown in Cases 3, 5 and 6.

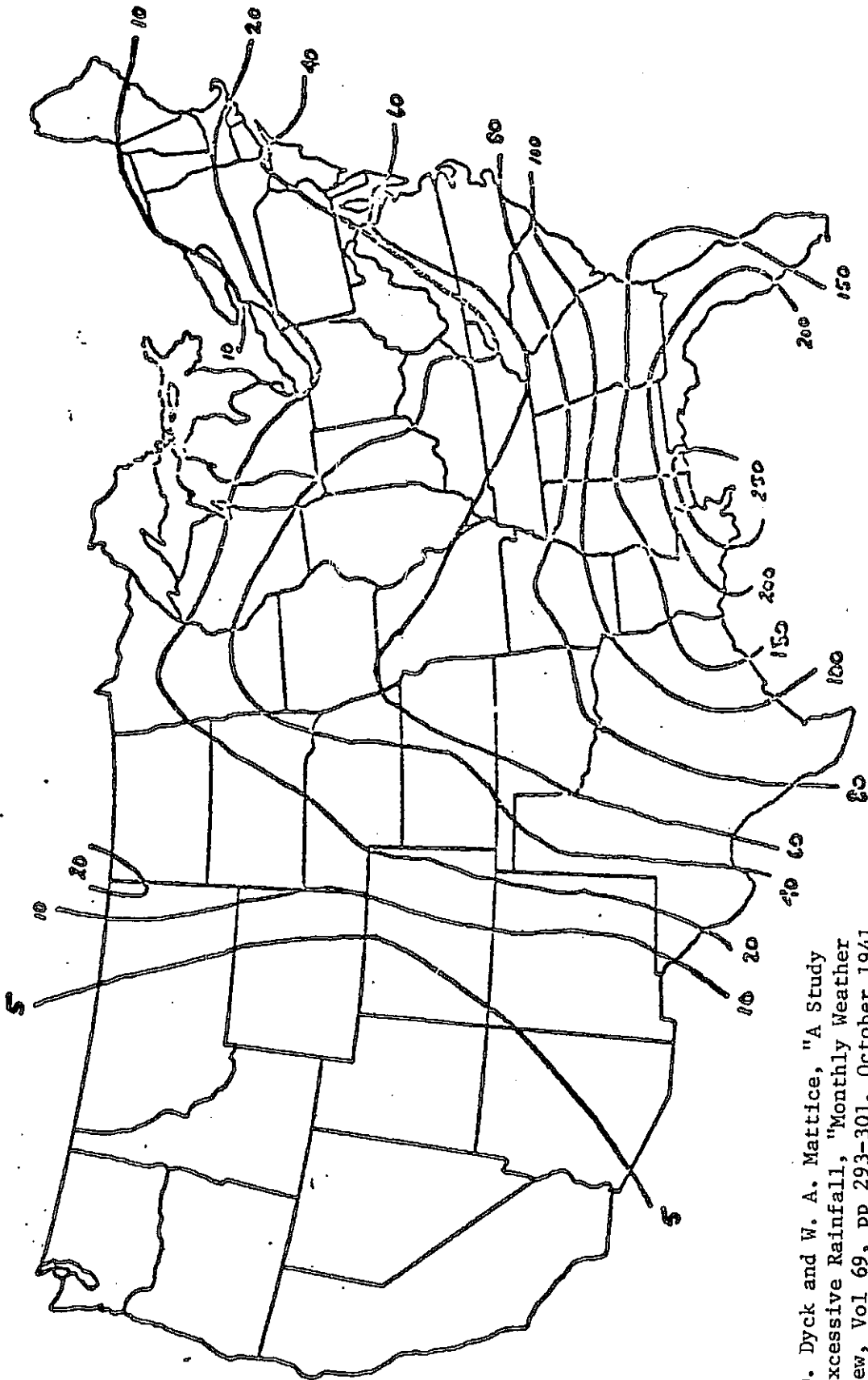
#### Link Calculations for Satellite Electronic Mail

There are a number of trade-offs to be considered in the design of satellite electronic mail regardless of the frequency used for the link transmissions. Among these are the techniques for converting from "hard copy" to "bits", the allowable end-to-end bit error rate (BER), the addressing codes and routing codes for each digital message, encryption techniques for privacy, and techniques for making electronic mail transmissions resistant to jamming. There are also many operational issues such as allowable costs relative to other mail transfer techniques, "break-even" volumes, "break-even" distances, schedules, (daily, weekly, monthly, holidays, etc.) load averaging techniques, end-to-end delays, alternate routing, techniques for preventing lost messages, etc.

This section, together with Appendix B, deals with link calculations using 14 GHz and 20 GHz uplinks and 12 GHz and 30 GHz downlinks. For purposes of these calculations, state-of-the-art minimum-shift-keying (MSK) modems are assumed. It has been assumed that a link BER of  $10^{-7}$  was acceptable and that where lower end-to-end BER rates are required they will be obtained by use of forward error correction codes (FEC) applied to each message with repeat (ARQ) of messages which are received with an unacceptably high BER.

Satellite transmissions at frequencies above 10 GHz are highly susceptible to rain and cloud attenuation and depolarization. In addition, high altitude ice crystals under seemingly clear skies conditions can also cause significant depolarization. Since the weather and upper atmosphere conditions vary widely with the location and season. Figures 4-9 and 4-10 illustrate the variability of intense rainfall over CONUS and the associated attenuations at 21 GHz. Figure 4-3 illustrates the increase in rain attenuation for 20/30 GHz over 12/14 GHz.

To maintain a constant BER with location requires increased link margins through increased EIRP, larger antennas and transmitter power and G/T for locations with higher rainfall. The lower the EIRP and the G/T the lower the equipment costs of the earth station. However, the smaller the antenna the larger the required high power amplifier to provide the desired uplink EIRP. Since the high power amplifiers are usually the most costly initially and in terms of maintenance of an earth station's rf complement, there is an economical minimum size for the antenna. At 14 GHz this minimum is typically around 4.5 to 5 meters. However, there is a strong trend to minimize the earth station antenna for urban areas for architectural or esthetic reasons. Thus, in the



N. D. Dyck and W. A. Mattice, "A Study of Excessive Rainfall, "Monthly Weather Review, Vol 69, pp 293-301, October 1941

Figure 4-9 Number of Total Occurrences of 1-Inch Per Hour or Greater Rainfall Rate for a 30-Year Period

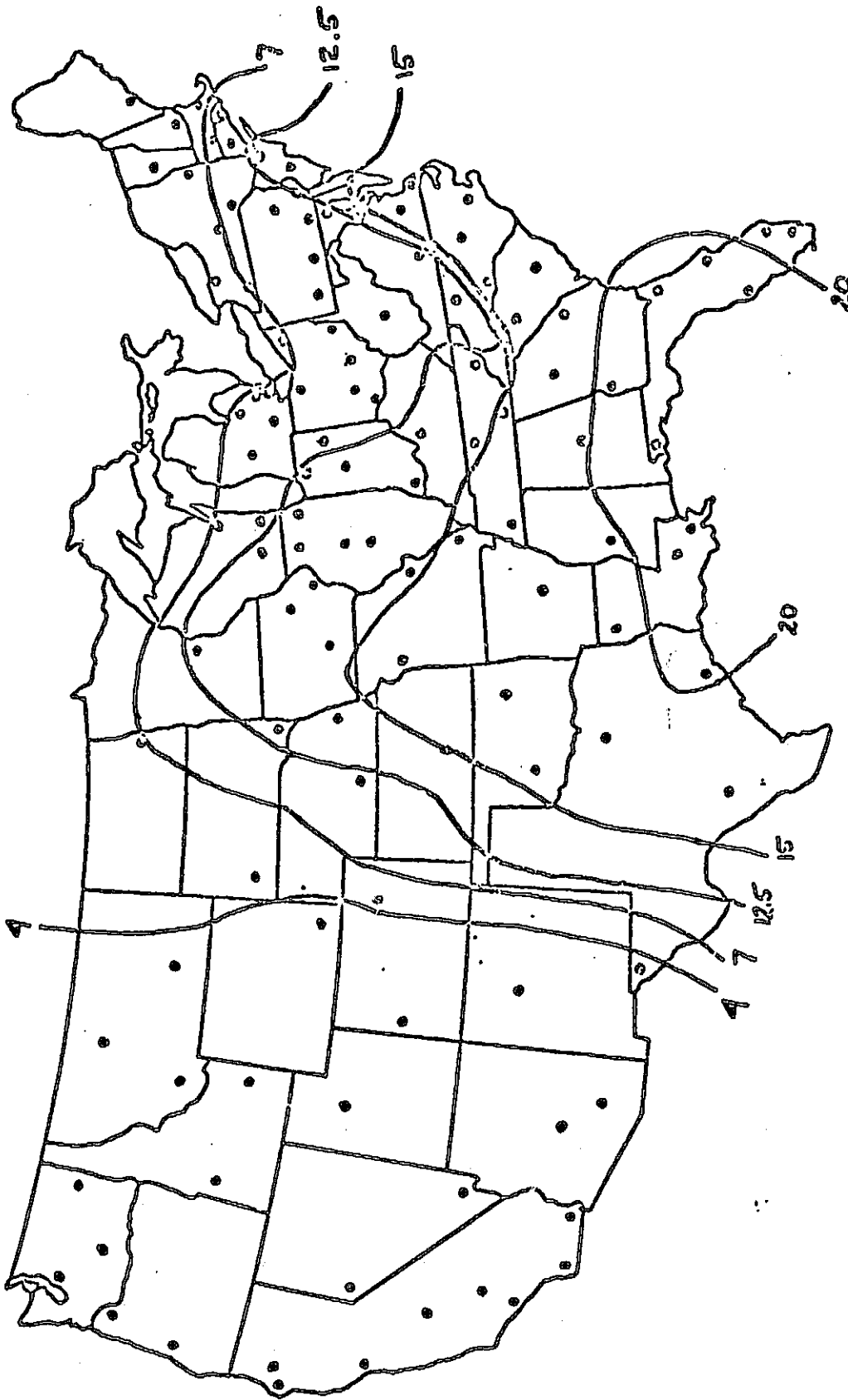


Figure 4-10 Regions Where Indicated db of Attenuation at 12 GHz  
is Exceeded for 0.01 Percent of the Time.



following sections link calculations are also developed for smaller antenna earth stations.

One of the primary advantages of a large platform communication satellite is that it can provide large antennas and large power levels to permit very small earth stations. However, with such a satellite operating in a shared band such as 6 GHz and 14 GHz, the link performance tends to be interference limited.

Specifically, on the uplink, the use of a large antenna on the satellite permits a low uplink EIRP at the earth station with respect to achieving a desired uplink carrier-to-thermal noise ratio,  $(C/N_{th})_u$ . However, increasing the satellite antenna increases the gain to interfering signals received at the satellite. Thus, once the link parameters have reached the point where the uplink carrier-to-interference ratio,  $(C/I)_u$ , is dominating the link performance, there is no advantage to increasing the size of the satellite antenna in order to permit further decreases to the earth station uplink EIRP. Given a required uplink EIRP, there is also an interference trade between the size of the earth station antenna and the power amplifier level. This trade is dominated by the allowable interference which the earth station is permitted to input to other satellites which share the same uplink frequency band and which are positioned in orbit near the large platform satellite. For a given interference level to the adjacent satellites and a given uplink EIRP, there is a minimum allowable transmit antenna size at the earth stations.

Similarly on the downlink side, the ability of large platform satellites to permit small receiving earth stations by generation of large downlink EIRP tends to be limited by interference considerations. The interference from the platform satellite to other receiving earth stations is the primary limit on the satellite downlink. One of the primary limitations on the size of the receiving earth station antenna is the interference received from adjacent in-orbit satellites which share the same downlink frequency band, the other (often more important) is terrestrial interference.

A very important parameter for the links is the amount of rain margin which is provided. This, in turn, depends upon the flexibility in transmission schedules, percentage of outages allowed, and the techniques used to control transmission errors other than high carrier-to-noise ratios. Fortunately, most mail does not have the transmission urgency that telephone conversations have, so that it is permissible to temporarily cease transmissions during periods of local intense rain attenuation periods at the user locations. This approach greatly reduces the design margins for rain and the associated costs. However, outages at the central routing/switching control station cannot be as easily tolerated since this effects all users simultaneously. Hence, it is very important that this station be located in a low rain incidence area. However, it must be recognized that there is probably no location in the United States which at some point in time will not receive a very heavy rain. Thus, a choice must be made for the control station of:

- A. Providing for very large rain margins even though an intense rain condition would be very rare.
- B. Providing for a backup station at another location at a distance sufficient to ensure both stations will not be subject to the same rainstorm.
- C. Permitting a temporary shutdown of the system when a rare rain event occurs at the control station

Time has not permitted complete investigations of all the above trade-offs and issues. However, calculations shown in Appendix B include sections which are believed to be reasonably practical choices of parameters for electronic mail service.

#### 4.4.3 Applications Test Satellite Design Parameters

##### Antenna Complement

Table 4-10 summarizes some of the potential communication antennas for the Advanced Test Platform Satellite. The telemetry antennas are not included. These antennas can be used to continue and expand the ATS-6 and CTS experiment including advanced electronic mail experiments. For economy reasons several reflector antennas could be combined instead of using separate antennas for each frequency. Refer to Interim Report NAS9-15718 for additional descriptions of the multiple-feed switched beam reflector antenna concepts.

##### Basic Transponder for Electronic Mail Experiments

Figure 4-11 shows a basic block diagram for a four-channel transponder for electronic mail experiments. Many transponders of the type shown in Figure 4-11 may be employed depending upon the magnitude of the ground-based portion of the experiment. One channel is sized for transmissions between 5-meter 12/14 GHz earth stations and the central 20/30 GHz control earth station as described in Section 4.2.2. These channels employ tunnel diode preamplifiers and FET power amplifiers with levels of 1 and 5 watts respectively at 12 and 30 GHz. The other channels are for smaller 12/14 GHz earth stations or for 5-meter 12/14 GHz earth stations operating in very high rainfall regions. These channels employ a parametric up-converter at 14 GHz and a cooled FET low-noise amplifier at 20 GHz. These channels employ TWT amplifiers with power levels of 20 and 25 watts at 12 GHz and 30 GHz respectively.

The two 14/30 GHz channels can be cross-connected through switching as desired. Similarly, the two 20/12 GHz channels can be cross-connected. Also, shown in Figure 4-11 is a 20 GHz to 30 GHz channel which employs 20 GHz cooled FET receivers and 30 GHz TWT amplifiers through the cross-connection switching. This path is provided for the small 20/30 GHz earth stations in the semi-arid locations as described in Appendix B. These channels interface with four separate large reflector antennas with multiple feeds for beam steering as described elsewhere. Table 4-11 summarizes the characteristics of these channels.

Table 4-10 Summary of Possible Applications Test  
Platform Satellite Antennas

<u>TYPE</u>	<u>ANTENNA DIAMETER (METERS)</u>	<u>NOMINAL FREQUENCY (GHz)</u>	<u>MULTIPLE FEEDS</u>
Reflector	9.8	2.2	YES
Reflector	20.5	4	YES
Reflector	13.8	6	YES
Reflector	7.5	12	YES
Reflector	6.4	14	YES
Reflector	5.1	20	YES
Reflector	3.0	30	YES
Horn	-	2.2	NO
Horn	-	4	NO
Horn	-	12	NO
Horn	-	18	NO
Horn	-	30	NO
ARRAY	-	1.5-1.6	YES
ARRAY	-	VHF	YES
ARRAY	-	VHF	YES
ARRAY	-	2.2	YES
Reflector	0.8	12/14	NO

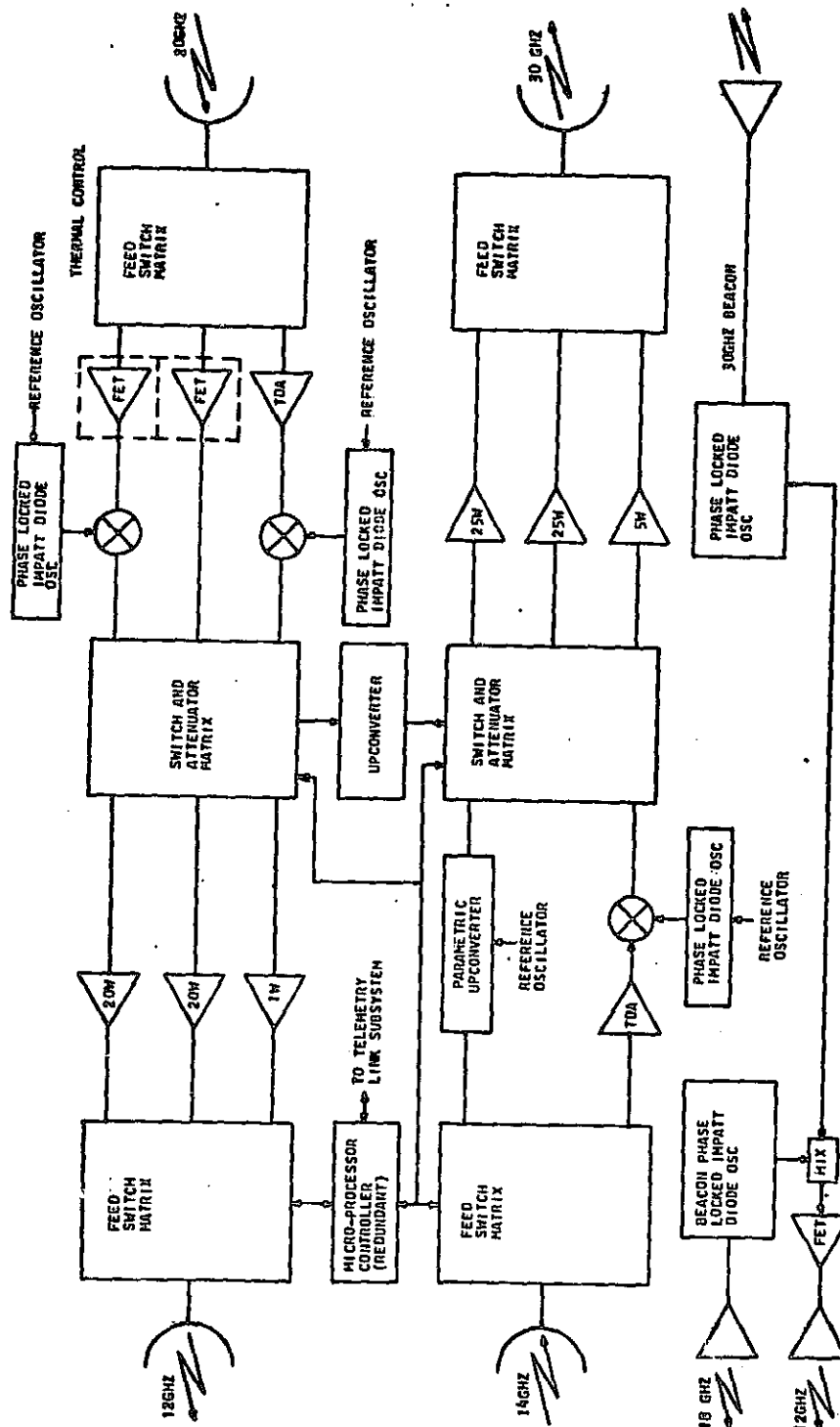


Figure 4-11 Basic Two-Channel Transponder Block Diagram  
for Electronic Mail Experiment

Table 4-11 Characteristics of Transponders in Figure 4-11

MODE	NOMINAL FREQUENCY (MHz)	BANDWIDTH (MHz)	POLARIZATION	ANTENNA FIELD OF VIEW	ANTENNA GAIN (dB)	G/T dB/K	TRANSMIT POWER (WATTS)	ETRP (dBW)
Receive from 5-M Stations	14	36 to 54	Linear	200 X 300 KM	55.8	24	-	-
Transmit To 5-M Stations	12	36 to 54	Linear	200 X 300 KM	56.8	-	1	54.8
Receive From Small East Coast Stations	14	36 to 54	Linear	200 X 300 KM	55.8	21	-	-
Transmit to Small East Coast Stations	12	36 to 54	Linear	200 X 300 KM	56.8	-	20	67.8
Receive From Control Station	20	36 to 54	Linear	200 X 300 KM	57	22	-	-
Transmit To Control Station	30	36 to 54	Linear	200 X 300 KM	56	-	5	61
Receive From Small Western Stations	20	36 to 54	Linear	200 X 300 KM	57	25	-	-
Transmit to Small Western Stations	30	36 to 54	Linear	200 X 300 KM	56	-	25	68
Beacon	12	-	Ortho Linear	10°	15.7	-	0.2	9
Beacon	18	-	Ortho Linear	10°	16.6	-	0.15	7.9
Beacon	30	-	Ortho Linear	10°	16.5	-	0.1	5.8

Also, shown in Figure 4-11 are symbolic blocks for generating 12, 18 and 30 GHz beacon signals for propagation experiments. These signals would be broadcast on orthogonal polarizations through small antennas for large area coverage.

#### Basic Transponder for Continuation of CTS Experiments

Figure 4-12 shows the basic block diagram for the CTS experiments. The CTS educational TV experiments employs two small mechanically steerable 0.8m diameter antennas with  $2.5^\circ$  beams. As long as separate frequency bands are employed, there should be no difficulty in carrying out CTS and electronic experiments simultaneously. Some of the limitations of the CTS satellite are:

- a) Mechanically steered beams with relatively short life in terms of number of scans
- b) Only two beams and transponders so that the many CTS experimental users have to time-share (every other day for example) the satellite

With the space and power capacity of the platform type of satellite many antennas can be operated simultaneously. In addition, feed-switched or phase array types of antennas can be employed.

If desired for economic reasons, the CTS experiments can be configured to use some of the same modules (such as the 14 GHz TDA's and 12 GHz power amplifiers) shown in Figure 4-11. This could mean time sharing between the electronic mail experiments and the CTS experiments. The CTS transponders have a bandwidth of 85 MHz. With the greater power and larger antenna sizes available on the large platform type of satellite, the wider bandwidth would permit simultaneous transmission of two analog color TV program or three digital color TV programs of excellent quality. Alternatively, larger numbers of simultaneously good to fair quality TV transmissions can be provided within an 85 MHz bandwidth with proper choice of the parameters.

Table 4-12 summarizes the CTS ETV transponder characteristics.

#### 4.4.4 Basic Transponders for Continuation of ATS-6 Experiments

A block diagram representation of the ATS-6 Communications Subsystem for continuing the following experiments is given in Figure 4-13.

- a. Coherent mode
- b. Non-coherent mode
- c. PLACE experiment
- d. Data relay experiment
- e. RFI experiment

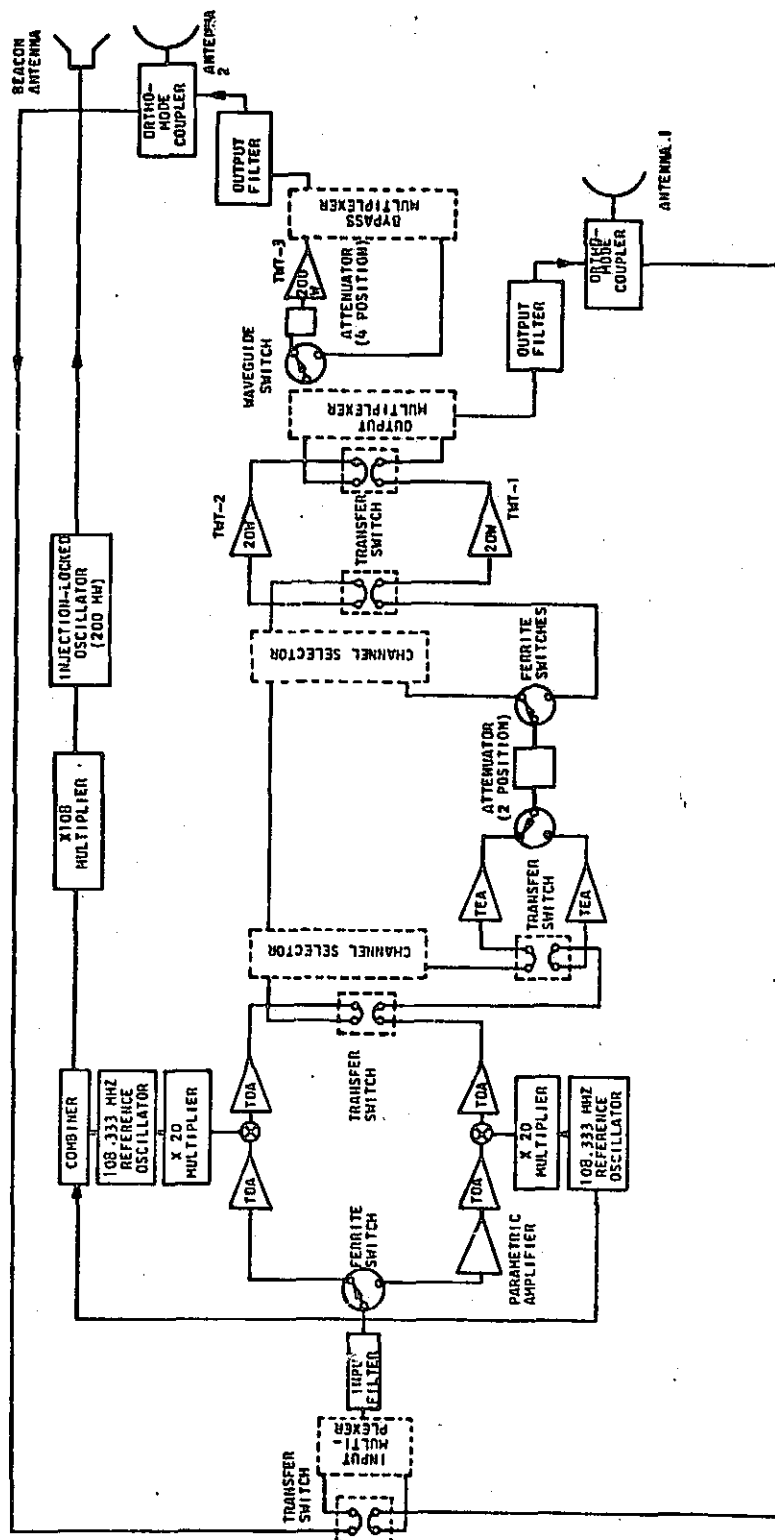




Table 4-12 Baseline CTS 12/14 GHz Transponder Characteristics

Uplink Frequency Band	14.0 to 14.5 GHz
Downlink Frequency Band	11.7 to 12.2 GHz
Uplink Half Power Beamwidth	2.5° (two steerable)
Downlink Half Power Beamwidth	2.5° (two steerable)
On-Axis Receive Flux Density for Transponder Saturation	-91.5 dBW/m <sup>2</sup>
Receive G/T	Peak 6.2 dB/°K
EIRP (Single carrier saturated)	Maximum 60 dBW
Bandwidth	85 MHz
Maximum Group Delay over Passband	62 Nanoseconds at <u>±</u> 18 MHz
Input Filter Group Delay Ripple Period	12 MHz
Gain Variation Across Bandwidth	0.25 dB
Gain Slope Across Bandwidth	0.01 dB/MHz
Input Filter Gain Slope	
-6 to +6 MHz	0.04 dB/MHz
+6 to +12 MHz	0.07 dB/MHz
+12 to +18 MHz	0.5 dB/MHz
Single Carrier AM/PM Conversa- tion Coefficient at -10 dB Input	3.3 deg/dB
Output Filter Gain Slope	
-18 to -12 MHz	0.05 dB/MHz
-12 to +12 MHz	0.01 dB/MHz
+12 to +18 MHz	0.07 dB/MHz



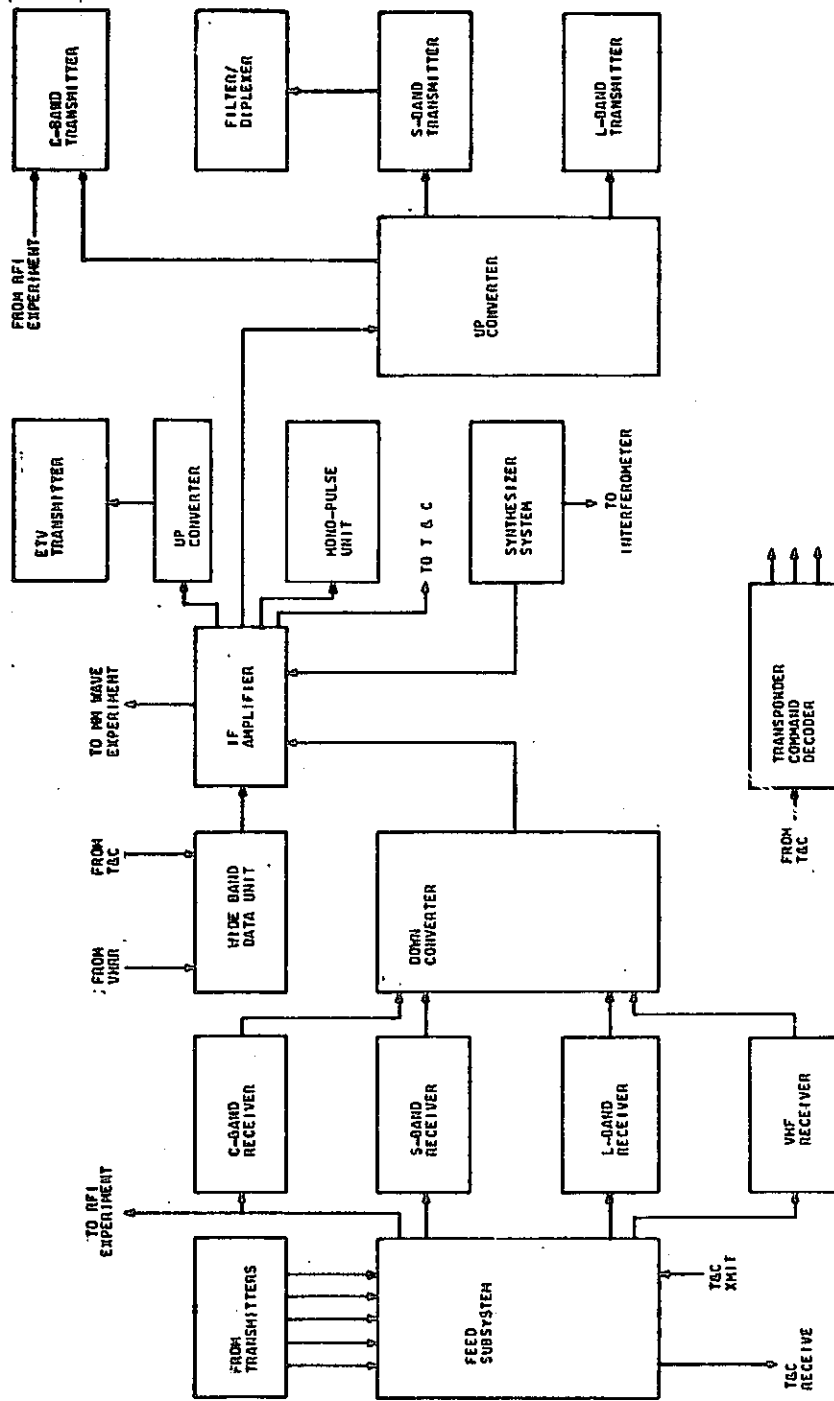


Figure 4-13 Communications Subsystem (Simplified Block Diagram)



- f. ETV experiment
- g. VHF radiometer data transmission
- h. Radio beacon

The baseline ETV transponder is described in Table 4-13. The communication subsystem characteristics in Figure 4-13 are summarized in Table 4-14.

Table 4-13 Baseline ATS-6 Type 2.6/6 GHz TV Transponder Characteristics

Transmit Frequencies

Channel A	2569.2 MHz
Channel B	2570.0 MHz

Receive Frequencies

Channel A	6350.0 MHz
Channel B	6149.2 MHz

Uplink Beamwidth 0.4°

Downlink Beamwidth 0.9°

On-Axis Receive Flux Density  
for Transponder Saturation -91 dBW/m<sup>2</sup>

Receive G/T Peak 13.5 dB/°K

EIRP (Single Carrier  
Saturated) Peak 53 dBW

Bandwidth 36 MHz

Maximum Group Delay  
over Passband 62 Nanoseconds at ±18 MHz

Input Filter Group Delay  
Ripple Period 12 MHz

Gain Variation Across  
Bandwidth 0.25 dB

Gain Slope Across Bandwidth 0.01 dB/MHz

Input Filter Gain Slope

-6 to +6 MHz	0.04 dB/MHz
<u>±</u> 6 to <u>±</u> 12 MHz	0.07 dB/MHz
<u>±</u> 12 to <u>±</u> 18 MHz	0.5 dB/MHz

Single Carrier AM/PM Conversa-  
tion Coefficient at -10 dB Input 3.3 deg/dB

Output Filter Gain Slope

-18 to -12 MHz	0.05 dB/MHz
-12 to +12 MHz	0.01 dB/MHz
+12 to +18 MHz	0.07 dB/MHz

Table 4-14 ATS-6 Communications Subsystem Characteristics

MODE	NOMINAL FREQUENCY (MHz)	BANDWIDTH (MHz)	POLARIZATION	ANTENNA FIELD OF VIEW (DEGREES)	RECEIVER			TRANSMITTER			
					PEAK GAIN(dB)	MIN G/T OVER FOV (dB/K)	G/T (PEAK) (dB/K)	TRANSMITTER OUTPUT POWER (WATTS)	MIN ERP OVER FOV (dB/M)	ERP (PEAK)	ERP (PEAK)
C-Band Receive	6350 6150	40	Llinear	0.4	49.0	10.5	13.5	-	-	-	-
C-Band Transmit	3750 3950	40	Llinear	0.6	46.0	-	-	21.0	51.5(1) 47.2(2)	54.5(1) 50.2(2)	-
Horn C-Band Receive	6350 6150 5950	40 12	Llinear	20	16.5	-20	-17	-	-	-	-
Horn C-Band Transmit	3950 3750 4150 3950	40	Llinear	10	16.6	-	-	21.0	25.0(1) 20.7(2)	28.0(1) 23.7(2)	-
C-Band Receive	6150	500	Horizontal Vertical RCP	0.4	48.5	NA	NA	NA	NA	NA	NA
S-Band Receive Scan	2750	40	RCP	9	40.5	-	-	-	-	-	-
S-Band Transmit On-Axis	2075	12	RCP	-	39.5	-	-	20.0	-	-	50.5
S-Band Transmit Scan	2075	12	RCP	9	39.0	-	-	20.0	48	-	-
S-Band Receive On-Axis	2250 40	12 40	RCP	-	40.5	-	9.5	-	-	-	-
L-Band Pencil Beam	1650	12	RCP	1.5	38.5	2.5	5.5	-	-	-	-
L-Band Fan Beam Transmit	1550 12	40 12	RCP	1.5	38.5	-	-	40.0	49.0	51	-
L-Band Fan Beam Receive	1650 12	40 12	RCP	1 X 7.5	31.5	5.0	-2	-	-	-	-

Table 4-14 Communications Subsystem Characteristics (Continued)

MODE	NOMINAL FREQUENCY (MHz)	BANDWIDTH (MHz)	POLARIZATION	ANTENNA FIELD OF VIEW (DEGREES)	RECEIVER		TRANSMITTER		
					PEAK GAIN (dB)	MIN G/T OVER FOV (dB/K)	TRANSMITTER OUTPUT POWER (WATTS)	MIN ERP OVER FOV (dB/W)	ERP (dB/W)
S-Band Transmit Scan	2075	12	RCP	9	39.0	-	20.0	48	-
S-Band Receive On Axis	2250	12 40	RCP	-	40.5	-	9.5	-	-
L-Band Pencil Beam	1650	12	RCP	1.5	38.5	2.5	5.5	-	-
L-Band Pencil Beam Transmit	1550	40 12	RCP	1.5	38.5	-	40.0	49.0	51
L-Band Fan Beam Receive	1650	40 12	RCP	1 X 7.5	31.5	5.0	-2	-	-
L-Band Fan Beam Transmit	1550	40 12	RCP	1 X 7.5	31.5	-	40.0	42.0	45
VHF Receive	150	6	RCP	15	17	-20	-18	-	-

Table 4-14 ATS-6 Communications Subsystem Characteristics (Continued)

MODE	NOMINAL FREQUENCY (MHz)		BANDWIDTH (MHz)	ANTENNA FIELD OF VIEW (DEGREES)		RECEIVER		TRANSMITTER			
						PEAK GAIN(dB)	MIN G/T OVER FOV (dB/K)	G/T (dB/K)	TRANSMITTER OUTPUT POWER (WATTS)	MIN ERP OVER FOV (dB/W)	ERP (dB/W)
L-Band Fan Beam Transmit	1550	40	12	1 X 7.5	RCP	31.5	-	-	40.0	42.0	45
VHF Receive	150	6		15	RCP	17	-20	-18	-	-	-
VHF Receive	148.26 154.2	.03		15	RCP	17	-20	-18	-	-	-
VHF Transmit	136.23 137.11	2		15	RCP	17	-	-	2.0	17	20
S-Band Transmit	2569-2 2670.3	40 40		0.9(3)	LCP	43.2	-	-	12 12	44.54(3)	53

{1} SINGLE CARRIER OPERATION  
{2} DUAL CARRIER OPERATION  
{3} EITHER OF TWO OFFSET BEAMS

APPENDIX A  
CONSTRUCTION PROJECT DRAWINGS

The following drawings are included in this appendix.

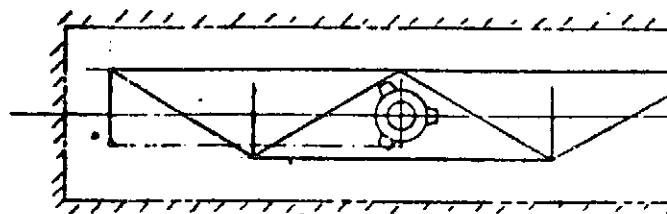
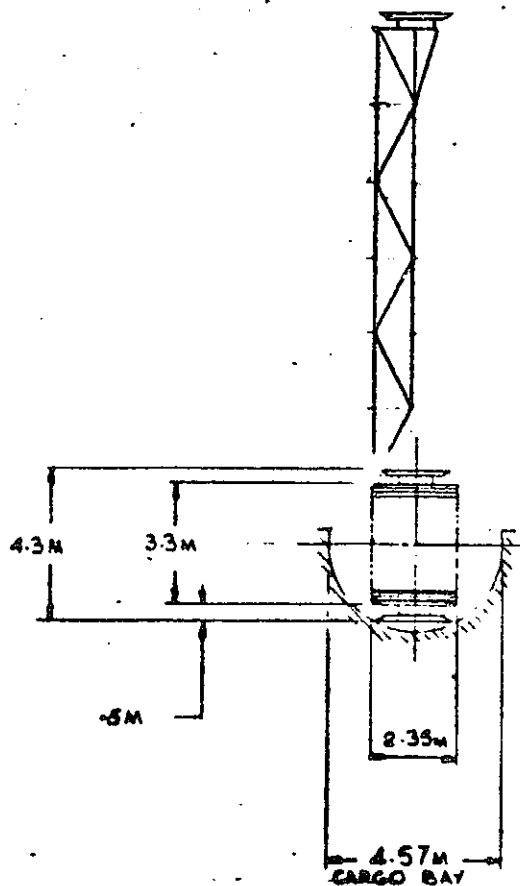
	<u>Page</u>
Drawing No. 42662-4, SPS Flight Test Vehicle Configuration, Deployable SEPS Propulsion, Single Bay (3 Sheets)	A-3,4
Drawing No. 42662-28, Generic Deployable Solar Array (2 Sheets)	A-9,10

PRECEDING PAGE BLANK NOT FILMED A-2

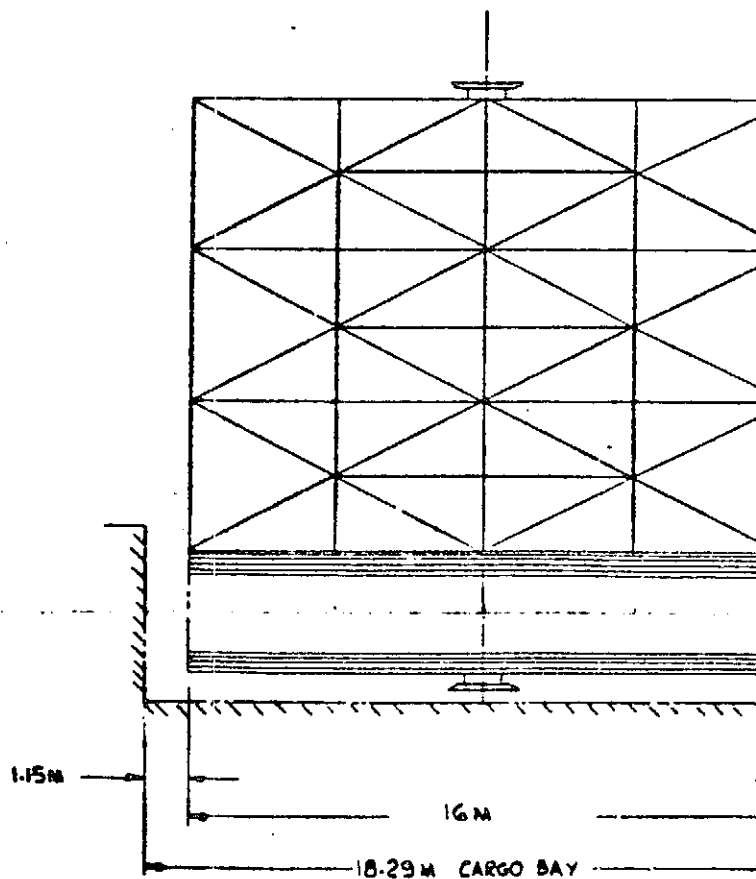
STACKED HEIGHT

2 DOCKING PORTS @ 19.7"	39.4"	1.0 M
63 FOLDED SECTIONS @ 2.00"	126.0"	3.2 M
2 FOLDED ENDS @ 2.00"	4.0"	0.1 M
	<u>169.4"</u>	<u>4.3 M</u>

FOLDOUT FRAME /

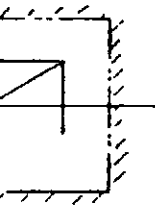


PLAN VIEW SHOWING TRUSS IN  
STOWED POSITION IN CARGO BAY

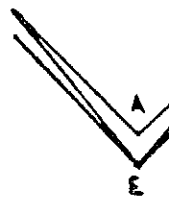
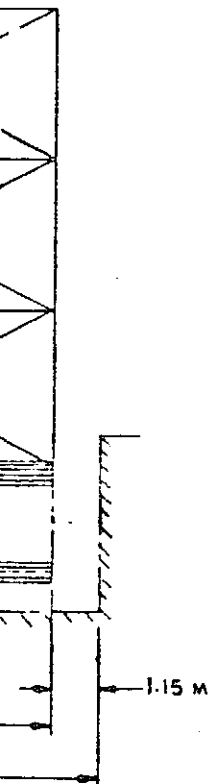


SCALE 1/100



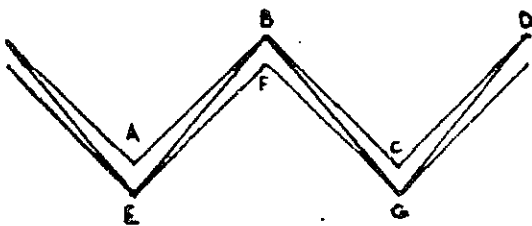
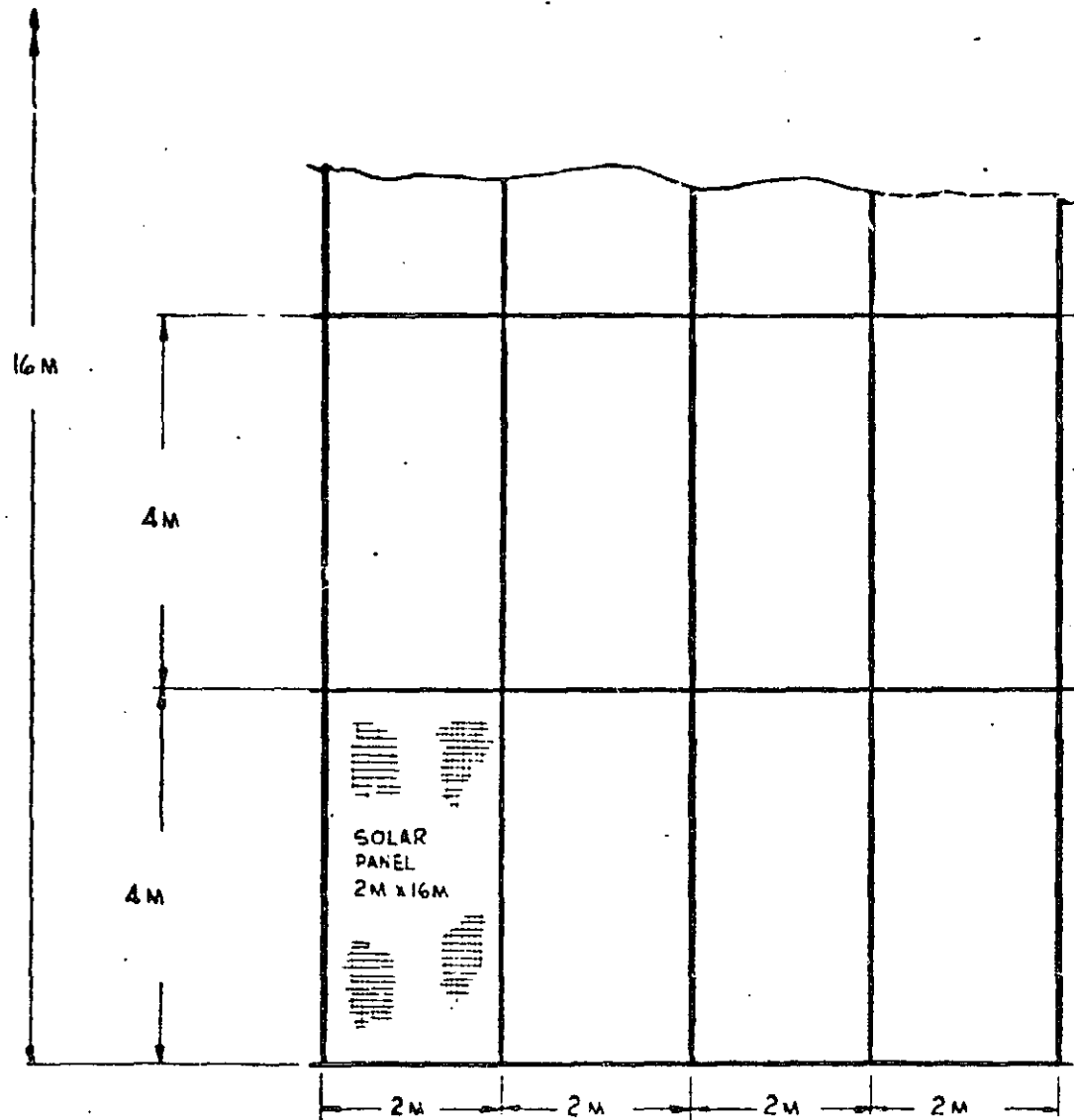


FOLDOUT FRAME 2

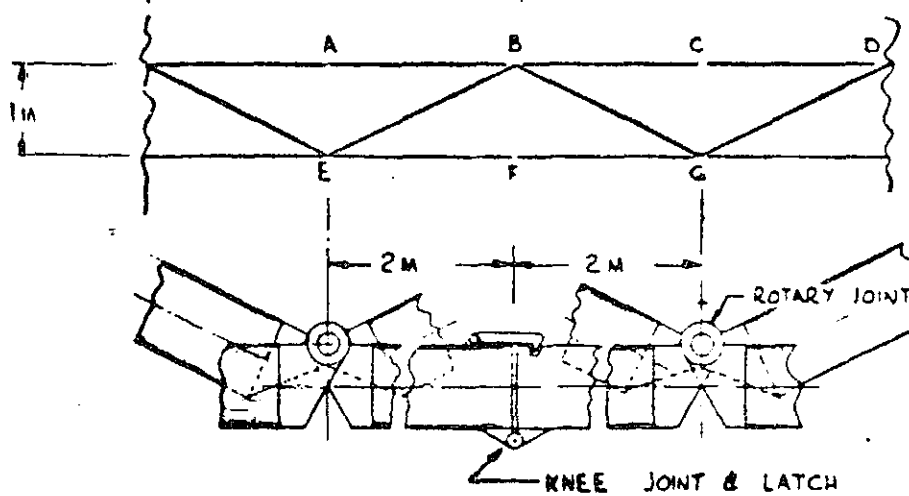


HALF

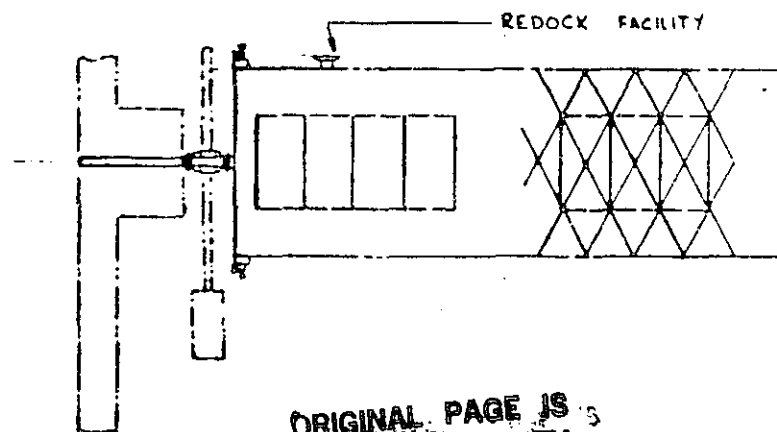
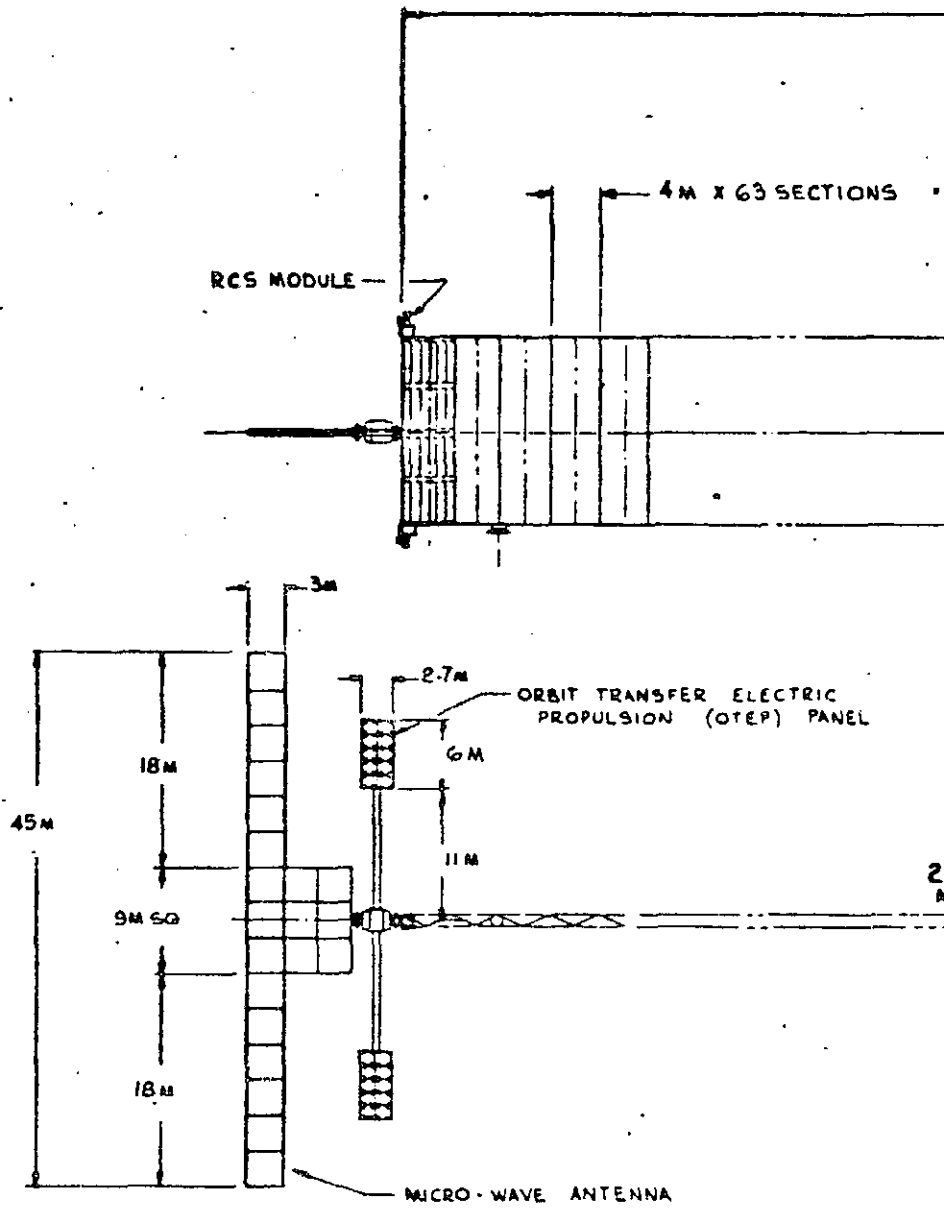
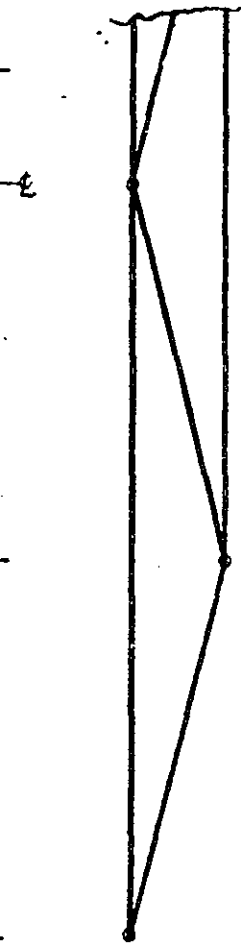
# FOLDOUT FRAME 3



HALF FOLDED POSITION



FOLDOUT FRAME 4

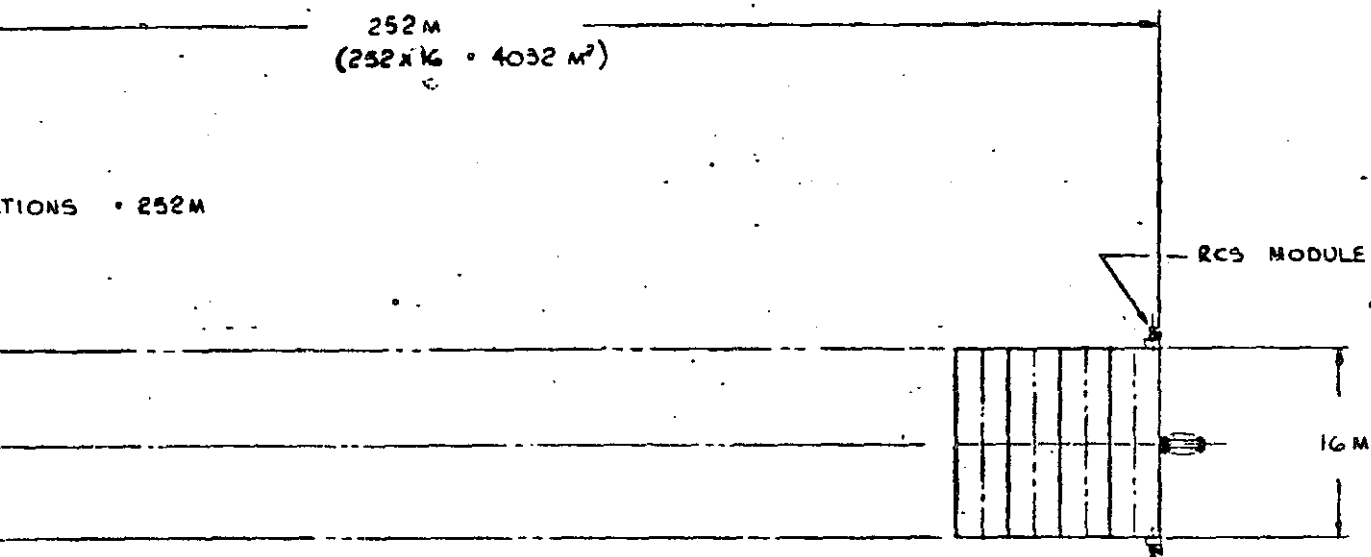


ORIGINAL PAGE IS  
OF POOR QUALITY

17M WIDE X 236 M LONG • 4012 M<sup>2</sup>  
(4M X 59 SECTIONS)

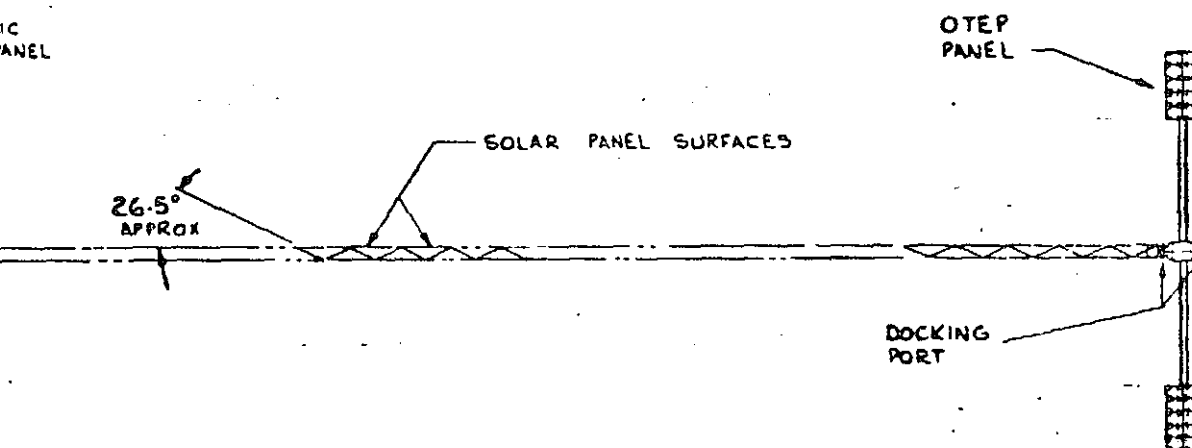
252 M  
(252 X 16 • 4032 M<sup>2</sup>)

CTIONS • 252 M

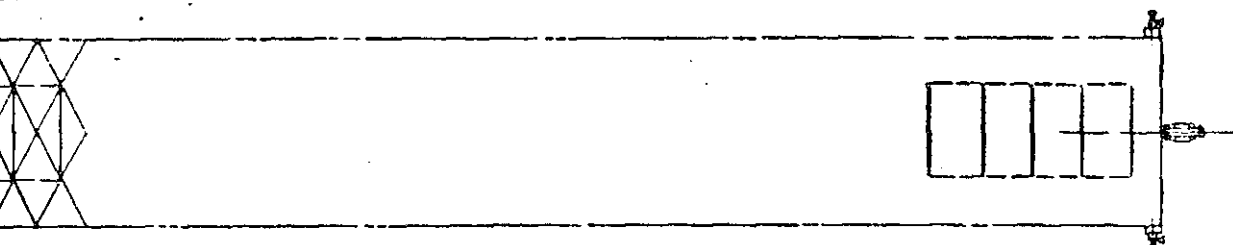


STRUCTURAL CONFIGURATION SCALE 1/320

IC  
ANEL

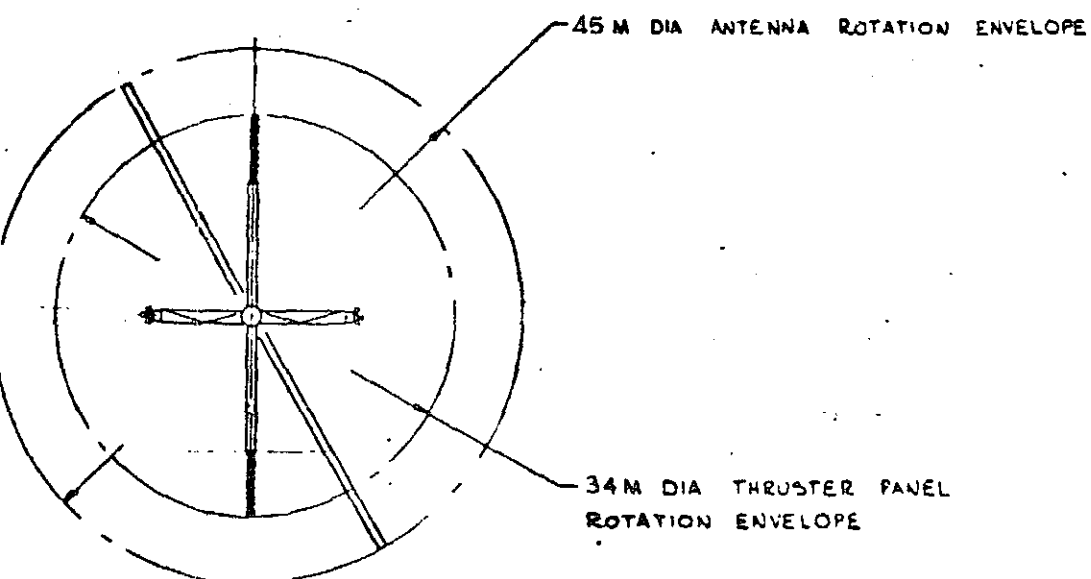


ILITY



FOLDOUT FRAME S

ORIGINAL PAGE IS  
OF POOR QUALITY



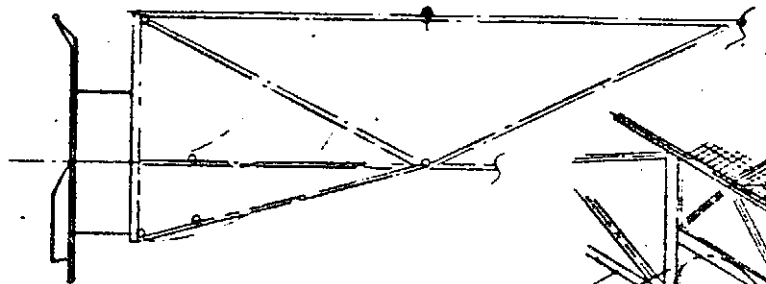
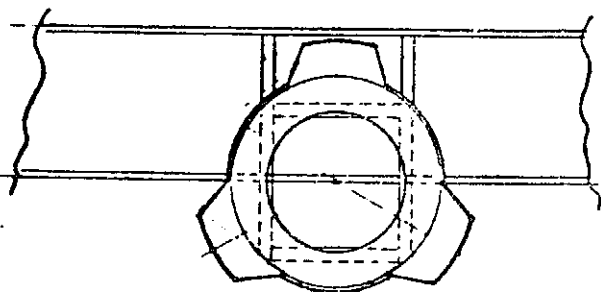
~~POULLOUT FRAME~~ 6

A-3,4

SPS No 1

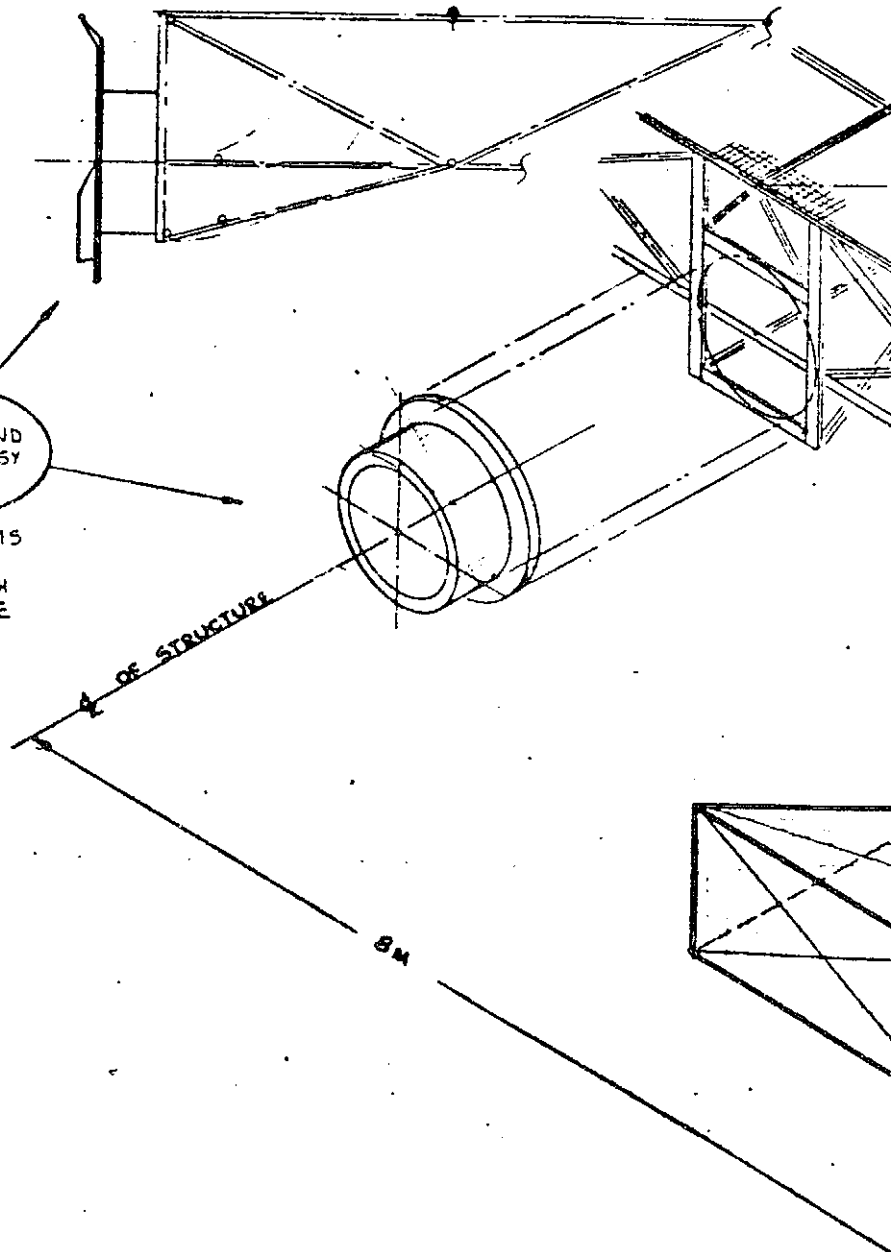
DESIGN	REV 1	DATE 24-78	ROCKWELL INTERNATIONAL CORPORATION SPACE DIVISION 1111 LAKESHORE BOULEVARD, IRVINE, CALIFORNIA 92614
NOTED			
SPS FLIGHT TEST VEHICLE CONFIG DEPLOYABLE SEPS PROPULSION SINGLE BAY.			42662-4 SHEET 1 OF 3

ORIGINAL PAGE IS  
OF POOR QUALITY

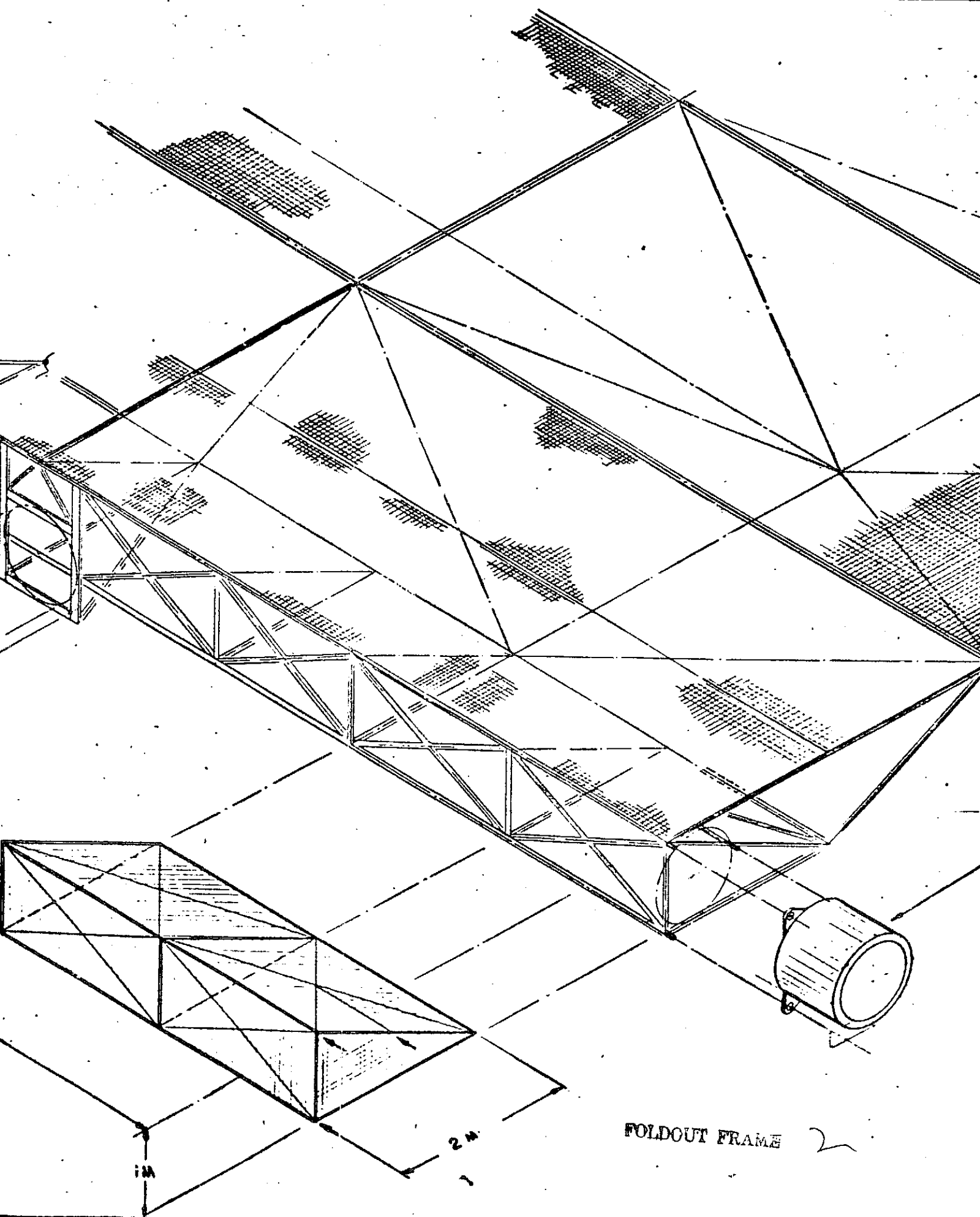


DOCKING  
PORT EACH END  
FOR OTEP ASSY

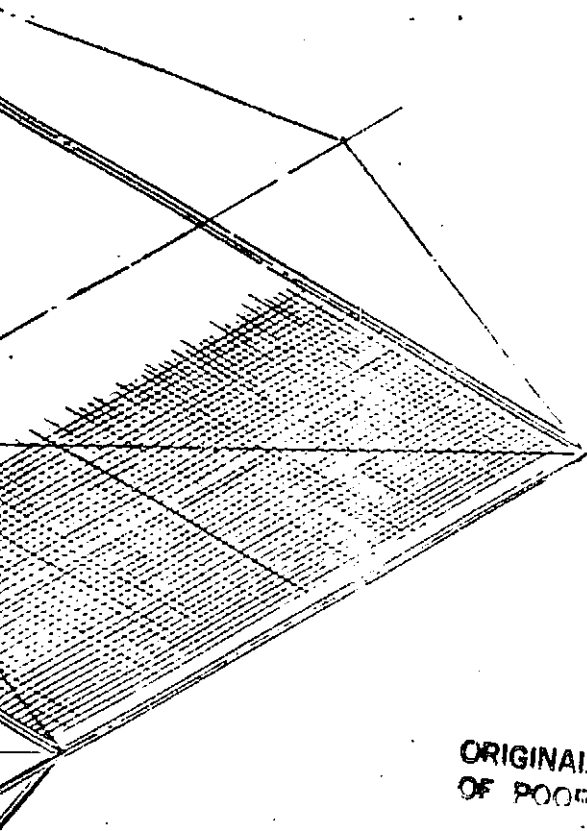
DOCKING PORT IS  
ATTACHED TO &  
DEPLOYED WITH  
THE STRUCTURE



FOLDOUT FRAME



# 3 FOLDOUT FRAME



ORIGINAL PAGE IS  
OF POOR QUALITY

DOCKING  
PORT AT EACH  
OF 4 CORNERS  
FOR RCS MODULES

DOCKING PORT IS INSTALLED  
USING RMS DURING DEPLOYMENT  
OF THE STRUCTURE.  
PORT IS ATTACHED BY SELF  
ALIGNING BALL LOCK SLEEVES  
& PINS.

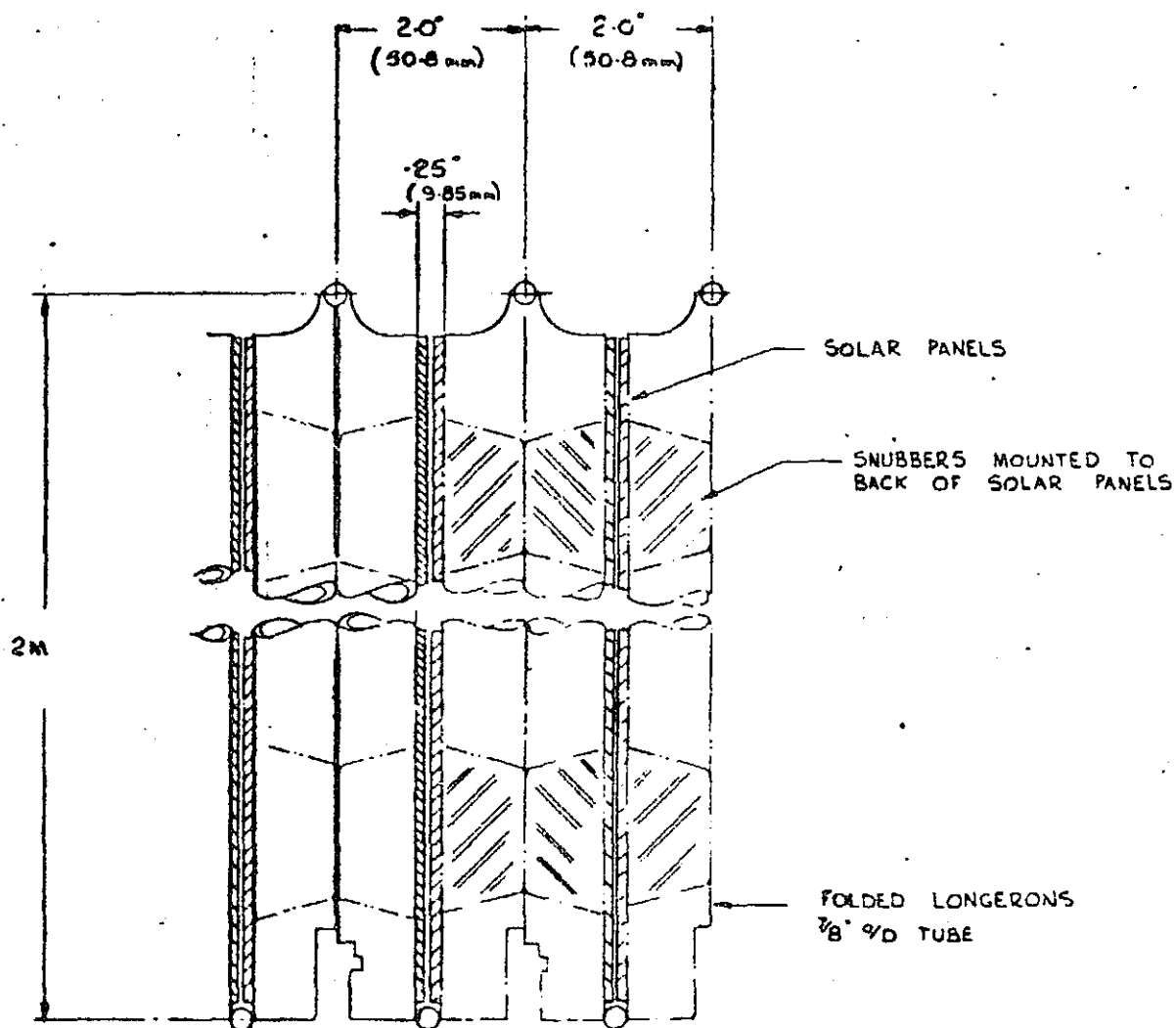
A-5,6

SPS No. 1

SCALE	DATE	ROCKWELL INTERNATIONAL CORPORATION	
1/25	10-26-74	SPACE DIVISION	
SPS FLIGHT TEST VEHICLE CONFIG			
DEPLOYABLE SEPS PROPULSION			
SINGLE BAY			
			42662-4
			SHEET 2 of 3



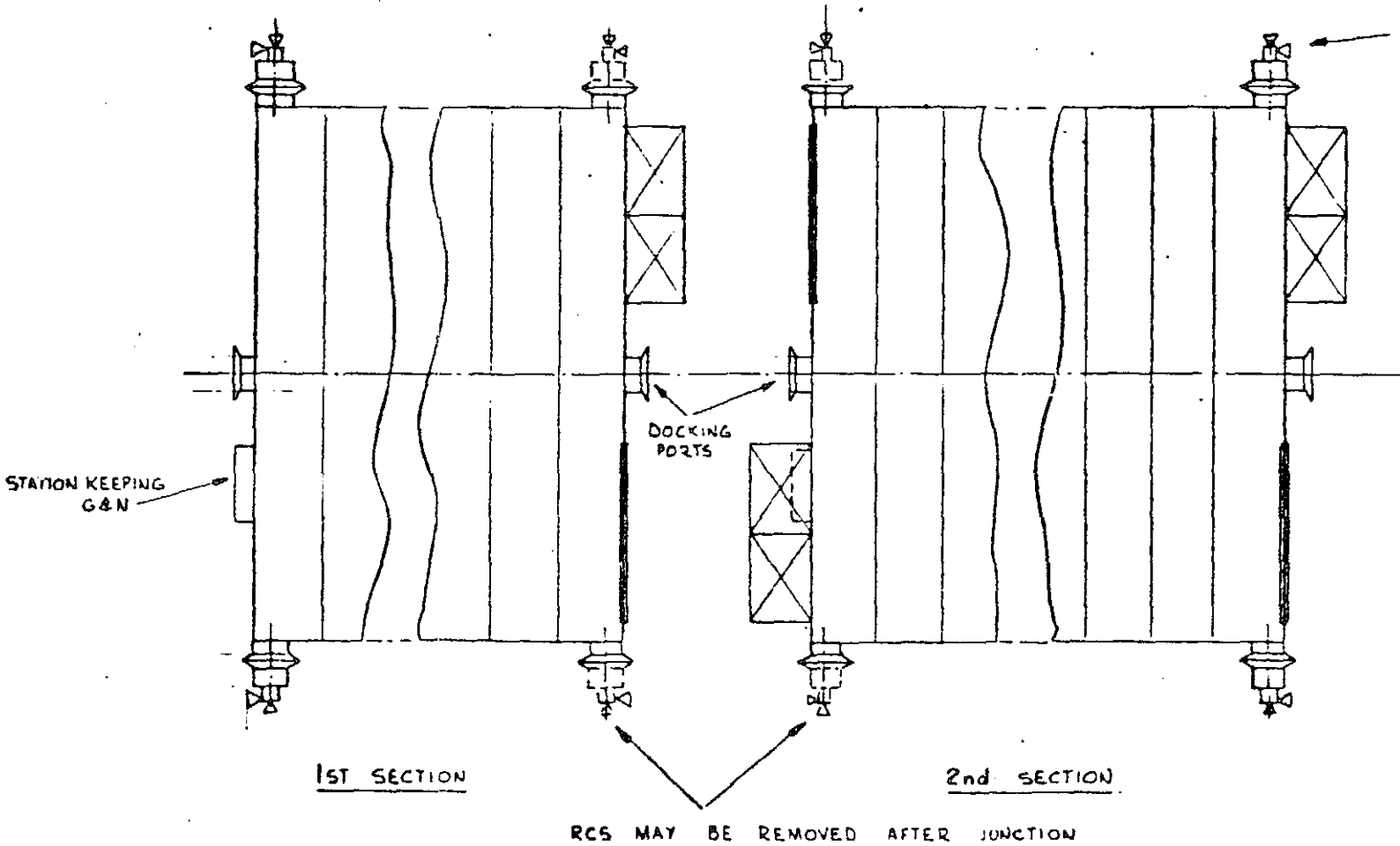
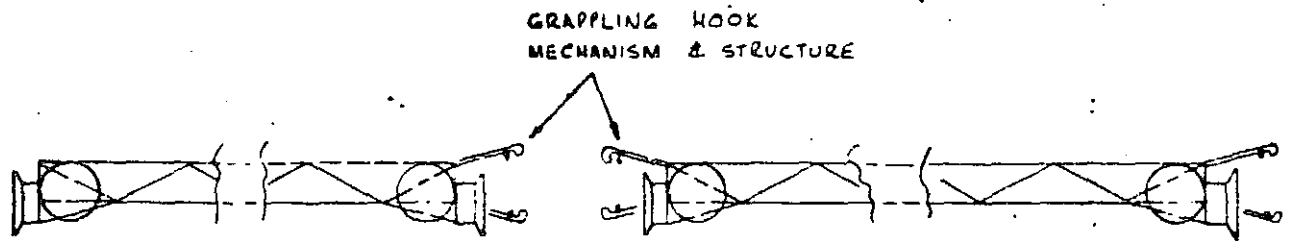
# FOLDOUT FRAME



FOLDED SOLAR PANELS

SCALE  $\frac{1}{1}$

ORIGINAL PAGE IS  
OF POOR QUALITY



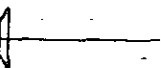
FOLDOUT FRAME 2

METHOD OF JOINING TWO SECTIONS  
SCALE 1/100

OF FOLDOUT FRAME



← DOCKING PORTS WITH  
RCS MODULES



FOLDOUT FRAME 3

A-7,8

SPS No. 1

DESIGNED BY	R. HAST	ROCKWELL INTERNATIONAL CORPORATION
DATE	10-2-75	SPACE DIVISION
NOTED		1111 LAKEMORE AVENUE, SUITE 100, CARLSBAD, CALIFORNIA 92008
SPS FLIGHT TEST VEHICLE CONFIG		42662-4 SHEET 3 OF 3
DEPLOYABLE SEPS PROPULSION		
SINGLE BAY		

18.27M

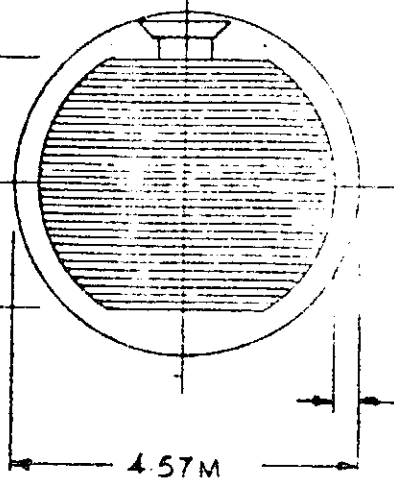
16M

1.13 M

FOLDOUT FRAME

ORIGINAL PAGE IS  
OF POOR QUALITY63 SECTIONS @  
2" STACK HEIGHT

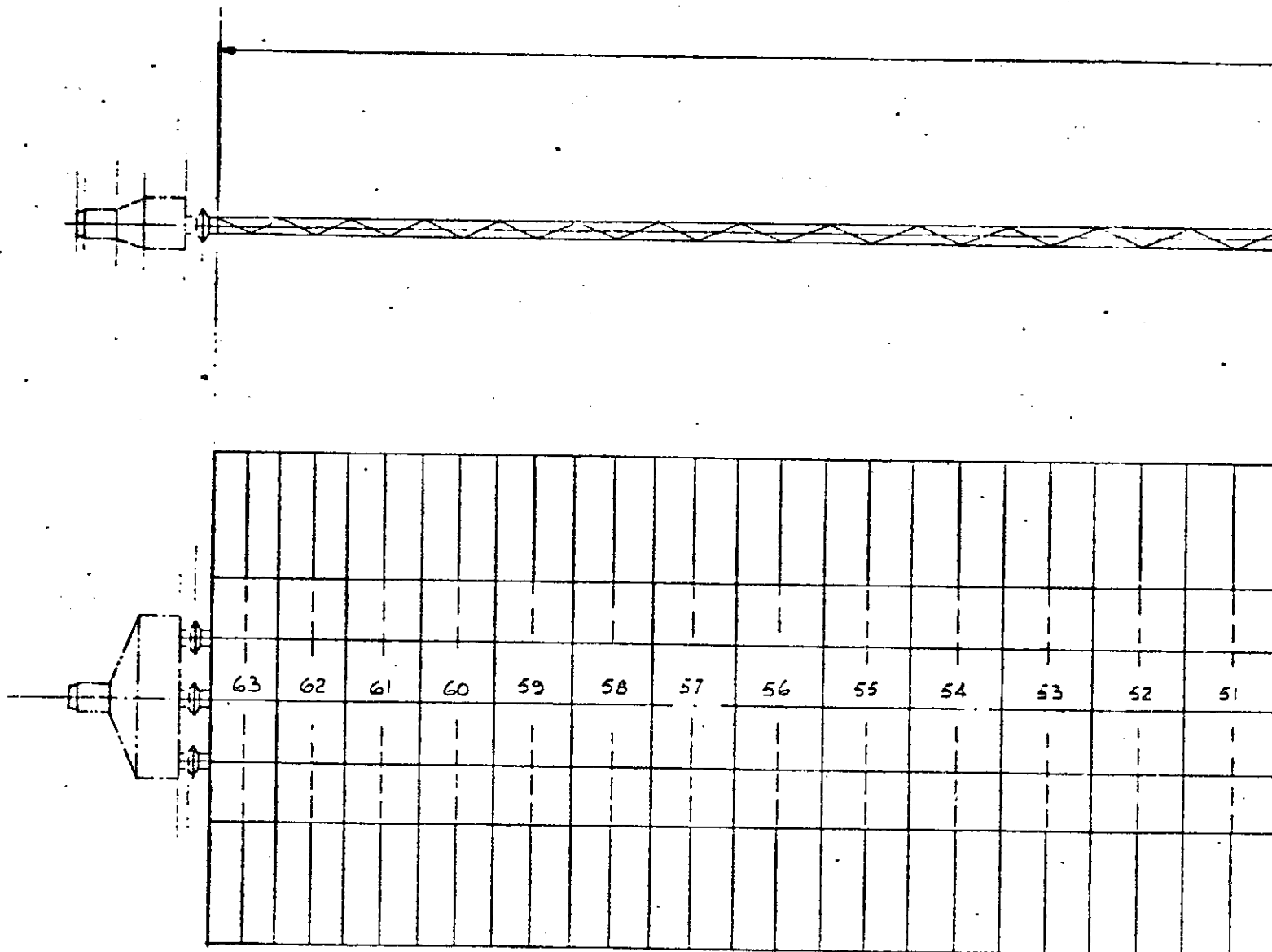
3.2 M

PACKAGING IN  
ORBITER

SCALE:- 1/50

0.30 M

4.57 M



FOLDOUT FROM

2

ORIGINAL PAGE IS  
OF POOR QUALITY

[illegible]

3 FOLDOUT FRAME

12

63 BAYS

1.77 M

[illegible]

**FOUR OUT FRAME**

41

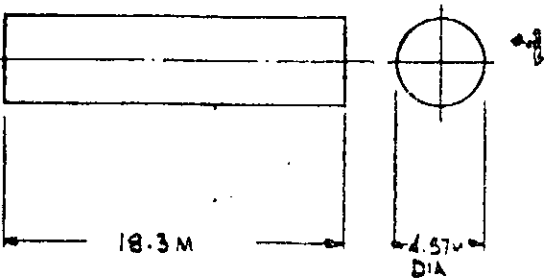
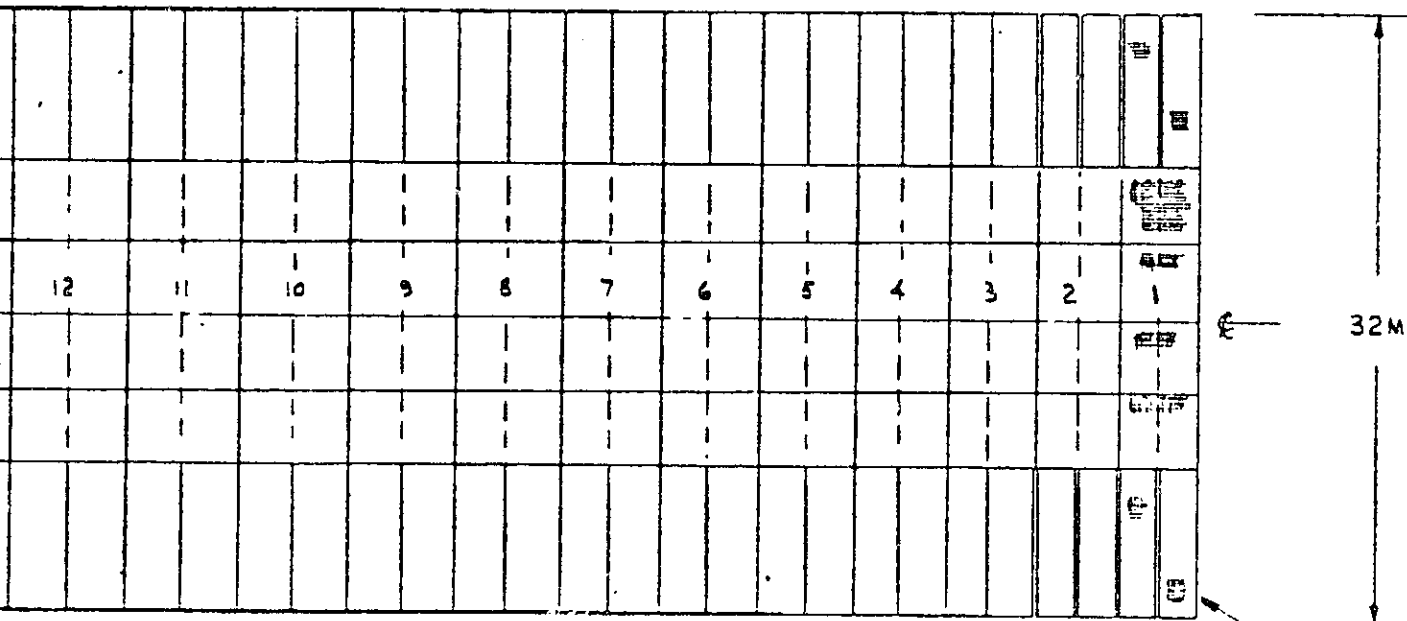
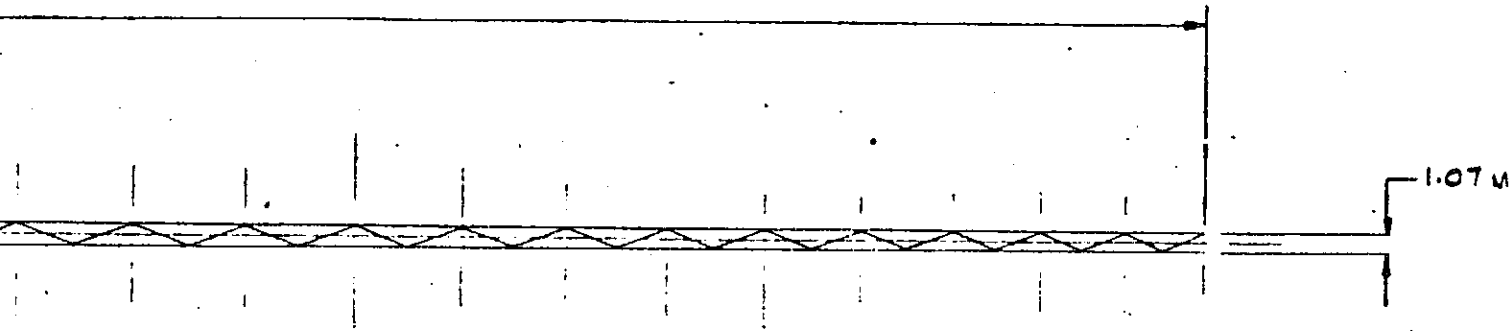
Si



8

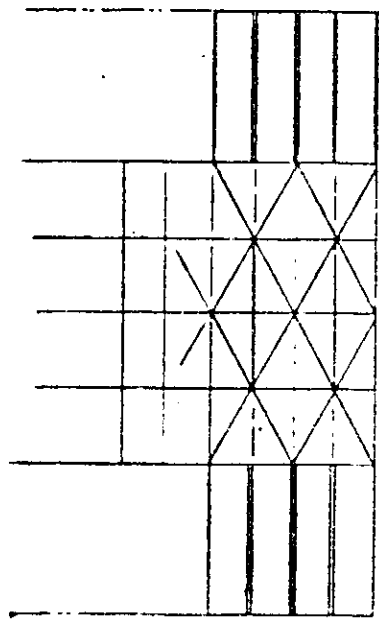
7

6



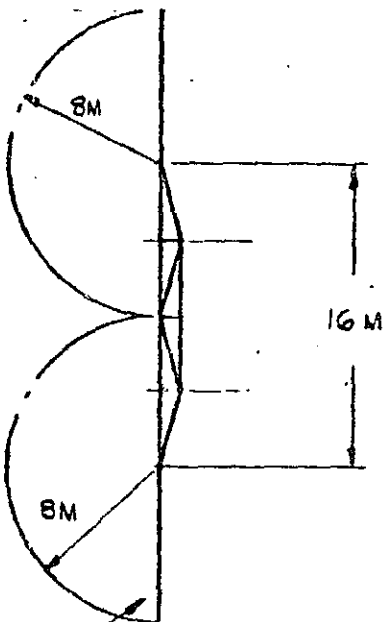
SHUTTLE CARGO BAY  
SAME SCALE AS MAIN VIEW

FOLDOUT FRAME 6



VIEW OF UNDERSIDE  
SHOWING STRUCTURE

# FOLDOUT FRAME



SOLAR PANEL WINGS  
RELEASED BY LANYARD  
DEPLOYED BY SPRING

BAY NO	LENGTH	HEIGHT
1, 63	4.296	1.07
2, 62	4.524	1.131
3, 61	4.734	1.183
4, 60	4.928	1.232
5, 59	5.110	1.277
6, 58	5.278	1.320
7, 57	5.434	1.358
8, 56	5.582	1.395
9, 55	5.718	1.430
10, 54	5.846	1.462
11, 53	5.966	1.496
12, 52	6.080	1.520
13, 51	6.184	1.546
14, 50	6.282	1.571
15, 49	6.372	1.593
16, 48	6.458	1.615
17, 47	6.536	1.634
18, 46	6.610	1.652
19, 45	6.676	1.669
20, 44	6.738	1.684
21, 43	6.794	1.698
22, 42	6.844	1.711
23, 41	6.890	1.723
24, 40	6.922	1.730
25, 39	6.966	1.742
26, 38	6.998	1.749
27, 37	7.022	1.755
28, 36	7.044	1.761
29, 35	7.060	1.765
30, 34	7.072	1.768
31, 33	7.078	1.769
32	7.080	1.770

ORIGINAL PAGE 18  
OF 2000 PAGES

2

1

REVISIONS				
ZONE	LTR	DESCRIPTION	DATE	APPROVED

D

C

GROSS AREA 32 M X 391.1 M • 12,515 M<sup>2</sup>  
 (105 FT X 1284 FT • 134,820 FT<sup>2</sup>)

IF SEP STD PANEL .75 M X 4 M IS USED  
 APPROX 70% AREA USAGE CAN BE ACHIEVED

70% X 12,515 M<sup>2</sup> = 8760 M<sup>2</sup>  
 AT 139 WATTS/M<sup>2</sup> • 1217 KW

B

FOLDOUT FRAME 8

A-9,10

DR BY		27-437		27-437	
CHK BY					
APPROVED BY					
Rockwell International Corporation Space Division 12214 Lakeside Drive • Gardena, California 90248					
GENERAL DEPLOYABLE SOLAR ARRAY					
SIZE	CODE IDENT NO	DRAWING NO			
L	03953	42333-28			
SCALE					

A

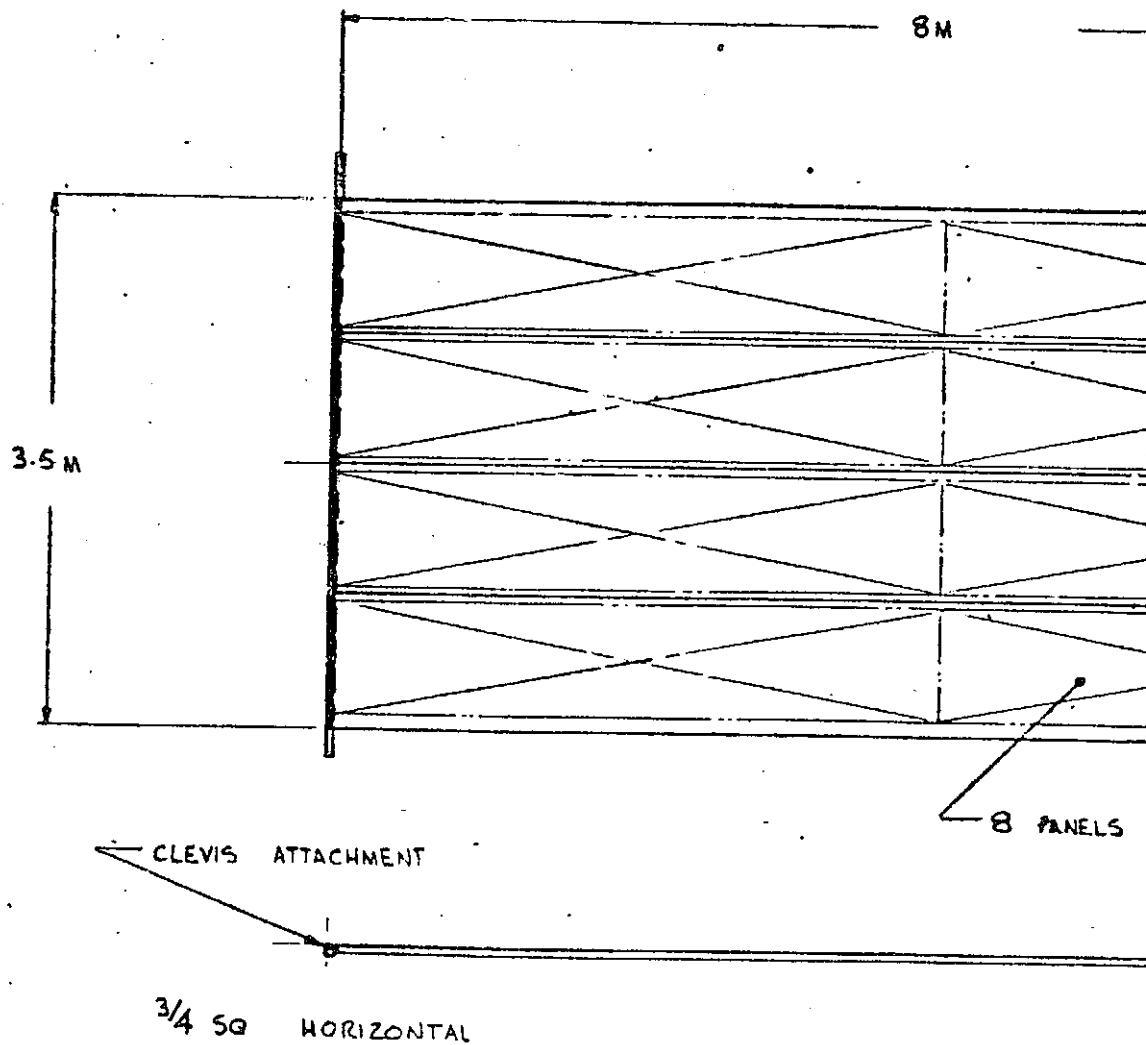
D

C

→

B

A



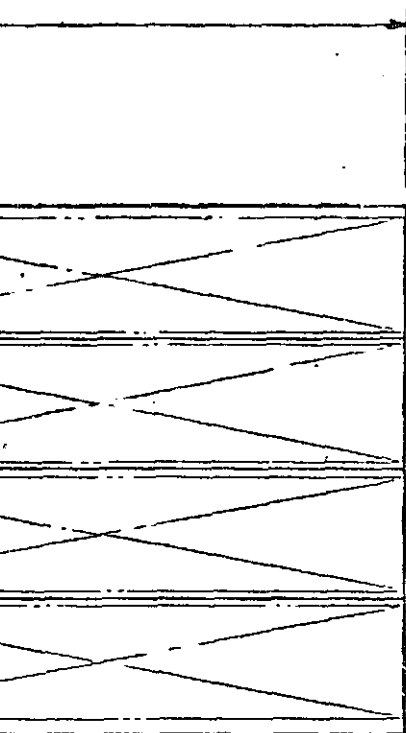
FOLDOUT FRAME

FOLDOUT FRAME

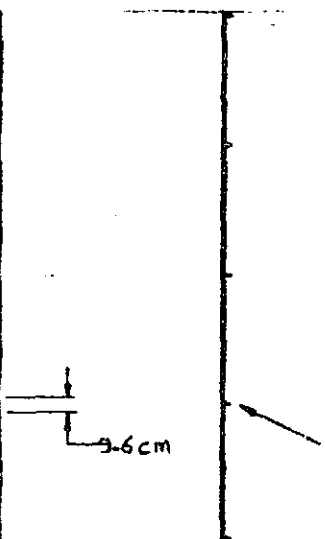
"WING" NO 32

SCALE:  $\frac{1}{25}$

ORIGINAL PAGE IS  
OF POOR QUALITY

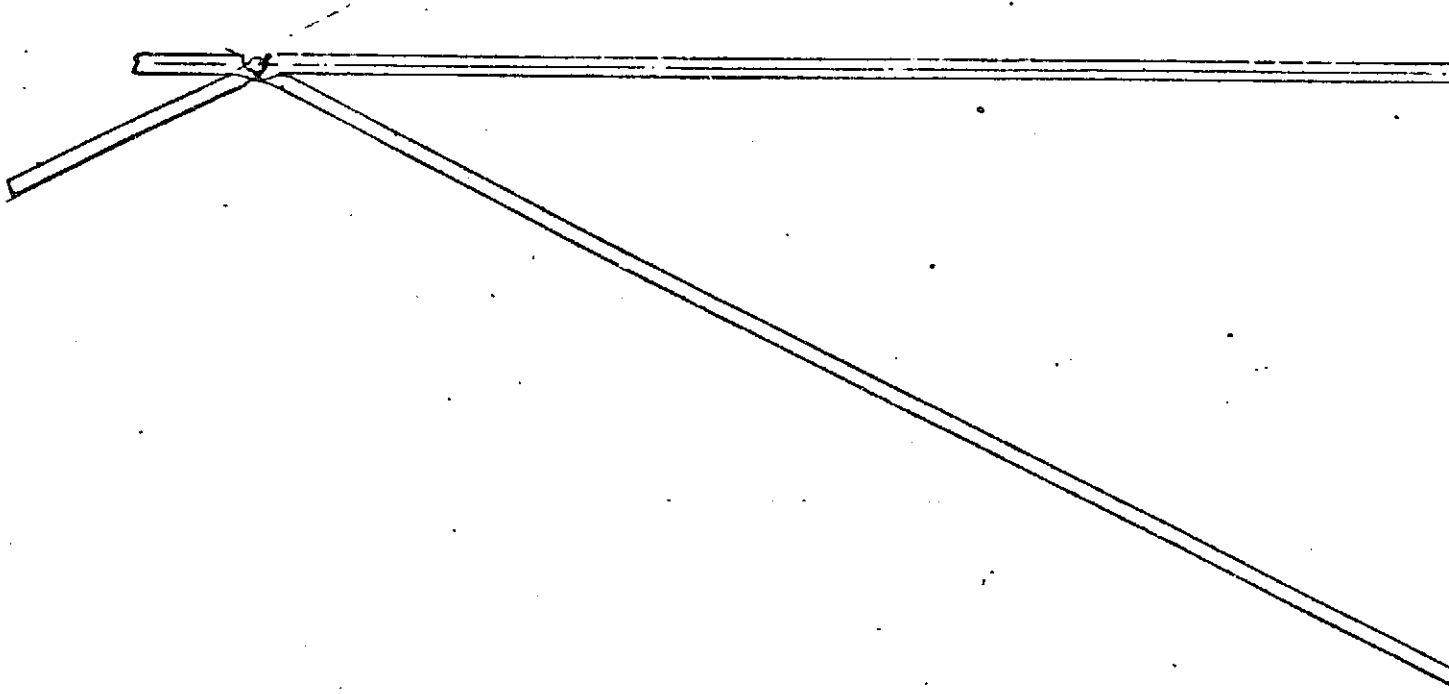


4 M x 754 M



RIB STIFFENERS  
5 PLACES

FOLDOUT FRAME 2



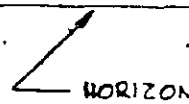
ORIGINAL PAGE IS  
OF POOR QUALITY

FOLDBOUT FRAME

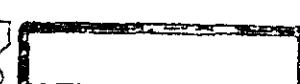
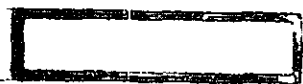
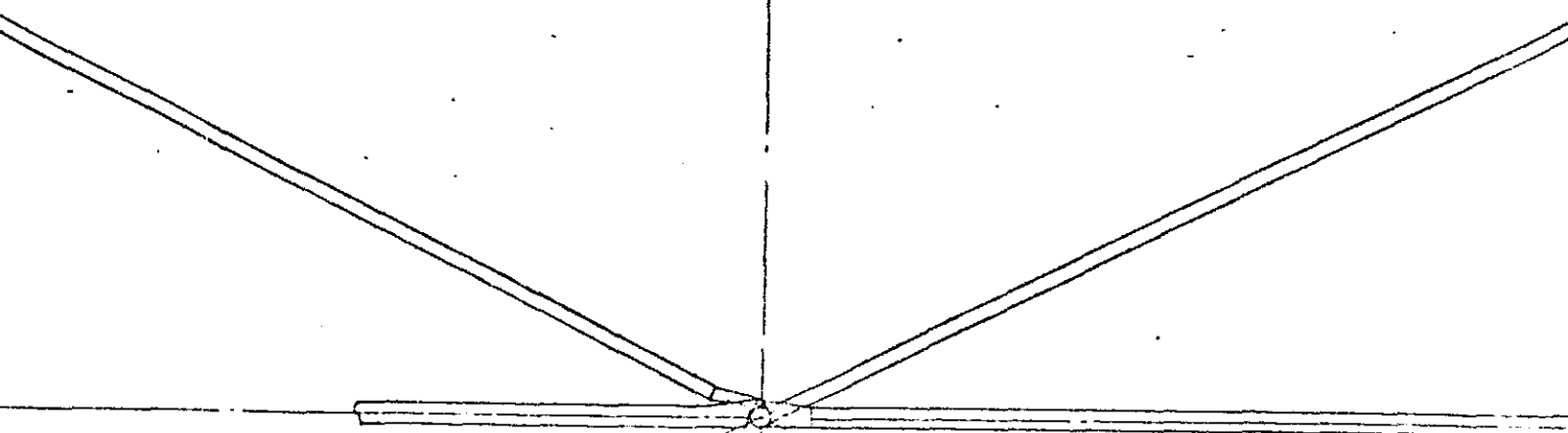
3



SECTION THROUGH HORIZ  
TUBE SHOWING "WING" IN  
POSITION WITH RIB STIFFE  
UNFOLDED



FOLDOUT FRAME 4



VIE  
WI

HORIZONTAL  
STOWED  
SENER

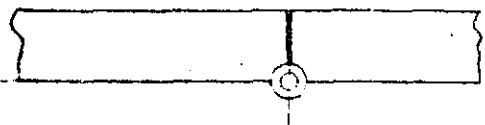
HORIZONTALS

DIAGONAL

FOLDOUT FRAME

HORIZONTALS

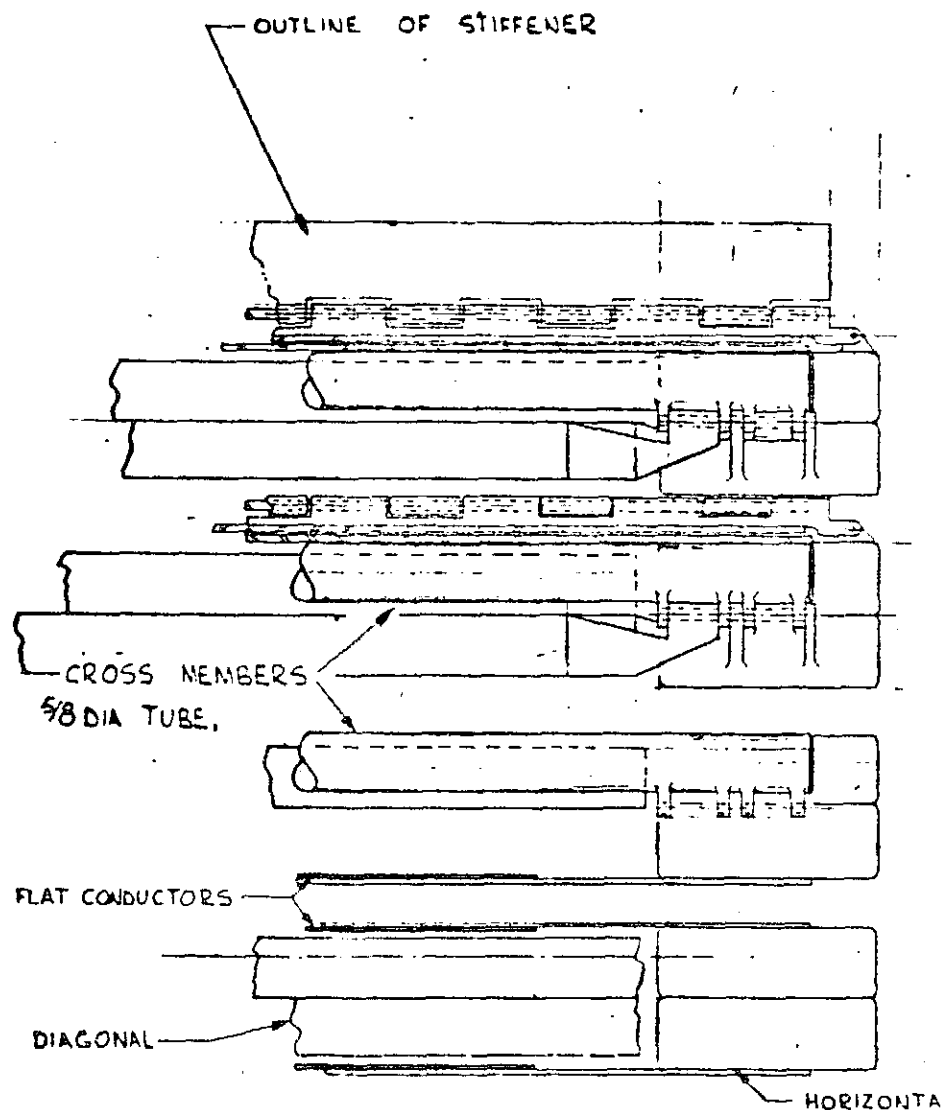
VIEW OF TYPICAL BAY  $\frac{1}{4}$  SCALE  
WITH DETAIL VIEWS FULL SIZE



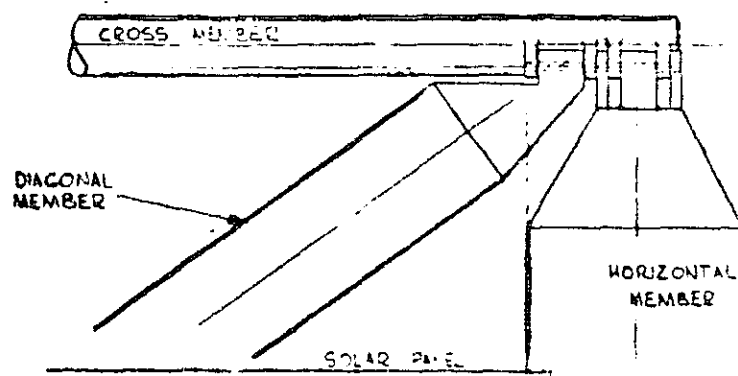


FOLDOUT FRAME

6



ORIGINAL PAGE IS  
OF POOR QUALITY



1/2" SPACE FOR STOWING SOLAR PANELS  
E "WING" STRUCTURE.

FOLDOUT FRAME 7

SPRING LOADED TO DEPLOY  
STIFFENERS FOR "WINGS."

HORIZONTAL MEMBERS  
SHOWN. DIAGONALS OMITTED  
FOR CLARITY.

FIXED SOLAR  
PANELS.

SOLAR PANEL "WING."

DIAGONAL MEMBERS 5/8 x 1/4" TUBE

FLAT CONDUCTORS  
APPROX .042" MAX

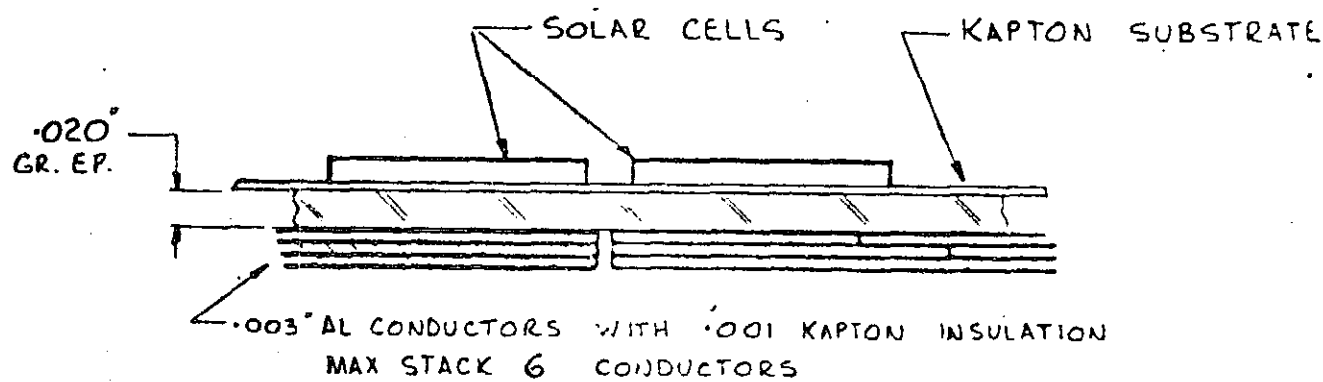
HORIZONTAL MEMBERS  
SUPPORTING THE MAIN (FIXED)  
SOLAR ARRAY PANELS  
3/4 x 2 1/4" TUBE

VIEW SHOWING FOLDED STRUCTURE

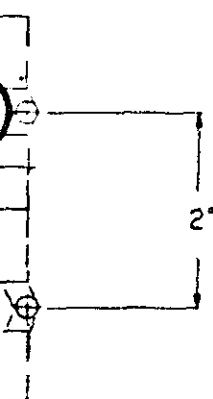
SCALE - FULL SIZE

ORIGINAL PAGE IS  
OF POOR QUALITY

REVISIONS				
ZONE	LTR	DESCRIPTION	DATE	APPROVED



SECTION THRO SOLAR BLANKET  
NO SCALE



WELDOUT FRAME 8

A-11,12

SIZE	CODE IDENT NO	DRAWING NO.
1	03953	42232-28

## APPENDIX B

### LINK CALCULATIONS

#### B.1 LINK CALCULATIONS FOR 12/14-GHz EARTH STATIONS AT USER LOCATIONS

##### B.1.1 C/N Requirements

Assuming a BER of  $10^{-7}$  for a single-hop link, and a 36 Mbps transmission rate in a 36-MHz bandwidth, the C/N ratio required for an MSK modem is 15.7 dB. (Figure B-1). This includes 3.8 dB of margin for inter-symbol interference

The general expression for the link C/N is:

$$\left(\frac{C}{N}\right)_{\text{total}} = \left[ \left(\frac{C}{N_{\text{th}}}\right)_u^{-1} + \left(\frac{C}{I}\right)_u^{-1} + \left(\frac{C}{N_{\text{th}}}\right)_d^{-1} + \left(\frac{C}{N_{\text{th}}}\right)_d^{-1} + \left(\frac{C}{N}\right)_d^{-1} \right]^{-1} \quad (\text{B-1})$$

We assume no system operating in the 20 to 30 GHz band to interfere with Satellite Electronic Mail System. Therefore, Equation B-1 can be written as:

$$\left(\frac{C}{N}\right)_{\text{total}} = \left[ \left(\frac{C}{N_{\text{th}}}\right)_u^{-1} + \left(\frac{C}{N}\right)_u^{-1} + \left(\frac{C}{N_{\text{th}}}\right)_d^{-1} \right]^{-1} \quad (\text{B-2})$$

Now, we shall compute each one of the ratios on the right-hand side of Equation 2.

##### B.1.2 (C/I)<sub>u</sub> Calculation at 14 GHz

$$\left(\frac{C}{N}\right)_u = E_W - E_I + G_S + P_A + B_A \quad (\text{B-3})$$

Where  $E_W$  = EIRP on main axis from electronic mail earth station

$E_I$  = EIRP off-axis in dBW from STS or SBS earth station

$G_S$  = Satellite gain in dB advantage (or disadvantage) which depends upon the elevation angles of the electronic mail earth station and interference system (SBS or CTS) earth station. In the absence of actual site information, we assume  $G_S = -3.5$  dB for worse case design.

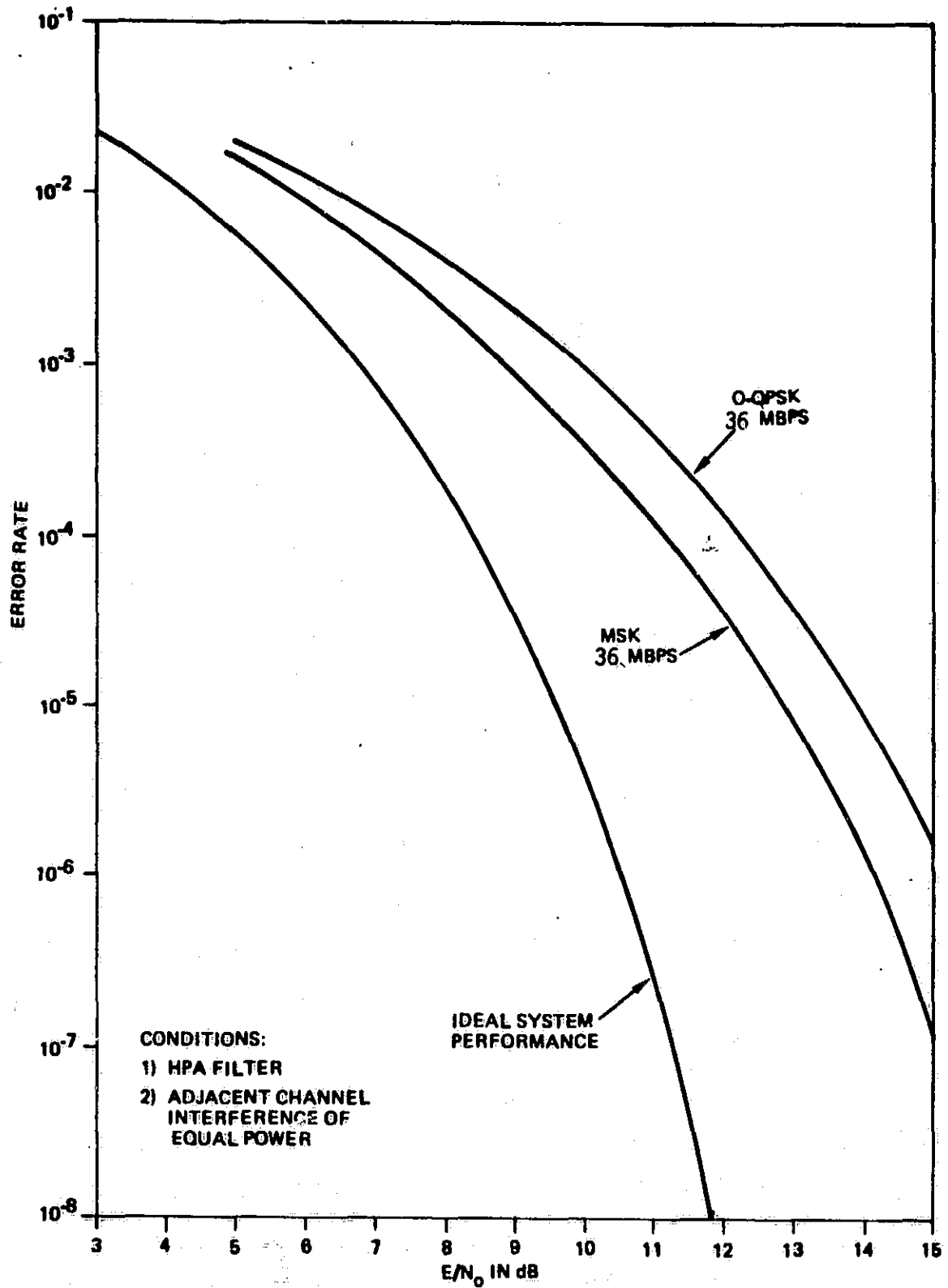


Figure B-1. Comparison of MSK and O-QPSK Performance over Satellite Channel with Adjacent Channel Interference and HPA Filter

$P_A$  = Polarization advantage (or disadvantage). We assume  $P_A = 0$  dB for worse case.

$B_A$  = This is a factor for when the interfering signal bandwidth is greater than the desired signal bandwidth; otherwise, it is assumed to be 0 dB.

The assumptions for the satellite parameters at 14 GHz are:

- Antenna diameter—6.4 m
- On-axis antenna gain—55.8 dBi

We assume that off-axis gain of the SBS and CTS transmitting antennas are given by the expression

$$G_{\text{off-axis}} = 32 - 25 \log \theta, \text{ dBi}, 1^\circ \leq \theta \leq 48^\circ \quad (\text{B-4})$$

where  $\theta$  is in degrees off axis.

The off-axis gains at the earth station are given as:

Angle (degrees)	Gain (dBi)
4.0	17.0
5.0	14.5
6.0	12.6

We will consider the uplink interference from two types of earth stations which could be operating at 14 GHz in the same urban area in which the electronic mail earth station is operating. The Satellite Business System (SBS) and the Communication Technology Satellite (CTS) are also known as Hermes. Table B-1 summarizes the uplink parameters for these stations.

Substituting the values in Equation B-3, we get the worse case spacing:

$$\left(\frac{C}{I}\right)_u = E_W - 47.5 - 3.5 + 1.3 \text{ dB} = E_W - 49.7 \text{ dB for SBS at } 4^\circ \text{ spacing, and}$$

$$\left(\frac{C}{I}\right)_u = E_W - 41 - 3.5 = E_W - 44.5 \text{ dB for CTS at } 4^\circ \text{ spacing.}$$

Of the two cases, the interference from the SBS type of earth station is potentially the greatest. It is current FCC practice to keep a  $5^\circ$  to  $6^\circ$  spacing relative to CTS which would decrease the CTS interference further.

Next, we consider the interference of the electronic mail earth station to an adjacent SBS or CTS satellite. The SBS and CTS satellite receive parameters are summarized in Table B-1. The  $(C/I)_{u\text{adj}}$  for the adjacent satellites is given by substituting into Equation B-3.

Table B-1. Uplink Parameters for Interference Calculations

Parameter	SBS Uplink	CTS Uplink
Earth station antenna size	5 meters	2.5 meters
Maximum power out	2000 W	400 W
Line loss	2.5 dB	2 dB
On-axis gain	55.5 dB	48.4 dB
EIRP on-axis	86 dBW	48.4 dB
EIRP at 6°	43.1 dBW	36.6 dBW
EIRP at 5°	46.0 dBW	39.5 dBW
EIRP at 4°	47.5 dBW	41.0 dBW
Antenna beamwidth	4.5°×3°	2.5°
Receive G/T (on axis)	1.5 dB/°K	6.2 dB/°K
Receive (G/T) beam edge	-4.5 dB/°K	3.2 dB/°K
Saturation flux density (on axis)	-83 dBW/m <sup>2</sup>	-91.5 dBW/m <sup>2</sup>

If we require that  $(C/I)_u$  26 dB, then we have the following minimum values of  $E_W$  for the earth station:

Angle (degrees)	Minimum $E_W$ for SBS Interference (dBW)	Minimum $E_W$ for CTS Interference (dBW)
4.0	75.7	70.5
5.0	74.2	69.0
6.0	72.3	67.1

Substituting again into Equation B-3,

$$\begin{aligned} \left(\frac{C}{I}\right)_{uadj} &= 86 - E_I - 3.5 \\ &= 82.5 - E_I \text{ for SBS} \end{aligned}$$

where  $E_I$  is the off-axis EIRP of the electronic mail station toward the adjacent satellite and

$$\begin{aligned} \left(\frac{C}{I}\right)_{uadj} &= 72.4 - E_I - 3.5 \\ &= 68.9 - E_I \text{ FOR CTS.} \end{aligned}$$

If we design for  $(C/I)_{uadj} \geq 30$  dB, then we see that the maximum value for  $E_I$  is 38.9 dBW and is set by CTS. Using the off-axis gain values assumed previously, then the maximum power levels into the satellite electronic mail earth station antenna become:

Angle (deg)	HPA Power Level (dBW)	EIRP (dBW)	Antenna Gain (dB)	Antenna Diameter (m)
4.0	21.9	75.7	53.8	4.0
5.0	24.4	74.2	49.8	2.9
6.0	26.3	72.3	46.0	1.8

Thus, from an interference standpoint, 1.8-m (5-ft) diameter earth station antennas with 600-W HPA's could be employed at 14 GHz for satellite electronic mail earth stations provided the in-orbit spacing to the adjacent satellite is 6 degrees or greater. However, from a cost tradeoff, it is more reasonable to employ 4.5- or 5-m-diameter antennas with 200-W HPA's. Further, this would allow adjacent satellite spacings of 4 degrees. Thus, for the remainder of the 12/14-GHz link calculations, a 5-m earth station antenna will be assumed.

### B.1.3 $(C/N_{th})_u$ Calculation at 14 GHz

The uplink C/N ratio is given by the expression

$$(C/N_{th})_u = E_W - L - M_p - M_r + 228.6 - 10 \log B + G/T_s \quad (B-5)$$

where  $E_W$  is the uplink EIRP in dBW

$L$  is the clear-weather path loss

$M_p$  is the margin in dB required for antenna pointing errors, polarization misalignment, etc.

$M_r$  is the rain margin in dB

$B$  is the bandwidth in Hz

$G/T_s$  is the receive gain-to-noise temperature ratio of the satellite in dB/°K

The resulting calculation is summarized in Table B-2.

Table B-2. Calculations of  $(C/N_{th})_u$  at 14 GHz

Uplink EIRP, $E_W$	72.3 dBW
Path loss at 14 GHz, $L$	-207.4 dB
Satellite $G/T_s$	24 dB/°K
Boltzmann's Constant	228.6
Noise bandwidth (36 MHz), $B$	-75.6 dB-Hz
Miscellaneous margin, $M_p$	-2.0 dB
Rain margin, $M_r$	-12 dB
$(C/N_{th})_u$	27.9 dB

The  $G/T_s$  of the satellite assumes a tunnel diode amplifier at the receiver input.



#### B.1.4 $(C/N_{th})_u$ Calculation at 30 GHz

With the interchange of earth station and satellite parameters, Equation B-5 can also be used to compute  $(C/N_{th})_d$ . For the 30-GHz downlink to the central routing control station, the following assumptions have been made.

- Satellite antenna diameter 3 m
- Satellite power amplifier level 5 dBW
- Satellite antenna gain 56 dBi
- Earth station antenna diameter 5 m
- Earth station antenna gain 61.0 dBi
- Earth station G/T 28.3 dB/°K

The link calculation is summarized in Table B-3.

Table B-3. Calculation of  $(C/N_{th})_d$  at 30 GHz

Satellite EIRP, $E_{ws}$	61 dBW
Path loss at 30 GHz, L	-214 dB
Earth station G/T	28.3 dB/°K
Boltzmann's Constant	228.6
Noise bandwidth (36 MHz), B	-75.6 dB-Hz
Miscellaneous margin, $M_p$	-2.5 dB
Rain margin	-5.1 dB
$(C/N_{th})_d$	20.7 dB

The G/T for the control earth station assumes a tunnel diode amplifier receiver. The antenna is large to provide adequate rain margin for low-rainfall areas and to make it relatively difficult for anyone to try to "copy" the mail through unauthorized receiving earth stations.

Rockwell has supplied one 50-ft without radome and one 120-ft-diameter antenna with radome for operation at 35 GHz for radio astronomy applications. Rockwell has performed feasibility studies for low-cost 30-GHz earth station antennas as large as 60-ft diameter which do not employ radomes.

#### B.1.5 Calculation of $(C/N)_{total}$ for 14-GHz Uplink and 30-GHz Downlink

Now, we can substitute the values into Equation B-2 under the worse case assumption of 1.2 dB of rain loss on the uplink, 5.1 dB of rain loss on the downlink, and interference from other 14-GHz uplink earth stations. That is, assuming two interfering sources, each with  $(C/I)_u = 26$  dB,  $(C/N_{th})_u = 27.9$  dB, and  $(C/N_{th})_d = 20.7$  dB. The  $(C/N)_{total}$  becomes 18.2 dB which exceeds C/N value required for a BER of  $10^{-7}$  by 2.5 dB.

#### B.1.6 $(C/N_{th})_u$ Calculation for 20-GHz Uplink

The satellite parameters assumed for the 20-GHz uplink calculations are:

- Satellite antenna diameter 5.1 m
- On-axis antenna gain 57 dBi
- Uplink satellite G/T 22 dB/°K

The control station parameters assumed for the 20-GHz uplink calculations are:

- Earth station antenna diameter 5 m
- On-axis antenna gain 57.8 dBi
- Power level into antenna 14.0 dBW

The  $(C/N_{th})_u$  calculations are summarized in Table B-4.

Table B-4. Calculation of  $(C/N_{th})_u$  at 20 GHz

Uplink EIRP, $E_W$ (assuming 50 W into antenna)	71.8 dBW
Path loss at 20 GHz, $L$	-210.5 dB
Satellite G/T	22 dB/°K
Boltzmann's Constant	228.6
Noise bandwidth (36 MHz), $B$	-75.6 dB-Hz
Miscellaneous margin, $M_p$	-2.5 dB
Rain margin, $M_r$	- 3 dB
$(C/N_{th})_u$	30.8 dB

#### B.1.1.7 $(C/I)_d$ Calculations for 12-GHz Downlink

First, assume that the 12-GHz satellites interfering with the electronic mail receiving earth stations are space in orbit at four degrees from the platform satellite since the uplink portion of the earth stations have been sized for 4-degree spacings. We substitute the following values for the CTS satellites which have a higher EIRP (58 dBW) than the SBS satellites (42 dBW):

$$(C/I)_d = E_W - E_I + G_{es} - G_o \quad (3-6)$$

Where  $E_W$  is the wanted satellite EIRP in dBW

$E_I$  is the interfering satellite EIRP in the direction of the electronic mail station = 58 dBW

$G_{es}$  is the on-axis antenna receive gain for the electronic mail station = 53.4 dBi

$G_o$  is the off-axis antenna receive gain for the electronic mail station = 17 dBi

Substituting,  $(C/I)_d = E_W - 58 + 53.4 - 17 = E_W - 21.6$  for CTS for

$$(C/I)_d = 26 \text{ dB, then } E_W \geq 47.6 \text{ dBW.}$$

Now consider the restrictions on  $E_W$  because of interference from the platform satellite into the CTS and SBS earth stations in the downlink beam. The assumption for the CTS and SBS earth stations at 12 GHz are summarized in Table B-5.

Table B-5. Summary of SBS and CTS 12-GHz Downlink Parameters

Parameter	SBS Downlink	CTS Downlink
Satellite EIRP	42 dBW	58 dBW
Earth station antenna size	5 m	2.5 m
On-axis gain	53.9 dBi	47 dBi
Gain at 4°	17 dBi	17 dBi

Substituting into Equation B-2 for the SBS case,  $(C/I)_d = 42 - E_I + 53.9 - 17 = 78.9 - E_I$ . If we set  $(C/I)_d$  at 26 dB, then  $E_I \leq 52.9$  dBW. For the CTS case, substituting into Equation B-7 results in  $(C/I)_d = 58 - E_I + 47 - 17 = 88 - E_I$ . Again, if  $(C/I)_d \geq 26$  dB, then  $E_I \leq 62$  dBW.

#### B.1.8 $(C/N_{th})_d$ Calculation for 12 GHz

The satellite parameters assumed for the 12-GHz downlink calculations are:

- Satellite antenna diameter 7.5 m
- On-axis antenna gain 56.8 dBi
- Transponder output power -2 dBW
- Satellite EIRP 56.8 dBW

The  $(C/N_{th})_d$  calculations are summarized in Table B-6 assuming a 5-m earth station antenna.

Table B-6. Calculation of  $(C/N_{th})_d$  at 12 GHz

Satellite EIRP	54.8 dBW
Path loss at 12 GHz	-206 dB
Earth station G/T, assuming $T_s = 184^\circ\text{K}$	31.2 dB/°K
Boltzmann's Constant	228.6
Noise bandwidth (36 MHz)	-75.6 dB-Hz
Miscellaneous margin, $M_p$	-1.5 dB
Rain margin, $M_r$	-11 dB
$(C/N_{th})_d$	17.9 dB

#### B.1.9 $(C/N)_{total}$ Calculation for 30-GHz Uplink, 12-GHz Downlink

By substituting the above values into Equation B-2, we can compute  $(C/N)_{total}$  under the worst-case assumption of 11 dB rain loss on the 12-GHz uplink. That is, assuming two interfering 12-GHz satellites, each with  $(C/I)_d = 26$  dB,  $(C/N_{th})_u = 33.8$  dB, and  $(C/N_{th})_d = 17.9$  dB, the  $(C/N)_{total}$  becomes 16.7 dB which exceeds the C/N required for a BER of  $10^{-7}$  by 1 dB.

## B.2 LINK CALCULATIONS FOR 20-GHz UPLINK AND 30-GHz DOWNLINK EARTH STATIONS

### B.2.1 General

This case assumes the same 20-GHz and 30-GHz links to the central control and switching earth station as in the preceding sections. However, this case assumes that there are user earth stations located in the semi-arid portions of the U.S. which are using other 20- and 30-GHz links for their transmissions. For the 20- and 30-GHz links, interference is assumed to be negligible.

### B.2.2 $(C/N_{th})_u$ Calculation for 20-GHz Uplink

Assuming the same satellite parameters as in Table B.1-6, except for a 3 dB higher G/T, the  $(C/N_{th})_u$  calculations are summarized in Table B-7.

Table B-7. Calculation of  $(C/N_{th})_u$  at 20 GHz

Uplink EIRP, $E_W$ (assuming 50 W into antenna)	56.7 dBW
Path loss at 20 GHz, L	-210.5 dB
Satellite G/T <sub>s</sub>	25 dB/°K
Boltzmann's Constant	228.6
Noise bandwidth (36 MHz), B	-75.6 dB-Hz
Miscellaneous margin, $M_p$	-1.5 dB
Rain margin, $M_r$	-3 dB
$(C/N_{th})_u$	18.7 dB

The uplink EIRP value of 56.7 dBW corresponds to a 3-ft-diameter antenna gain of 43 dBi with an input power of 12.7 dBW or 18.6 W. Such power levels are achievable with TWT's. With the advances in the state of the art, this power level should be achievable with parallel solid-state amplifiers. In addition to the attractiveness of solid-state amplifiers, there is the advantage of soft degradation if only one or two of the paralleled amplifiers fail at a time. Note also that the receiver noise temperature for the satellite uplink is not pushing the state of the art and could be improved by perhaps 3 dB, which would lower the required power output for the earth station power amplifiers.

### B.2.3 $(C/N_{th})_d$ Calculation for 30 GHz

Assuming the same satellite parameters as in Section B.1.4, except for the satellite power level, the  $(C/N_{th})_d$  calculations are summarized in Table B-8 for a 3-ft receiving antenna. The receive noise temperature for the earth stations are assumed to be 600°K. The power level into the satellite antenna is assumed to be 13 dBW or 20 W which is achievable with TWT's.

### B.2.4 Summary of 3-ft 20/30-GHz Earth Station $(C/N)_{total}$ Calculations

With link degradations of 3 dB and 5.1 dB on the up- and downlinks, respectively, the overall  $(C/N)_{total}$  for the above 3-ft-diameter earth station case is 15.7 dB which can provide  $10^{-7}$  BER over the satellite portion of the system. Such stations would be suitable for large portions of the western parts of the United States.

Table B-10. Calculation of  $(C/N_{th})_d$  at 30 GHz

Satellite EIRP, $E_{WS}$	68 dBW
Path loss at 30 GHz, L	-214 dB
Earth station G/T	18.3 dB/°K
Boltzmann's Constant	228.6
Noise bandwidth (36 MHz), B	-75.6 dB-Hz
Miscellaneous margin, $M_p$	-1.5 dB
Rain margin	-5.1 dB
$(C/N_{th})_d$	18.7 dB

### B.3 CODING

So far, in all the link calculations done, no allocation was made to the processing gain which can be obtained by including some kind of forward error-correcting coding scheme. Although coding adds one more dimension to the complexity of the system, it also gives an additional tradeoff possibility to the system designer. For example, if we consider a binary PSK system, without any forward error correction the required energy per bit-to-noise spectral density ratio ( $E_b/N_0$ ) to achieve a bit error rate (BER) of 1 in  $10^7$  is approximately 11.6 dB. If we use a rate 1/2 convolutional code with 8-level soft decision Viterbi decoder, the required  $E_b/N_0$  to achieve a BER of  $10^{-7}$  is 6.6 dB which is a 5-dB processing gain due to coding. The price we have to pay for this coding gain, besides increased system complexity, is the reduced throughput data rate for a given bandwidth or increased bandwidth for a given data rate. In Figure B-2, bit error probability as a function of  $E_b/N_0$  for several important codes in use is plotted and the coding gain at a BER of  $10^{-5}$  is tabulated in Table B-9.

The 5-dB coding gain found above can be used to reduce the antenna size or HPA size at all the earth stations. If we translate 5-dB coding gain into reduced antenna size, rather than 5 meters, we could employ 2-meter antenna size and yet achieve the required BER performance but double the bandwidth requirement. We have assumed additive white Gaussian noise in computing the coding gain. The coding gain can be substantially increased if the noise is non-Gaussian, such as that due to short-duration heavy rainfall.

The redundancy added to obtain the coding gain can also be used to combine the function of encryption in some way. Privacy is an important factor in any alternative to the present mail system and it becomes even more important by the very nature of satellite electronic mail system.

A detailed study is necessary to optimize the satellite electronic mail system in terms of cost, complexity, satellite utilization, the efficient use of space segment, and privacy. We may also add another possibility to the above list of studies. If the link budget margin due to rainfall is substantial and if the rainfall is only of short duration (one or two hours per day), the system can be turned off during that duration to that particular site for later transmission. This may be easily done by transmitting some kind of preamble before each message burst and measuring BER at the receive site and responding send/no-send to the transmit site. The buffering requirements and the actual protocols have to be analyzed for such a system.

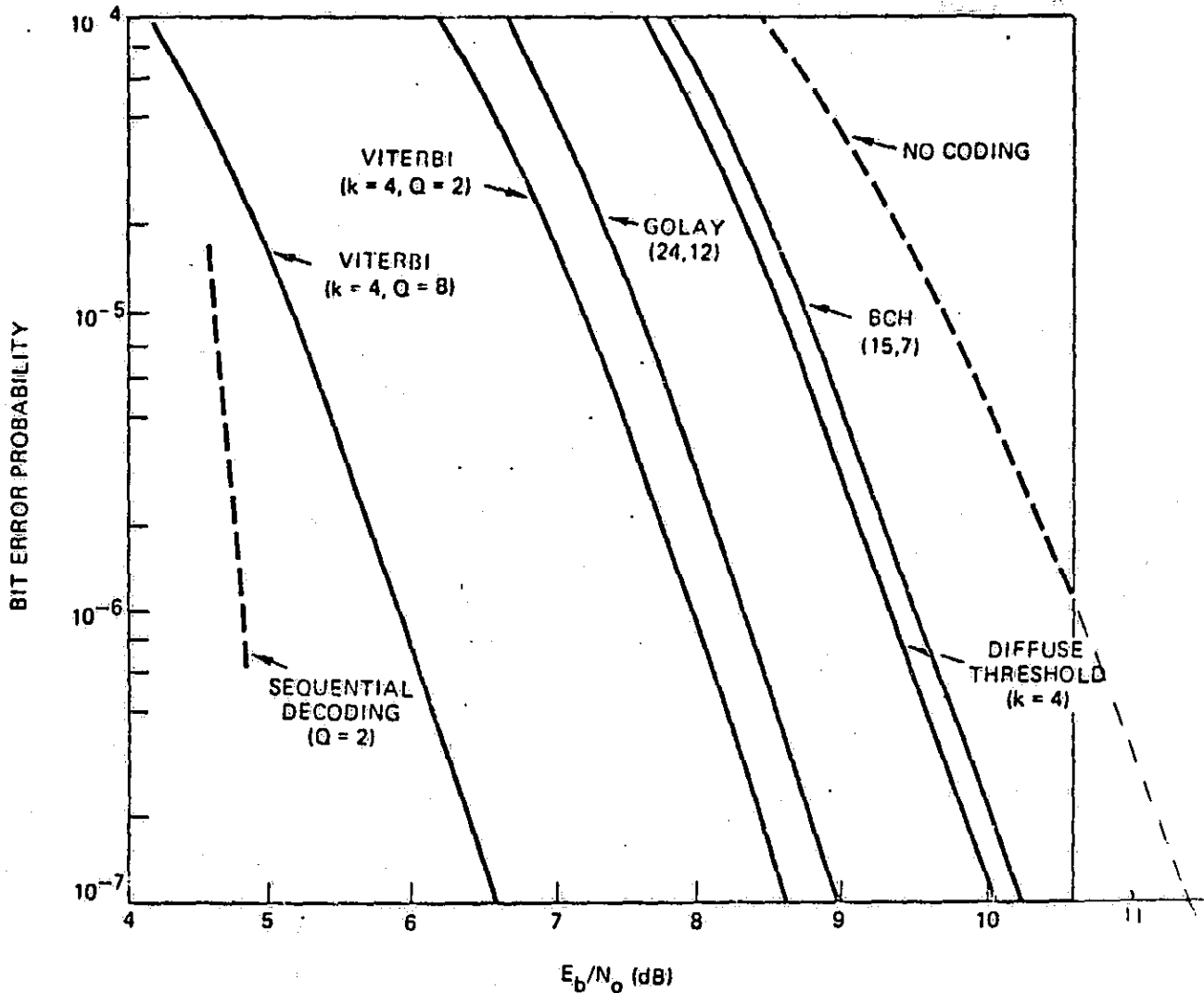


Figure B-2. Error Correction Code Performance with PSK Demodulation

Table B-9.  $E_b/N_0$  Coding Gain for Several Coded Systems

System	Required $E/N$ at $10^{-5}$ (dB)	Gain ( $E_b/N_0$ ) Uncoded— $E_b/N_0$ Coding (dB)
No coding	9.6	—
(15, 7) BCH	8.65	1.0
Threshold	8.5	1.1
Golay (24, 12)	7.5	2.1
Viterbi ( $Q = 2$ )	7.1	2.5
Viterbi ( $Q = 8$ )	5.1	4.5
Sequential ( $Q = 2$ )	4.6	5.0

All require 2:1 increase in channel bandwidth.

#### B.4 SUMMARY OF LINK CALCULATIONS

The preceding link calculations strongly indicate that it is well within the state of the art to provide electronic mail service using 12/14 GHz and 20/30 GHz TDMA data links with a large platform satellite. They further show that even with other 12/14 GHz satellites located as close as four degrees to the platform satellite operating in the same band, acceptable service to all users can be provided. They further show that it would be possible to employ small 20/30 GHz earth stations with 3-ft-diameter antennas for electronic mail service in areas where the rainfall and cloud attenuations are low.

## APPENDIX C

### TRAFFIC CAPACITY OF COMMUNICATIONS PLATFORM AS LIMITED BY ANTENNA SIDELOBES

#### C.1 INTRODUCTION

In the course of studying large multibeam antennas for long-haul domestic communication traffic, it became apparent that as the number of spot beams covering the U.S.A. increased beyond 50, a severe restriction on system capacity due to mutual interference could occur. This interference is due to the reception of energy from spots other than the one a given beam is pointed. The energy from many of these spots can be filtered out. However, the remaining spots utilize the same frequency band. Only the antenna which serves as a spatial filter can reduce this interference. The purpose of this paper is to determine the antenna sidelobe level needed for a given traffic capacity.

#### C.1 SYSTEM TRAFFIC CAPACITY

The system traffic capacity is dependent upon the desired carrier-to-interference ratio, the number of spot beams illuminating the U.S.A., the sidelobe level of the antennas, the bandwidth allocation, and the traffic distribution. To simplify the analysis, the traffic distribution will be taken to be uniform so that various trends will be more evident.

The carrier-to-interference ratio will be taken as

$$\frac{C}{I} = 24 \text{ dB}$$

Most authors choose 22 - 27 dB so that the interference does not seriously degrade the bit-error rate.

With the above choices, we can now solve for the remaining items parametrically using sidelobe levels of -40, -35, and -30 dB. Starting with

$$\frac{C}{I} = \frac{1}{S} \frac{M}{N} \quad (1)$$

where

- C = carrier level (watts)
- I = total interference level in given spot and frequency band (watts)
- N = number of spot beams
- $\frac{1}{S}$  = inverse sidelobe level (-40 dB sidelobe is 10,000)



M = number of frequency bands in which the total frequency allocation is divided. For example, if the allocation is 500 MHz, each transponder takes 36 MHz plus 4 MHz guard band. Then with two polarizations a maximum of 24 transponders per spot beam would be possible if the sidelobes were small enough. In actuality, 8, 6 or even fewer transponders per beam are used due to interference problems. Therefore, if Q = number of transponders per spot beam, then  $M = 24/Q$ .

Solving equation (1) using 40 dB sidelobes:

$$24 \text{ dB} = 40 \text{ dB} - 16 \text{ dB}$$

$$\text{Since } -16 \text{ dB} = \frac{1}{40}$$

$$\frac{M}{N} = \frac{1}{40} \text{ or } \frac{2}{80} \text{ or } \frac{4}{160} \text{ or } \frac{6}{240}$$

Again with 35 dB sidelobes

$$24 \text{ dB} = 35 \text{ dB} - 11 \text{ dB}$$

$$\text{Since } -11 \text{ dB} = \frac{1}{12.6}$$

$$\frac{M}{N} = \frac{1}{12.6} \approx \frac{2}{25} = \frac{4}{50} = \frac{6}{75}$$

Again with 30 dB sidelobes

$$24 \text{ dB} = 30 \text{ dB} - 6 \text{ dB}$$

$$\text{Since } -6 \text{ dB} = \frac{1}{4}$$

$$\frac{M}{N} = \frac{1}{4} = \frac{2}{8} = \frac{4}{16} = \frac{6}{24}$$

The results are plotted in Figure C-1 and tabulated with antenna size in Table C-1. In the March 1979 report, we used as an average

$$\frac{2 \text{ transponders}}{\text{spot beam}} \times \frac{3 \times 73 \text{ beams}}{\text{band}}$$

or 438 transponders in C band and 438 transponders in Ku Band. By going through the above calculations iteratively -36.5 dB sidelobes were found to be adequate for 219 beams and 438 transponders.

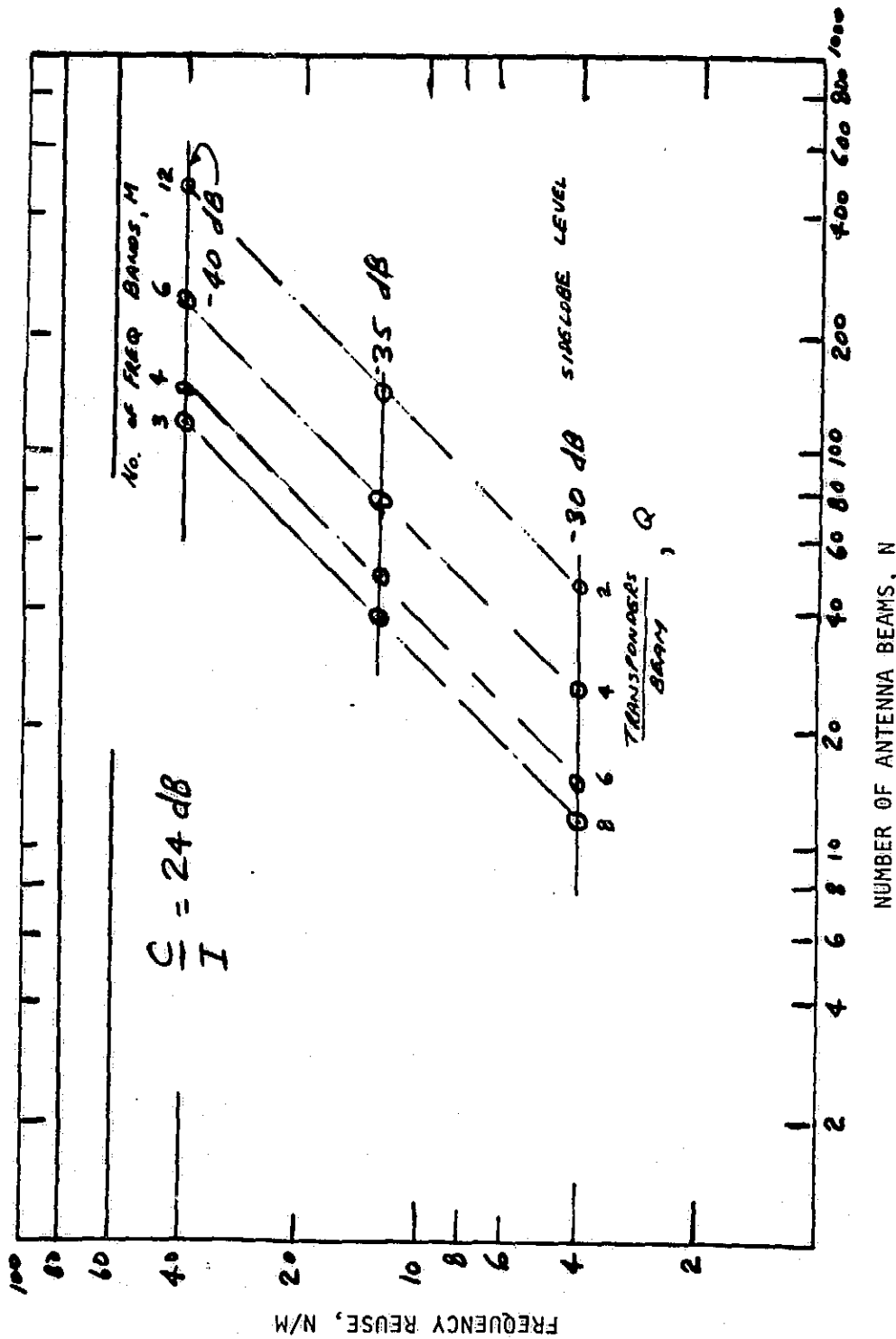
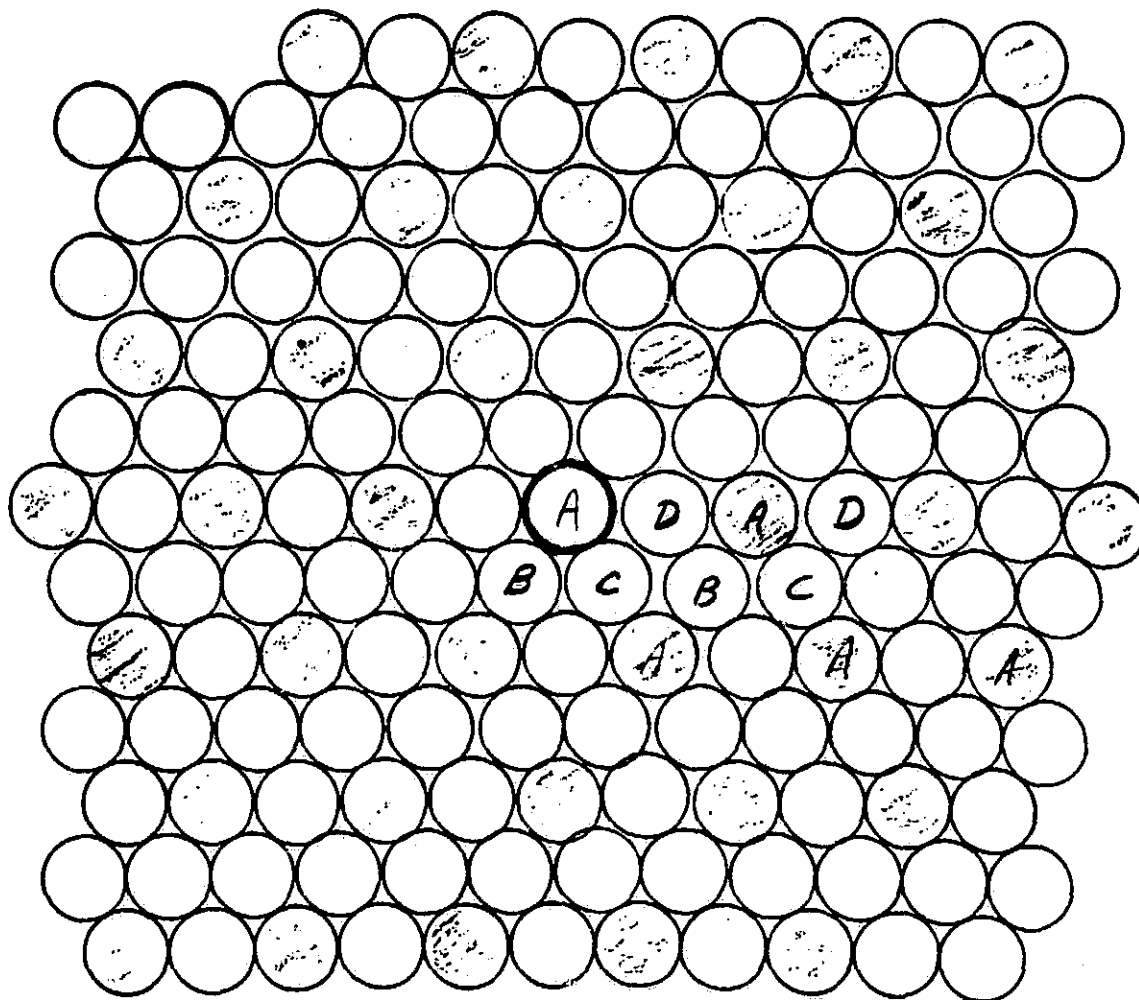


Figure C-1. Effect of Satellite Antenna Side Lobe Level on System Traffic Capacity

Table C-1. System Capacity Vs. Sidelobe Levels

Sidelobe Level	Frequency Re-Use N/M	Number of Spots N	Number of Bands M	Transponders per Beam (24/M) Q	Total Transponders NQ	Antenna Diameter
-40 dB	40	480	12	2	960	29 m
	40	240	6	4	960	21.5 m
	40	160	4	6	960	16.7 m
	40	120	3	8	960	14.3 m
-35 dB	~12.5	150	12	2	300	16.5
	~12.5	75	6	4	300	11.5
	~12.5	50	4	6	300	9.4
	~12.5	37.5	3	8	300	8.1
-30 dB	4	48	12	2	96	9.3
	4	24	6	4	96	6.5
	4	16	4	6	96	5.3
	4	12	3	8	96	4.5

Shown in Figure C-2 is one of several frequency reuse patterns. In this particular one, the frequency allocation of 500 MHz is divided into four bands, giving six transponders per beam. As N, the number of spot beams, increases the interference level increases. As M, the number of frequency divisions, increases the situation improves. The ratio N/M is the frequency reuse factor.



FREQUENCY ALLOCATION = 500 MHz = 24 TRANSPONDERS

M = FOUR FREQUENCY BANDS (A,B,C,D)

Q = SIX TRANSPONDERS PER SPOT BEAM

$$\text{INTERFERENCE LEVEL} = \left( \frac{N}{M} \times \frac{1}{\text{SIDELOBE LEVEL}} \right)$$

Figure C-2. Interference caused by Frequency Reuse